

INFORMATION TO USERS

This manuscript has been reproduced from the microfilm master. UMI films the text directly from the original or copy submitted. Thus, some thesis and dissertation copies are in typewriter face, while others may be from any type of computer printer.

The quality of this reproduction is dependent upon the quality of the copy submitted. Broken or indistinct print, colored or poor quality illustrations and photographs, print bleedthrough, substandard margins, and improper alignment can adversely affect reproduction.

In the unlikely event that the author did not send UMI a complete manuscript and there are missing pages, these will be noted. Also, if unauthorized copyright material had to be removed, a note will indicate the deletion.

Oversize materials (e.g., maps, drawings, charts) are reproduced by sectioning the original, beginning at the upper left-hand corner and continuing from left to right in equal sections with small overlaps.

ProQuest Information and Learning
300 North Zeeb Road, Ann Arbor, MI 48106-1346 USA
800-521-0600

UMI[®]

NOTE TO USERS

This reproduction is the best copy available.

UMI[®]

University of Alberta

Neural differentiation and excitability in flatworm stem cells

by



Sampson Kar Cheung Law

**A thesis submitted to the Faculty of Graduate Studies and Research in partial fulfillment of
the**

requirements for the degree of Master of Science

in

Physiology and Cell Biology

Department of Biological Sciences

Edmonton, Alberta

Fall 2005



Library and
Archives Canada

Bibliothèque et
Archives Canada

0-494-09214-9

Published Heritage
Branch

Direction du
Patrimoine de l'édition

395 Wellington Street
Ottawa ON K1A 0N4
Canada

395, rue Wellington
Ottawa ON K1A 0N4
Canada

Your file *Votre référence*

ISBN:

Our file *Notre référence*

ISBN:

NOTICE:

The author has granted a non-exclusive license allowing Library and Archives Canada to reproduce, publish, archive, preserve, conserve, communicate to the public by telecommunication or on the Internet, loan, distribute and sell these worldwide, for commercial or non-commercial purposes, in microform, paper, electronic and/or any other formats.

The author retains copyright ownership and moral rights in this thesis. Neither the thesis nor substantial extracts from it may be printed or otherwise reproduced without the author's permission.

AVIS:

L'auteur a accordé une licence non exclusive permettant à la Bibliothèque et Archives Canada de reproduire, publier, archiver, sauvegarder, conserver, transmettre au public par télécommunication ou par l'Internet, prêter, distribuer et vendre des thèses partout dans le monde, à des fins commerciales ou autres, sur support microforme, papier, électronique et/ou autres formats.

L'auteur conserve la propriété du droit d'auteur et des droits moraux qui protègent cette thèse. Ni la thèse ni des extraits substantiels de celle-ci ne doivent être imprimés ou autrement reproduits sans son autorisation.

In compliance with the Canadian Privacy Act some supporting forms may have been removed from this thesis.

Conformément à la loi canadienne sur la protection de la vie privée, quelques formulaires secondaires ont été enlevés de cette thèse.

While these forms may be included in the document page count, their removal does not represent any loss of content from the thesis.

Bien que ces formulaires aient inclus dans la pagination, il n'y aura aucun contenu manquant.


Canada

Abstract

Neurons have evolved to conduct electrical impulses using voltage-gated (Vg) ion channels. The suite of Vg-channels in the membrane gives rise to particular excitability properties. Despite our knowledge of excitability properties in mature neurons, little is known about the sequence of Vg channel expression during development. I examined this question by culturing stem cells, neoblasts, from the flatworm *Girardia tigrina*, inducing them to develop into neurons, then monitoring changes in electrical properties.

Neurally derived factors trigger neoblasts to develop into neurons which is indicated by the expression of a neuron-specific tubulin. There is also a specific pattern of changes in the electrophysiological properties of the maturing neurons that includes increasing membrane potential as K_{DR} channels begin to be expressed. With certain treatments some neurons also produce neurites that is coincident with the expression of K_A channels. These patterns of neurogenesis are conserved in many invertebrates, but are cell lineage specific.

Acknowledgements

This thesis represents an achievement I could not have attained without those dearest to me.

First and foremost, I would like to thank my Supervisor, Dr. Andy Spencer. My most sincere gratitude goes out to you for the support, encouragement, and unshakeable patience through thick and thin. You have always given me freedom to explore my ideas and motivate me by your example. Thank you for providing such a wonderful opportunity. Special thanks must also go to my Committee members, Dr. Declan Ali, Dr. Warren Gallin, and Dr. Jeff Goldberg for the enormous support they provided while I was in Edmonton. I am grateful they all welcomed me into their labs as a guest, shared their equipment and resources, and always gave insight and helpful discussion. Without my Committee, this project could not have been completed. Researchers from the 5th floor Zoology Wing, Dr. John Chang and Dr. Greg Goss were also invaluable, thank you for promoting such a rich environment for collaboration. The members of the Microscopy unit, Rakesh Bhatnager, Randy Mandryk, and Jack Scott provided many hours of help using the confocal microscope. The staff at the Bamfield Marine Sciences Centre were very kind and helpful over the course of many years living in Bamfield.

I must also acknowledge the wonderful people I have met over the course of this degree, their friendship and our lessons learned together made the time pleasant. K.C. Burns and Jen Dalen, Mike Nishizaki, and Kerry Marchinko made the time in Bamfield a delight. Mathis Stoeckle helped me laugh and have some fun. In Edmonton, Shawn Parries was always a thrill, and can still bring joy to any room he enters. Martin Tresguerres kept my interest in basketball alive. Those who shared our office space, Kee-Chan Ahn, Keith Todd, Shandra Doran, Liz Orr, Wang-peng Sun, and Scott Parks shared very insightful discussions about science and others.

I must thank my parents for loving support and encouragement, and Marisa, for everything.

Table of Contents

Introduction	1
1. Overview.....	1
2. Electrical excitability phenotypes are determined by Vg-ion channels.....	2
2.1. Differentiation of excitable cells: autonomous specification vs. inductive interactions.....	6
2.2. Electrical excitability regulates ubiquitous neural developmental events.....	9
2.2. Patterns in the sequence of Vg-ion channel expression – from worms to mice	13
2.3. Excitability of Invertebrate Cells and Sequence of Channel Acquisition.....	13
2.4. Excitability of Vertebrate Cells and Sequence of Channel Acquisition.....	16
3. Flatworms as a model system: evolutionary considerations in the development of excitability properties.....	19
3.1. Flatworms are basal bilaterians.....	19
3.2. Flatworms have limited Vg-channels subtypes and excitability phenotypes ...	22
3.3. Flatworm neurons do not arise from ectoderm.....	25
4. Neoblasts – A unique system of stem cells with neurogenic potential.....	26
4.1. Distribution and abundances of neoblasts.....	27
4.2. Ultrastructural evidence for different populations of neoblasts.....	28
4.3. Neoblasts are responsible for cellular replacement	29
4.4. Neoblast involvement in regeneration, and factors affecting their behaviour..	30
4.5. Regeneration of neural structures in flatworms.....	31
4.6. Potential neurogenic agents in flatworms	32
4.7. Cell culture of neoblasts.....	34
5. Objectives	35
5.1. Establish a method for isolating stem cell cultures in <i>Girardia tigrina</i>	36
5.2. Induce cultured stem cells to initiate neuronal differentiation.....	36
5.3. Examine the changes in electrophysiological properties stem cells undergo during differentiation	37
Materials and Methods	39
1. Collection and maintenance of animals	39

2. Cell dissociation and concentration of neoblasts	39
3. Identification of neoblasts in culture.....	40
4. Cell culture of neoblasts, viability and proliferation	41
5. Assay for identification of neurons from <i>Girardia tigrina</i>	41
6. Induction of neuronal differentiation in neoblasts by treatment with putative morphogens.....	41
7. Induction of neurite-outgrowth by plating neoblasts on different substrates	43
8. Electrophysiological properties of undifferentiated neoblasts.....	44
9. Recording solutions	45
10. Electrophysiological properties of differentiating neoblasts	45
11. Voltage-dependent activation properties of K ⁺ channels.....	46
12. Data analyses and statistical methods.....	47
Results	48
1. Primary cell culture and purification of neoblasts	48
1.1. Cell culture of neoblasts; viability and proliferation	49
2. Assay for positive neuronal identification	49
3. Differentiation of cultured neuroblasts	50
3.1. Neoblasts exposed to morphogenic agents express a neuron-specific tubulin .	51
3.2. Induction of neurite-outgrowth in differentiating neuroblasts.....	52
4. Electrophysiological properties of cultured neoblasts	54
4.1. Resting membrane properties of undifferentiated neoblasts.....	54
4.2. Resting membrane potential increases in differentiating stem cells.....	56
4.3. Vg-KDR channels from undifferentiated neoblasts.....	57
4.4. Vg-K _{DR} channels from differentiating neoblasts	58
4.5. Electrophysiological properties of differentiating neurons with neurites.....	60
4.6. Differences between differentiation neoblasts and mature adult neurons	62
Discussion	64
1. Isolation and purification of neoblasts from <i>Girardia tigrina</i>	64
1.1. Density- and size-dependent purification of neoblasts	64
1.2. Neoblasts are a heterogenous group of stem cells	66
1.3. Neoblast activity is regulated by extracellular osmolarity.....	67
2. Nervous system architecture and neuronal differentiation revealed by a monoclonal	

tubulin antibody	69
2.1. Tubulin expression is an early indicator of neural differentiation.....	70
3. Factors influencing neurogenesis in flatworms	71
3.1. Neoblasts consist of a heterogeneous group of pluripotent stem cells	72
3.2. Neuropeptides	73
3.3. Biogenic amines and transduction via intracellular signalling cascades	76
3.4. Cocktail treatments combining different factors are effective in promoting neurogenesis.....	78
3.5. Neuritogenesis and neurogenesis are initiated by different morphogens	79
4. Early developmental changes in electrical properties of differentiating neurons....	81
4.1. Hyperpolarization of the resting membrane potential	82
4.2. Expression of delayed rectifier K ⁺ channels	84
4.3. K _A channels are expressed in neoblasts developing neurites.....	86
4.5. Phylogenetic comparison of development of excitability properties.....	88
4.6. Summary of developmental changes occurring during neural differentiation..	92
4.7. Future directions	93
Literature Cited	147
Appendix 1. Properties of cultured brain neurons and neuroblasts from the marine polyclad <i>Notoplana atomata</i>	179
1. Effects of substrate and exogenous diffusible factors on neurite outgrowth in cultured brain neurons.....	180
A. Materials and Methods.....	180
B. Results	182
B.1. Neurite outgrowth is initiated early after plating and is unaffected by substrate	182
B.2. Effects of bFGF and 5-HT on neurite initiation and outgrowth.....	184
B.3. Neurite outgrowth is correlated with changes in Vg channel expression	186
B.4. Electrophysiological properties of Ca ²⁺ channels involved in neurite outgrowth	188
2. Neoblasts from the marine flatworm <i>Notoplana atomata</i>	189
A. Materials and Methods.....	189

B. Results	191
B.1. Isolation and purification of neoblasts	191
B.2. Neoblasts express a delayed rectifier-like K ⁺ channel	192
3. The architecture of the nervous system revealed by tubulin immunohistochemistry	193
A. Materials and Methods.....	193
B. Results	193
B.1. Neuron-specific tubulin reacts with the commercial antibody Tub Ab-4	193
4. Literature Cited	195
5. Appendix Figures.....	196

List of Figures

Figure 1. Individuals of <i>Girardia tigrina</i> used in experiments.....	95
Figure 2. Identification of cultured neoblasts using histological stains or DIC microscopy	96
Figure 3. Isolation and purification of neoblasts from whole organism dissociations	98
Figure 4. Neoblasts remain viable, with no signs of proliferation when cultured	100
Figure 5. Cultured brain neurons are immunoreactive against the neuron-specific antibody.....	101
Figure 6. An antibody against α - and β -tubulin specifically labels neurons in whole-mounts of <i>Girardia tigrina</i>	102
Figure 7. Neurons innervating the pigmented ocellus visualized using Tub Ab-4 immunolabelling	103
Figure 8. The ciliated margin of <i>Girardia tigrina</i> binds the fluorescent secondary antibody non-specifically in negative control treatments	105
Figure 9. Effects of various putative morphogen treatments on the expression of a neuron-specific tubulin in neoblasts culture for 24 h.....	107
Figure 10. Effects of various morphogen treatments on viability of cultured cells after 24 h.....	109
Figure 11. Treatment with morphogens induces differentiating neoblasts to develop neurite-like extensions	110
Figure 12. Differentiating neoblasts treated with A+G for 24 h develop neurite-like extensions.....	112
Figure 13. Membrane capacitance and time constant of differentiating neoblasts are unaffected by A+G treatment.....	113
Figure 14. Membrane capacitance and time constant of differentiating neoblasts are unaffected by the presence of Vg-K ⁺ channels.....	114
Figure 15. Resting V _m of differentiating neoblasts is affected by both treatment and the presence of Vg-K ⁺ channels.....	115

Figure 16. Resting V_m of control neoblasts are similar between whole-cell patch clamp and intracellular sharp electrode recordings	116
Figure 17. K^+ currents recorded from cultured neoblasts	117
Figure 18. Activation properties of V_g - K^+ channels recorded from undifferentiated neoblasts.....	119
Figure 19. The time constant of activation of delayed rectifier channels.....	121
Figure 20. Appearance of V_g - K^+ currents in cultured neoblasts	122
Figure 21. Maturation of a delayed rectifier K^+ current in differentiating neoblasts	123
Figure 22. K^+ current density increases in differentiating neoblasts	125
Figure 23. Activation properties of V_g - K^+ channels from differentiating neoblasts.....	127
Figure 24. The time constant of activation of V_g - K^+ channels from cells cultured for 24 h in control media and in the presence of A+G are similar and voltage-dependent	129
Figure 25. Developing neurons sprouting neurites had variable morphologies	131
Figure 26. Developing neurons extending neurites express delayed rectifier K^+ channels with the same activation properties as in adult brain neurons	132
Figure 27. The time constant of activation from K^+ channels in differentiating neuroblasts and adult neurons is similar and voltage-dependent.....	134
Figure 28. Whole-cell patch clamp recordings in solutions isolating for K^+ currents reveal that neoblasts sprouting neurites possess both an inactivating and non-inactivating component.....	135
Figure 29. Resting membrane properties of differentiating neurons expressing an A-type V_g - K^+ current.....	137
Figure 30. Delayed rectifier currents from differentiating neoblasts are smaller than those observed in adult brain neurons	138

List of Tables

Table 1. Early expression of Vg-ion channels during development – phylogenetic and cell lineage comparisons.....	140
Table 2. Composition of neurogenic treatments applied to neoblasts	143
Table 3. Composition of the different electrophysiological solutions used to determine resting membrane properties and indentify voltage-gated ion channels in neoblasts.....	144
Table 4. Summary of neuropeptides, neurotransmitters, and second messenger pathways involved in regulating neurogenesis	145
Table 5. Review table of changes occurring in differentiating neurons	146

List of Appendix Figures

Figure 1. Cultured brain neurons from <i>Notoplana atomata</i> develop growth cones within 3 h of plating and begin extending neurites soon after	196
Figure 2. Brain neurons from <i>N. atomata</i> developed growth cones during the first 24 h in culture in absence of exogenous biological factors	197
Figure 3. The rate of neurite outgrowth is similar between brain neurons cultured on polystyrene dishes and cells grown on 0.1% poly-L-lysine	198
Figure 4. The substrate on which brain neurons are cultured has no effect on the number of neurites extended	200
Figure 5. Treatment of brain neurons with bFGF increased the proportion of cells developing growth cones	202
Figure 6. Basic fibroblast growth factor applied exogenously had a slight inhibitory effect on neurite outgrowth.....	203
Figure 7. Basic fibroblast growth factor applied exogenously had no effect on the number of neurites extended.....	205
Figure 8. Serotonin increases the proportion of cultured neurons extending growth cones	207
Figure 9. Serotonin inhibits neurite outgrowth.....	208
Figure 10. Serotonin applied to brain neurons inhibited neurite extension	210
Figure 11. Appearance of Vg-Ca ²⁺ channels in cultured brain cells	212
Figure 12. Expression of Ca ²⁺ currents in brain neurons during neurite outgrowth requires <i>de novo</i> protein expression.....	213
Figure 13. Treatment with morphogens inhibits expression of Ca ²⁺ currents in brain neurons.....	214
Figure 14. Culturing brain cells from <i>N. atomata</i> resulted in an increase in the proportion of cells expressing a K _{DR} -like channel.....	215
Figure 15. The effect of diffusible factors on the proportion of cultured brain neurons expressing a K _A channel	216

Figure 16. Vg-Ca ²⁺ currents recorded in brain cells from <i>N. atomata</i>	217
Figure 17. Activation and steady-state inactivation properties of Vg-Ca ²⁺ channels recorded from brain neurons.....	219
Figure 18. Expression of Ca ²⁺ channels increases during the first 24 h in cultured brain neurons.....	221
Figure 19. Isolation and purification of neoblasts from whole organism dissociations of <i>Notoplana atomata</i>	222
Figure 20. Neoblasts purified using Percoll gradients can be identified using histological stains	224
Figure 21. Effect of diffusible morphogens on the expression of a neuron-specific tubulin in neoblasts cultured for 7 days	225
Figure 22. Vg-K ⁺ currents recorded in undifferentiated neoblasts	227
Figure 23. Activation properties of Vg-K ⁺ channels from differentiating neoblasts.....	229
Figure 24. The time constant of activation of Vg-K ⁺ channels from cells cultured for 24 h in control media and in the presence of A+G are similar and voltage-dependent	231
Figure 25. Cultured brain neurons can be identified in culture by immunoreactivity towards the Tub Ab-4 antibody	233

Introduction

1. Overview

Electrically excitable cells use specialized voltage-gated (Vg) ion channels for the generation and rapid propagation of electrical signals (Kandel *et al.*, 2000; Hille, 2001). Despite our considerable knowledge of the electrical excitability properties of mature neurons, relatively little is known about the pattern by which ion channels are expressed during development (Spitzer, 1979; Ribera & Spitzer, 1998). Emerging excitability properties have been shown to regulate critical developmental processes of neurons including cell proliferation, morphological differentiation (Ming *et al.*, 2001), as well as migration (Komuro & Rakic, 1998), specification (Borodinsky *et al.*, 2004) and the establishment of the mature electrical phenotype (Dallman *et al.*, 1998). The roles of specific types of Vg channels during development are only beginning to be understood.

Given the high diversity of mature excitability phenotypes in neurons, and the many developmental processes governed by Vg channels, it is of interest to determine whether the sequence of Vg ion channel expression is important. If the sequence of Vg ion channel expression is conserved among cells with dissimilar mature phenotypes, this may suggest that electrically excitable cells are constrained by an ancestral developmental program. On the other hand, if the sequence of Vg ion channel insertion into the membrane differs among cellular lineages, this may explain the diversity of excitability phenotypes in mature cells.

I therefore suggest the following null hypothesis, “A common, conserved developmental pattern is expressed in all developing electrically excitable cells within the Metazoa, resulting in a similar sequence of ion channel expression during differentiation among excitable tissues with different cell lineages and in evolutionarily divergent organisms.”

If differences in the developmental pattern exist, they are most likely manifested in cell lineages and organisms that are not closely related. The Platyhelminthes should be a suitable taxon to study and determine whether the pattern of Vg ion channel acquisition is significantly divergent from that of other major lineages, for example, the chordates. Modern flatworms are thought to resemble the common ancestor of the Bilateria (Hyman, 1951; Zrzavy *et al.*, 1998; Giribet *et al.*, 2000; Rieger & Ladurner, 2001). They may have retained features of a basal genetic program, and consequently, the sequence of ion channel insertion in developing flatworm cells may reflect that of the ancestral bilaterian. This suggests that the incorporation of ion channels in developing excitable cells from flatworms will help to determine if the differentiation pattern of neurons has been conserved during the diversification of modern metazoans. The objective of this study was to develop a stem cell culture system using flatworm tissues to examine neurogenesis *in vitro* and the sequence of electrophysiological changes that stem cells undergo as they differentiate into neurons.

2. *Electrical excitability phenotypes are determined by Vg-ion channels*

Neurons can vary in morphology, neurotransmitter expression, and excitability properties among other features. The defining characteristic of electrically excitable cells is the way they utilize regenerative electrical signals to process and transmit information. Although neurons share mechanisms to produce excitation in the form of action potentials (APs), there is considerable diversity in the shape of action potentials and the patterns of discharge. The diversity of mature neuronal phenotypes and the complexity of connections between neurons is responsible for the many complex behaviours and functions attributed to the nervous system. Differences in excitability phenotypes may arise from factors such as the type of ionic species (Ca^{2+} , Na^+ , or both) carrying inward current that lead to depolarization and action potentials or sub-threshold electrical signals. However, major determinants of excitability phenotype are the properties of the channels carrying outward potassium currents that specify coding parameters such as the dynamic range for generating APs (Duzhyy *et al.*, 2004), spike amplitude and shape (Martin-

Caraballo & Greer, 2000), firing frequency (Liu & Kaczmarek, 1998) and adaptation (Faber & Sah, 2004), firing patterns (Connor & Stevens, 1971a; Dodson *et al.*, 2002) and other properties. Some neurons do not fire action potentials (e.g. interneurons in central ganglia, Dicaprio, 1989; Kandel *et al.*, 2000), others produce rhythmical changes in membrane potentials (e.g. neurons in the suprachiasmatic nucleus controlling circadian rhythms; Cloues & Sather, 2003). Some excitable cells are designed to generate slow APs (e.g. cardiac muscle; Sanguinetti *et al.*, 1996), while others are adapted for extremely fast bursts of APs (e.g. cochlear neurons; Macica *et al.*, 2003). These are just a few of the numerous excitability phenotypes that exist in the vertebrate nervous system and other metazoans.

Regulation of the specific types of Vg-ion channels and levels at which they are expressed will determine the precise electrical signal produced. Varying the types and expression levels of Vg-channels gives rise to the enormous diversity in excitability phenotypes. Of the various types of Vg-ion channels, K⁺ channels seem to play a critical role in determining excitability properties of neurons (Hille, 2001). In addition to producing the repolarizing phase of the action potential (Hodgkin *et al.*, 1952a; 1952b; 1952d), Vg-K⁺ channels are integral in setting and maintaining the resting membrane potential (Hallows & Tempel, 1998), determining the duration and shape of APs, controlling the rate of firing (Connor & Stevens, 1971b; Hille, 2001), and presumably playing significant roles in all other excitability phenotypes. Based on the large number of genes encoding for Vg-K⁺ channels (between 30-100 genes identified from each of the genomes from human, *Drosophila*, and *C. elegans*; Bargmann, 1998; Miller, 2000), and variation arising from alternative splicing (Kamb *et al.*, 1987; Swartz *et al.*, 1988; Wei *et al.*, 1990), the theoretical combinations and differences in expression levels of these channels suggest that the range of possible electrical phenotypes is almost limitless. However, expression patterns will be limited to those that produce functional phenotypes in the host organism that are not at a significant selective disadvantage. Non-permissive sequences of ion channel expression would be those that lead to cell death through sustained depolarizations and excessive calcium entry, except that such changes may be

advantageous during programmed cell death and apoptosis. Unlikely sequences of channel expression would be those that put the host at a disadvantage at any stage during maturation eventually leading to a lowered reproductive success. In those species where embryonic or larval neurons are retained in the adult it will often be necessary for the phenotype to change during development to accommodate changing physiological and behavioural patterns.

A number of human channelopathies are known to be due to K⁺ channel mutations; these include cardiac arrhythmias, ataxia, convulsions, epilepsy, diabetes, deafness, and schizophrenia among many others (Miller, 2000; Shieh, 2000), and there will be variable degrees of selection against these genotypes. Although disease states that result from an improper balance in density or distribution of voltage gated channels have not been well documented, they might be expected to occur if there are errors in the feedback mechanisms regulating channel density and trafficking of channels. Neuronal differentiation is controlled by evolutionarily conserved genes and gene clusters, including the homeodomain genes (Gilbert, 1997; Jessell, 2000; Bertrand *et al.*, 2002), many of which are linked in cascades of developmental events. Therefore the patterns of differentiation will also be constrained by the evolutionary history of the taxon of interest.

In summary, there has been selection for specific patterns of ion channel expression that do not generate defective excitability configurations during differentiation to the mature phenotype. Furthermore we can expect to find sets of permitted phenotype platforms from which relatively minor changes in channel make-up can produce the diversity seen in adult neurons. This seems likely since most neurons must experience the same developmental events including: fate-specification, migration, morphological differentiation, neurotransmitter specification, and maturation of excitability properties (reviewed below). In a generalized scenario, maturing neurons might be expected to undergo a transition between two different excitability states. There is an immature state during early differentiation when populations of Vg-channels are functionally expressed to regulate developmental activities; and a mature state, where electrical signalling serves

to code information regarding sensory or motor functions. In addition, there is also a transition between properties of excitable cells in the embryonic, larval, juvenile stages and adults (Davis *et al.*, 1995; Moody, 1998). In neurons from embryos and juveniles, neurons are often already involved in both regulating further development and in pre-adult behaviour (Sun & Dale, 1998; Kuang *et al.*, 2002). In a few examples transdifferentiation can occur and the complement of ion channels expressed in mature cells (juvenile or adult) can become modified or altered due to developmental or regenerative signals (Schmid, 1992; Lin *et al.*, 2000). An alternative mode of development exists where embryonic/juvenile neurons are resorbed or undergo apoptosis (Truman, 1983; 1984; Marois & Carew, 1997b). This suggests that in these instances, the excitability properties of mature cells can not revert to immature platforms. In this scenario, it is likely that the adult excitability phenotype can not be achieved from modifications of the embryonic/juvenile cells, highlighting the conservation in the establishment of excitability properties.

These observations stimulate many questions regarding the development of electrical excitability properties and the role evolution has played in shaping patterns of expression in extant organisms. Since all multicellular animals share common body patterning genes (e.g. *Hox* cluster genes), has evolution selected for similar patterns of Vg-ion channel populations in developing neurons among distant clades? Furthermore, what is the relative importance of autonomous vs. extrinsic control of neuronal differentiation. Many invertebrates undergo determinate cleavage where neuronal differentiation is invariant and mostly regulated by a genetic program specific to that neuronal type. This contrasts with most of the chordates and some invertebrates where differentiation tends to be site specific. Alternatively, there may be few similarities in Vg-channel expression ontogeny between different clades or lineages.

2.1 Differentiation of excitable cells: autonomous specification vs. inductive interactions

Early in the development of excitable cells in vertebrates, through neural induction, specific embryonic cells are specified to become either neurons or muscle cells, the former being derived from the ectoderm and the latter from the mesoderm (Gilbert, 1997). These cells must proliferate, migrate to their final location and then acquire mature electrical characteristics. How developing excitable cells determine the specific repertoire of Vg-ion channels is not well understood. There are both autonomous (intrinsic) signals, cytoplasmic determinants acquired during cleavage events; and inductive (extrinsic) cues received from surrounding tissues that determine cell fate and control cellular differentiation (Davidson, 1990; 1991; 2001). Presumably, both types of signalling also play integral roles in defining the precise subset and correct levels of Vg-ion channel expression. The importance of intrinsic vs. extrinsic signals appears to vary, with many invertebrates often relying exclusively on intrinsic signals and vertebrates utilizing a combination of both, but with a stronger emphasis on extrinsic inductive signalling (Easter *et al.*, 1985). There are examples in basal invertebrates (*Hydra*) where position specific cell fate-specification is known to occur (Bode *et al.*, 1973; Fujisawa, 1989; Teragawa & Bode, 1990), but many other invertebrates appear to rely exclusively on intrinsic cell-fate determination (reviewed below).

In vertebrates and *Drosophila*, neuronal differentiation occurs by the progressive switch from progenitors responding initially only to extrinsic inductive signals, and then relying on intrinsic cues to control latter processes (Gilbert, 1997; Davidson, 2001). During gastrulation, neuronal cell fate is controlled by proneural genes, including transcription factors of the basic helix-loop-helix (bHLH) class, and other immediate early genes that can be either activated by extrinsic or intrinsic determinants (reviewed by Cepko, 1999; Chitnis, 1999). These factors promote cells to enter neuronal lineages and initiate commitment to differentiation by: inhibiting adjacent cells from entering neural lineages; inhibiting self-commitment to non-neural lineages; regulating the cell-cycle; and

influencing neuronal subtype specification (reviewed by Bertrand *et al.*, 2002). These systems produce gradients of inductive cues, and cell fate is ultimately determined by the position of progenitor cells along these gradients. For example, during development of the vertebrate CNS, signalling gradients are produced along both the cephalocaudal and dorsoventral body axes. The fate of developing neurons is determined by the concentration and identity of inductive signals. Along the cephalocaudal axis, members of the *Hox* gene clusters are expressed at different segmental regions implicating gene products in fate-specification and patterning (Gilbert, 1997). Other factors that are secreted and also involved in neural specification include but are not limited to bone morphogenic proteins, Wnts, fibroblast-, and epidermal growth factors (reviewed by Jessell, 2000). The progression from extrinsic control to predominately intrinsic control occurs after cell cycle exit and the birth of differentiating neurons through continual activation of intracellular signalling cascades and transcriptional autoregulation (reviewed by Edlund & Jessell, 1999). Intrinsic control of neuronal cell-fate has been well described in both *Drosophila* and in mammals. In asymmetric mitosis, a neuroblast functions as a stem cell, divides and renews itself with each division and produces a second daughter which then becomes fate-restricted and differentiates (Jan & Jan, 2000). This process occurs by controlling the asymmetric localization of cell fate determinants, and directing the mitotic spindle to allow for unequal segregation of cytoplasmic factors and different daughter cell sizes (Chia & Yang, 2002). Several neuronal cell fate determinants have been identified; including the gene products Notch, Numb, Prospero, Mastermind (Shen *et al.*, 2002; Yedvobnick *et al.*, 2004); as have genes controlling the unequal distribution of these molecules; *bazooka*, *frizzled*, *dishevelled*, and *flamingo* (reviewed by Jan & Jan, 2000; Cayouette & Raff, 2002). This switch in fate-regulation appears to confer developmental plasticity. Extrinsic cues will drive large populations of neurons to undergo early developmental changes, but later changes are driven by intrinsic cues. The importance of extrinsic cues is supported by both transplantation and ablation studies, where neuroblasts acquire different fates in order to replace a neuronal type that is lacking or at low density.

This pattern is in sharp contrast with neural specification in most invertebrate groups. Detailed cell lineage maps can often be traced from the zygote through to larvae, juveniles or adults. In protostomous invertebrates, neuronal subtype is established by a genetically specified, patterned development. Examples can be found in both of the major clades of prostomes, including the Ecdysozoa (*C. elegans*, Sulston *et al.*, 1983), and the Lophotrochozoa (*Chaetopterus*, Goldstein, 1950; Jeffery, 1985; Leech, Weisblat *et al.*, 1984; Shankland, 1987; Smith & Weisblat, 1994; *Gastropoda*, Damen & Dictus, 1994). Ablation experiments reveal that organisms undergoing determinate cleavage are unable to replace cell lineages that are destroyed, often resulting in serious or lethal developmental deficiencies (Render, 1991; Smith & Weisblat, 1994)

In the cnidarians, there are numerous excitability phenotypes including non-spiking cells with graded membrane depolarizations (Arkett & Spencer, 1986), electrically coupled cells with both short and long APs (Anderson & Mackie, 1977; Spencer, 1981; Spencer *et al.*, 1989), bursting neurons (Arkett & Spencer, 1986) and even neurons that support both Ca^{2+} and Na^{+} dependent APs (Mackie & Meech, 1985). Another prominent example of the diversity of excitability phenotypes among the invertebrates can be found in the stomatogastric ganglion of crustaceans. Within this ganglion, are cells and circuits that modulate complex motor behaviours (Harris-Warrick *et al.*, 1989; Katz, 1991). There are cells with oscillating membrane potentials, with rapid patterns of burst activity, phasic and tonic motor neurons, that all show high degrees of neuromodulation in order to produce the different complex swimming and feeding behaviours required to match foods with different consistencies (Hartline & Maynard, 1975; Russell & Hartline, 1978; Wiens & Atwood, 1978; Lnenicka & Atwood, 1985a; Millar & Atwood 2004).

Given that many invertebrates can produce a considerable diversity of excitability phenotypes, what effect does cell fate inflexibility have on the patterns of Vg-ion channel acquisition during development? Perhaps invertebrates have retained an ancestral form of neuronal determination, sufficient to generate relatively simple nervous systems and physiologies, and the patterns of Vg-channel populations expressed during differentiation

also reflect an evolutionarily conserved program. The differences among vertebrates and protostomous invertebrates suggest that control over Vg-ion channel expression may be restricted by cell lineage in organisms with determinate cleavage, whereas organisms displaying extrinsic control over cell fate have a more plastic mode of developing excitability properties.

2.2 Electrical excitability regulates ubiquitous neural developmental events

Perhaps the earliest and most dramatic evidence that excitability plays a role during development was first presented by Hubel and Wiesel (1962) when they deprived one eye of a cat from visual experience and demonstrated profound changes in the size of visual fields. It was later shown that depriving afferent input into the developing visual cortex prevented the formation of naturally occurring ocular dominance columns (Stryker & Harris, 1986; Crair, 1999). Also, the occurrence of “spontaneous” activity, electrical activity that is not triggered by either sensory or motor operations, before neural networks are formed, suggests that spontaneous activity is important for early developmental events (reviewed by Moody, 1998). These two contrasting modes of electrical activity appear to serve different functions. Use-dependent activity seems to play a role later in development, regulating synaptic construction (Constantine-Paton *et al.*, 1990; Shatz, 1990; Katz & Shatz, 1996), and circuit wiring (Hubel & Wiesel, 1962; 1963; 1965). In contrast, spontaneous activity tends to be involved in several early developmental events.

Spontaneous activity has been implicated in numerous early developmental events and will be reviewed in the subsequent sections using examples from both the invertebrates and vertebrates. Ubiquitous developmental processes affected by Vg ion channels include: (1) cell survival, proliferation, and migration; (2) morphological differentiation, including neurite outgrowth and extension, growth cone control and target finding; (3) neurotransmitter expression and receptive phenotypes; (4) ion channel trafficking to membranes through autoregulation of Vg channel complement by activity; (5) embryonic and larval behaviour.

Survival of developing neurons in both vertebrates and invertebrates appears to require a baseline level of excitability. In both chick ciliary ganglion (Collins *et al.*, 1991) and the embryonic cockroach brain (Benquet *et al.*, 2001), slow Ca^{2+} spikes or waves are required to keep neurons alive. Reducing excitability induces cell death, whereas hyperexcitability can promote cell survival. Obviously, there are limitations to the supportive abilities of hyperexcitability since excessive activity can cause Ca^{2+} -induced toxicity and death (Meyer, 1989). This may reflect the importance of the developmental regulation of Vg-channel identity and expression levels in generating a permissible excitability phenotype. It may be necessary for an immature neuron to express specific excitability properties before further differentiating. A role for excitability in controlling neuronal migration has also been discovered. Developing neurons in the vertebrate cortex and spinal cord must migrate during the time between mitosis and morphological differentiation (Rakic, 1972; Leber & Sanes, 1995). Komuro & Rakic (1992; 1996; 1998) have followed migrating neurons in the mouse cerebellum by staining cells with DiI, and have shown that both the amplitude and frequency of Ca^{2+} spikes are positively correlated with migrational speed, and that Ca^{2+} enters through an N-type voltage-gated calcium channel (VGCC). Migration of developing neurons has also been well characterized in the invertebrates (Goodman & Spitzer, 1981a; Tagher *et al.*, 1984), and it is likely that the mechanisms and role of Ca^{2+} entry through VGCC's is similar to the vertebrates, since all cells move using similar mechanisms (Stossel, 1993).

Morphological differentiation is also controlled by electrical activity. For example, developing myocytes from *Xenopus* require a basal level of spiking for proper myofibrillar organization and for sarcomere assembly (Ferrari *et al.*, 1996). More is known about how electrical activity regulates neuronal morphology. Spiking has been shown to control neurite extension, outgrowth, axonal elongation and guidance in both vertebrates and invertebrates. Excitability stimulates neurite initiation, enhances outgrowth, and controls the number of primary neurites and secondary branching in cultured neurons from the cockroach brain (Benquet *et al.*, 2001). In the pond snail

Helisoma trivolvis, excitability can either enhance or inhibit neurite elongation in the CNS (Cohan & Kater, 1986; Mattson & Kater, 1987). The behaviour of growth cones in this system appears to depend on the size of transient Ca^{2+} signals elicited by activity where low levels of intracellular Ca^{2+} induce outgrowth, and periods of high activity leading to high levels of intracellular Ca^{2+} can inhibit neurite extension (Cohan *et al.*, 1987; Mattson & Kater, 1987). A similar effect is seen in neurons from *Xenopus*. In this system, there are also two responses to excitability; slow waves in spinal motor neurons lasting up to 45 min can inhibit neurite extension *in vitro* (Gu & Spitzer, 1995; Gomez *et al.* 2001) and *in vivo* (Gomez & Spitzer, 1999); whereas hyperexcitability in retinal ganglion cells promotes outgrowth and target finding (McFarlane & Pollock, 2000). The precise pattern of electrical activity seems to be the deciding factor in determining the response of a growth cone (Petersen & Cancela, 1999; 2000; Ming *et al.*, 2001).

Neurotransmitter phenotype is also affected by spontaneous activity in differentiating neurons. In the grasshopper, the dorsal unpaired median neurons of the embryonic CNS become responsive to, and begin producing, neurotransmitters during a similar time course as the appearance of action potentials (Goodman & Spitzer, 1979; Goodman *et al.*, 1979; 1981b). In *Xenopus*, the frequency of Ca^{2+} based spikes is critical in controlling the acquisition of neurotransmitter phenotype. Most spinal neurons produce GABA but blocking electrical activity can inhibit or delay its expression (Gu & Spitzer, 1995; Watt *et al.*, 2000). Recently Borodinsky *et al.* (2004) were able to demonstrate that transmitter phenotype is not exclusively regulated by intrinsic factors as previously thought (reviewed by Goridis & Rohrer, 2002), but also depends upon electrical activity. They were able to alter patterns of Ca^{2+} spiking by inducing hyperexcitability or by reducing activity by overexpressing Na^+ or K^+ channels respectively. Normal activity or enhanced activity led to an increase in GABAergic neurons, whereas decreasing activity resulted in neurons switching to a glutamatergic or cholinergic fate (Borodinsky *et al.*, 2004).

Electrical activity appears to have an autoregulatory function in controlling the suite of ion channels developing excitable cells express. This is true in ascidian muscle cells

where activity during a critical period early during differentiation is required for subsequent expression of an $I_{K(Ca)}$ (Dallman *et al.*, 1998). Not all Vg channels are regulated by activity; a slow non-inactivating K^+ current, and inward rectifier, and an inward Ca^{2+} current are expressed during this period and are unaffected by spontaneous activity. In this example, electrical activity leads to a negative feedback loop to reduce and alter patterns of activity since the Ca^{2+} spikes are shortened in duration by the rapidly activating $K_{(Ca)}$ channels (Dallman *et al.*, 1998). Vg- K^+ channels are also regulated by excitability in the vertebrates. Activity in *Xenopus* spinal neurons causes an enhancement of an I_{Kv} and induces Kv channels to acquire faster activation kinetics (Gu & Spitzer, 1995). In the developing CNS of the mouse, altering activity by overexpressing a Shaker-type K^+ channel causes mis-expression of several other classes of Kv channels (Sutherland *et al.*, 1999).

Embryonic and larval behaviours are also determined and regulated by changes in excitability properties. Sun & Dale (1998) showed that as embryonic amphibians develop into larvae, changes in K^+ channel expression result in changes in the swimming motor pattern. Embryonic spinal motor neurons possess only K_{DR} and $K_{(Ca)}$ channels, and produce bursts of spontaneous activity. As larvae emerge, there is no change in the overall size of K^+ currents, but the I_{DR} decreases along with an increase in the $I_{K(Ca)}$ that results in termination of swimming bursts.

Virtually all developing excitable cells, independent of their mature excitability phenotype or origin must undergo the changes described above during differentiation. Thus, it would seem very likely that patterns in the sequence of events occurring would also result in a very specific mode of Vg-ion channel expression.

2.3 Patterns in the sequence of Vg-ion channel expression – From worms to mice

When comparing the sequence of Vg-ion channel expression in developing excitable cells among different cell lineages and across divergent animal phyla one common feature emerges. This is that most developmental events are regulated by activity induced increases in intracellular Ca^{2+} levels. The source of Ca^{2+} varies, as some developing excitable cells first express Ca^{2+} based APs while others have only Na^+ based spikes, and some rely on a combination of both ions. In several systems a developmental switch occurs where the initial ionic species contributing to APs changes. These patterns will be reviewed in the subsequent section with an emphasis on the phylogenetic relationships between the species studied. This review will focus on several features of Vg-ion channel acquisition including: the specific sequence of Vg-channels expressed, the first Vg-channel to appear (Vg- K^+ vs. Na^+ or Ca^{2+} channels), whether Vg- K^+ channels appear before action potentials, the main ionic species underlying action potentials, whether Vg-currents are present prior to morphological differentiation, and whether there are changes in expression levels and kinetics of specific Vg-channels.

2.4 Excitability of Invertebrate Cells and Sequence of Channel Acquisition

The most basal organism where developmental changes in Vg-channel expression has been studied is the nematode *Caenorhabditis elegans*. Both oocytes and embryonic neuroblasts possess Vg- Cl^- channels that function in activation of meiosis and in processes that alter cell shape, including passage from the ovaries into the spermatheca during fertilization (Rutledge *et al.*, 2001; Christensen & Strange, 2001). These channels disappear in mature muscles and neurons, however the role they play during differentiation remains unknown. To date, no Vg- K^+ channels have been recorded from neuroblasts (Strange, 2002; Francis *et al.*, 2003), but it has been shown that developing embryonic muscles express *Shaker* and *Shal*-type channels, along with an ATP-

dependent Ca^{2+} channel, and a Ca^{2+} -dependent K^+ channel (Santi *et al.*, 2003; Salkoff, pers. comm.). These channels are also found in mature pharyngeal muscle (Franks *et al.*, 2002) however, the time course of changes in expression of these channels or the developmental roles they play are not known. The *C. elegans* genome contains genes for many Vg ion channels, but there appear to be no genes for Vg- Na^+ channels (Bargmann, 1998). It seems unlikely that even this relatively derived species has lost the otherwise ubiquitous TTX-sensitive Na^+ channel. Since only a few electrophysiological studies have been undertaken (reviewed by Francis *et al.*, 2003), it may be discovered that one of the divergent Ca^{2+} sequences actually encodes a Vg-channel that has significant Na^+ permeability (Bargmann, 1998). There is indirect evidence for the existence of Vg- Na^+ channels in pharyngeal muscle as Ca^{2+} -dependent APs are abolished in the absence of extracellular Na^+ (Franks *et al.*, 2002). Whether developing neurons first express a Ca^{2+} - or Na^+ -dependent AP remains unknown.

Studies of the annelid *Hirudo medicinalis* have examined the temporal sequence of the appearance of Vg-channels (Schirmacher & Deitmer, 1991; Meis & Deitmer, 1997). Developing neurons cultured from the embryonic segmental ganglia express four types of K^+ currents, two delayed rectifiers, an A-type current, and a Ca^{2+} dependent current. All cells in the ganglion appear to express a delayed rectifier current, and there are no changes in activation kinetics or current density during maturation. Sixty seven percent of these cells also express a Ca^{2+} -dependent K^+ current that also does not undergo changes in either kinetics or expression levels. In contrast, the prevalence of ganglion cells with A-type channels does change, with nearly a four-fold (from 16% to 70%) increase over 6 days in the proportion of cells expressing A currents. Potassium channels are always present before the appearance of inward currents (Schirmacher & Deitmer, 1991). The appearance of both Na^+ and Ca^{2+} currents occurs in parallel, with the increase in outward currents, but the appearance of Na^+ currents precedes Ca^{2+} currents by one day of embryonic development (Schirmacher & Deitmer, 1991). The cation(s) responsible for the upstroke of action potentials appears to depend on the identity of the cell, some cells have Na^+ -based APs alone, and some have APs dependent upon both Na^+ and Ca^{2+}

(Schirrmacher & Deitmer, 1989). There is no apparent switch in the main cation driving APs (Schirrmacher & Deitmer, 1991; Meis & Deitmer, 1997).

The sequence of Vg-ion channel expression in *Drosophila* depends on the cell lineage and mature phenotype of the excitable cell, with differences occurring between neurons and muscle. In the mesodermally derived developing flight muscle of pupae, cells first begin to develop more polarized resting potentials, presumably by incorporation of potassium channels with leak currents (Salkoff & Wyman, 1981). Subsequently, an A-type channel is the first Vg-channel to appear, followed by a delayed rectifier 24 h later, and a Ca^{2+} channel 24 h after that (Salkoff & Wyman, 1981; 1983; Salkoff, 1985). This pattern is similar to developing muscle from embryonic myoblasts with two slight differences. The Ca^{2+} channels appear first in embryonic muscle, which would seem like a significant difference. However, both the delayed rectifier and A-type currents then appear within several minutes. One major difference is the appearance of a Ca^{2+} -dependent K^+ channel during maturation (Broadie & Bate, 1993b). These sequences are much different in developing neurons where K_{DR} channels are always expressed first. These patterns are in stark contrast with the developing embryonic CNS, where a delayed rectifier is the first channel to appear at 14 h after egg laying, followed by a calcium current with two components 2 h later, a Na^+ current at 16 h, and an A-type K^+ current at 17 h (Baines & Bate, 1998). The appearance of Vg- K^+ channels before inward currents is also observed in the developing photoreceptors in *Drosophila* (Hardie, 1991).

There have been many studies of developing tunicates that take advantage of known cell lineages. Prior to invagination of the blastopore, muscle precursors only express an inwardly rectifying K^+ channel (Block & Moody, 1987). Developing muscles experience an increase in resting V_m during gastrulation (Takahashi *et al.*, 1971) and display regenerative action potentials that have both a Ca^{2+} and Na^+ component, whereas mature muscles display only Ca^{2+} spikes (Miyazaki *et al.*, 1972). Immature muscle cells in ascidian larvae develop both a transient Ca^{2+} channel, and a delayed rectifier K^+ channel at similar times, with both contributing to the establishment of spontaneous activity

during development (Davis *et al.*, 1995; Dallman *et al.*, 1998; Moody, 1998; Dallman *et al.*, 2000). As muscles mature, they lose the inward rectifier K^+ channels temporarily while retaining and increasing expression of the Ca^{2+} and outward K^+ channels. Mature muscle cells also express a second high-voltage activated (HVA) Ca^{2+} channel and two rapidly inactivating K^+ channels along with a Ca^{2+} activated K^+ channel (Davis *et al.*, 1995). This change in the population of expressed Vg-channels is associated with a change in excitability phenotype from spontaneous, slow Ca^{2+} spikes to fast spikes in mature muscle. This change in properties is autoregulated by expression of the Ca^{2+} -activated K^+ channel, which functions to reduce and limit spontaneous firing (Dallman, 1998). Early and sustained Ca^{2+} influx is thought to regulate Ca^{2+} -dependent developmental programs, whereas fast Ca^{2+} spikes that appear later control larval swimming (Dallman *et al.*, 2000). These patterns may be unique to muscle lineages since in cleavage-arrested embryos, cells previously fated to develop into muscles but induced by cell contact to develop into neurons expressed Na^+ -dependent APs (Takahashi & Tanaka-Kunishima, 1998). In developing neuronal blastomeres, Vg- Na^+ , Ca^{2+} , and delayed rectifier K^+ channel are observed. Although it has been shown that there is a coordinated expression of both Na^+ and K^+ currents (Ono *et al.*, 1999), the role of Ca^{2+} channels during maturation remains unclear (Nakajo & Okamura, 2004).

2.5 Excitability of Vertebrate Cells and Sequence of Channel Acquisition

Possibly the most-studied species for examining the development of excitability properties and channel incorporation is the amphibian *Xenopus laevis*. Studies have focussed primarily on neurons from the embryonic spinal cord and developing myoblasts from the surrounding myotomes (reviewed by Spitzer *et al.*, 2000). In this organism, the pattern of Vg-channel acquisition is predominantly influenced by cell lineage, with different sequences observed in neurons and muscle (reviewed by Ribera & Spitzer, 1990b; Spitzer *et al.*, 2000; see below). Spinal neurons in this region represent a heterogeneous population including sensory, motor, and interneurons (Bixby & Spitzer, 1984; Spitzer & Ribera, 1998). Ion channels appear in a characteristic pattern, with

delayed rectifier K^+ channels appearing within minutes of both Ca^{2+} and Na^+ channels (O'Dowd *et al.*, 1988; Ribera & Spitzer, 1990a; Olsen, 1996). During development, there is a progression from Ca^{2+} -dependent APs to spikes carried by both Ca^{2+} and Na^+ , and finally APs that are only Na^+ -dependent (Spitzer & Lamborghini, 1976). This transition is reflected in the changes observed in whole-cell currents during the first few days after neurons begin to sprout neurites. Approximately 6 h after developing neurons begin migratory movements, I_{KDR} , I_{Na} , and I_{Ca} appear at roughly the same time, and continue to increase in density until neurite initiation begins (Olsen, 1996). During neurite elongation, Ca^{2+} currents are presumably mature, since there are no changes in their density, voltage-dependence, or activation rate (O'Dowd *et al.*, 1988). During the same period, there is a 2-fold increase in Na^+ current density, a 3-fold increase in I_{KDR} and the activation time constant of the K_{DR} channels is halved. Soon after, a Ca^{2+} -dependent K^+ channel is expressed, followed by an A-type K^+ current (O'Dowd *et al.*, 1988; Ribera & Spitzer, 1990). Upregulation of the delayed rectifier current shortens the AP and changes its ionic dependence (Lockery & Spitzer, 1992; Vincent *et al.*, 2000), whereas expression of the A-type K^+ channel functions to prevent repetitive firing (Ribera & Spitzer, 1991). In contrast to the pattern of channel expression observed in neurons, developing myocytes display a different sequence of Vg-ion channel expression. APs in developing muscle are always Na^+ dependent, thus there is no developmental switch in ionic dependence (Ribera & Spitzer, 1991). Also, there are always well defined K^+ currents prior to development of action potentials (Ribera & Spitzer, 1991). The first Vg channels to appear are inward rectifiers, followed by delayed rectifier K^+ channels, Na^+ channels, and lastly Ca^{2+} channels (Ribera & Spitzer, 1991; Spruce & Moody, 1992). A second significant difference between the development of neurons and myocytes is the presence of Vg-channels in neurons prior to morphological differentiation as opposed to myocytes, where no channels are present when cells develop their morphological phenotype (Ribera & Spitzer, 1991). Ca^{2+} signals are also important in developing muscle and are believed to induce upregulation of both Na^+ and K_{DR} currents (Linsdell & Moody, 1995).

A conserved characteristic of neuronal differentiation in vertebrates is that APs initially express a plateau, but APs later shorten due to an increase in expression of K^+ channels (Spitzer *et al.*, 2000). In chick ganglionic and limb motoneurons, $V_g K^+$ channels always appear first, and there is no shift in the ionic dependence of APs (they are always Na^+ -based), while AP shortening depends on expression of a Ca^{2+} -dependent K^+ channel (Bader *et al.*, 1983; Bader *et al.*, 1985; Gottmann *et al.*, 1988; McCobb *et al.*, 1990). A similar pattern is found in rat motoneurons, where initially, K_{DR} and K_A currents are well established and regulate perinatal repetitive firing (Martin-Caraballo & Greer, 2000). After birth, there is an increase in membrane excitability and in the repetitive firing rate that is important for synaptogenesis, and increase in synaptic transmission, and complex motor behaviour that occurs due to an increase in the expression levels of K_{DR} , K_A , and Ca^{2+} -dependent K^+ channels (Ziskind-Conhaim, 1988; Gao & Ziskind-Conhaim, 1998; Martin-Caraballo & Greer, 2000). Developmental shortening of the AP is also observed in retinal ganglion cells from fish (Olson *et al.*, 2000), neurons of the cerebral cortex of mouse (Bahrey & Moody, 2003), and moto- and sensory neurons in the cat (Cameron *et al.*, 1990).

Since so many aspects of neuronal differentiation are regulated by electrical activity and there is often a distinct temporal pattern in these developmental events, it seems reasonable that there are also patterns in the development of excitability properties. A summary of the changes occurring in developing neurons is found in **Table 1** with an emphasis on the phylogenetic position of the organism and on the cell lineage from which the excitable cells are derived. To address the questions presented above, it was important to find an organism that would provide contrast to the systems and organisms previously studied.

3. Flatworms as a model system: evolutionary considerations in the development of excitability properties

Members of the phylum *Platyhelminthes* provide an excellent opportunity to address many of the questions presented above. Most studies have focussed on the chordates (see above) and since flatworms are quite distantly related, selective forces have acted independently on these two taxa over a long evolutionary period. First, flatworms occupy a unique phylogenetic position, retaining many features reminiscent of the ancestral bilaterian (Smith & Tyler, 1985; Zrzavy *et al.*, 1998; Giribet *et al.*, 2000). The pattern of electrical changes during neurogenesis in flatworms may also reflect a primitive mode of generating neuronal phenotypes. The second rationale for selecting flatworms as a study species are the paucity of Vg-K⁺ channel subtypes found in the flatworms and the limited number of excitability phenotypes observed (Buckingham and Spencer, 2000). This suggests that there are few permutations of excitability states, which in turn might limit the sequence of ion channel acquisition during neuronal differentiation. Another motivation for selecting the flatworms as a study organism to examine the pattern of ion channel insertion into differentiating excitable cells is because neurons in flatworms are derived from a different cell lineage than neurons in the chordates (reviewed below). This may have resulted in differences in the developmental programs regulating neurogenesis, and hence result in a difference in the sequence of electrophysiological changes. Taken together, these arguments suggest that flatworms may provide a sharp contrast to the patterns of changes occurring in chordate excitable tissues and provide useful information regarding the evolution of neuronal development. Each of these points will be expanded further in the subsequent sections.

3.1 Flatworms are basal bilaterians

Although the *Platyhelminthes* share some features with the vertebrates including; a triploblastic arrangement, bilateral symmetry, and anterior-posterior and dorsal-ventral

body-plan organization; they are among the simplest metazoans (Hyman, 1951; Brusca & Brusca, 1990; Giribet *et al.*, 2000). This led previous investigators to propose several hypotheses suggesting that extant flatworms closely resembled the ancestral organism bridging the gap between the Radiata and the Bilateria (Ehlers, 1995; Giribet *et al.*, 2000; Rieger & Ladurner, 2000). One theory that continues to gain acceptance among students of the Turbellaria is the planuloid-acoeloid theory first proposed by Libbie Hyman (Hyman, 1951). This view placed flatworms as the most primitive extant relatives to the ancestral primitive bilaterian (Hyman, 1951; Ax, 1987; Brusca & Brusca, 1990; Willmer, 1990). This classification has been called into question by recent DNA sequence analyses that place flatworms within a new taxonomic group known as the Lophotrochozoa (Adoutte *et al.*, 1999; Knoll & Carroll, 1999; Valentine *et al.*, 1999; Adoutte *et al.*, 2000). This rearrangement has largely been based on sequence data available for the small subunit ribosomal RNA molecule and comprises a monophyletic group of organisms with either a lophophore (tentacles around the mouth used for feeding), or a trochophore larvae. A group of flatworms, the polyclads do undergo spiral cleavage to develop a trochophore larva (Boyer *et al.*, 1998; Henry *et al.*, 2000) but most other flatworms possess neither of the characteristic traits (Baguna & Boyer, 1990). One interesting result of this regrouping is the question of whether the ancestral lophotrochozoan had an acoelomate or coelomate design.

There remains much controversy surrounding the placement of the *Platyhelminthes* as a derived clade among the Bilateria. Much of this controversy arises from the problematic Acoela. On the basis of 18s rRNA data, this group has been placed as emerging at the base of the Bilateria (Carranza *et al.*, 1997; Littlewood *et al.*, 1999; Ruiz-Trillo *et al.*, 1999) unrelated to other flatworms. This placement is also supported by their unique diel cleavage pattern (Boyer *et al.*, 1996; Henry *et al.*, 2000). Combined, this data would separate acoels from all other flatworms, however, acoels do share many morphological synapomorphies and developmental patterns similar to the Nemertodermatida (Karling, 1974; Tyler & Rieger, 1977; Smith & Tyler, 1985; Ehlers, 1985, 1986), including the absence of protonephridia, and morphological similarities in the shaft region and rootlets

of epidermal cilia (Tyler & Hooge, 2004). Recent molecular data suggests that the Nemertodermatida themselves belong with all other Platyhelminthes (Carranza *et al.*, 1997; Zrzavy *et al.*, 1998; Littlewood *et al.*, 1999), thus placing the flatworms near the base of the Bilateria. Also, phylogenetic trees based on 18s rRNA sequences most likely suffer from long-branch attraction, as it has been reported that the rates of nucleotide substitution in Platyhelminthes is three to five times the rate in other taxa (Ruiz-Trillo *et al.*, 1999; Tyler *et al.*, 1999)

Long-branch attraction would affect the base of the bilaterian lineage because typical outgroups used for these analyses (including the Radiata) have diverged from the triploblasts for so long that they may have accumulated so many changes as to saturate the resolving power of 18s rDNA sequence data (Giribet & Wheeler, 1999). Only recently have systematists begun comprehensive analyses including both morphological and molecular characters on all metazoan phyla to produce total evidence trees (Zrzavy *et al.*, 1998; Giribet *et al.*, 2000). These results place the modern flatworms as the closest relatives to the last common bilaterian ancestor (LCBA). More recently the validity of hypotheses that remove the flatworms as intermediate and basal taxa have been called into question by renewed support for the clade Coelomata (Wolf *et al.*, 2004). Phylogenetic analyses of over 500 sets of orthologous proteins among *C. elegans*, *D. melanogaster*, and *H. sapiens* suggest that the arthropods and chordates group more closely together, and that non-coelomate organisms may have diverged from a basal bilaterian lineage prior to the separation with coelomates (Wolf *et al.*, 2004). Taken together, this supports the view that the Platyhelminthes are basal members of the Bilateria.

Whether modern flatworms represent a primitive bilaterian closely resembling the LCBA or if they are a derived clade that has lost many of the features retained in other lophotrochozoans remains unresolved. Despite this controversy, the flatworms do represent a taxon that can provide phylogenetic clues concerning the ancestral pattern of

electrophysiological changes occurring in differentiating neurons due to their distant relationship with all other taxa studied to date.

3.2 Flatworms have limited Vg-channels subtypes and excitability phenotypes

There appears to be a limited diversity of excitability phenotypes in adult flatworm neurons conferred by a limited number of Vg-gated ion channels. Action potentials have only been recorded from the marine polyclad *Notoplana*. Use of both extracellular and intracellular recording techniques has revealed only a limited number of firing patterns. Studies involving *Notoplana acticola* brain cells have demonstrated silent cells, neurons using graded potentials, and cells with firing rates between 3 to 100 Hz (Keenan & Koopowitz, 1981; Keenan & Koopowitz, 1984b; Koopowitz, 1989). These action potentials are mediated by at least five types of Vg-ion channels. There appear to be at least two types of Vg-Na⁺ channels, a TTX-sensitive Na⁺ channel that is responsible for the rising phase of the action potential and a TTX-insensitive channel. There is a Ca²⁺ current that may play a role in synaptic potentials, and two types of Vg-K⁺ channels. One K⁺ channel has fast activation kinetics and is blocked by TEA⁺, and the other is a Ca²⁺-activated K⁺ channel (Keenan & Koopowitz, 1984). In a closely related polyclad, *Notoplana atomata*, Buckingham and Spencer (2000; 2002) have recorded both silent cells and neurons that display extremely high frequency firing with rates above 75 Hz in the brain of *Notoplana atomata*. There appear to be only three types of Vg-channels responsible for this pattern. A rapidly activating and inactivating inward current, presumed to be Na⁺ based, and two types of Vg-K⁺ currents. Both potassium channels have relatively positive activation thresholds and extremely fast activation kinetics. One is a high voltage activated non-inactivating delayed rectifier type channel, and the other is a rapidly inactivating A-type K⁺ channel (Buckingham & Spencer, 2000; Buckingham & Spencer, 2002). Two types of Ca²⁺ currents have also been observed in cultured brain neurons and are correlated with the growth of neurites in culture (**Appendix 1**).

Other published accounts of electrophysiological studies of flatworms have used the endoparasitic trematodes, and the triclads for voltage-clamp studies of ionic currents. The first experiments were performed on cultured muscle cells from the parasitic trematode *Schistosoma mansoni*. Using single channel and whole cell recordings from cultured muscle cells, it has been shown that at least three types of Vg-K⁺ channels are present. In all muscle cells examined, a high conductance Ca²⁺-dependent K⁺ channel that is Ba⁺ sensitive but TEA⁺ insensitive is observed (Blair *et al.*, 1991). Currents through these channels are negligible in whole-cell preparations where muscle cells express large Vg-currents similar to delayed rectifiers and A-type currents (Day *et al.*, 1993). Three distinct muscle morphologies are identifiable, each with different resting membrane potentials and complements of Vg-K⁺ channels. Both the K_{DR} and K_A channels activate near -20 mV, and are insensitive to TEA⁺. The A-type like channels activate rapidly within 15 ms, and are completely inactivated after 100 ms (Day *et al.*, 1993). Through molecular cloning, a *Shaker*-related K⁺ channel has also been identified and characterized showing rapid activation and inactivation (Kim *et al.*, 1994). The cloned A-type channel activates at membrane potentials positive of -20 mV, peaks after 8 ms, is insensitive to TEA⁺, but is blocked by 4-aminopyridine (Kim *et al.*, 1994). Two types of Ca²⁺ channels have been found by indirect analyses in *Schistosoma* muscle. A dihydropyriding-sensitive Ca²⁺ channel is involved in muscle contraction (Day *et al.*, 1994), as are ryanodine-sensitive channels on the sarcoplasmic reticulum (Day *et al.*, 2000). In these preparations, neither action potentials, nor inward currents have been demonstrated directly.

Studies of cultured neurons from the marine ectoparasite, *Bdelloura candida*, have also revealed an ability to elicit high frequency action potentials. Firing rates of up to 300 Hz have been recorded from dissociated brain cells (Blair & Anderson, 1993). These properties are produced by four types of Vg-ion channels. There is a fast, rapidly inactivating TTX-sensitive Na⁺ current, a Ca²⁺ current, and two types of Vg-K⁺ currents; a rapidly inactivating 4-AP sensitive A-type current, and a sustained non-inactivating current (Blair & Anderson, 1993).

Voltage-clamp studies have also been performed on muscle cells from the triclad *Girardia tigrina* (Cobbett & Day, 2003). Action potentials could be elicited, but unlike the Na⁺ based action potentials in brain neurons, muscle cells use Ca²⁺ influx through VGCC's to generate spikes. Whole-cell patch clamp recordings on cultured muscle cells expose at least three types of Vg ionic currents. There is at least one type of Ca²⁺ channel involved in action potential formation, but the data suggest that there is both an inactivating and non-inactivating component (Cobbett & Day, 2003). There also appear to be two K⁺ currents, a transient rapidly inactivation current, and a sustained current.

Taken together, voltage-clamp experiments using flatworms have uncovered only a few types of Vg ion channels even though a wide range of distantly related taxa have been studied. This suggests that there has been evolutionary conservation in the way excitable cells in flatworms have been shaped. Consistently, in both brain neurons and muscle cells, there appear to be only a few types of Vg-K⁺ channels. All cells display a sustained, delayed rectifier-like outward current, and many cells also possess a transient A-type-like channel. The scarcity of K⁺ channels found in flatworms suggests very limited possibilities in terms of generating different excitability patterns.

The paucity of K⁺ channel subtypes determined by electrophysiological recordings has also been corroborated by attempts to sequence and clone Vg-K⁺ channels. K⁺ channel sequences have been isolated from DNA libraries constructed for *Notoplana*. These have revealed only 4 types of Vg-K⁺ channels. Two have been cloned and expressed in *Xenopus* oocytes revealing irregular properties. One channel produces a sustained delayed rectifier type current that has slower activation kinetics than K_{DR}'s described from cultured neurons, but show characteristic *Shaw* delayed rectifier properties. The second cloned channel is related by sequence to the *Shaw* subfamily of *Shaker* K⁺ channels, but unlike other channels in this class that display typical delayed rectifier activity, this channel from *Notoplana* displays inward rectifying properties similar to those observed in the K_{ir} channels (Klassen *et al.*, personal communication). Given the

limited number of Vg-K⁺ channels found in flatworms, this suggests that the developmental events and the sequence of Vg-ion channel insertion in the membrane may be limited and more accessible for comparative studies.

3.3 Flatworm neurons do not arise from ectoderm

In chordates, neural precursors develop from an infolding of the embryonic ectoderm during gastrulation. Cell type specification is regulated by interactions between neighbouring cells in the gastrula. Excitable tissues arise either directly from the neurectoderm, or through neural inductive processes where body-patterning gene products regulate cell fate (Gilbert, 1997).

In flatworms, development is mostly determinate whereby fate specification is regulated by cytological determinants passed down from previous cell divisions. This has been shown by ablating specific blastomeres in larvae (Boyer 1971; 1987; 1989; 1992), although the same author provided evidence that cell-cell interactions also played a role. The exact mode of gastrulation in flatworms depends on whether they exhibit the archoophoran or neophoran taxa (Hyman, 1951). The archoophorans are considered ancestral within the flatworms and include the acoels, polyclads and macrostomids. They produce oocytes that are yolky and typically undergo unmodified spiral determinate cleavage, occasionally with the generation of distinct germ layers (Kato, 1940). The neophorans (including triclads) contain oocytes devoid of yolk. Instead, yolk glands produce separate yolk cells that accompany eggs and are later incorporated into the developing blastula through gastrulation type events. The externalization of yolk dramatically alters the mode of early embryogenesis. Cleavage events occur irregularly and produce a solid mass of internalized cells referred to as the mesenchyme that generates primordial organs. Only after organ primordia begin to develop does an epithelium arise surrounding both the mesenchyme and the yolk cells (Baguna & Boyer, 1990; Younossi-Hartenstein *et al.*, 1999; Hartenstein & Ehlers, 2000; Younossi-Hartenstein & Hartenstein, 2000). Unlike the chordates, the neophoran nervous system

arises from a primordial mass of mesenchymal cells that later develop into the brain. Neurons form two bilaterally symmetrical hemispheres at the anterior end and an invariable pattern of pioneer neurons begin to form commissures between the two hemispheres as well as pairs of dorsal and ventral tracts that extend toward the posterior regions (Younossi-Hartenstein, 1999; Hartenstein & Ehlers, 2000). These neuroblasts continue to divide and produce the developing orthogonal pattern of the flatworm nervous system.

The differences in cell lineages that generate neurons in neophoran flatworms (internalized embryonic mesenchymal cells) as opposed to other taxa (neurectoderm) suggests that genetic mechanisms controlling embryogenesis and neurogenesis in particular might also be different or modified. Therefore the sequence and pattern of Vg-ion channel insertion into developing neurons might reflect these differences, and again provide a useful contrast to other animal groups where neurons arise from neurectoderm. One difficulty that arises when studying neurogenesis is determining a starting point to record electrophysiological changes. Soon after specification and before cells are morphologically identifiable, changes in electrical properties and Vg-channel expression levels begin to occur. Thus, it might be more useful to perform studies on cells that have not been committed to a specific fate so that the earliest developmental events can be monitored. Flatworms provide such an opportunity because they possess totipotent stem cells that can be isolated from adults. These stem cells, called neoblasts, are a group of undifferentiated mesenchymal cells (Baguna & Boyer, 1990). Thus, not only are neoblasts useful for this study because of their undifferentiated state, but also because of their mesodermal origin.

4. Neoblasts – A unique system of stem cells with neurogenic potential

The considerable regenerative abilities of flatworms have been attributed to neoblasts (Levetzow, 1939; Bronsted, 1955; Lender, 1960; Wolff, 1962; Baguna, 1998). These stem cells have specific morphological and histological features that are useful for

identification. Neoblasts tend to be small spherical cells 8-12 μm in diameter, with a large nucleus approaching 90% of the cells internal area when seen in sections (Pedersen, 1959b; Hay & Coward, 1975; Rieger *et al.*, 1999). Within the nucleus, a large nucleolus, or several smaller nucleoli are often seen using light microscopy (Pedersen, 1959b; Hay & Coward, 1975). When stained with a basophilic dye, the DNA is observed to be arranged into many distinct heterochromatin condensations (Pedersen, 1959a, Hay & Coward, 1975). The thin rim of scanty cytoplasm is basophilic, comprised mostly of RNA as determined by histological staining and can be removed by treating neoblasts with ribonucleases (Pedersen, 1959b). The cytoplasm also contains abundant free ribosomes, and is rich in chromatoid bodies that are often associated with small clusters of mitochondria; but lack both endoplasmic reticulum and a Golgi apparatus (Pedersen, 1959b; Hay & Coward, 1975). Neoblasts retain these distinctive morphological characteristics both in fixed and live tissues (Pedersen, 1959a; Pedersen, 1959b; Pedersen, 1961; Betchaku, 1973). A method to selectively stain neoblasts was developed by Pedersen (1959b), and provides a useful way to identify all neoblasts. However it does not provide help in determining whether these populations are homogenous or if multiple subtypes exist. Techniques other than light microscopy such as electron microscopy and immunohistochemistry have provided a more descriptive view of the population of neoblasts found within the flatworms.

4.1 Distribution and abundances of neoblasts

Neoblasts comprise a variable proportion of the total cells in flatworms depending on the species studied. In planarians, approximately 20-35% of all cells are neoblasts (Hay & Coward, 1975; Baguna & Romero, 1981; Baguna *et al.*, 1989, Romero & Baguna, 1991), compared with 15% in acoels (Gschwentner *et al.*, 2001). There is little pattern to the distribution of neoblasts *in vivo*. In triclad, they are usually found ventrally, in two bands extending along either side of the pharynx, but never anterior to the eyes (Pedersen, 1959b; Baguna, 1976a; Newmark & Sanchez Alvarado, 2000). The mitotic state of neoblasts has been characterized with respect to their location with up to 20% of

neoblasts immediately anterior to the pharynx actively undergoing mitosis (Baguna, 1976a). In acoels, the pattern of neoblast distribution appears almost uniform throughout the entire organism (Gschwentner *et al.*, 2001). The distribution and high abundances of neoblasts seem to suggest a generalized role in cellular replacement.

4.2 *Ultrastructural evidence for different populations of neoblasts*

Because most cells within flatworms are small (4-15 μm) and share some morphological similarities with neoblasts it can sometimes be difficult to identify them. Ultrastructural studies (Hay & Coward, 1975; Morita & Best, 1984b; Palmberg, 1990; Rieger *et al.*, 1999) have successfully identified three subtypes of neoblasts based on the complement of cytoplasmic constituents and nuclear structure. In the first two subtypes, neoblasts are characterized by a lack of cytoplasmic organelles except for ribosomes and mitochondria and are devoid of basal bodies (Palmberg, 1991; Rieger *et al.*, 1999). These stages are separable by nuclear morphology, where in the first stage heterochromatin is scattered and produces a 'checkerboard' pattern and in the second stage heterochromatin begins to form strands and clump together. The first stage presumably represents a population of mitotic stem cells, whereas in the second stage, nuclear rearrangement most likely represents a stem cell where genetic processes involved with differentiation are active. In the third stage of development, neoblasts acquire a rough endoplasmic reticulum, Golgi apparatus, and many basal bodies in one pole (Palmberg, 1991). Cells without basal bodies appear to be fully functional (mitotic and totipotent) neoblasts, whereas cells with basal bodies appear to have begun cellular differentiation. In the third stage, the heterochromatin strands become more prominent and attach to the nuclear lamina. The functional significance of the changes in nuclear structure has not yet been studied, but may well represent activation of immediate early genes involved in fate specification. When and how neoblasts become fate-specified remains unknown.

4.3 Neoblasts are responsible for cellular replacement

Neoblasts appear to exist in a state of readiness for both mitosis and activation as a first step to cellular differentiation. The morphology of neoblasts suggests that they do not perform any functional tasks, but instead are prepared to undergo massive gene activation. The heterochromatin organization of DNA suggests that gene expression in neoblasts is highly selective and can be activated rapidly (Harbers et al., 1982), and the abundance of ribosomes in the cytoplasm suggests that protein translation can also be activated rapidly. These findings along with the relatively high mitotic rates of neoblasts throughout the organism suggest that neoblasts play a significant role in normal cell turnover along the length of an animal (Baguna, 1984a). Also supportive of the role of neoblasts as replacement cells is the similarity in the mitotic index between normal and starved animals (Baguna, 1976a).

Evidence supporting neoblasts as the only cells in flatworms capable of undergoing mitosis is diverse and unambiguous. Histological evidence reveals that neoblasts are the only cells found in various mitotic states (Baguna, 1974a; Baguna, 1976a; Baguna, 1976b; Morita & Best, 1984b). Studies involving both tritiated-thymidine (H^3) (Palmberg, 1986; 1990) and more recently BrdU incorporation (Newmark & Sanchez Alvarado, 2000; Ladurner *et al.*, 2001; Gschwentner *et al.*, 2001) show quite convincingly that only neoblasts undergo DNA replication and mitosis. It has also been shown that neither epidermal nor gastrodermal cells undergo mitosis, and that the main source of cells replacing these tissues comes from neoblasts (Drobysheva, 1986; 1997; Ishii, 1995; Drobysheva & Mamkaev, 2001). The strongest data that suggests neoblasts function in normal cell turnover is the presence of cells with morphologies intermediate between undifferentiated neoblasts and differentiated states. Several intermediate cell types have been observed in both light and electron microscopic preparations; including epidermal (Skaer, 1965; Hori, 1983a), mucosal, rhabdite-forming, pigment-forming, neurosecretory cells (Lentz, 1967a; Hay & Coward, 1975), neurons, gastrodermal, flame cells (Lentz, 1967b; Palmberg, 1990), muscle (Morita & Best, 1984a), germ cells (Gremigni, 1974)

and saggitocyst-producing gland cells (Gschwentner *et al.*, 2001). Finally the totipotency of neoblasts is explicit from their vital role in regeneration as described below.

4.4 Neoblast involvement in regeneration, and factors affecting their behaviour

The extraordinary regenerative power of flatworms has long been recognised (Bronsted, 1955; Lender, 1960; Wolff, 1962; Salo & Baguna, 2002). Perhaps the most dramatic experiment was first performed by T.H. Morgan (1898) when he observed that whole organisms could be regenerated from tissues pieces a mere $1/279^{\text{th}}$ of the original animal, or only approximately 1×10^4 cells (Montgomery & Coward, 1974). Regeneration in flatworms most likely involves a mixture of events, with morphallaxis occurring early, followed by epimorphosis. Morphallactic regeneration involves the remodelling of pre-existing cells to recreate damaged parts. Evidence for this process in flatworms was provided by X-ray irradiation and grafting experiments. X-ray irradiation abolishes the regenerative abilities of flatworms by preventing neoblasts from replicating and differentiating (see ref in Bronsted, 1955; Lender, 1960). Grafting experiments show that in X-ray irradiated organisms with non-irradiated grafts, cells from the non-irradiated donors adjacent to damaged areas are integral in early regenerative events before the regenerating blastema forms (Lender, 1960). During the epimorphic phase, neoblasts migrate from proximal regions and form the regenerative blastema. The blastema that forms is a collection of old cells, and neoblasts that proliferate and differentiate to repair the damaged area (Wolff, 1962; Salo & Baguna, 1989a; Palmberg, 1991, Newmark & Sanchez Alvarado, 2000). Cells originally within the blastema do not divide (Morita & Best, 1984b; Salo and Baguna, 1984), thus it seems that there is a continuous migration and proliferation of neoblasts during regeneration (for recent reviews see; Baguna *et al.*, 1994; Baguna *et al.*, 1998; Salo & Baguna, 2002). There is a peak in mitotic activity near the blastema between 2-5 h, followed by a second peak after 48 h. This has been interpreted to signify that neoblasts directly adjacent to the forming blastema rapidly

enter mitosis and enter the region, together with a migration of neoblasts from proximal regions followed by a second round of mitosis (Baguna 1976b).

Given the crucial role of neoblasts during regeneration, it has been suggested that neoblasts, or at least a subset are totipotent. Direct evidence to support this claim was provided by Baguna *et al.* (1989b) when they injected isolated neoblasts from non-irradiated hosts into irradiated animals. The hosts regained regular mitotic activities and were capable of regenerating all types of tissue. Although these experiments do not definitively prove that neoblasts are totipotent since specific progenitors may exist for every cell type damaged, they do suggest that neoblasts are at least pluripotent stem cells capable of acquiring a neuronal phenotype. Definitive proof that neoblasts are totipotent would require long-term labelling of a single neoblast and tracking its commitment into all cell types of the animal.

4.5. Regeneration of neural structures in flatworms

There have been fewer regeneration studies restricted to the nervous system, but studies have shown that most flatworms are capable of completely regenerating both the CNS and PNS (Hyman, 1951). One exception is the order Polycladida. These marine flatworms are capable of regenerating lost peripheral tissues including the nervous system, however, head-amputated animals are unable to restore this area (Olmsted, 1922b; Levetzow, 1939; Hyman, 1951). This contrasts with the planarians where animals are able to regenerate the brain after it is removed. The regenerative limitation in polyclads is restricted to the brain. Regions in the head other than the brain are able to regenerate, however, when the whole brain or portions of it are removed, they are not regenerated (Faisst *et al.* 1980). This may be a result of the thick sheath surrounding the brain that could possibly restrict migration of neoblasts into this region. This seems probable since polyclads are the only flatworms with thick sheaths surrounding the brain, and are also the only members of the flatworms that have been found to be incapable of regenerating the brain. Also, animals with brains removed and receiving transplanted brains will make

connections between the donor brain and the hosts severed cerebral nerves and the paired ventral nerve cords (Davies *et al.* 1985). Hence it appears that only cells within the sheath are unable to be replaced. The second possible cause for this inability to regenerate the lost brain is the role that the nervous system and particularly the factors it produces plays during flatworm regeneration.

4.6 Potential neurogenic agents in flatworms

The nervous system may produce neurogenic agents that induce regeneration in flatworms. As early as 1922 Olmsted showed that the polyclad brain was incapable of regeneration, however, all the tissue surrounding the brain could regenerate. Even in flatworms that are capable of regenerating the entire nervous system, amputation experiments removing varying masses of nervous tissues results in changes in the rate and schedule of regeneration (Palmberg, 1990). This has led to the suggestion that the brain plays a significant role in controlling regeneration. Further evidence for the role of the nervous system in regeneration comes from two separate methods. One approach has focussed on identifying substances produced by the nervous system during regeneration using both immunocytochemical and transplantation techniques. The second approach involves isolating regenerative substances using biochemical techniques and then exposing regenerating fragments to these substances.

Experiments that evaluate the rates of regeneration during asexual reproduction and grafting have implicated a number of neuronal factors. Biogenic amines, neuropeptides and growth factors seem to play the most important roles in activating neoblasts and stimulating differentiation. Neurons near the regenerating blastema show immunoreactivity against serotonin (5-HT), FMRFamide and RF-amide peptides, small cardioactive peptide, neuropeptide F, and EGF (Reuter *et al.*, 1986; Reuter & Palmberg, 1990; Reuter & Gustaffson, 1996; Kreshchenko *et al.*, 1999). During asexual reproduction, immunoreactivities appear in a specific order depending upon the region undergoing regeneration. When the ventral nerve cords begin to regenerate, 5-HT-like

immunoreactive neurons are the first to appear, followed by RF-amide and neuropeptide F, and finally EGF-positive cells (Reuter *et al.*, 1986; Reuter & Palmberg, 1990; Reuter & Gustaffson, 1996). This order is different when the stomatogastric nervous system regenerates, in this case peptidergic neurons appear first followed by serotonergic neurons.

By applying factors exogenously, it has been shown that many products of the nervous system greatly enhance regeneration rates, and directly influence neoblasts. These have included: neurosecretory factors (Friedel & Webb, 1979); the intracellular signalling molecules cGMP and cAMP (Lenicque, 1976; Weinstein & Gavurin, 1977); polyamines (Forbes *et al.*, 1979; Collet & Salo, 1983); several neuropeptides including substance P (Salo & Baguna, 1986), *Hydra* head-activator and substance K (Baguna *et al.*, 1988); and the growth factors, EGF and FGF (Baguna *et al.*, 1988). Antagonists to neurotransmitters (3-HT, 5-HT, norepinephrine, ACh) and cAMP have also been applied and shown to inhibit regeneration (Lenicque, 1976; Franquinet, 1979; 1981). Using biochemical methods, the concentrations of several biogenic amines have been shown to increase during regeneration, including 3-HT, 5-HT, and norepinephrine (Franquinet, 1979; 1981; Martelly & Franquinet, 1984). The involvement of 5-HT seems likely since 5-HT immunoreactive neurons are seen to extend into the blastema very early during regeneration (Reuter & Gustaffson, 1996). Other factors including external Ca^{2+} concentrations also influence regeneration, with elevated levels appearing to enhance the rate (Martelly, 1983; 1986). Calcium ions increase cAMP production and activate DNA and RNA synthesis (Martelly, 1984b). These findings have led to the proposal that a 5-HT activated, cAMP-dependent intracellular signalling cascade is involved in regeneration. Serotonin is presumed to activate a G-protein coupled receptor that leads to a cascade that involves upregulation of cAMP levels via adenylyl cyclase activation, followed by activation of either PKA or CaM kinase (Martelly *et al.*, 1981; Moraczewski, 1981; Morawska *et al.*, 1981). These protein kinases then presumably proceed to modulate other as yet unidentified enzymes that regulate nucleic acid synthesis (Moraczewski *et al.*, 1986) and possibly regulating transcription and translation (Martelly & Franquinet, 1984).

These techniques have several limitations. It is difficult to determine precisely what molecules are involved by using transplantation experiments because immunocytochemical evidence does not preclude a non-regenerative role for the neuronal substances produced. Biochemical techniques introduce unwanted variance because it is extremely difficult to isolate specific tissues from an acoelomate, thus the tissue producing each factor is not properly identified. The most direct way to show a physiological role for such factors in regeneration would be to expose cultured neoblasts to substances produced by the nervous system, then monitor differentiation events.

4.7 Cell culture of neoblasts

Many previous attempts to maintain neoblasts in culture have met variable results. Until recently, few if any of the methods have been reproduced, and there has been little effort to implement a standard technique for isolation and culturing neoblasts. This may be in large part due to the multitude of species that have been used in such studies and the difficulties in devising cell culture media. A recent review of previous efforts to culture neoblasts has highlighted the importance of several factors in designing culture media as well as the isolation methods to obtain the highest yield of viable cells (Schurmann & Peter, 2001). Early attempts suffered from inconsistencies in the nutrients and osmolalities (Murray, 1927; Betchaku, 1967; Franquinet, 1973). Teshirogi & Tohya (1988) were the first group to determine the concentrations of amino acids from planarian extracts. Not until Schurmann & Peter (1993) systematically determined the osmolalities of various planarian tissues has an adequately isosmotic medium been used.

Techniques used to isolate cells have been hampered by the random distribution of neoblasts, and by the acoelomate condition. It is not practical to isolate tissues and body regions to produce sufficiently high concentrations of neoblasts. The earliest efforts involved cutting animals into small fragments, and then gently shaking or squishing preparations to release neoblasts (Betchaku, 1967; Franquinet, 1973). These methods

were useful for obtaining neoblasts, but could not produce enough cells for cultures to remain healthy, or for use in biochemical experiments. Franquinet (1981) first obtained neoblasts from whole worms by dissociating animals using a Dounce tissue grinder. This technique produced cell suspensions from whole worms but no efforts were made to specifically purify neoblasts. Purification of neoblasts was first performed by culturing cells on glass as neoblasts preferential adhered over other cells (Schurmann & Peter, 1988). Later, density-dependent separation of neoblasts was introduced. Baguna *et al.* (1989a) obtained enriched cultures first by passing neoblasts through a series of progressively smaller nylon meshes, then further purifying cells by using discontinuous Ficoll gradients. This procedure yielded neoblast cultures up to 85% pure with viabilities higher than 90% immediately following dissociation, but reduced to 60-70% after two days and up to twenty days (Baguna *et al.*, 1989a). A similar method was also used for several other species, but with the introduction of enzymatic methods to prevent cells aggregating during serial filtrations and Percoll separations (Schurmann *et al.*, 1998). Most recently, a review of previous cell culture methods was conducted and the most useful techniques were combined (Schurmann & Peter, 2001). This has resulted in the development of isolation procedures and culture media that allow 57% of neoblasts to survive for 31 days. These procedures have provided an excellent framework for isolating neoblasts in order to test the effects of various factors promoting neuronal differentiation. They also provide a useful system to perform the first electrophysiological experiments on neoblasts.

5. Objectives

Ideally, this study would have been performed on a basal member of the Platyhelminthes. The marine polyclad *Notoplana* was initially selected for this study since there was already data describing Vg-channels in this genus and a culture system for neurons had been established (Buckingham & Spencer, 2000). It was possible to isolate stem cells from *Notoplana*, but experiments using *Girardia* showed that this animal would be a

better candidate due to technical considerations. Experiments performed on *Notoplana atomata* are described in **Appendix 1**.

*5.1 Establish a method for isolating stem cell cultures in *Girardia tigrina**

Stem cells in adult flatworms are generally dispersed evenly throughout the organism. Because flatworms lack a true coelom, it is difficult to target specific tissues and cell types for cell culture. Previous attempts to develop a cell line from flatworms have been unsuccessful; however, there have been recent advances in generating primary cultures of stem cells. Because there is no particular model species representative of the flatworms, and most studies have used a variety of species, genera, and orders, methods developed in other flatworm groups needed to be tested to determine specific methodologies that can be adopted and applied with *Girardia tigrina*. The first objective of this study was to establish a technique for isolating relatively pure populations of stem cells that could be maintained long enough to induce those cells to develop into neurons and to measure electrophysiological changes.

5.2 Induce cultured stem cells to initiate neuronal differentiation

Despite the wealth of knowledge concerning neoblasts and their role in cell renewal and in regeneration, there have been no published accounts of neoblasts induced to differentiate in culture. The second objective of this study was to provide direct evidence that neoblasts could differentiate into neurons *in vitro*. Previous experiments have suggested that flatworm neoblasts have neurogenic potential (Morgan, 1898, Palmberg, 1990). Both immunocytochemical and biochemical experiments have provided a long list of chemicals presumed to be involved in activating and instructing neoblasts to migrate and begin cellular differentiation. Cultured neoblasts have not been exposed to these factors to determine their effect on differentiation. A goal of this study was to determine which factors might be involved in inducing neoblasts to develop into neurons.

Another goal was to determine whether stem cells from flatworms displayed any similarities to those from more derived taxa. More specifically, this study would determine if methods used to culture and stimulate stem cells in more derived taxa were transferable to flatworms. This might suggest that cellular mechanisms promoting neurogenesis have been conserved among evolutionary divergent organisms. This study examined the role of broad-spectrum inductive morphogens (retinoic acid), growth factors (bFGF and EGF), neurotransmitters (3-HT and 5-HT), neuropeptides (RF-amide), and agents affecting intracellular messenger systems (dibutyryl-cAMP, IBMX, and PMA) in neural fate-specification.

5.3 Examine the changes in electrophysiological properties stem cells undergo during differentiation

The main objective of this study was to develop a system where the electrical changes stem cells undergo during differentiation could be measured using the whole-cell patch clamp technique. To track the earliest changes, adult stem cells were used as opposed to neuroblasts in embryos because we assume that adult stem cells are undifferentiated electrically and exist as a single population with respect to their complement of Vg-ion channels. This also allowed us to address the question whether all neoblasts exist in a similar undifferentiated state, with unlimited differentiation potential.

First, the resting membrane properties of undifferentiated neoblasts were observed in culture over the first 24 h after plating. Also, the suite of Vg-ion channels present in these cells was examined, by characterizing the voltage dependent properties of activation. Stem cells were then exposed to factors inducing them to develop morphologically into neurons. The same electrophysiological properties were recorded from undifferentiated neoblasts, developing neurons, and adult brain neurons to compare the extent of electrical differentiation caused by treatments.

Together, these experiments will determine the extent to which mechanisms regulating neurogenesis are conserved. Specifically, this study will reveal which if any morphogenic agents are capable of inducing stem cells to develop into neurons and uncover the early electrical changes differentiating cells undergo. This study will also reveal insights upon the neurophysiology of flatworms by providing a descriptive profile of the resting membrane properties of neurons, and of the kinetic properties of the suite of Vg-ion channels found in flatworms.

Materials and Methods

1. Collection and maintenance of animals

Girardia tigrina (0.2-2.5 cm) (**Fig. 1**) from an established laboratory strain were kept in glass aquaria with continuously flowing water (18-22°C) from the freshwater system at the University of Alberta Aquatics Facility. Animals had continual access to embryos from *Helisoma trivolvis* but were starved for 3 days before use in experiments. Worms were transferred into an artificial rinsing solution containing 0.01% (w/v) gentamycin sulphate in artificial pond water (APW) (0.265% w/v Instant Ocean, Aquarium Systems) for 24 h to reduce the bacterial load in the surface mucosal layer prior to cell culture experiments.

2. Cell dissociation and concentration of neoblasts

Planarians were rinsed in 0.1% (w/v) gentamycin sulphate in saline (in mM: 51.3 NaCl, 1.7 KCl, 4.1 CaCl₂, 1.5 MgCl₂, 5.0 HEPES, pH 7.40, 160 mOsmol/L) for 1 min then transferred into a dissociation solution containing 0.05% protease (Type XIV, 5.2 units/mg from *Streptomyces*, Sigma, USA) and 0.014% dithiotheritol in modified isotonic planarian medium (IPM) developed by Schurmann & Peter (2001) but with a final osmolality of 178 mOsmol/L. Ten to twenty *Girardia* (0.5-1.5 cm) were dispersed in 10 ml of dissociation solution using a Dounce tissue grinder with a large-clearance pestle. Approximately 20 strokes were required to dissociate individuals into adequately small pieces. Tissue fragments were incubated for 10 min at 18°C on a shaker table in the dissociation solution to allow sufficient enzymatic penetration. Fragments of DNA released from cells were digested by adding 2.5 mg type I DNase (Sigma, USA) for 5 min at 37°C with gentle agitation. DNase was added to digest DNA released from damaged cells, and was necessary to prevent cells from clumping which would interfere with Percoll separation. The cell suspension was gently triturated through

syringe needles of progressively smaller bore sizes (18-G, 23-G, 27-G, and 30-G) to break up any remaining fragments. Cells were washed three times by centrifugation at 500 x g for 5 min each at 4°C. The resulting pellet was re-suspended by triuration through 18-G then 30-G syringe needles. The cell suspension was filtered through a 40 µm filter (Falcon) before layering onto a preformed Percoll gradient with four discontinuous layers (1.03 g/ml, 1.05 g/ml, 1.07 g/ml, and 1.09 g/ml). Cells were separated using an Eppendorf (Model 5810 R) centrifuge with a swinging bucket rotor at 2000 x g for 45 min at 4°C. Cells were collected by aspiration from the sharply defined boundaries between Percoll layers. The resulting cell suspensions were transferred to centrifuge tubes to wash away the Percoll. Each fraction was diluted by adding five parts IPM, centrifuged and washed three times at 500 x g for 5 min at 4°C in modified IPM. The pellets were re-suspended in IPM, counted and diluted to a final cell concentration of 1×10^5 cells/ml.

3. Identification of neoblasts in culture

For morphological identification of neoblasts, 200 µl of the cells from each fraction were plated onto clean charged glass slides (Fisher Biotech, ProbeOn Plus) and allowed 30 min to settle and attach. Cells were fixed by flooding slides with Zenker's fixative for 30 min. Cells were washed clean of fixative using 0.01 M PBS (in mM; 2.5 NaH₂PO₄•H₂O, 7.5 NaHPO₄•7H₂O, 150 NaCl). Neoblasts were stained using azure A – eosin B for 30 min (Pedersen, 1959) to accentuate nuclear structure and the extremely basophilic rim of cytoplasm. Cells were dehydrated with a quick rinse in acetone, cleared in toluene, and then mounted using a permanent mounting medium (Vector Laboratories). Slides were examined using a Leica DMR microscope. Cells were randomly distributed within the 1.5 cm area of a glass coverslip. Gridlines 1 mm apart were demarcated along the X and Y axes producing 196 sampling regions. Neoblasts were counted by randomly selecting 10 sub-samples from each slide and counting all cells within the field of view. Images were captured and digitized using a Nikon DXM 1200 CCD camera for subsequent identification of neoblasts in culture.

4. Cell culture of neoblasts, viability and proliferation

For culture, 200 μ l of neoblasts (at 1×10^5 cells/ml) were plated on 35 mm polystyrene dishes (Falcon 353001, BD Labware, USA) coated with 0.01% poly-L-lysine to promote adherence. Cells were allowed 30 min to settle, and then dishes were flooded with 1.8 ml of IPM. Dishes were kept in the dark at 18°C until required for counting. Cells were collected by re-suspension using a cell scraper (Falcon 353086, BD Labware, USA), then aspirated and counted using a haemocytometer. Cells were collected at 0 h, 6 h, 24 h, and 72 h and the total number of cells, the number of live cells and the number of dead cells was determined. The proportion of viable cells was determined by staining dead cells with Trypan Blue (Sigma, USA), then calculating the ratio of live to dead cells. For experiments requiring incubation times greater than 72 h, culture medium was exchanged every 3 days allowing cells to be kept for over 3 weeks with no signs of morphological differentiation or proliferation.

5. Assay for identification of neurons from *Girardia tigrina*

Prior to recording from neoblasts neuron specific immuno-labelling was required to determine which treatments stimulated differentiation. Two antibodies shown to label neuronal precursors and mature neurons in flatworms (Younossi-Hartenstein *et al.*, 1999; Robb & Sanchez Alvarado, 2002) were tested to determine if they would be suitable neuronal markers in *Girardia*.

Whole worms (2-5 mm in length) were killed by submersion in 2% HCl in dH₂O for 30 s. Worms were rinsed several times in 0.01 M PBS then fixed in 4% paraformaldehyde in PBS at 4°C for 2-4 h. Tissues were rinsed in three, 10 min changes of PBS on a shaker table, and then tissues were permeabilized and cleared in 6% H₂O₂ in 0.4% PBTx overnight. This bleaching of tissues removed much of the autofluorescent pigmentation found on the dorsal surface of worms. Tissues were rinsed in 0.4% PBTx then treated with blocking solution (5% normal goat serum), 3.3 mg/ml bovine serum albumen (BSA),

in 0.4% PBTx for 2-4 h at room temperature with agitation. Tubulin containing cells were labelled using either a mouse IgG monoclonal antibody against acetylated α -tubulin (Sigma) (diluted 1:2000 in blocking solution) or a polyclonal antibody against α - and β -tubulin (Tubulin Ab-4, Clones DM1A + DM1B, NeoMarkers, Fremont CA) (diluted 1:100) for 12 h at room temperature. Primary antibodies were washed away using three, 20 min changes of blocking solution. Then tissues were treated with a secondary antibody, Alexa Fluor 488 conjugated goat anti-mouse IgG (Molecular Probes) diluted 1:500 in blocking solution for 15 h at room temperature. The same secondary antibody was used to react with both primary antibodies. Secondary antibody was removed by three, 20 min rinses with 0.4% PBTx, followed by three, 20 min changes of 0.01 M PBS before mounting with 1 part 0.01 M PBS to 9 parts glycerol and viewed using a Leica TCS-SP2 multiphoton confocal laser scanning microscope (CLSM). Pre-absorption controls were performed as above except that primary antibodies were first treated with either acetylated α -tubulin, or α -tubulin for 24 h at 4°C with gentle agitation before exposing antibodies to the tissues. Negative controls were performed by omitting the primary antibody completely. Images were processed using Adobe Photoshop 7.0, where only the brightness, contrast and signal color balance were adjusted to optimize the signal to noise ratio.

Whole worms were killed by a brief immersion (30-45 s) in 2% HCl in dH₂O, and then fixed immediately in cold 4% paraformaldehyde (4°C) for 2-4 h. Tissues were rinsed several times with 0.01 M PBS, and then dehydrated through an ethanol series (30%, 50%, 70%, 90%, 95%, 100%) before clearing in 100% xylene. Tissues were transferred into hot paraffin for 2-3 h before embedding in paraffin overnight. Sagittal sections, either 8 μ m or 15 μ m thick, were cut and consecutively mounted onto charged glass slides. Samples were de-paraffinized in xylene and rehydrated through an ethanol series. Tissues were permeabilized in 0.4% PBTx and blocked with 5% NGS and 3.3 mg/ml BSA. Samples were incubated with α -tubulin antibodies (NeoMarkers) diluted 1:500 in blocking solution for at least 12 h. Tissues were washed, and a goat anti-mouse IgG conjugated with Alexa Fluor 488 (Molecular Probes) diluted 1:500 was applied for 12 h.

Tissues were washed thoroughly with 0.4% PBTx and 0.01 M PBS and mounted with glycerol prior to examination under the Leica TCS-SP2 multiphoton CLSM.

Brain neurons were processed for immunocytochemistry by dissociating the head region, anterior to the eyes into a single cell suspension by grinding tissues in a Dounce tissue grinder in proteolytic enzymes (0.05% protease), rinsing the enzyme away and plating cells onto acid washed, glass slides coated with 0.01% poly-L-lysine. Cells were allowed 30 min to settle and adhere before slides were flooded with cold 4% paraformaldehyde. Slides were then processed for tubulin staining as described above, but with shorter incubation times, 1 h in each of the 1° and 2° antibody treatments.

6. Induction of neuronal differentiation in neoblasts by treatment with putative morphogens

Neoblasts were cultured on glass slides (Lab-Tek 16 well chamber slides, Nalge Nunc Inc.) in the presence of 14 putative neurogenic inducers for 24 h, and then fixed to examine whether neoblasts had begun to express neuron-specific tubulin. A list of working concentrations and the exact composition of each treatment is listed in **Table 2**. After 24 h, cells were fixed using 4% paraformaldehyde in 0.01M PBS for 30 min. Slides were rinsed 3X using 0.01 M PBS. To prevent non-specific binding, cells were incubated in a blocking solution (5% NGS, 3.3 mg/ml BSA, in 0.1% PBTx) for 30 min at RT. Cells were exposed to the neuron-specific polyclonal mouse IgG α -Tubulin Ab-4 (NeoMarkers) diluted 1:1000 in blocking solution for 0.5-2 h, then rinsed using 3 changes of blocking solution. Alexa Fluor 488 conjugated to goat anti-mouse IgG diluted 1:1000 in blocking solution was applied for 0.5-2 h, and then rinsed using 3 changes of 0.1% PBTx. Cells were washed in 3 changes of 0.01 M PBS, and then mounted in 1 part 0.01 M PBS to 9 parts glycerol and viewed using a Leica TCS-SP2 multiphoton CLSM. The proportion of cells positively labelled against tubulin was compared among treatments using a one-way ANOVA and an *a posteriori* Tukey's multiple comparisons test to determine differences among treatments.

7. Induction of neurite-outgrowth by plating neoblasts on different substrates

Purified neoblasts were plated onto glass slides coated with different substrates in an attempt to promote neurite outgrowth and extension. Previously, it was shown that neurite outgrowth is influenced by the substrate neurons are cultured on (Asami *et al.* 2002). Neoblasts were plated on 0.01% poly-L-lysine, 0.1% poly-L-lysine, or 5 $\mu\text{g}/\text{cm}^2$ laminin. Slides were coated for 1 h with poly-L-lysine, rinsed 3 times with ddH₂O, then allowed to air dry for 1-3 h before plating cells. Laminin was applied to culture surfaces and allowed to air dry for 3 h prior to plating cells. Both the proportion of cells expressing neuronal tubulin and the proportion of cells sprouting processes were compared among treatments using a Two-way ANOVA and an *a posteriori* Tukey's multiple comparisons test.

8. Electrophysiological properties of undifferentiated neoblasts

To determine the baseline excitability characteristics of undifferentiated neoblasts, measurements of the resting membrane potential (V_m), input resistance (R_i), membrane time constant (τ), and membrane capacitance (C_m) were recorded in either the current-clamp mode using sharp electrode recordings with a Model 5A current-clamp amplifier (Getting Instruments) or the voltage-clamp mode and whole-cell patch-clamp technique (Hamill *et al.*, 1981) using an AxoPatch 200B amplifier, and digitized using pClamp 8.2 software (Axon Instruments). Membrane potentials were measured using both types of amplifiers, input resistance was measured with the current-clamp amplifier by injecting a brief 1 nA current, τ and C_m were measured using the patch-clamp amplifier using the online protocols.

Recording electrodes were pulled from thin-walled, filamented borosilicate glass using a Flaming / Brown P-97 Micropipette puller. Patch pipettes were fire-polished using a

Narashige MF-830 microforge. Sharp electrodes had tip resistances between 40 and 80 M Ω when filled with 3M KCl. Patch electrodes had resistances between 1.5 and 8 M Ω when filled with pipette solutions. Seal resistances averaged 4.02 \pm 0.76 G Ω (n=180) and the whole-cell configuration could be achieved by applying gentle suction. Data for whole-cell currents were analyzed only if the seal resistance was >500 M Ω , access resistances no greater than 10 M Ω , and holding currents no greater than 0.5 nA. Series resistance was compensated to at least 50%, resulting in a maximum voltage error of 2.5 mV. Capacitative currents were subtracted using the amplifier, and leakage currents were subtracted using the online *P/N* protocol, by applying *N* inverted copies of the voltage waveform with an amplitude of 1/*N*, prior to the experiment, then subtracting the sum of the pre-pulse currents from the main experiment. Patch clamp recordings were acquired using a sampling rate of 10 kHz. All recordings were performed at room temperature.

9. Recording solutions

Table 3 shows the compositions of the various extracellular bathing solutions and pipette solutions used for electrophysiological experiments. Neoblasts were plated on 35 mm polystyrene dishes coated with 0.01% poly-L-lysine and allowed to settle for 30 min before electrophysiological experiments were conducted. Dishes were flooded with the extracellular recording medium and rinsed several times prior to whole-cell, patch-clamp experiments. Cells were selected for recording by randomly moving the stage of an inverted Nikon Diaphot microscope with phase contrast optics, then finding the cell nearest to the centre with the distinct morphological features of cultured neoblasts, including a large nucleus and a prominent nucleolus or nucleoli.

10. Electrophysiological properties of differentiating neoblasts

Resting membrane properties (membrane potential, V_m ; input resistance, R_i , membrane time constant, τ ; membrane capacitance, C_m), the presence of V_g ion channels and their

kinetic properties were measured in cells exposed to the two treatments that were found to be most effective in stimulating neuronal differentiation. One treatment (A+G) contained dibutyryl cAMP (100 μ M), IBMX (100 μ M), PMA (100 nM), and 5-HT (150 μ M), a second treatment was *Helisoma* brain-conditioned medium (BCM). Treatments were stopped at various time intervals up to 35 h to determine and compare the electrophysiological properties of untreated, freshly dissociated neoblasts to neoblasts plated on different substrates.

11. Voltage-dependent activation properties of K^+ channels

Vg- K^+ currents recorded from undifferentiated neoblasts and developing neuroblasts were analysed by comparing current-voltage (I-V) relationships, voltage-dependency of steady-state activation, and the voltage-dependency of the time constant of activation.

Current-voltage relationships were produced by stepping the holding command potential through a series of 100 ms depolarizing pulses in 10 mV increments between -90 mV to +70 mV from a holding potential of -70 mV. Steady state currents were obtained by averaging the current measured between 50 ms and 90 ms after the beginning of the depolarizing test pulse. Mean steady-state currents were standardized to the maximum current evoked by depolarizing to +70 mV and plotted against the voltage of the test pulse.

The voltage-dependence of activation was measured by analyzing tail currents to avoid the necessity of measuring the reversal potential. Steady-state currents were evoked by stepping the holding potential from -70 mV through a series of 10 mV depolarizing steps between -90 and +70 mV for 35 ms. The holding potential was then stepped down to -100 mV to evoke instantaneous tail currents. Tail currents were fitted to a single exponential function to determine their amplitude, then standardized to the maximum current and plotted against the depolarizing test pulse. Data from individual neoblasts were fitted to a multi-stage Boltzmann function: $G_{(V)} / G_{\max} = 1 / (1 + e^{(V_{50} - V)/S})$, where

$G(V)$ is conductance, G_{\max} is the maximum conductance, V_{50} is the voltage of half-activation, V is the membrane potential, and S is the slope factor.

The voltage-dependence of the time constant of activation (τ_n) was determined by evoking currents using 10 mV voltage steps from the holding potential of -70 mV to a series of values between -90 mV to +70 mV for 250 ms. The rising phase of outward currents was fitted to the four-stage Hodgkin-Huxley model of activation with first order kinetics. Mean values for τ_n were plotted against the voltage of the test pulse to determine whether time in culture or treatment had an effect on either the rate of activation, or its voltage-dependence.

12. Data analyses and statistical methods

Data are expressed as means \pm S.E.M. unless otherwise specified. Data were analyzed using SYSTAT 9 and plotted using SigmaPlot 2001 (Version 7.0) for Windows. Individual treatment of data and the statistical tests used for analysis are described in the figure legends.

Results

1. Primary cell culture and purification of neoblasts

Primary cultures of all cell types obtained by dissociating whole worms into suspensions using enzymatic and mechanical trituration yielded consistent results with few if any cell aggregates remaining. Cellular debris could be removed by washing at least three times by centrifugation. Using preformed discontinuous Percoll gradients and isopycnic centrifugation was the simplest and most consistent way of obtaining neoblast-rich suspensions that were viable. The morphology of neoblasts was obvious in all Percoll layers, but could be quite variable, and included spindle-, pear-, or spherical cells (**Fig. 2**). Often, single or multiple nucleoli were readily observed in both stained cells (**Fig. 2a**), and in live cells using DIC microscopy (**Fig. 2b**, solid arrow). Muscle cells were the most common type of contaminating cell in neoblast cultures (**Fig. 2a and b**, dashed arrows). Staining with azure-A and eosin-B was the simplest diagnostic method for identifying neoblasts. Using these morphological and histological features that characterized neoblasts, the percentage of neoblasts isolated from each Percoll layer was determined. The total number of cells recovered from the bottom of each of the density interfaces (1.03-, 1.05-, 1.07-, 1.09 g/ml) was similar (**Fig. 3a**). Cells were aspirated from the boundary between two successive Percoll layers, thus, cells from the 1.07 g/ml category were mostly recovered from above the interface, but may have contained some cells from the top of the 1.09 g/ml layer. Neoblasts were found in all density layers, but at the greatest density in the 1.07 g/ml Percoll layer (**Fig. 3b**). The percentages of neoblasts collected compared with all cell types were $1.0 \pm 0.6\%$, $3.0 \pm 1.6\%$, $68.8 \pm 7.3\%$, and $16.5 \pm 1.7\%$ from the 1.03-, 1.05-, 1.07-, and 1.09 g/ml layers respectively (n = 5 for each layer).

1.1 Cell culture of neoblasts; viability and proliferation

Cultured neoblasts could be maintained in culture for more than 3 weeks provided the medium was changed every 3 days. It was important to establish whether, over time, cell mortality or proliferation might alter the proportion of neurons in culture. Selective mortality or proliferation of specific cell types would introduce variability in proportional measurements. Initially, 2×10^4 cells were plated and both the proportion of living cells (cells with intact membranes capable of excluding Trypan Blue) and the proportion of viable cells (proportion of living to dead cells) were monitored for 72 h. The number of living cells, of all types, in primary cultures remained high after 24 h (**Fig. 4**). After 72 h in culture, nearly half the cultured cells had died, leaving cellular debris that needed to be washed away to maintain cultures without bacterial contamination. The percentage of viable cells remained high even after 72 h ($78.8 \pm 2.2\%$, $n=5$), suggesting that the remaining living cells were relatively healthy (**Fig. 4**). There were no significant signs of mitosis or any type of cellular proliferation in cultured neoblasts over the time course followed (**Fig. 4**).

2. Assay for positive neuronal identification

A method of identifying neurons in culture was required to determine the efficacy of treatments designed to induce neoblasts to differentiate into excitable neurons. Two commercially available antibodies, previously shown to label neurons in other flatworm groups (Younossi-Hartenstein *et al.*, 1999; Robb & Sánchez Alvarado, 2002), were tested to determine whether they immunologically label only neurons in *Girardia tigrina*. Whole animals, paraffin sections and dissociated neurons in culture were screened against a monoclonal α -acetylated tubulin antibody (Sigma, USA), and a polyclonal α - β -tubulin antibody (NeoMarkers, Fremont, CA).

Whole-mounts and saggittal sections revealed that the α -acetylated tubulin antibody labelled neurons of the CNS and PNS. However, cilia were also labelled in the ventral epidermis, the gut lining, and the lining of the reproductive organs. In culture, both ciliated cells (probably epithelial cells and flame cells, not shown) and neurons were labelled by α -acetylated tubulin antibody (**Fig. 5**).

The polyclonal α -, β -tubulin antibody, which specifically labels neurons in triclads (Robb & Sanchez Alvarado, 2002), labelled most, if not all neurons, but did not cross-react with the tubulin in cilia. Confocal sections of whole-mounts reveal that both neurons of the CNS and PNS label positively against this polyclonal antibody (**Fig 6**). The brain, which is situated in the ventral region anterior and immediately posterior to the eyes, labelled intensely, as do the series of paired nerves exiting the brain which innervate the subepidermal plexus (**Fig. 6**). Sensory neurons were distinctly visible originating in the ocelli (**Fig. 7**) and the chemoreceptive auricles (**Fig. 6**). The pair of ventral nerve cords extends to the posterior margins of the animal, with nerves exiting both medially and laterally, matching the classical 'orthogonal' pattern of the nervous system in platyhelminthes. The periphery labelled strongly, with sensory-cell dendrites extending into the epidermal lamina and to the surface of the epidermis along all the lateral margins of the animal (**Fig. 8**). The body margins showed a high degree of non-specific aggregation of secondary antibody, and do not represent immunoreactivity to ciliated cells as the pattern of staining was identical in both negative and preabsorption controls. Thus, the commercially available antibody from NeoMarkers was used in differentiation experiments as a simple assay for neuronal identity in differentiating neoblasts in culture.

3. Differentiation of cultured neoblasts

Neoblasts were treated with various putative morphogens to induce neurogenesis. Agents were chosen because either they are produced during regeneration or development of flatworms, or because they are effective in inducing neurogenesis in other stem cell systems. Treatments included broad spectrum morphogens (retinoic acid), growth factors

(bFGF and EGF), neurotransmitters and neuropeptides (3-HT, 5-HT, and RF-amide), and agents (dibutyryl-cAMP, IBMX, and PMA) capable of stimulating intracellular messenger cascades. Culture medium conditioned with brains from the pond snail *Helisoma trivolvis* was also tested. The exudates from snail brains are presumed to contain various growth factors, neurotransmitters, and neuropeptides (Wong *et al.*, 1981; Wong *et al.*, 1984). Neoblasts were cultured in the presence of these diffusible factors to determine which, if any, treatments could increase the proportion of cells expressing neuronal tubulin.

All treatments were tested using a single slide with 16 individual culture wells to minimize among trial variability. The power settings for the argon laser were constant, however, gain settings were changed among trials to maximize the signal to noise ratio. This did not affect within trial comparisons because these settings were first calibrated using control treatments, and remained identical for the remaining cultures in that trial. Images were captured and digitized, then analyzed using Adobe Photoshop 7.0 to determining the proportion of tubulin-positive cells.

3.1 Neoblasts exposed to morphogenic agents express a neuron-specific tubulin

Neoblast cultures isolated and fixed immediately after plating had a small percentage of contaminating mature adult neurons indicated by neuronal tubulin cross-reactivity ($5.7 \pm 2.3\%$, $n = 5$, see **Fig. 9a**). The percentage of immuno-positive cells almost doubled after 24 h in control isotonic medium to $10.4 \pm 1.4\%$ (Tukey's multiple comparisons test, $p < 0.05$, $n = 5$). Treatment with PMA, RA, 5-HT, bFGF, DMSO, and dibutyryl-cAMP plus IBMX for 24 h increased the percentage of tubulin-positive cells when compared to the 0 h control, however, they did not significantly change the percentage when compared to the 24 h control or each other (ANOVA, $p < 0.001$, $n = 40$, Tukey's multiple comparisons test, $p > 0.05$, **Fig. 9a**). Treatment with the remaining 8 differentiation cocktails induced an increase in tubulin-positive cells when compared to both 0 h and 24

h controls. Seven of those treatments induced a 1.6 to 2.4-fold increase in neurons when compared to the 24 h control, and one treatment induced a 3-fold increase in tubulin-positive cells (ANOVA, $p < 0.001$, $n = 40$, Tukey's multiple comparisons test, $p < 0.05$, **Fig. 9b**). This treatment with dibutyryl-cAMP, IBMX, and 5-HT (cocktail A+G) was therefore used in further studies to monitor the electrophysiological changes that occur in neoblasts as they differentiate into neurons.

Changes in the proportion of tubulin expressing cells could have been due to the selective mortality of non-neuronal cells caused by the treatments. Or conversely the treatment might increase the survival of neurons relative to other cell types. To rule out these alternatives, the number of all types of living cells was recorded after 24 h in each of the differentiation treatments (**Fig. 10**). After 24 h in control medium, $80.2 \pm 4.0\%$ ($n = 5$) of the cells plated remained alive. Treatment with all the other agents resulted in survival rates between $63.6 \pm 0.1\%$ (retinoic acid, $n = 5$) to $82.4 \pm 0.0\%$ (bFGF, $n = 5$), but there were no statistical differences between the mean survival rates for any treatment when compared with the control (ANOVA, $p > 0.05$, $n = 75$, Tukey's multiple comparisons test, $p > 0.05$). If mortality of non-neuronal cells alone was the cause of the observed increase in the percentage of tubulin expressing cells (**Fig. 9a and b**) only a maximum increase of 1.5-fold (retinoic acid, **Fig. 10**) in the number of tubulin expressing cells would be observed. However, since differentiation treatments induced an increase of greater than 1.5-fold in the proportion of tubulin-immunoreactive cells (**Fig. 9a and b**), the increase in neuronal tubulin expressing cells could not be explained by selective mortality alone. This suggests that the increase in tubulin positive cells is likely the result of the differentiation treatments and not due to the selective mortality of non-neuronal cells.

3.2 Induction of neurite-outgrowth in differentiating neuroblasts

Since expression of tubulin in neurons is often associated with the growth and extension of processes, it was important to examine whether treatments not only induced tubulin expression, but also caused neoblasts to sprout neurites. It is known that

neurotransmitters, neuropeptides, growth factors and other diffusible agents are capable of inducing neuroblasts to develop growth cones and stimulating axonal extension (Asumi *et al.*, 2002). Tubulin immunoreactive cells were counted as before, but the percentage of cells extending processes equal or greater than one soma diameter in length was also determined.

When neuroblasts were cultured on 0.01% poly-L-lysine coated glass slides, only a small percentage of cells in control media produced neurite-like extensions ($0.3\pm 0.3\%$, $n = 5$ for 0 h, $0.5\pm 0.3\%$, $n = 5$ for 24 h) (**Fig. 11a**). Generally, treatments that did not significantly increase the percentage of tubulin positive cells also had no effect on the percentage that grew neurites (Treatments: B, G, D, and K, Kruskal-Wallis one-way analysis of variance, $p > 0.05$, $n = 120$). Exceptions to this were treatments with dibutyryl-cAMP plus IBMX (treatment A), and with retinoic acid (treatment F). Both these treatments did not increase the percentage of tubulin-expressing cells (**Fig. 9a**); however, they did increase the percentage of neurons sprouting processes (**Fig. 11b**). Many of the treatments that significantly increased the percentage of tubulin-expressing cells also significantly increased the number of cells sprouting neurite-like extensions (Treatments: A+D, J, A+F, BCM, and A+G; Kruskal-Wallis one-way analysis of variance, $p < 0.05$, $n = 120$) (**Fig. 11b**). Exceptions included treatments: H, E, and C, which induced cells to express neuronal-tubulin, but not to sprout neurites (**Fig. 11a**). Neuroblasts exposed to dibutyryl-cAMP, IBMX, PMA, and 5-HT (treatment A+G) showed the largest increase in both tubulin-expression, and growth of neurite-like extensions ($3.7\pm 0.8\%$, $n = 5$) (**Fig. 9b, 11a**). Differentiating neuroblasts treated with A+G for 24 h retained the high nucleus to cytoplasm ratio even in cells sprouting neurite-like extensions (**Fig. 12**).

Because treatment with A+G had little effect on the survivorship, and increased both the percentage of cells expressing neuronal tubulin and sprouting neurites, differentiating neuroblasts under these treatments were selected for electrophysiological experiments.

4. Electrophysiological properties of cultured neoblasts

An electrophysiological profile of undifferentiated stem cells was accumulated by measuring cellular electrical properties that influence neuronal excitability. These included resting membrane properties (V_m , R_i , τ , C_m), the presence of V_g ion channels, and the kinetic properties of those channels. Measurements of C_m should reflect the surface area of the cell, giving an indirect measure of whether cell size or complexity is affected by treatments. The membrane time constant is a measure of the time required for the membrane to hold or release charge, and is proportional to both C_m and R_m . R_m in turn, is directly proportional to the input resistance of a cell. Thus, τ provides an indirect measurement of input resistance. Input resistance was also measured directly through sharp electrode recordings.

Whole-cell, patch-clamp recordings of neoblasts were first performed in regular isotonic planarian medium, and then in salines with normal ion complements for recordings of whole-cell currents from freshly dissociated neoblasts. There were no perceivable inward currents recorded from either undifferentiated or differentiating neoblasts at 0 h. Hence solutions designed for isolating K^+ currents were used and whole-cell currents measured.

4.1 Resting membrane properties of undifferentiated neoblasts

Neoblasts were selected randomly for both patch-clamp and intracellular recordings. The holding potential was set to -90 mV prior to achieving whole-cell access, and then pulse trains of 20 mV were applied at 5 Hz to measure both membrane capacitance and the time constant of current decay. Membrane capacitances of undifferentiated neoblasts varied between 1.08 and 19.22 pF and did not change with time in culture (ANCOVA, $p > 0.05$, $n = 68$) (**Fig. 13a**). This suggests that cell size remained constant in neoblasts cultured in control IPM. The membrane time constant varied between 30.6 and 145.7 ms and was likewise unaffected by time in culture (ANCOVA, $p > 0.05$, $n = 59$) (**Fig. 13b**).

Both C_m and τ remained unchanged within the first 24 h in differentiating neoblasts treated with A+G (ANCOVA, $p > 0.05$, (τ) $n = 115$, (C_m) $n = 132$) (**Fig. 13**).

Comparisons of C_m and τ were also made in cells where $V_g\text{-K}^+$ currents were observed. The presence of $V_g\text{-K}^+$ channels had no effect on either of these parameters and no interaction between the presence of $V_g\text{-K}^+$ channels and time in culture was observed (ANCOVA, $p > 0.05$, (τ) $n = 115$, (C_m) $n = 132$) (**Fig. 14a, 14b**).

Resting membrane potentials measured using whole-cell, patch-clamp were determined by first establishing whole-cell recordings in the voltage-clamp mode, then switching to a slow current-clamp where currents were maintained at zero, and the voltage followed. In undifferentiated freshly dissociated neoblasts, the resting V_m was relatively unpolarized (-25.9 ± 2.3 mV, $n = 25$), and remained unchanged when cultured in IPM for as long as 30 h (-27.8 ± 2.2 mV, $n = 11$) (ANOVA, $p > 0.05$, $n = 52$) (**Fig. 15a**, black bars).

It is possible that measurements of membrane potential using the patch-clamp amplifier may not be accurate because the amplifier lacks a bridge circuit and is therefore not a true voltage follower. For comparison, resting membrane potential measurements were also conducted using sharp electrode intracellular recordings and a current-clamp, voltage following amplifier (Model 5A amplifier, Getting Instruments). Cells were chosen randomly as before, and impaled by manually penetrating cells using a piezoelectric micromanipulator. The voltage drop was distinct and immediate, suggesting that electrodes penetrated the cells cleanly. Cells could be maintained stably in this recording mode for longer than 15 min. Input resistance was measured in addition to membrane potential. Co-cultured muscle cells were impaled as a control to determine if the general health of cultures might influence resting V_m and R_i measurements. Muscle cells had a relatively polarized mean resting V_m of -50.8 ± 1.7 mV ($n = 4$). This result along with previous experiments that examined neoblast viability suggests that cell cultures were healthy.

The mean resting V_m of neoblasts recorded using sharp electrodes from freshly dissociated neoblasts cultured for 0-5 h was -17.5 ± 3.6 mV ($n = 6$) and did not change after 20-25 h in culture (-24.0 ± 1.6 mV, $n = 3$) (ANOVA, $p > 0.05$, $n = 13$) (**Fig. 16a**, white bars). There was no significant difference between resting membrane potentials recorded using sharp electrode (white bars) and whole-cell patch clamp methods (black bars) (ANOVA, $p > 0.05$, $n = 65$) suggesting that the accuracy of measurements made using whole-cell patch clamp may be appropriate and sufficient in neoblasts under these conditions. The mean input resistance in 0 h neoblasts was 141.5 ± 4.2 M Ω ($n = 5$) and there was no effect of time in culture on R_i after 24 h (122.5 ± 9.8 M Ω , $n = 5$) (unpaired t -test, $p > 0.05$, $n = 5$) (**Fig. 16b**).

4.2 Resting membrane potential increases in differentiating stem cells

Both the presence of V_g - K^+ channels, and the induction of neuronal differentiation by a cocktail of dibutyryl-cAMP, IBMX, and 5-HT (treatment A+G) increased the resting membrane potential of neoblasts. Neoblasts possessing V_g - K^+ channels had mean resting potentials of -30.9 ± 1.6 mV ($n = 45$) compared to -19.0 ± 1.2 mV ($n = 32$) in neoblasts without V_g - K^+ channels (**Fig. 15b**). This difference was present at all time periods measured (Two-way ANOVA, $p < 0.05$, $n = 77$), but there was no statistical difference between mean resting V_m among time periods in cells with V_g - K^+ channels (Tukey's multiple comparison's test, $p > 0.05$). The resting V_m of neoblasts without V_g - K^+ channels was similarly uninfluenced by the time cells remained in culture (Tukey's multiple comparison's test, $p > 0.05$) (**Fig. 15b**).

Differentiating neoblasts treated with A+G for 24 h developed more negative resting membrane potentials than in controls. After treatment for greater than 10 h, neoblasts had a mean resting V_m of -40.2 ± 1.8 mV ($n = 8$) compared to -25.9 ± 2.3 mV ($n = 25$) in untreated cells at 0 h. Both treatment alone, and the combination of treatment with A+G and time in culture significantly increased the resting membrane potential (Two-way ANOVA, $p < 0.05$, $n = 69$) (**Fig. 15a**).

4.3 V_g - K_{DR} channels from undifferentiated neoblasts

The whole-cell configuration could often be maintained for 30 min. To determine both the percentage of cells with K^+ currents, and the current-voltage properties of these channels, cells were held at -70 mV before a series of 10 mV steps from -90 mV to +70 mV were imposed for 200 ms. In response to these pulses, 42.9% ($n = 28$) of neoblasts, recorded within the first 5 h after being cultured in IPM, displayed outward currents that appeared to have a single non-inactivating component (**Fig. 17a**). In control neoblasts, this was the only current observed. These currents activated at potentials more positive than approximately -50 mV (**Fig. 17b**). The current-voltage properties remained unchanged after 24 h (**Fig. 17b**).

Activation properties were used to characterize the K^+ channels found in neoblasts and to compare changes in expression with time in culture and the effect of various treatments. The voltage-dependence of activation was measured by analyzing tail currents to avoid the necessity of measuring the reversal potential. Steady-state currents were evoked by stepping the holding potential from -70 mV through a series of 10 mV depolarizing steps between -90 and +70 mV for 35 ms. The holding potential was then stepped down to -100 mV to evoke instantaneous tail currents. After 0-5 h in culture, K^+ channels from neoblasts had a V_{50} of 22.6 ± 5.6 mV ($n = 4$) and a slope factor of 14.9 ± 2.8 ($n = 4$) (**Fig. 18a**). These properties remained unchanged in neoblasts cultured for 24 h (Kruskal-Wallis one-way analysis of variance, $p > 0.05$, $n = 12$) where the V_{50} was 30.0 ± 6.6 mV ($n = 8$) and the slope was 27.5 ± 5.4 ($n = 8$) (**Fig. 18b**).

The time constant of activation was similarly unaffected by the time neoblasts remained in culture (Kruskal-Wallis one-way analysis of variance, $p > 0.05$, $n = 12$). The steep rising phase of the evoked currents was fitted using the Hodgkin-Huxley model of K_{DR} activation with first-order kinetics. Mean values for τ_n were plotted against the evoking pulse potential, and then fitted to a three-parameter exponential decay function to describe the voltage-dependence of τ_n (**Fig. 19**). Activation time constants were shorter

when test pulses more positive than -50 mV were applied. When a -50 mV depolarizing test pulse was applied, τ_n was 2.6 ± 0.4 ms in 0h neoblasts ($n = 4$), and 1.0 ± 0.4 ms in 24 h cells ($n = 6$). The activation time constant reached a minimum value at potentials more positive than approximately -20 mV. When a +70 mV test pulse was applied, the activation τ was 0.7 ± 0.4 ms ($n = 4$) and 0.4 ± 0.1 ($n = 4$) ms for 0 h and 24 h cells respectively. The values of τ_n were not different from those observed in K_{DR} channels recorded from mature brain neurons (**Fig. 19**, solid curve).

4.4. *Vg-K_{DR} channels from differentiating neoblasts*

The percentage of cultured neoblasts expressing a K^+ current was influenced both by time in culture and by treatment with A+G (**Fig. 20**). When cultured in control IPM, the percentage of cells expressing a K^+ current increased from 42.9% ($n = 28$) at 5 h to 82.4% after 24 h ($n = 17$). This increase in cells expressing K^+ currents was proportional to the time in culture for both treated and untreated cells (**Fig. 20**). Treatment with A+G caused neoblasts to express the K^+ currents earlier. A significantly greater number of treated cells expressed Vg- K^+ channels after 5 h, 66.7% ($n = 6$) (Chi-square test, $p < 0.05$, $n = 34$). This percentage increased to 85.0% ($n = 20$) in cells treated for up to 30 h with A+G, but was not significantly different from control cells at the same time (Chi-square test, $p > 0.05$, $n = 48$). Taken together, these data suggest that time in culture alone is sufficient to induce neoblasts to express a Vg- K^+ channel, however, treatment with A+G expedites this process and Vg- K^+ currents are found in treated cells sooner.

In addition to the proportion of cells expressing Vg K^+ currents, the magnitude of currents was compared between control and treated cells to determine if expression levels in differentiating cells were affected by treatment with A+G. Currents were evoked from a holding potential of -70 mV through a series of depolarizing steps and the K^+ currents recorded. **Figure 21** shows representative current traces recorded from differentiating neoblasts treated with A+G at specified time periods. The majority of neoblasts showed

no observable K^+ currents immediately after isolation (**Fig. 21**, top left panel). Measurable currents became apparent after 5 h in culture and expression increased gradually up to 24 h (**Fig. 21**). After 24 h treatment with A+G, neoblasts developed currents that ranged between 33.0 to 1107.1 pA ($n = 37$).

After currents were standardized to membrane capacitance, it was revealed that differentiating cells develop larger currents than in control treated neoblasts (**Fig. 22**). Currents were evoked by depolarizing cells from a holding potential of -70 mV to +30 mV (**Fig. 22a**), or +50 mV (**Fig. 22b**). Mean current density of control cells up to 15 h was not larger than the mean electrical noise from recordings (Kruskal-Wallis one-way analysis of variance, $p > 0.05$, $n = 36$) at either +30 or + 50 mV (**Fig. 20a, 20b**). Potassium current density in control cells did increase above ambient noise levels after 24 h in culture to 0.09 ± 0.02 pA/ μm^2 ($n = 10$) and 0.14 ± 0.04 pA/ μm^2 when depolarized to +30 and + 50 mV respectively (**Fig. 22a, 22b**), and was significantly larger than control cells at all other time periods (ANOVA, $p < 0.05$, $n = 55$). In differentiating cells treated with A+G, mean K^+ current density increased significantly when compared to control cells, but time had no influence on the size of currents (ANCOVA, $p < 0.05$, $n = 87$). Current density increased from 0.09 ± 0.03 pA/ μm^2 ($n = 13$), 0.12 ± 0.04 pA/ μm^2 ($n = 8$), to 0.17 ± 0.07 pA/ μm^2 after 5, 10, and 20 h respectively. After 24 h treatment with A+G, mean current density decreased to 0.10 ± 0.3 pA/ μm^2 but the decrease was not statistically significant (**Fig. 22a, 22b**).

The voltage-dependence of activation and the time constant of activation of $V_g\text{-}K^+$ channels in treated and untreated cells were similar. Activation was measured as described above and the data were fitted to a Boltzmann function as before. The voltage of half-activation was markedly rightward shifted in A+G treated cells when compared to many other delayed rectifier K^+ channels (Hille, 2001). The V_{50} of activation in the control (22.0 ± 4.0 mV, $n = 9$) was not significantly different from the value observed in control cells (27.5 ± 5.4 mV, $n = 8$) (ANOVA, $p > 0.05$, $n = 17$) (**Fig. 23a**). Treatment with A+G for 24 h had no effect on the slope factor from the fitted curve of the

Boltzmann function (ANOVA, $p > 0.05$, $n = 17$). The curve had a shallow slope, indicated by the relatively high value for the slope factor of 30.0 ± 6.6 ($n = 8$) and 21.0 ± 2.5 ($n = 9$) for control and treated cells respectively (**Fig. 23b**).

The rate of activation and the voltage dependence of τ were similarly unaffected by treatment with A+G (**Fig. 24**). As with channels recorded from 0 h and 24 h control neoblasts, channels from cells exposed to A+G for 24 h had the slowest rates of activation when depolarized to -50 mV (2.6 ± 1.3 ms, $n = 5$), which reached a minimum at approximately -20 mV and were fastest at +70 mV (0.9 ± 0.3 ms, $n = 9$). There were no statistical differences between values obtained from the three parameter exponential function used to describe the voltage dependence of τ between control and treated cells (repeated measures ANOVA, $p > 0.05$, $n = 5$).

Taken together, these results suggest that differentiating neoblasts treated with A+G express K^+ channels sooner than control cells, and that K^+ channel expression continues to increase over the first 24 h, most likely due to an increase in the density of K^+ channels in the membrane. Results also show that although expression levels differ, the specific channel type expressed in both control and untreated cells are indistinguishable based on the voltage dependence of activation, the rate of activation, and the voltage dependence of τ .

4.5. *Electrophysiological properties of differentiating neurons with neurites*

In addition to expressing neuronal tubulin, some differentiating neoblasts also sprouted neurite-like processes. Of the cells expressing neuronal tubulin, $3.7 \pm 0.8\%$ ($n = 5$) of those cells also grew processes. The morphology of these cells was highly variable (**Fig. 12, 25a, 25b**). Cells were observed to exhibit monopolar (**Fig. 25a**), bipolar (**Fig. 25b**), and multipolar (**Fig. 12, 25a**) morphologies, with both homopolar (**Fig. 25b**) and heteropolar (**Fig. 12, Fig. 25a**) arrangements. After 24 h treatments, differentiating neoblasts with processes could still be distinguished from contaminating mature neurons

on the basis of their large nucleus to cytoplasm ratio (**Fig. 25a**). Those neurons that were already mature in the tissue prior to isolation tended to have nucleus to cytoplasm ratios much smaller than in neoblasts. Changes in the electrophysiological properties of differentiating neoblasts, the presence and types of Vg-K⁺ channels, channel activation kinetics, and the types of Vg-K⁺ channels present were compared with undifferentiated neoblasts, differentiating neoblasts without processes, and mature brain neurons.

The percentage of neoblasts sprouting neurites after 24 h and possessing K_{DR} channels was 100% (n = 8) compared to 82.4% (n = 17) in 24 h control cells, and 85.0% (n = 20) in A+G treated cells without neurites. The percentage of cells expressing K_{DR} channels was significantly larger in cells sprouting neurites compared to those without neurites (Chi-square test, p < 0.05, n = 45). The delayed rectifier channels of A+G treated neoblasts with neurites had similar voltage dependence of activation as adult neurons (**Fig. 26a**). Channels activated at approximately -50 mV and had half-activation voltages of 19.7±4.4 mV (n = 10) and 22.1±2.9 mV (n = 10) for adult neurons and A+G treated neoblasts with neurites respectively and did not differ significantly (ANOVA, p > 0.05, n = 20) (**Fig. 26b**). The slope factors for the fitted Boltzmann distributions for adult neurons (21.7±2.1, n = 10) and A+G treated cells with neurites (21.2±2.3, n = 10) were also statistically similar (ANOVA, p > 0.05, n = 20) (**Fig. 26a, 26b**).

The rate of activation for K_{DR} channels in adult neurons and neurite-sprouting neoblasts were voltage dependent and had similar fit parameters when modelled with a three-parameter single exponential decay function (**Fig. 27a, 27b**). The rate of activation was slowest at -50 mV approaching 2.3±1.6 ms (n = 10) for adult neurons, and 1.6±0.7 ms (n = 10) for neurite-sprouting neoblasts. The rate of activation reached a maximum at potentials more positive than -20 mV with asymptotic fit values of 0.5±0.1 ms (n = 10) and 0.58±0.03 ms (n = 10) for adult neurons and A+G treated cells respectively (**Fig. 27b**). These did not differ significantly from the τ of activation for any potentials between -20 mV and +70 mV (repeated measures ANOVA, p > 0.05, n = 10). The linear and exponential constants, describing the rate of decrease in the τ of activation, were

statistically similar in both adult brain neurons, and neoblasts with neurites (Kruskal-Wallis one-way analysis of variance, $p > 0.05$, $n = 20$) (**Fig. 27b**).

Both the τ_n and voltage dependent steady-state activation properties of neurite-sprouting neoblasts were similar to the K_{DR} channels recorded from undifferentiated neoblasts and of A+G treated neoblasts without processes. This suggests that all cells from all these categories express the same type of K_{DR} channel.

Whole-cell recordings revealed that in addition to expressing a K_{DR} current, neurite-sprouting cells also expressed an A-type K^+ current (50%, $n = 8$) (**Fig. 28**). No A-type currents were recorded from undifferentiated neoblasts ($n = 68$) or differentiating cells without processes ($n = 31$), but they were expressed in 42.9% ($n = 14$) of adult brain neurons. The A-type currents activated and inactivated rapidly, reaching peak values within 2 ms of the test pulse (**Fig. 28a**). The current-voltage relationship reveals that the ratio of inactivating to non-inactivating currents was voltage dependent and larger at more positive potentials (**Fig. 28b**).

The mean membrane time constant for cells with K_A currents (78.9 ± 5.7 ms, $n = 6$) was not significantly different from cells without K_A currents (83.5 ± 2.2 ms, $n = 45$) (unpaired t -test, $p > 0.05$, $n = 51$) (**Fig. 29a**). It was hypothesized that the membrane capacitance in cells with K_A currents would be larger than in cells without K_A currents because the former also began sprouting processes. Although the C_m measured from cells with K_A currents was larger (8.8 ± 0.7 pF, $n = 7$) than in cells without (7.4 ± 0.4 pF, $n = 67$), the means did not differ statistically (unpaired t -test, $p = 0.07$, $n = 74$) (**Fig. 29b**).

4.6. Differences between differentiating neoblasts and mature adult neurons

Although differentiating neoblasts share similarities with cultured adult neurons including expression of a neuron-specific tubulin, sprouting of neurite-like extensions, a large resting V_m , and expression of both voltage-gated K_{DR} and K_A channels, there

remain some important differences that suggest that treatment with dibutyryl-cAMP, IBMX, PMA, and 5-HT for 24 h do not induce neoblasts to mature completely into neurons. Two of the most striking differences are the size of Vg-K⁺ currents and the lack of inward currents.

Delayed rectifier currents from differentiating neoblasts are smaller than those observed in adult brain neurons (**Fig. 30**). K_{DR} currents recorded from A+G treated neoblasts ranged between 33.0 to 1077.1 pA (n = 37) (**Fig. 30a, 30b**) whereas currents from brain neurons ranged between 76.0 to 3704.8 pA (n = 8) when a depolarizing test pulse to +70 mV was applied in the same ionic solutions. When cells were depolarized to +30, +50, and +70 mV and the resulting currents normalized to the membrane area, K_{DR} current density was consistently 3.3 times smaller when recorded from developing neoblasts (n = 37) compared to adult neurons (n = 8) (Kruskal-Wallis one-way test of analysis, p < 0.05, n = 62) (**Fig. 30d**).

When neoblasts were recorded in salines with full ionic complements and with general pipette solutions, no inward currents were observed (n = 27). This suggest that either the A+G treatment alone is insufficient for inducing neoblasts to express inward currents, or that the duration of application was insufficient. When salines and pipette solutions designed for isolating Ca²⁺ currents were used, no discernable inward currents were recorded in cells exposed to control media (n = 24), A+G for 24 h (n = 10), or *Helisoma* brain-conditioned media (n = 10). When extracellular solutions contained Ca²⁺ (2 mM), most cells displayed residual outward currents (n = 23). Even when Ca²⁺ was replaced with Ba²⁺ (2 mM), in an attempt to block K_{DR} channels, small, 10-20 pA, residual outward currents remained (n = 21).

Discussion

1. Isolation and purification of neoblasts from Girardia tigrina

I have developed a reproducible technique to selectively culture neoblasts from *Girardia tigrina* at sufficient purities and viabilities to be used for cellular biology and electrophysiological experiments. Previous attempts to develop cell isolation protocols from flatworms have highlighted the importance of controlling the culture medium and of selective filtration. Sorting cells by size and density appears to be the simplest and most effective way of obtaining viable cultures of neoblasts (Baguna *et al.*, 1989; Schurmann *et al.*, 1998; Schurmann & Peter, 2001).

1.1. Density- and size-dependent purification of neoblasts

Using discontinuous Percoll gradients, neoblasts are recovered from all density layers, but are most concentrated at the boundary between the 1.07 g/ml and 1.09 g/ml layers. The density of neoblasts recorded in this study is slightly higher than in previous reports, where neoblasts were concentrated at the boundary between the 1.05 g/ml and the 1.07 g/ml layers (Schurmann *et al.*, 1998). Differences in neoblast density can be attributed to species specific differences or differences in the culturing procedures. Solutions used during the cell dissociation process in this study had slightly higher osmolalities, 178 mOsmol/L, than the 125 – 139 mOsmol/L reported by Schurmann *et al.* (1998). This combined with differences in the medium's pH may have resulted in the disparity of measured densities. Schurmann *et al.* (1998) used osmolality values obtained directly from tissues of *Schmidtea (Dugesia) polychora* and *D. tahitiensis* obtained from freezing point depression studies, whereas in this study, Percoll gradients were prepared using 0.15 NaCl, as per the manufacturer's suggestion (Amersham Biosciences), then supplemented with a fixed volume of culture medium. Although the mechanisms used to regulate cellular volume are unknown in planarians, if neoblasts from the *G. tigrina* have

similar masses to those in other planarians, an increase in extracellular osmolarity could be assumed to cause an obligatory decrease in cellular volume and consequent increase in density (Lang *et al.*, 1998). Although the precise densities *in situ* remain unknown, I observed that neoblasts are robust with respect to their ability to respond to changes in osmolarity (personal observations). In one instance where neoblasts were isolated in a medium with an osmolality of 290 mOsmol/L, cells remained viable for several days after plating.

The viability of neoblasts, determined by a Trypan Blue exclusion, immediately following the culturing procedure was always above 90%, similar to the values observed in *Schmidtea (Dugesia) mediterranea* (Baguna *et al.*, 1989). Cultures retained viabilities above 80% for over 3 days, but were not observed for any longer periods. Presumably, neoblasts from *Girardia tigrina* could have been maintained in culture for longer durations, as has already been done in *Schmidtea (Dugesia) polychroa*, where neoblasts retain viabilities above 80% for 15 days with no morphological signs of differentiation (Schurmann & Peter, 2001). There was no effect on neoblast viability upon treatment with morphogenic treatments. Cell viabilities reported here appear sufficient for electrophysiological experiments as judged by reasonably large resting potentials. Neoblasts cultured using similar protocols and in comparable conditions have been shown to retain their activities. For example, X-ray irradiated host animals lose their regenerative abilities, but when cultured neoblasts are injected from non-irradiated donors, hosts are capable of fully regenerating all structures (Baguna *et al.*, 1989). This suggests that culturing neoblasts in our study had little effect on their capacity to differentiate. The same authors report an increase in neoblast mitosis when they are injected into host animals, however, I never observed neoblasts undergoing mitosis in any of the cultures. Mitosis of neoblasts has been observed to occur in culture, but only at rates near 1% (Schurmann *et al.*, 1998; Schurmann & Peter, 2001). Attempts to induce mitosis using growth factors were unsuccessful. The density of neoblasts in flatworms is species-specific and depends on the age and feeding status of an animal (Baguna, 1974; 1976a; 1976b; Baguna & Romero, 1981; Romero & Baguna, 1991; Nimeth *et al.*, 2004).

It remains to be seen if neoblasts recovered from animals in different physiological states have similar properties.

1.2. Neoblasts are a heterogeneous group of stem cells

Although the relative densities of neoblasts may vary with species and culture methods, techniques employing tissue grinders, dithiothreitol to reduce the mucus load, mechanical sieves, and brief treatment with proteinases appears to remain an efficient method of isolating and purifying stem cells from flatworms. I was able to produce neoblast cultures of ~70% purity which is slightly lower than in previous reports. Neoblast cultures with >85% purity were obtained from *Schmidtea mediterranea*, (Baguna *et al.*, 1989). This difference may reflect the methods used for identification since in the past gland cells, and nerve cells have been incorrectly identified as neoblasts (Lender, 1960; Wolff, 1962; Hay & Coward, 1975). This study relied on both phase-contrast microscopy and a histological stain used to specifically label neoblasts (Pedersen, 1959b; Schurmann *et al.*, 1998; Rieger *et al.*, 1999), whereas Baguna *et al.* (1989) used only phase-contrast microscopy. Because many planarian cells fit the general description of a neoblast, “*small cells (8-15µm), rounded or pear-shaped*” (Baguna *et al.*, 1989), it would be easy to overestimate the number of neoblasts recovered if phase-contrast microscopy is used alone. Future studies need to focus on a precise method to label or separate neoblasts based on molecular markers.

Recent techniques have been developed that may provide a solution to misinterpretations of neoblast identities. Because neoblasts are the only mitotic cells in the flatworms, continuous labelling of neoblasts with BrdU can now be used to determine neoblasts that have recently undergone mitosis (Ladurner *et al.*, 2000; Newmark & Sanchez Alvarado; Gschwentner *et al.*, 2001). This may require a re-evaluation of what we consider to be a neoblast to include only mitotic cells, compared to the classical description of small, morphologically undifferentiated cells, with a high nucleus to cytoplasm ratio (Pedersen, 1959b; Schurmann *et al.*, 1998; Rieger *et al.*, 1999). Further advances in neoblast cell

culture techniques should focus on whether subtypes of neoblasts exist based on functional characteristics and differentiation potential. Some relatively simple methods to find neoblast specific markers might be to generate molecular expression profiles using reverse transcriptase PCR (Koos & Seidel, 1990). Subtypes of neoblasts might express different surface cell markers and display different intracellular properties that could be exploited for separation using flow cytometry (Loken, 1980). Our attempts to use flow cytometry to purify suspensions of neoblasts based on size and internal complexity were unsuccessful. Brain cells from *Dugesia japonica* have already been separated using fluorescence-activated, cell-sorting by labelling neurons with specific molecular markers and confirming their identity with a voltage-sensitive fluorescent dye (Asami, *et al.*, 2002). Results from this study suggest that resting membrane potential may be a useful marker for undifferentiated neoblasts, since they have relatively unpolarized resting membrane potentials when compared with some other cell types such as muscles.

1.3. Neoblast activity is regulated by extracellular osmolarity

Neoblasts isolated in this study share many of the morphological features described in previous reports including a high nucleus to cytoplasm ratio, small size (~6-10 μm), and a round or pear shape (Pedersen, 1959b; Baguna *et al.*, 1989; Schurmann *et al.*, 1998). I observed some variation in morphology, the most notable difference was that neoblasts did not develop fine cell extensions (Betchaku, 1967; Schurmann *et al.*, 1998; Schurmann & Peter, 2001). Betchaku (1967) first reported that neoblasts exhibit a characteristic change in morphology when cultured. Within 24 h of plating, cells extend a long primary process and then a shorter secondary process in the opposite direction which is subsequently retracted. The development of cellular processes was presumed to be a mechanism by which neoblasts migrate, by attaching to anchored parenchymal gland cells then shortening contractile elements within the process (Betchaku, 1967). Cell extensions have also been observed by others and appear to be dependent upon a mild to strong hypotonic environment (Teshirogi & Tohya, 1988; Schurmann & Peter, 2001). Neoblasts reported here most likely did not develop processes since our culture medium

was mildly hypertonic. Also, it seems unlikely that the developing neurons sprouting processes in *Girardia tigrina* are similar to those described in previous accounts as I observed neurite-like processes that were broader, and often had lamellopodial and filopodial-like extensions. The cell extensions also showed strong immunoreactivity towards a neuron-specific antibody. In addition, neurites in this study did not degenerate after 24 h as did processes that formed when neoblasts were cultured in a study by Schurmann & Peter (2001). Although Schurmann and Peter (2001) briefly describe the influence of collagen I on the development of neoblast processes, it remains to be seen whether extracellular matrix components also influence neurite extension in developing neurons.

It has been suggested that changes in osmolarity alone might act to induce neoblast activation and differentiation during regeneration. In *G. tigrina*, wound-healing requires as long as 30 min for the epithelium to close up around the opening (Baguna *et al.*, 1994), exposing underlying tissues to an osmotic perturbation from the surrounding medium. The osmotic shock associated with tissue damage might induce gene expression through either stretch-activated channels (Syntichaki & Tavernarakis, 2003), or through the activities of ion co-transporters or exchangers (Lang *et al.*, 1998; Goss *et al.*, 2001). There is indirect evidence for the presence of a Na^+/H^+ exchanger in the epidermis of both parasitic and free-living flatworms (Prusch, 1976; Pax & Bennett, 1990; Ikeda, 2004), but whether neoblasts express these proteins is unknown. Osmotic shock is also known to stimulate a mitogen-activated protein kinase (MAPK) cascade in both yeast and mammalian cells (Galcheva-Gargova *et al.*, 1994; Matsuda *et al.*, 1995; Stariha & Kim, 2001). These responses are often in response to hyperosmotic conditions, and can be independent of ion exchangers (Kapus *et al.*, 1999; Sheikh-Hamad & Gustin, 2004), and can also involve Janus kinase 2 and Ca^{2+} /calmodulin (Garnovskaya *et al.*, 2003). The ubiquitous presence of osmoregulatory mechanisms in cells suggests that external osmolarity may also influence neural specification in flatworm neoblasts.

The results presented here confirm the validity of cell culture techniques previously developed (Schurmann *et al.*, 1998; Schurmann & Peter, 2001), as an effective method to quickly obtain high quantities of viable neoblasts to be used for physiological experiments. Longer term studies and the systematic characterization of the ways neoblasts respond to extrinsic factors are possible. An important step in planarian cell culture will be to identify factors that promote mitosis and proliferation so that a stable cell line of neoblasts can be produced.

2. Nervous system architecture and neuronal differentiation revealed by a monoclonal tubulin antibody

The central nervous system of *G. tigrina* is arranged in the classic flatworm ladder-like orthogon, with a bi-lobed brain, and longitudinal nerve cords connected by transverse commissures, with the main nerve cords located on the ventral side (Bullock & Horridge, 1965; Reuter *et al.*, 1998; Halton & Maule, 2004). Both the ventral and dorsal submuscular plexuses comprising the peripheral nervous system are apparent in confocal reconstructions of whole animals. The nervous system revealed by tubulin immunohistochemistry using the Tub Ab-4 antibody (NeoMarkers) appears to label more elements than in other reports where only antigenicity towards serotonergic, cholinergic and peptidergic neurons was examined (Minichev & Pugovkin, 1979; Maule *et al.*, 1990; Reuter *et al.*, 1995c; Reuter *et al.*, 1998). Although serotonin appears to be the dominant biogenic amine in all flatworms studied, all the classical neurotransmitters (ACh, norepinephrine, dopamine, histamine, glutamate, γ -amino butyric acid, nitric oxide) and 32 neuropeptides have been demonstrated in flatworms (reviewed by Halton & Maule, 2004). It is unknown whether the tubulin antibody used in this study cross-reacts with every mature neuronal phenotype, however, it appears to label the majority of neurons.

2.1. Tubulin expression is an early indicator of neural differentiation

This study supports the hypothesis that neuron-specific tubulin expression is an early event during neuronal fate specification and differentiation. Neuronal precursors began expressing neuron-specific tubulin within 24 h after treatment with various morphogens. In embryonic stem cells and neuronal precursors from mammals, neuron-specific tubulin expression can begin before termination of the last cycle of mitosis and precedes neurofilament expression (Meininger & Binet, 1989; Memberg & Hall, 1995). Several mammalian tubulin isoforms have been identified to be exclusively neuron-specific (Frankfurter *et al.*, 1986; Edde *et al.*, 1987), but there have not yet been neuron-specific tubulin isoforms isolated from the flatworms. Several commercially available antibodies appear to label neuroblasts in developing embryos (Younossi-Hartenstein & Hartenstein, 2000; Younossi-Hartenstein *et al.*, 2000; 2001), and several other antibodies are known to cross-react with both neurons, ciliated epidermal cells, and cilia alone (Bueno *et al.*, 1997; Robb & Sanchez Alvarado, 2002). In both species of flatworms examined in this study acetylated- α -tubulin (Sigma, St. Louis, MO) labelled both neurons and cilia. The Tub Ab-4 (Neomarkers) antibody reacts with neurons specifically in the species studied, but labels both neurons and cilia in *Dugesia dorotocephala* (Robb & Sanchez-Alvarado, 2002). The reactivity of neuronal tubulin towards commercially available antibodies in flatworms appears to be species-specific.

This study clearly shows that neoblasts express tubulin very early during neuronal differentiation and not as a result of another developmental event such as mitosis. In the marine triclad *Sbussowia dioica*, it has been suggested that tubulin is produced in neoblasts early during regeneration, but is localized in proliferating cells (Tekaya *et al.*, 1996). These authors also suggest that microtubule expression produces a scaffold for neoblasts migration into the regenerating blastema. However, it has been shown previously, that local proliferation of neoblasts is not enhanced during regeneration (Salo & Baguna, 1984; Salo & Baguna, 1989). If tubulin was expressed due to neoblast mitosis, constitutive tubulin-immunoreactivity would be seen in all regions of high cell

proliferation, which was not observed (Tekaya *et al.*, 1996). A comparable study in a freshwater triclad showed a very similar pattern of tubulin immunoreactivity during regeneration, but the authors found that tubulin expression was localized only in regenerating sensory neurons found at the epithelial surface (Robb & Sanchez Alvarado, 2002). Once the genes for neuron-specific tubulin are isolated from planarians, it will be important to assess RNA transcript expression using *in situ* hybridization techniques, to determine the precise cells where tubulin expression is enhanced during regeneration.

Subcellular tubulin expression patterns may provide information regarding how far neoblasts have progressed through neural differentiation. This cellular distribution of tubulin could be used to distinguish between mature neurons and developing neurons since the differentiating neoblasts observed express tubulin before any other gross changes in morphology occur, including nuclear restructuring. Early expression of class III- β -tubulin is commonly used in mammalian systems to detect neuronal phenotypes before any other neuron-specific characteristics are seen (Miller *et al.*, 1987; Memberg & Hall, 1995; Laferriere *et al.*, 1997). Developing *G. tigrina* neoblasts always retained their large and prominent nucleus, and tubulin was expressed only in the thin layer of surrounding cytoplasm. This study emphasizes the importance of finding an alternative means to identify neoblasts, since cells that retained an undifferentiated appearance when examined under phase-contrast microscopy had already begun to develop neuronal characteristics. The Tub Ab-4 antibody seems particularly useful in this species as an assay for neuronal differentiation since it appeared to label the entire nervous system and was not restricted to specific subtypes of neurons.

3. *Factors influencing neurogenesis in flatworms*

I investigated the putative effects of several morphogenic substances on neoblasts to determine if any treatments could stimulate neurogenesis. In addition to demonstrating that stem cells could be driven to differentiate into neurons, I showed that neoblasts had different sensitivities when exposed to morphogenic treatments. Since only a small

proportion of all neoblasts responded to these treatments, it is likely that that neoblasts are a heterogeneous group of stem cells at various stages of cellular differentiation, and have different fate potentials. Also there is a small percentage of neoblasts that will differentiate under controlled conditions, suggesting that approximately 5% of morphological neoblasts in *Girardia* have already been specified to develop into neurons.

3.1 Neoblasts consist of a heterogeneous group of pluripotent stem cells

Neoblasts have long been regarded as a system of totipotent stem cells, capable of generating all the cells of the organism (Baguna *et al.*, 1989; Sanchez Alvarado, 2000; Newmark & Sanchez Alvarado, 2002; Salo & Baguna, 2002). Classical studies have demonstrated the remarkable regenerative capabilities of flatworms and the likelihood that neoblasts are totipotent (Morgan, 1898; Bronsted, 1955; Lender, 1960; Baguna *et al.*, 1989). More recently it has been suggested that there may be several smaller populations of pluripotent stem cells that are capable of generating all the cell types (Agata & Watanabe, 1999; Ladurner *et al.*, 2000; Ogawa *et al.*, 2002b). My results suggest that the later explanation is more accurate, since I did not find any single treatment that was capable of inducing all neoblasts to differentiate. However, my data does not preclude the possibility that a small subset of neoblasts is truly totipotent. This could only be tested by following a single neoblast, and showing that it was capable of self-renewal, and that its progeny were capable of developing into every cell phenotype observed in the animal. This may soon be possible, since cell culture techniques in flatworms are improving and cell-specific molecular markers are now beginning to be discovered. For example: TCEN is a marker for body positional elements (Bueno *et al.*, 1995); TNEX is expressed during regeneration (Fernandez-Rodriguez *et al.*, 2001); CNS-specific genes have been identified (Agata *et al.*, 1998; Tazaki *et al.*, 1999; Ogawa *et al.*, 2002; Marsal *et al.*, 2003; Cebria *et al.*, 2002a; 2002b; 2002c; Salo & Baguna, 2002), as have markers for the epidermis, testis, gland cells, and gut (Shinozawa *et al.*, 1995). It now seems possible to test whether all stem cells in flatworms are totipotent, or if as this study

suggests, neoblasts are a group of heterogeneous pluripotent stem cells with different cell-fate potentials.

Although neoblasts were morphologically similar, the suite of membrane receptors for diffusible ligands was highly variable. There appear to be subpopulations of neoblasts capable of responding to neuropeptides and growth factors, biogenic amines, and stimulators of second messenger cascades. Previous reports have suggested a role for all these factors in regulating regeneration of the nervous system (Reuter *et al.*, 1986; Salo & Baguna, 1986; 1989; Reuter & Palmberg, 1990; Reuter & Gustaffson, 1996; Kreshchenko *et al.*, 1999), but I provide the first direct evidence that these types of factors can regulate neurogenesis in the flatworms. My results demonstrate the importance of factors produced by the nervous system in directing neuronal fate-specification.

3.2. Neuropeptides

Flatworms produce a wide assortment of neuropeptides, many of which have been implicated in activating neoblasts during regeneration. Immunoreactivity towards 26 mammalian and 6 invertebrate neuropeptides has been described in the nervous systems of flatworms (Wilgren *et al.*, 1985; Day & Maule, 1999; Reuter *et al.*, 2001). Six native flatworm peptides have also been isolated, two homologues of neuropeptide F (NPF) (Maule *et al.*, 1991; Curry *et al.*, 1992) and four FMRF-amide-related peptides (FaRPs) (Maule *et al.*, 1993b; 1994; Johnston *et al.*, 1995; 1996). In worms undergoing regeneration, immunoreactivity towards FMRF-amide and RFamide increases in the area of the blastema, and because they are the first elements of the nervous system to develop it has been suggested that they act as wound signalling hormones in *Microstomum lineare* (Palmberg & Reuter, 1990; Reuter & Palmberg, 1989; Reuter & Gustaffson, 1996). Here I show that RF-amide is bioactive when applied exogenously to neoblast cultures, and that FaRPs play at least two roles in flatworms, inducing neuronal specification and promoting neurite outgrowth. FaRPs have also been shown to be

myoexcitatory and possibly play a neuromuscular role (Day *et al.*, 1994). Studies of FaRP structure have revealed an absolute requirement for the phenylalanine residue (-Famide) (Day *et al.*, 1996; 1997). This explains the sensitivity of flatworm cells to a truncated cnidarian RF-amide peptide, and reveals that both neoblasts and neuroblasts express a receptor for FaRPs. The mechanism of FaRP activity is unknown, and no receptors have been identified, but signal transduction of FaRP responses in muscle involve G proteins, phospholipase C, and protein kinase C, and likely involve a typical GPCR signalling cascade (Totten *et al.*, 2002).

Growth factors were also effective in promoting neurogenesis when applied to cultured neoblasts from *G. tigrina*. Epidermal growth factor, but not basic fibroblast growth factor applied alone was sufficient to promote neuronal tubulin expression, however, bFGF applied in conjunction with dibutyryl-cAMP and IMBX also induced neurogenesis. Immunoreactivity towards epidermal growth factor and basic fibroblast growth factor have both been demonstrated in flatworms (Reuter & Kuusisto, 1992; Gustafsson *et al.*, 1995), as well as immunoreactivity to EGF and FGF receptors in planarians (Baguna *et al.*, 1990; Cebria *et al.*, 2002a; 2002c). Epidermal and fibroblast growth factor have both been shown to stimulate proliferation and differentiation in neural progenitors in mammalian stem cells, but the response is cell specific (Gritti *et al.*, 1996; Kuhn *et al.*, 1997; Gritti *et al.*, 1999). In vertebrate systems, both FGF proteins and FGFR's are also expressed early in the developing nervous system in regions where cells are undergoing proliferation or neurogenesis (Wanaka *et al.*, 1990; 1991; Cameron *et al.*, 1998a). In both adult and embryonic brain neuroblasts, FGF's mainly regulate the proliferation of neuronal precursor cells, and differentiation occurs only after FGF is removed (Bogler *et al.*, 1990; McKinnon *et al.*, 1990; Gritti *et al.*, 1996). The results from this study do not rule out a mitogenic effect for either EGF or FGF in flatworms. Since neoblast cultures were only followed for the first 24 h, there may be latent mitogenic effects of these growth factors.

EGF has been implicated in stimulating cell proliferation in flatworms, and asexual reproduction is inhibited by anti-EGFR (Baguna *et al.*, 1989; Fairweather & Skuce, 1995). In our study, EGF did not induce mitosis in neoblasts after 24 h, even though EGF treatments in regenerating animals double the mitotic index over the same period (Salo & Baguna, 1986). Expression patterns of EGF receptors in mammals suggest a pivotal role in controlling neuroblast proliferation (Kornblum *et al.*, 1997), but *in vitro* evidence suggests that EGF is only mitogenic in distinct stem cell populations (Reynolds & Weiss, 1992; Lillien & Cepko, 1992).

Our data show that FGF is a potent morphogen in flatworms and acts to induce neuronal differentiation. The role of FGF in neuronal differentiation has been described in flatworms and recently, FGF receptors have been cloned from *Dugesia japonica* where expression is restricted to brain tissues. The restriction of FGFR's to neuroblasts and neurons in planarians is unusual, but suggests they play a pivotal role in neuronal development. Ectopic expression of FGFR's causes brain tissues to form throughout the body (Cebria *et al.*, 2002a; 2002c). These receptors are also found in the regenerating blastema so neoblasts might also express them (Cebria *et al.*, 2002b). Two days after wounding there is a marked increase in FGFR expressing cells, which then decreases after 3 days, and returns to normal levels after 7 days (Cebria *et al.*, 2002b). These authors suggest that only uncommitted stem cells migrating towards the wound site express FGFR's, but this would imply that FGFR expression would be found in unwounded animals, and in non-nervous tissue which they never observed. I suggest that cells expressing FGFR's are not totipotent, but are neuroblasts already committed to neuronal lineages. This is supported by the evidence that bFGF alone is insufficient to promote neurogenesis. In addition, all *G. tigrina* neoblasts can respond to FGF, thus, it appears that FGFR's are only expressed after cell-fate has been specified.

3.3. Biogenic amines and transduction via intracellular signalling cascades

In this study, I demonstrate that both dopamine (3-HT) and serotonin (5-HT) are important factors in regulating neuronal fate-specification. Treatment with dopamine alone successfully induced tubulin expression, whereas 5-HT treatment required the addition of activators of second messenger cascades or the presence of other brain derived factors (*Helisoma* brain-conditioned media has been shown to include 5-HT, Ahn *et al.*, unpublished results). The presence of serotonin has been demonstrated in every class of flatworms, with extensive immunological staining in both the CNS and the PNS (reviewed by Halton & Maule, 2004). In intact animals, these substances have been shown to play an important role in neuromuscular communication (Alegri *et al.*, 1983; Pax *et al.*, 1984; Day *et al.*, 1994a). During planarian regeneration, previous studies have only implicated biogenic amines through indirect evidence, such as through the pattern of immunoreactivity arising during regeneration (Rieger, 1998). Here, for the first time, a direct role of biogenic amines in neural fate-specification in planarians is demonstrated.

Many indoleamines and catecholamines have been shown to promote regeneration, and 5-HT containing neurons are the first regenerative nervous system elements in some groups of flatworms (Reuter, *et al.*, 1986; Salo & Baguna, 1989; Reuter & Palmberg, 1990; Reuter & Gustaffson, 1996). During regeneration of planarians, both 3-HT and 5-HT have been demonstrated to enhance cell proliferation (Martelly *et al.*, 1981; Martelly & Franquinet, 1984), whereas a 5-HT derivative, melatonin, is known to inhibit asexual reproduction (Morita & Best, 1984c). Four sequences for putative G protein-coupled 5-HT receptors have also been identified from *Girardia tigrina* and show significant sequence homology to *Drosophila* and human G-protein coupled receptors (Saitoh *et al.*, 1997). During differentiating of neurons in *Girardia tigrina*, serotonin and dopamine presumably act through these G-protein coupled receptor to enhance intracellular cAMP levels via adenylyl cyclase. There is evidence that 3-HT and 5-HT signals are transduced by an intracellular cAMP-dependent kinase (PKA) signalling cascade (Martelly *et al.*, 1981), and 5-HT may also act through a CaM-kinase dependent cascade (Moraczewski,

1981; Morawska *et al.*, 1984; Martelly *et al.*, 1986). The concentrations of PKA and CaM-kinase within regenerating fragments peak during the first 18 h in culture and remain elevated for several days (Martelly *et al.*, 1981). These protein kinases might then modulate other as yet unidentified enzymes that control RNA and DNA synthesis, and influence transcription and translation (Martelly & Franquinet, 1984). Martelly & Franquinet (1984) show that 5-HT applied alone inhibits RNA synthesis but when 5-HT is applied in conjunction with DB-cAMP, RNA synthesis is recovered. This is consistent with my findings that 5-HT alone had no effect on neoblasts, but when applied with DB-cAMP, neuronal tubulin expression was promoted. Our data show that biogenic amines induced signalling in differentiating neoblasts to regulate expression of at least two types of proteins, neuronal tubulin and Vg-K⁺ channels. The rapid changes in morphological and electrophysiological characteristics occurring during the first 24 h of differentiation suggest that transcripts for these proteins could already be present in neuroblasts. Future studies should target the assortment of genes activated during neuronal differentiation.

Intracellular signalling via a protein kinase C (PKC) cascade has also been implicated to regulate neoblast activity and regeneration in planarians. Regeneration is enhanced when wounded animals are exposed to treatment with substance P by a specific membrane receptor that is presumed to activate a typical PKC signalling cascade (Salo & Baguna, 1986). Phorbol ester treatment of intact worms induces abnormal tumour-like growths, similar to those observed in mammals, suggesting that PKC may regulate cellular activity and proliferation in a similar manner (Nishizuka, 1984; Hall *et al.*, 1986a, 1986b). When *G. tigrina* neoblasts were treated with the phorbol ester PMA, a potent activator of PKC, there was no increase in neuronal tubulin expression. This implies that PKC signalling may not be important during the earliest stages of neural fate-specification and differentiation. DB-cAMP and IBMX application was expected to increase intracellular cAMP levels and activated PKA signalling, but when applied alone also had no effect on tubulin synthesis. Interestingly, when PMA was applied with DB-cAMP and IBMX, neoblasts were induced to express neuronal tubulin. This suggests that one of these signalling pathways might regulate fate-specification and the second pathway may

control tubulin expression. These results draw attention to the role of multiple factors in controlling different aspects of neural differentiation.

3.4. Cocktail treatments combining different factors are effective in promoting neurogenesis

The application of a single morphogenic factor was often insufficient in promoting neural differentiation in *G. tigrina* (**Table 4**). However, when those same factors were applied in conjunction with other agents (especially those increasing intracellular cAMP), neuronal tubulin expression was enhanced. This is very common among neural progenitors in the developing mammalian spinal cord and adult brain and in embryonic stem cells, where multiple factors are often required to induce differentiation (Bogler *et al.*, 1990; Gritti *et al.*, 1996; Liem *et al.*, 1997; Schuldiner *et al.*, 2000). The process of neural development requires independent cues to induce fate-specification and to activate differentiation (Lillien & Cepko, 1992; Murphy *et al.*, 1994; Lillien, 1998).

Our results show that cAMP dependent pathways are critical for controlling either fate-specification or inducing differentiation. When either bFGF or 5-HT was applied alone, neoblasts did not begin to differentiate morphologically, whereas when they were applied with DB-cAMP and the phosphodiesterase inhibitor IBMX, neoblasts began to express neuronal tubulin. This suggests that cAMP-dependent signalling is required for neoblasts to express receptors for bFGF and 5-HT. Artificially elevated intracellular cAMP may mimic the activity of an as yet unidentified receptor's function. Although no signalling pathways have been fully characterized from any flatworm cells, there are many extracellular-signal-regulated kinases that may control neurogenesis. Tyrosine kinase receptors (Trks) have been shown to mediate neurotrophin induced signals for cell survival, differentiation, exit of the cell cycle and apoptosis (Kaplan, & Miller, 1997; Tessarollo, 1998). At least one type of Trk has been indirectly demonstrated in flatworms, with one type responsive to nerve growth factor. When intracellular cAMP levels were artificially elevated in *G. tigrina*, this may have activated a signalling

pathway involved in regulating neural fate-specification (Robinson & Cobb, 1997; Benoit *et al.*, 2001), and application of the additional morphogens may have induced differentiation. It will be important to determine what intracellular signalling pathways are active during neurogenesis, and to determine the specific function of these cascades.

3.5. Neuritogenesis and neurogenesis are initiated by different morphogens

A small proportion of developing neurons in *G. tigrina* begin to sprout neurites in response to exogenously applied morphogenic factors. Because such a small number of developing neurons began sprouting neurites, it is probable that neurogenesis and neurite production in flatworms are controlled by different substances. Neurite production is not an early developmental event such as expression of tubulin or Vg-K⁺ channels, and requires additional cues. Although upwards of 30% of neoblasts began expressing neuronal tubulin after 24 h treatments using dibutyryl-cAMP, IBMX, and 5-HT, only a relatively small percentage of those cells (~10%) also began sprouting neurites. Cells that sprouted neurites may represent neuroblasts already fate-specified, and treatment with the morphogens functioned only in promoting neurite outgrowth. As described above, the actions of 5-HT are presumed to be mediated through a cAMP-dependent pathway in flatworms (Martelly & Franquinet, 1984), and cAMP-dependent signalling has been shown to regulate neurite outgrowth in mammals (Tojima *et al.*, 2003). Serotonin also been shown to promote neurite outgrowth in both invertebrate (Goldberg *et al.*, 1992) and vertebrate (Lieske *et al.*, 1999; Lotto *et al.*, 1999) systems. Our results show that in fate-specified neuroblasts, cAMP alone was sufficient to promote neurite outgrowth. These artificially elevated cAMP levels may have mimicked the effect of a membrane receptor and stimulated the effects of an extracellular-signal-regulated kinase (ERK) (Grewal *et al.*, 1999).

Several factors may explain why there were only a small proportion of neurons developing neurites. First, it has been shown that many potential morphogens inhibit neurite outgrowth. In mature brain neurons of *Notoplana atomata*, neurite outgrowth is

regulated by both bFGF and 5-HT. The initiation of neurite production and the development of growth cones was enhanced in a dose-dependent manner by these factors, however, neurite extension and elongation are inhibited (**Appendix 1**). There are many examples of neurite outgrowth inhibition induced by 5-HT in both invertebrates (Haydon *et al.*, 1984; 1987; McCobb *et al.*, 1988; Murrain *et al.*, 1990) and in vertebrates (Lankford *et al.*, 1988; Liebl & Koo, 1993; Lima *et al.*, 1994). Levels of cAMP are also important during neurite elongation, low concentrations can promote outgrowth whereas higher levels cause inhibition (Song & Poo, 1999). Secondly, there may be separate cues for fate-specification and neurite outgrowth. Some factors when applied together may have interactive effects (McCobb *et al.*, 1988) and there are growth factors that may regulate neurite outgrowth that were not examined in this study. Nerve growth factor may be an important regulator of neurite outgrowth in flatworms. When wounded, *Dugesia gonocephala* are exposed to NGF, and there is a considerable increase in the neuronal processes in regenerating tissue (Palladini *et al.*, 1988). This is similar to the responses observed both *in vivo* and *in vitro* from the vertebrates (Levi-Montalcini & Booker, 1960; Levi-Montalcini & Angeletti, 1968; Campenot, 1977) and invertebrates (Ridgeway *et al.*, 1991). NGF is known to activate Trk receptors that can regulate neurite outgrowth (Kimpinski *et al.*, 1997), but Trk receptors have not yet been found in the flatworms. Trk receptors activated by NGF have been shown to activate multiple signalling pathways including those involving phospholipase C (reviewed by Greene & Kaplan, 1995), resulting in activation of PI3-kinase, Ras, and MAPK (Kaplan & Miller 1997; Robinson & Cobb, 1997). The treatments in this study of *G. tigrina* did not target these signalling cascades and may explain the lack of significant neurite outgrowth.

Substrate is also an important regulator of neurite outgrowth. In *Dugesia japonica*, poly-L-lysine, fibronectin, and laminin have all been shown to promote neurite outgrowth in dissociated brain neurons (Asami *et al.*, 2002). Substrate-dependent neurite outgrowth has also been well documented in other systems (Sanes, 1989; Miller & Hadley, 1991; Wildering *et al.*, 1998; Hopker *et al.*, 1999). Microfilament interactions can also be important for neurite initiation (Sutter & Forscher, 2000; Tang & Goldberg, 2000;

Rodriguez *et al.*, 2003), but it remains unknown whether developing neuroblasts in our system have begun to express actin. Lastly, Vg-ion channels and excitability have been shown to play important roles in directing neurite outgrowth in invertebrates (Cohan & Kater, 1986; Cohan *et al.*, 1987; Mattson & Kater, 1987; Benquet *et al.*, 2001) and vertebrates (Gu & Spitzer, 1995; Peterson & Cancela, 1999; McFarlane & Pollock, 2000; Ming *et al.*, 2001), but the differentiating neurons I observed had not yet expressed detectable inward currents and were not excitable.

It is likely that regenerating neurons and developing neuroblasts can often be exposed to similar signals (Wilkgren, 1990; Halton & Maule, 2004), but it will be important to determine what receptors are expressed in each subtype of neuroblast, and whether they can activate similar signal transduction pathways. In the future it will be possible to use the *G. tigrina* culture system to specifically target fate-specified neuroblasts and treat with factors presumed to only control neurite outgrowth in order to separate the different roles of the tested morphogens in promoting fate-specification and neuritogenesis.

4. Early developmental changes in electrical properties of differentiating neurons

In the present study, the first electrophysiological recordings and measurements were made from stem cells in flatworms. I was able to establish a baseline profile of the resting membrane properties of *G. tigrina* neuroblasts and showed that undifferentiated cells do not exhibit any changes in the membrane time constant, capacitance, or resting membrane potential when cultured. These properties have been shown to remain unchanged in mammalian neural progenitor cells prior to differentiation (Amagai *et al.*, 1983; Hogg *et al.*, 2004). However, the resting electrical profile of neuroblasts changed rapidly and dramatically during the first day of neuronal differentiation, and these changes could be related to the expression of cytoskeletal proteins and Vg-ion channels during neurogenesis. As developing neurons began to express Vg-K⁺ currents the activation kinetics of these channels did not change, but the magnitude of whole-cell

currents increased, presumably due to an increase in the number of channels expressed. The importance of obtaining an electrophysiological profile is highlighted by certain distinguishing characteristics of neoblasts. Most notable is the relatively unpolarized resting membrane potential of undifferentiated neoblasts.

As cells develop to become excitable, we would expect to observe a decrease in the input resistance and a change in the membrane capacitance if cell size also changes (Junge, 1992; Grigaliunas *et al.*, 2002). No changes in the input resistance due to treatment with 5-HT, DBcAMP, and IMBX, nor by expression of Vg-K⁺ channels was seen in *G. tigrina*, but this might be expected as the cells had not yet become excitable. Also, the input resistance may not begin to decrease until inward currents begin to develop (Ziskind-Conhaim, 1988). Membrane capacitance was also unaffected by morphogenic treatments or expression of K⁺ channels, suggesting that membrane complexity and folding was not occurring. The membrane capacitance began to increase in cells sprouting neurites, but not significantly, most likely because extensions remained relatively short over the time period examined.

4.1. Hyperpolarization of the resting membrane potential

The resting membrane potential of undifferentiated neoblasts was relatively unpolarized, which is often interpreted as a damaged plasma membrane in unhealthy cells. Although relatively depolarized resting membrane potentials are not as uncommon as might be expected (Amagai *et al.*, 1983; Jensen, 1987; Skalióra *et al.*, 1993; Reiff & Guenther, 1999), there was evidence that *G. tigrina* neoblast cultures were relatively healthy. First, the membranes were intact, as shown by our Trypan blue viability assay. Furthermore, our estimation of resting membrane potential may have been underestimated due to our use of the whole-cell patch clamp configuration (Mathias *et al.*, 1990; Magistretti *et al.*, 1996; Tyzio *et al.*, 2003). However, I have shown that using an independent measure of resting potential, namely sharp electrode recordings, gave similar values, and that co-cultured muscle cells had hyperpolarized membrane potentials similar to those previously

described in *Girardia tigrina* (Corbett & Day, 2003). Lastly, the resting membrane potential did become hyperpolarized after neurons began to express Vg-K⁺ channels during neuronal differentiation. Polarization of the membrane potential has significant effects on membrane excitability. Specifically, hyperpolarized membrane potentials can contribute by increasing the proportion of Vg-channels available to produce depolarizing currents by removal of inactivation. Conversely, a depolarized membrane potential could increase excitability by activating high-voltage activated inward currents, such as Vg-channels producing transient Ca²⁺ currents that are necessary in regulating early developmental events (Cohan *et al.*, 1987; Komuro & Rakic, 1998; Gomez & Spitzer, 1999; Borodinsky *et al.*, 2004).

Changes in the resting membrane potential may have arisen due to changes in the selective permeability of the membrane to ions. We demonstrate that membrane permeability of K⁺ is altered through the expression of delayed rectifier channels. At the resting membrane potentials recorded from undifferentiated neoblasts, the K_{DR} channels would be open and explain in part the hyperpolarization observed. Additionally, there may have been an increase in the expression of leak channels permeable to K⁺ that could also have resulted in a hyperpolarization (Salkoff & Wyman, 1981; Hille, 2001). However, the changes in resting K⁺ conductance do not entirely explain the shift in membrane potential, since untreated neoblasts develop K_{DR} channels, but do not show a significant increase in the resting membrane potential. It is likely that a Na⁺/K⁺-ATPase is also expressed or activity increases during early neuronal differentiation. These electrogenic pumps have been shown to hyperpolarize the resting membrane potential (Trotier & Doving, 1996; Volkov *et al.*, 2000; Hille, 2001). Previous studies have shown that treatment with 5-HT and growth factors can regulate the expression and activity of Na⁺/K⁺-ATPases causing the membrane to hyperpolarize (Broadie & Sampson, 1986; Hernandez, 1992). Also, Na⁺/K⁺-ATPases have been shown to be developmentally regulated during neuronal differentiation in Purkinje neurons of both pre- and postnatal rats (Molnar *et al.*, 1999; Biser *et al.*, 2000), thus it would seem likely that they also contribute to the change in resting membrane potential we have observed in flatworm

neoblasts. Future studies should focus on separating the relative effects of selective ion permeability vs. the actions of an electrogenic pump in regulating membrane potential. This could be achieved by changing extracellular K^+ concentrations and by using the selective inhibitor of Na^+/K^+ -ATPases, ouabain, to determine if any shifts in the resting membrane potential result.

4.2. Expression of delayed rectifier K^+ channels

This study reveals that the first Vg-ion channels expressed in neoblasts differentiating into neurons are delayed rectifier K^+ channels. We show that nearly 50% of neoblasts already possess K_{DR} channels at the time of isolation. K_{DR} channels are also expressed in undifferentiated stem cells from the mouse embryo (Simonneau *et al.*, 1985), human neural progenitors (Luskin *et al.*, 1999; Piper *et al.*, 2000), and oligodendrocyte progenitors in the rat CNS (Borges *et al.*, 1995). The presence of delayed rectifier K^+ channels alone may not be indicative of neural differentiation (Hribar *et al.*, 2004), since they are also expressed in many non-neuronal cells (Rudy, 1988). By applying 5-HT exogenously and elevating intracellular cAMP levels, we could induce 30% of the remaining neoblasts to also express K_{DR} channels. There was also an increase in cells expressing K^+ channels under control conditions, but treatment induced neoblasts to express K^+ currents sooner. Thus, expression of K^+ channels may have been in a response to specific culture conditions, and possibly due to osmotic shock induced gene expression (discussed above). The proportion of neoblasts expressing Vg- K^+ channels increased within 5 h revealing rapid activation of gene expression.

There was no time-dependent change in the activation kinetics measured from K_{DR} channels in differentiating neoblasts and the activation kinetics did not differ from those recorded in mature brain cells. Potassium channels found in *Girardia* have a markedly rightward shifted voltage of half-activation, wider range of activation, and more rapid rate of activation when compared to other delayed rectifier channels (Hille, 2001). These properties seem to be a common feature among Vg- K^+ channels in flatworms (Day *et al.*,

1993; Kim *et al.*, 1995; Buckingham & Spencer, 2000) and allows for both an extremely high frequency of firing in neurons and an increase in the coding range (Buckingham & Spencer, 2002). Although the activation properties of K_{DR} channels recorded from neoblasts have similar kinetics of activation, the magnitude of currents was much smaller than those recorded from brain neurons. Although both neoblasts and adult brain neurons were similar in size, whole-cell currents from adult brain cells were 3-fold larger in magnitude, indicating that maturation of K^+ currents took longer than 24h.

In this study, I observed a morphogen-induced increase in the size of whole-cell delayed rectifier currents that was not observed in the control. During differentiation of neoblasts there was a substantial increase in the mean current density that may have been due to either an increase in the number of channels expressed, or due to an increase in the single channel conductance of K_{DR} channels. Increases in the magnitude of delayed rectifier K^+ currents are observed during the first few days of differentiation in the medicinal leech (Schirmacher & Deitmer, 1989; 1991), *Drosophila* (Salkoff & Wyman, 1981; 1983; Salkoff, 1985), ascidians (Dallman *et al.*, 1998; Dallman *et al.*, 2000), *Xenopus* (O'Dowd *et al.*, 1988; Ribera & Spitzer, 1990), chick (Bader *et al.*, 1983; 1985), and rat (Ziskind-Conhaim, 1988; Gao & Ziskind-Conhaim, 1998). In all these examples, delayed rectifier K^+ channels are important in shaping developing excitability, and are always expressed after neurite initiation.

Developing neurons most often express Vg- K^+ channels before any other type of Vg-ion channel, but K^+ currents often arise simultaneously with inward currents to give rise to AP's and produce an excitable cell (Olson, 1996; Baines & Bate, 1998; Spitzer *et al.*, 2000; Bahrey & Moody, 2003). The appearance of K^+ currents before inward currents and action potentials is presumably important in preventing hyperexcitability and Ca^{2+} -induced toxicity (Meyer, 1989). Over the time course of our study, we never observed inward currents in differentiating neoblasts, suggesting that K_{DR} channels were important in regulating early developmental events. The increase in transient K^+ current size occurred concurrently with the expression of neuronal tubulin and before neurite

initiation, thus, they may function in regulating morphological development. The increase in delayed rectifier current may also have contributed to the developmental hyperpolarization of the resting membrane potential (see above). We did not test whether delayed K^+ channels contributed directly to the resting membrane potential, but this has been shown to occur by blocking K_{DR} with Ba^{2+} in rat embryonic spinal neurons (Nakamura *et al.*, 2001). However, flatworm K_{DR} channels can not be blocked by either Ba^{2+} or pharmacological agents (e.g. TEA⁺ or 4-AP) (Buckingham & Spencer, 2000; data from this study not shown), thus, we could not test this assumption. Once efficient pharmacological blockers for flatworm K_{DR} channels are discovered, their role in setting the resting membrane potential and in promoting morphological development can be examined.

4.3. K_A channels are expressed in neoblasts developing neurites

Transient outward currents resembling those produced by typical A-type K^+ channels were observed in a small group of differentiating neurons. A-type currents were only observed in cells that also possessed a non-inactivating K^+ current. The currents activated extremely rapidly, but with a similar time course as the sustained outward current. We did not test the pharmacological sensitivity of these currents, but similar channels reported from the flatworms suggest they might be blocked by 4-AP, and are insensitive to TEA⁺ (Blair & Anderson, 1993; Day *et al.*, 1994; Kim *et al.*, 1995; Buckingham & Spencer, 2000). The precise role of K_A currents in shaping excitability in flatworms has not yet been determined, but these channels seem to be expressed only in cells with either distinctive morphologies or with specific electrophysiological properties.

In *G. tigrina*, K_A currents were expressed in approximately 10% of differentiating neurons, and were only ever found in cells extending neurites. In the marine triclad *Bdelloura candida*, K_A currents are only observed in 5% of dissociated brain neurons, and also only in cells that developed axons (Blair & Anderson, 1993). Combined with observations that K_A channels are restricted to cells with neurites in the marine polyclad

Notoplana (Buckingham & Spencer, 2000), it might be assumed that K_A channels function to regulate the distinctive high frequency-firing patterns in axons. But unlike many I_A currents that allow for high-frequency firing in vertebrate systems (Liu & Kaczmarek, 1998; Wang *et al.*, 1998), modelling experiments have shown that high-frequency firing in flatworm neurons is not dependent upon the expression of I_A (Buckingham & Spencer, 2002). Instead these authors suggest that K_A channels function in regulating spatially localized currents in dendrites. Muscle cells from *Schistosoma* also express K_A channels, but only in cells that exhibit complex branching morphologies (Day *et al.*, 1993).

The results demonstrating that K_A channels are only expressed in cells developing distinctive morphologies is commonly observed in other systems. I_A is expressed early during the developmental of hippocampal pyramidal neurons, shortly after neuronal morphology is recognizable (Wu & Barish, 1992), and K_A channels are expressed during membrane expansion (Wu *et al.*, 1998). Morphological changes occurring during development are often accompanied by changes in the number and distribution of K_A channels (Harris *et al.*, 1992; Purves *et al.*, 1994). Changes in expression of K_A channels are also observed in regenerating axons after axotomy. In cultured neurons, expression of I_A currents increases dramatically as neurons regenerate axons after axotomy in the leech *Hirudo* (Tribut *et al.*, 1999), and in the snail *Helisoma* (Achee & Zoran, 1996), suggesting that their expression is localized to axons. Restriction of K_A channels to axons is common in invertebrates where neuronal somata often do not possess Na^+ channels, and action potentials are restricted to axons (Brismar & Gilly, 1987).

Our results demonstrate that a specific neuronal morphology influences or is coincident with the expression of a transient A-type like K^+ current. From our knowledge of when and where K_A channels are expressed in other excitable cells from flatworms, we predict that inward currents will also appear shortly after K_A currents mature further. Since no pharmacological agents have been discovered that effectively block the sustained I_{DR} , we did not observe any emerging inward currents. Also, since K_A channels are expressed in

flatworm neurons that are capable of high-frequency firing, our results suggest that we have successfully induced neoblasts to differentiate into neurons with this excitability phenotype. As neurites develop further, it will be important to monitor whether any additional changes in K_A channel expression occur.

4.5. Phylogenetic comparison of development of excitability properties

The changes in the electrical properties and the sequence of ion channel acquisition that was observed followed a specific temporal sequence suggesting a highly regulated developmental program. When treated with 5-HT and by elevating intracellular cAMP levels, differentiating neoblasts first developed more hyperpolarized resting membrane potentials that occurred concurrently with expression of neuron specific tubulin, and the appearance of a delayed rectifier K^+ current. Subsequently, developing neurons began to sprout neurite-like extensions, and expressed an A-type current. During the duration of our experiment, we never observed inward currents or action potentials. There are two important characteristics regulating excitability properties that can be compared with other animal groups. First, Vg-ion channel appeared before gross morphological changes including neurite extension. Second, K_{DR} channels were the first Vg-ion channels to appear, before cells expressed inward currents and became excitable.

This sequence of events mirrors those observed in many organisms. In the few invertebrate species studied, a very similar sequence of changes occurs in developing neurons. In the annelids, K_{DR} channels appear first, with little subsequent changes in current size or activation kinetics (Schirrmacher & Deitmer, 1991). Although these authors do not report changes in resting membrane properties or changes in K_{DR} expression, they only examined cells that had already begun to sprout neurites. This demonstrates the significance of our study system, where we could begin examining electrophysiological changes immediately after undifferentiated stem cells had been isolated. In leech neurons a K_A channel is then expressed, and I_A increases over a period of 6 days. Subsequently, both Ca^{2+} and Na^+ currents appear, and cells become excitable

(Schirrmacher & Deitmer, 1989; 1991). In two species of arthropods studied, *Drosophila* and *Schistocerca nitens*, developing neurons first develop hyperpolarized resting membrane potentials, and then express K_{DR} channels (Goodman, *et al.*, 1980; Hardie, 1991; Baines & Bate, 1998). In *Drosophila* ganglionic neurons, this is followed by expression of inward currents carried by Ca^{2+} and Na^+ , and then maturation of I_A (Baines & Bate, 1998). In developing photoreceptors from *Drosophila* and dorsal unpaired motor neurons from *Schistocerca*, expression of the K_{DR} is followed by establishment of an A-like current (Goodman, *et al.*, 1980; Hardie, 1991).

These data suggest that the sequence of developmental events occurring during neuronal differentiation have been conserved among the Lophotrochozoa and Ecdysozoa. Despite the variability in mature excitability and neurotransmitter phenotypes in these examples, they all share a similar sequence of changes suggesting that among these phyla, neurons must progress through a specific intermediate excitability platform. First, the resting membrane must become hyperpolarized which will change the proportion of channels available and remove inactivation that would arise from depolarized resting potentials. This is followed by expression of a suite of Vg- K^+ channels that may both contribute to the hyperpolarization of the resting V_m (Nakamura *et al.*, 2001), and be important in preventing hyperexcitability (Meyer, 1989).

The sequence of developmental events is similar among the invertebrate and vertebrate groups studied, except that in the vertebrates, several types of ion channels are often observed to appear simultaneously. In the developing vertebrate neurons, there appear to be two different patterns of development. In the chick and quail, Vg- K^+ channels always appear before inward currents develop (Bader *et al.*, 1983; Gottmann *et al.*, 1988), whereas in amphibians and mammals, Vg- K^+ channels appear at the same time as Ca^{2+} and Na^+ channels (Barish, 1986; Ziskind-Conhaim, 1988a; Olson, 1996; Gao & Ziskind-Conhaim, 1998; Martin-Caraballo & Greer 2000; Spitzer *et al.*, 2000; Bahrey & Moody, 2003). This second mode of development has not been observed in invertebrate systems and may reflect the differences in the complexities of invertebrate and vertebrate nervous

systems. In the latter mode of development, inward currents appear much sooner than in invertebrate examples. This may reflect the importance of spontaneous excitability that has been well described in vertebrates (reviewed by Moody, 1998; Spitzer *et al.*, 2000; Spitzer *et al.*, 2004). Emerging excitability properties are known to regulate early developmental events including fate specification (Borodinsky *et al.*, 2004), morphological differentiation (Gu & Spitzer, 1995; Ming *et al.*, 2001), migration (Kumuro & Rakic, 1998), and the maturation of the excitability phenotype (Dallman *et al.*, 1998). Vertebrate neuronal development is characterized by a progressive switch from extrinsic to intrinsic regulation of neuronal development (Edlund & Jessell, 1999), but invertebrates often develop following predictable cellular fate-maps (Sulston *et al.*, 1983; Weisblat *et al.*, 1984; Burke *et al.*, 1991). Thus, developing neurons in vertebrates may need to express inward currents and become excitable sooner in order to regulate other subsequent developmental events. In invertebrates, the nervous system is relatively simple and neuronal development can arise through a systematic sequence of genetically programmed events (Davidson, 1990)

The pattern and sequence of electrical changes also seems to depend upon the final excitability phenotype a stem cell becomes. In both invertebrates and vertebrates, neurons and muscle cells follow different sequences of changes. In both *C. elegans* and *Drosophila* muscle cells, Ca^{2+} channels are always first to appear, followed by Vg-gated and Ca^{2+} -dependent K^+ channels (Broadie & Bate, 1993b; Santi *et al.*, 2003). The appearance of inward currents before K^+ channels in muscle cells is surprising in light of what has been observed to occur during neuronal differentiation and may reflect the lineage giving rise to these cells. Here we show that neoblasts specified to become neurons acquire Vg- K^+ channels first even though they are derived from embryonic mesoderm. It will be interesting to note whether neoblasts specified to become muscle cells will express inward or outward currents first. If the intermediate excitability platforms are determined by the mature excitability phenotype (muscle vs. neuron), then we would expect that neoblasts would acquire inward currents first. However, if the

germ layer from which stem cells arise is important, then we might expect that developing muscle would express Vg-K⁺ channels first.

In developing vertebrate neurons, Ca²⁺ channels often appear before Na⁺ channels and are important in allowing for plasticity during morphological development (Gu & Spitzer, Gomez & Spitzer, 1999; Spitzer *et al.*, 2004). In contrast, because invertebrate neurons appear to rely on genetic programs, Ca²⁺-dependent signalling may not occur so early. It will also be important to examine whether the emerging excitability properties we observed are important in future developmental events such as neurotransmitter specification and synapse formation. We have developed a useful system for examining the role excitability properties play during neuronal development in the flatworms.

It must be acknowledged that the results and conclusions made in this study may not be completely representative of flatworm neurogenesis *in vivo*. The results may only partially describe the changes in electrophysiological properties occurring as neoblasts develop into neurons. Inconsistencies between *in vitro* and *in vivo* results have been observed in many aspects of neuronal development such as responsiveness to neurotrophic factors (Levi-Montalcini & Cohen, 1956; Arakawa *et al.*, 1990; Oppenheim *et al.*, 1992) and expression of Vg-channels (Kuo *et al.*, 2005). Discrepancies may arise because factors found *in vivo* are absent from the culture conditions (Becker *et al.*, 1998), leading cells to lose their mature characteristics through dedifferentiation (Perrier *et al.*, 2000). Additionally, the culturing process may disrupt the intracellular environment and result in different cellular behaviours (Sudlow & Gillette, 1997). It will be critical for future studies to address whether the results obtained here are useful in describing the changes occurring in developing neoblasts *in vivo*.

4.6 Summary of developmental changes occurring during neural differentiation

I have described a useful *in vitro* system whereby we can isolate neural progenitors and expose them to various morphogenic agents that can induce neurogenesis. I have also established baseline electrical properties in undifferentiated neoblasts and have shown that a patterned sequence of changes occurs as they develop morphologically and electrophysiologically.

Neoblasts from flatworms are induced to differentiate into neurons with application of extracellular ligands. We show that neoblasts are a heterogeneous group of stem cells that can be activated by a wide range of factors. There are probably different populations of neoblasts expressing receptors for FMRF-amide related proteins, epidermal and basic fibroblast growth factors, dopamine and serotonin. Neurogenesis requires the activity of cAMP-dependent signalling cascades and PKC activity. In response to these treatments, neoblasts begin to express a neuron-specific tubulin and in some instances sprout neurites. We would like to suggest a putative scheme for activation of neoblasts. During regeneration, severed neurons may release biogenic factors into surrounding tissues and stimulate a subset of neoblasts (those expressing the appropriate receptors for extracellular morphogens) to differentiate (Reuter & Gustaffson, 1996). Neoblasts most likely respond to gradients of cues and the axial polarity of surrounding tissues regulates the phenotypes of neurons required (Kato *et al.*, 2001; Agata *et al.*, 2003). Many morphogenic factors have been shown to exhibit pleiotropic effects (Cameron *et al.*, 1997), thus it will be important to determine the precise role of these factors in cell proliferation, differentiation, cell migration, survival, and maturation. It will also be interesting to determine how long neoblasts remain responsive to mitogenic and morphogenic compounds after they have exited the cell cycle. Neoblasts may become activated during regeneration by either osmotic shock (Baguna *et al.*, 1989), or by exposure to diffusible factors. Diffusible factors may stimulate extracellular-signal regulated protein kinase cascades involving cAMP-dependent kinase and PKC pathways

that activate expression of tubulin and Vg-K⁺ channel genes. I have developed a system where future studies can elucidate the precise signalling mechanisms activated during neuronal fate-specification.

Differentiating neurons show electrophysiological changes that follow a characteristic sequence of events shared by other invertebrates including annelids and arthropods. Differentiating neurons first develop hyperpolarized resting membrane potentials, and the first Vg-ion channels to appear are K_{DR} channels. I show that these channels may function to establish the resting membrane potential, however, a Na⁺/K⁺-ATPase may also be involved. Neurons that sprout neurites also develop K_A channels that may function to regulate spatially localized currents within axons and may also regulate neurite outgrowth. Expression of K_A channels in developing neurons suggests they will acquire a high-frequency firing phenotype that has been described in other flatworm neurons. However, the differentiating neurons in this *G. tigrina* culture system have not yet become mature, since they exhibit smaller outward currents, and have not yet begun to express inward currents. The ground work is in place for future studies that monitor the sequence of electrical changes occurring during neurogenesis, and where later developmental events can be examined.

4.7 Future directions

The first step in advancing the progress made in this study will be to follow developing neoblasts for longer periods and determine if inward currents develop. Additionally it will be of interest to know if differentiating neoblasts also express specific neurotransmitters. It will also be important to separate factors inducing differentiation from those that induce neurite-outgrowth. Future studies can also address whether the various treatments that promote tubulin expression also induce the electrophysiological changes as those described here. It will be interesting note whether the precise sequence of developmental events observed here are also expressed in neoblasts induced to differentiate using other triggers. For example, will neoblasts treated with other factors

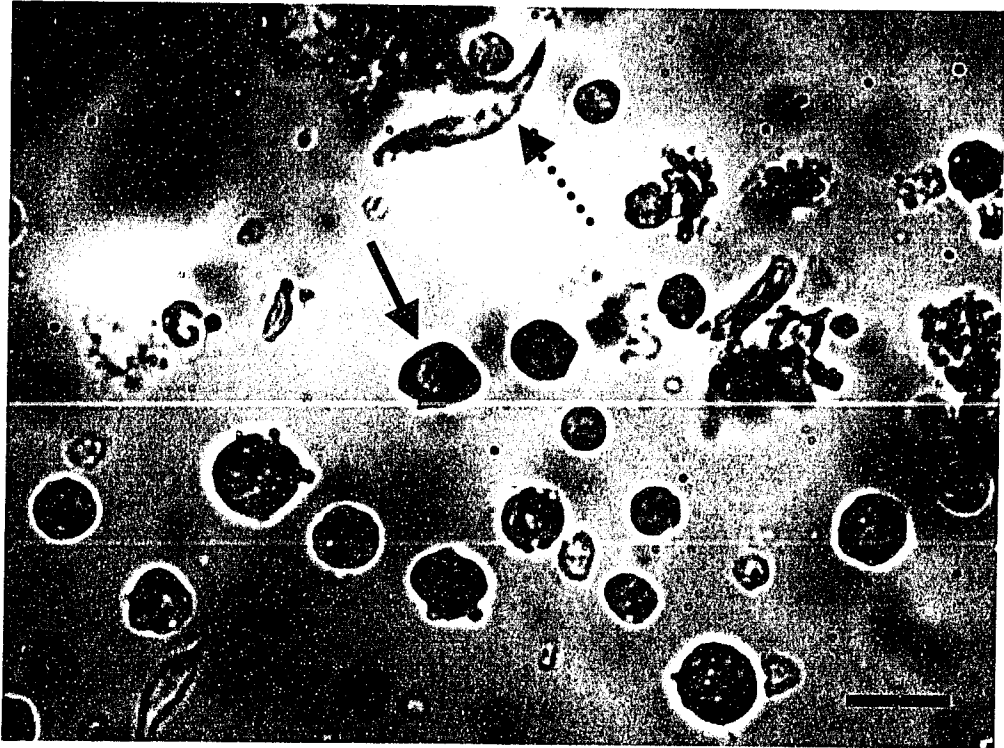
acquire similar excitability properties and show other neuronal characteristics such as neurotransmitter expression.



Figure 1. Individuals of *Girardia tigrina* used in experiments varied in length between 0.5 cm and 1.5 cm. Smaller individuals, presumably juveniles were used for whole-mount immunocytochemistry, whereas larger adults were used for cell culture experiments. Scale bar = 1 mm.

Figure 2. Identification of cultured neoblasts using histological stains or DIC microscopy. **(a)** Positive identification of neoblasts was readily made by using Lillie's (1954) buffered azure-A eosin-B staining. This method stained the prominent nucleus, which has a diameter equal to nearly 90-95% of the entire cell diameter. The thin rim of surrounding cytoplasm stained dark blue (solid arrow), as do the nucleoli. Muscle cells were found in most cultures as the main source of non-neoblast contaminating cells (dashed arrow). **(b)** Live neoblasts could also be readily identified using Nomarski DIC optics. The characteristic morphological features of neoblasts (large nucleus, and prominent nucleolus) are easily observed (solid arrow). Other contaminating cells found in the 1.07 g/ml Percoll layer were ciliated flame cells, and club cells (dashed arrow). Scale bars: 10 μ m.

(a)



(b)

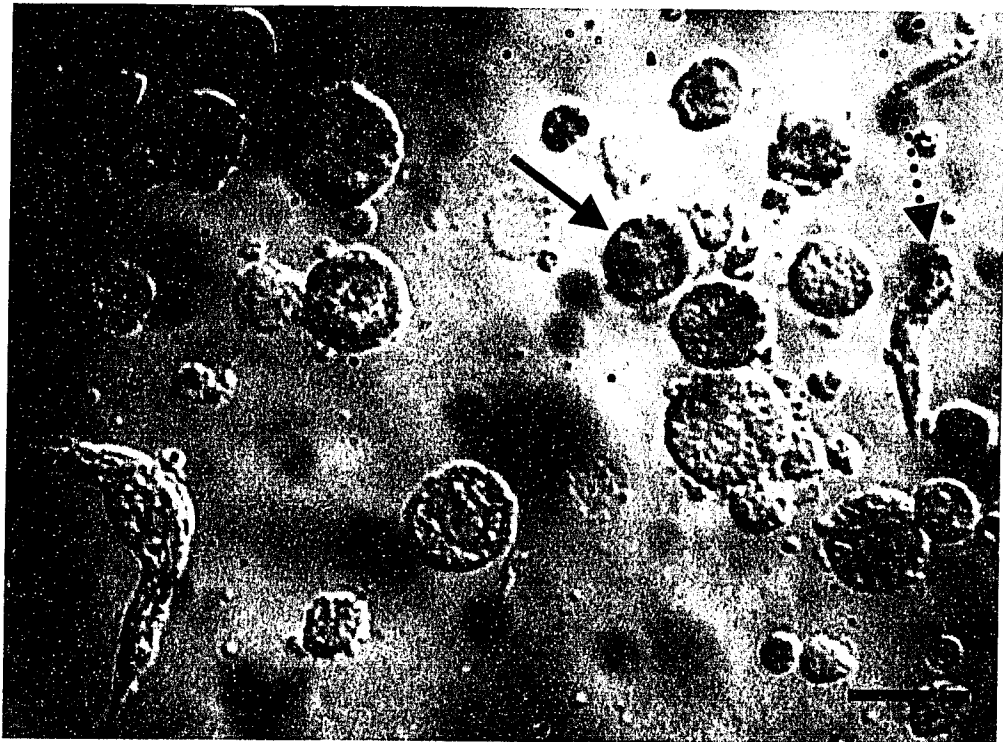
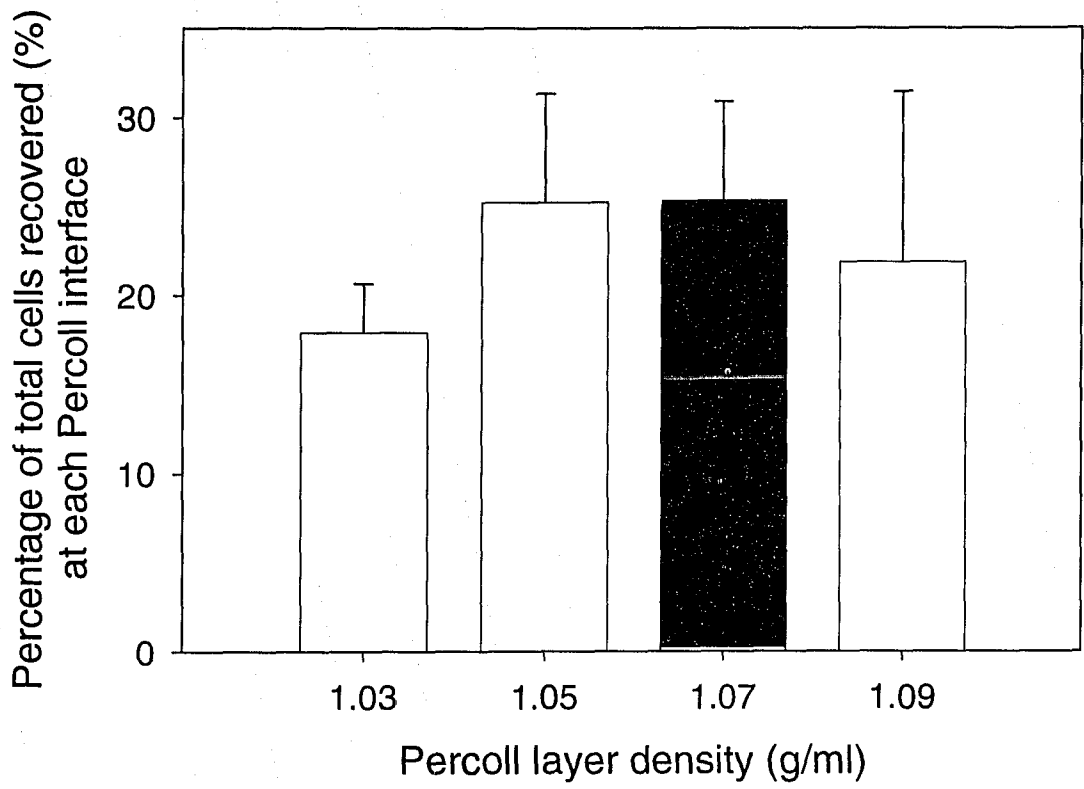
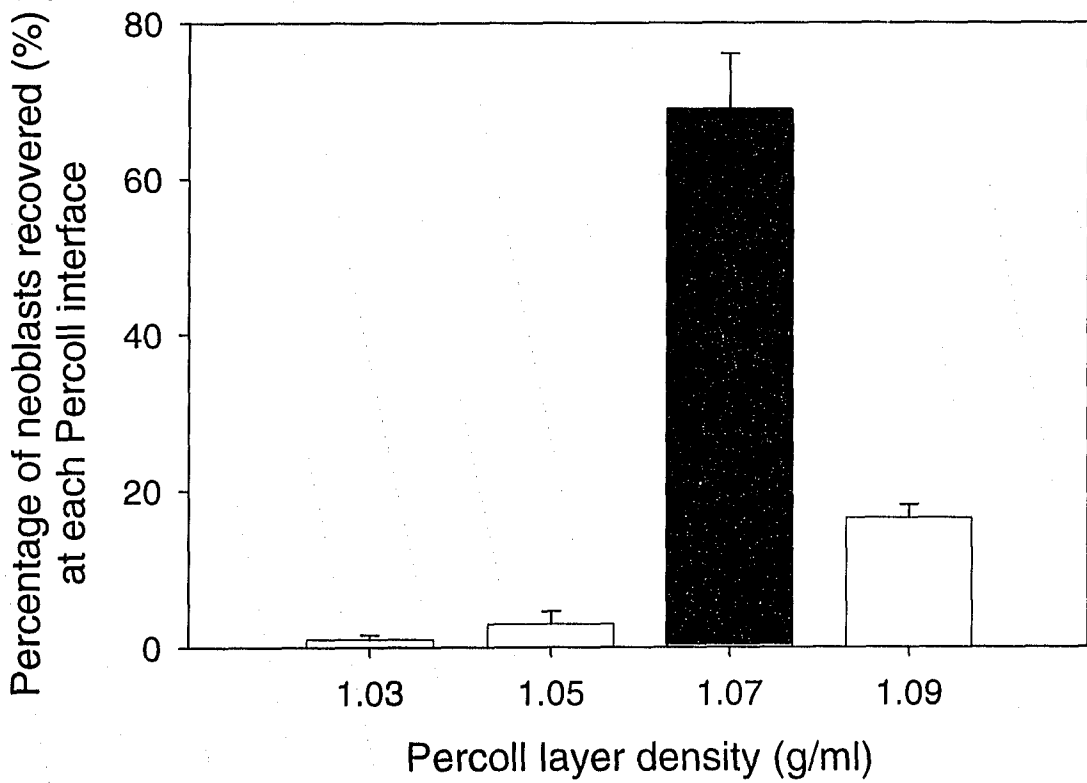


Figure 3. Isolation and purification of neoblasts from whole organism dissociations. 10-20 animals were ground and triturated into single cell suspensions and separated by density using discontinuous Percoll gradients. **(a)** The percentage of cells recovered from the boundary between each layer was similar when four discontinuous layer gradients were used to separate cells. Cells recovered from the interface at each layer were then processed for histological staining to determine the percentage of neoblasts recovered (n = 5 trials). The total number of cells does not add to 100% presumably because not all cells were found at the interfaces where cells were aspirated. The layer with the highest percentage of stem cells is in black. **(b)** Neoblasts were identified by histology and could be found in all layers, with the highest percentages in the 1.07 g/ml layer (n = 5 trials). The approximately 31.5% of contaminating cells from this density layer were comprised mainly of muscle cells, ciliated flame cells, and club cells. The layer (1.07 g/ml) treated with putative neurogenic triggers is highlighted in black. Error bars represent the S.E.M.

(a)



(b)



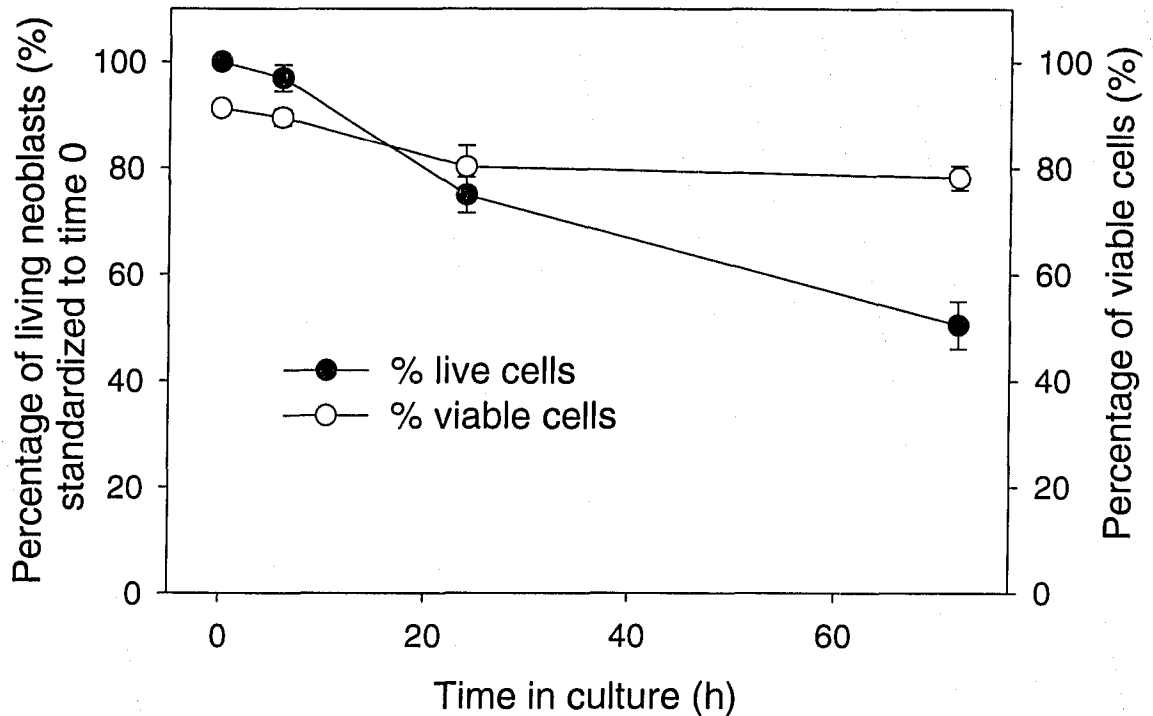


Figure 4. Cultured neoblasts remain viable, with no signs of proliferation when cultured in isotonic planarian medium on 0.01% poly-L-lysine coated glass slides. Following neoblast isolation, 2×10^4 cells were plated and the number of living cells was followed for 72 h. The percentage of living neoblasts (left axis) in primary cultures remained high after 24 h in culture ($74.9.0 \pm 3.37\%$, $n = 5$), but decreases after 72 h in culture ($50.5 \pm 4.5\%$, $n = 5$). The viability of cells (percentage of living cells as determined by a Trypan Blue exclusion assay, right axis) remains relatively high after 72 h ($78.2 \pm 2.2\%$, $n = 5$) when compared to the viability of initial cultures at 0 h ($91.3 \pm 1.3\%$, $n = 5$). Data represent 5 trials. Error bars represent the S.E.M.

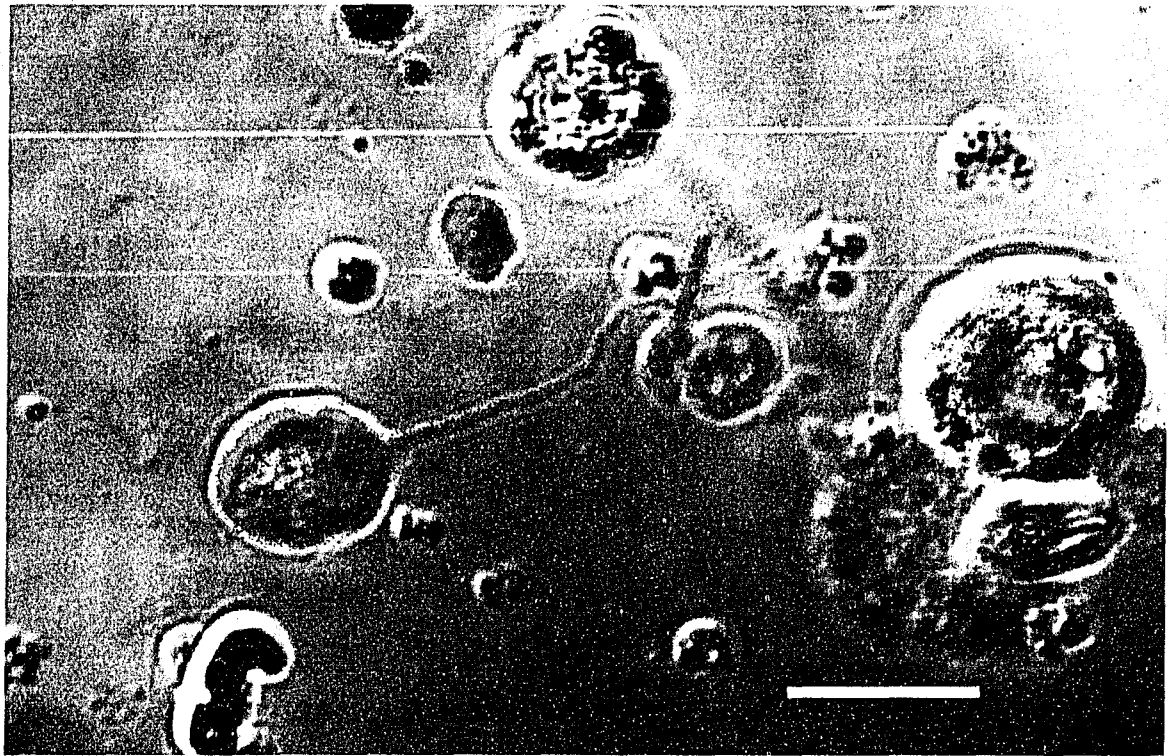


Figure 5. Cultured brain neurons are immunoreactive against the neuron-specific antibody. Nearly half of the neurons cultured on $0.0025 \mu\text{g}/\text{cm}^2$ laminin developed neurites within the first 24 h in culture. Cultured neurons varied with some monopolar (shown), bi-, but mostly multipolar morphologies. The size of neurons also varied, with the majority of cells between $3\text{-}7 \mu\text{m}$ in diameter. Scalebar: $20 \mu\text{m}$.

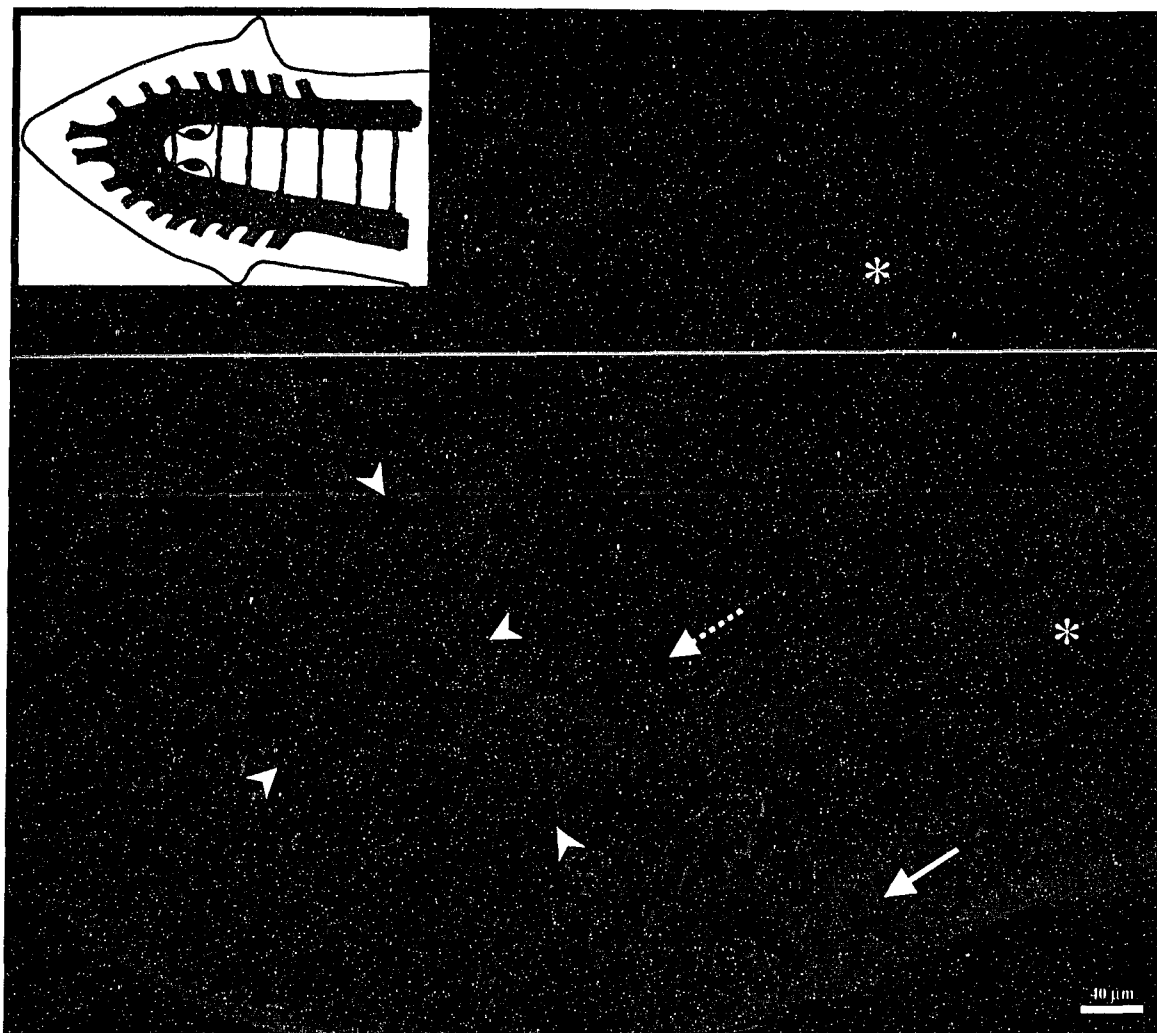
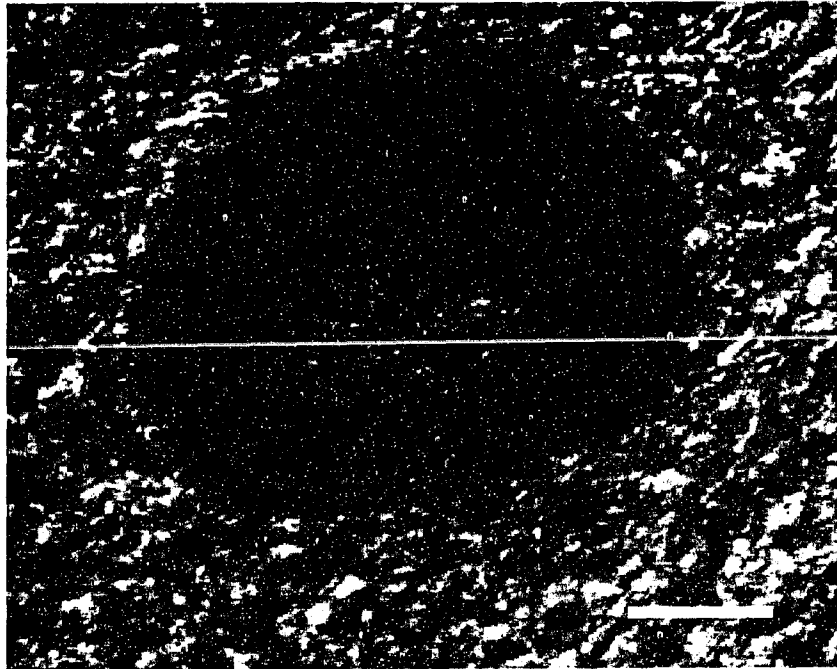


Figure 6. An antibody against α - and β -tubulin specifically labels neurons in whole-mounts of *Girardia tigrina*. The orthogonal arrangement of the nervous system that is characteristic of Platyhelminthes is apparent. The brain (arrow heads) with its series of bilaterally symmetrical nerves innervating a submuscular plexus and neurons entering the eyes (dashed arrows) and auricles (solid arrows) can be seen. Paired ventral nerve cords (asterisks) extend from the brain along the length of the body. The same antibody was used to determine if stem cells differentiated into neurons. See inset for diagrammatic representation of the brain. Scalebar: 40 μ m.

Figure 7. Neurons innervating the pigmented ocellus visualized using Tub-Ab-4 immunolabelling. **(a)** Cells within the ocellus observed in a whole mount of *Girardia tigrina* imaged using DIC microscopy are presumed to be light sensitive sensory neurons that form an optic nerve that enters the brain. **(b)** Neuronal cell bodies and axons can be labelled using the neuron-specific tubulin antibody Tub-Ab-4. Scale bars:20 μm .

(a)



(b)

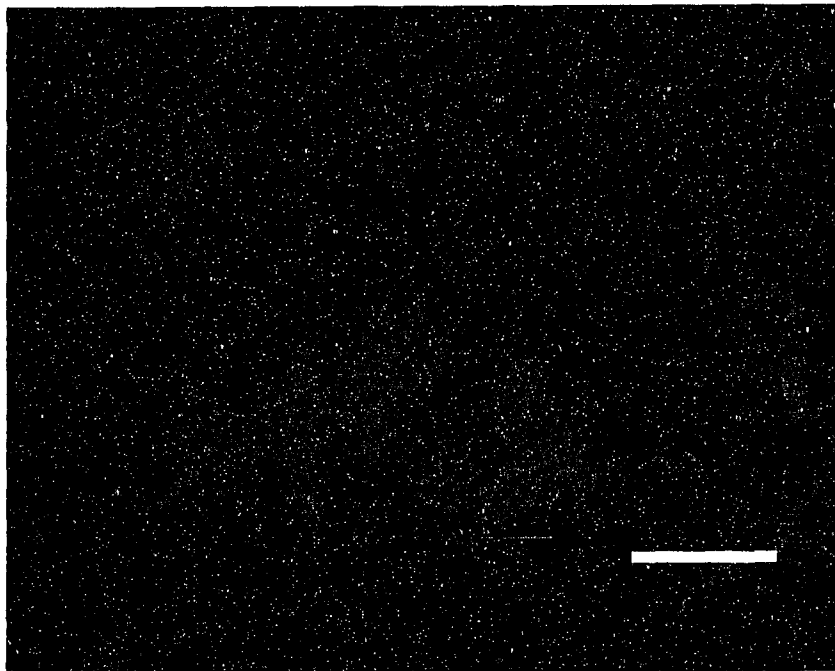
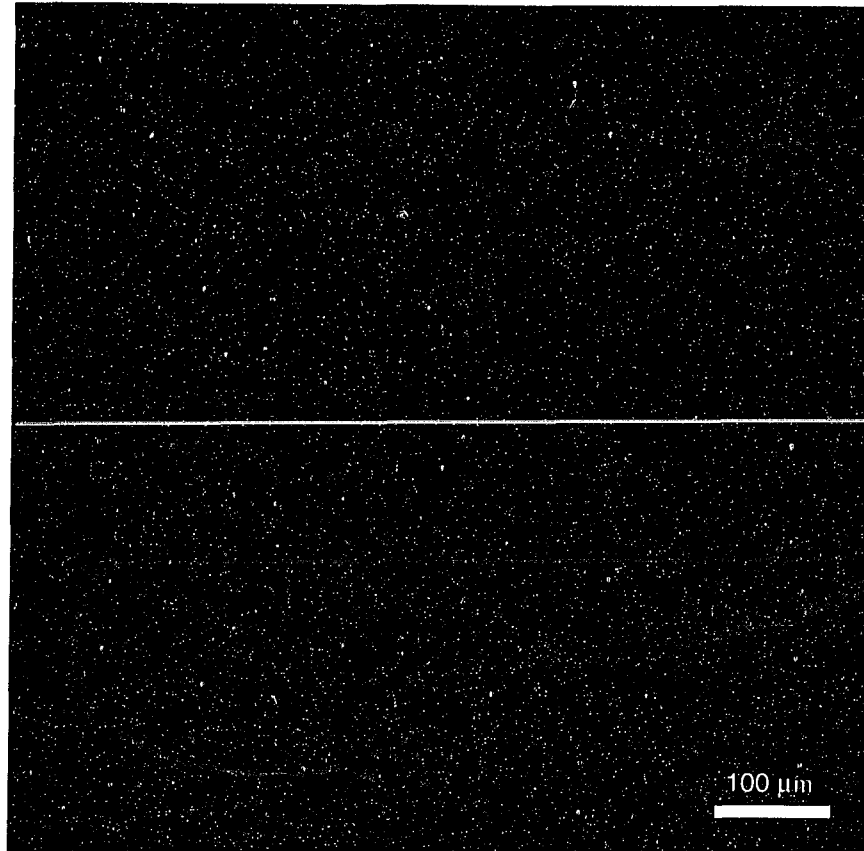
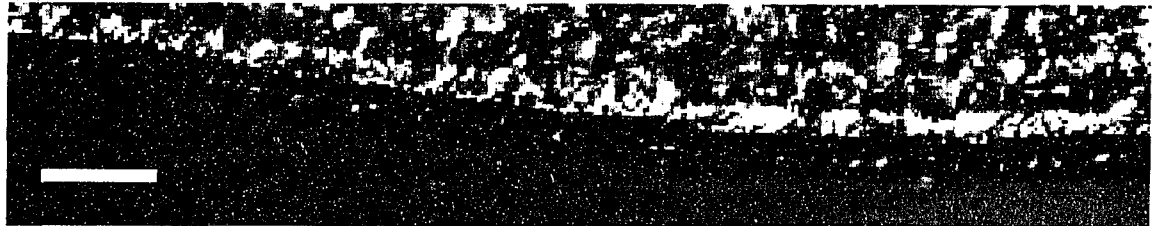


Figure 8. The ciliated margin of *Girardia tigrina* binds the fluorescent secondary antibody non-specifically in negative control treatments. **(a)** In experiments where the primary antibody reactive against tubulin was removed from the protocol, the lateral ciliated margins accumulate and bind the Alexa 488 conjugated secondary antibody non-specifically. Note that regions of the margin where no non-specific staining was observed was due to a non-flat specimen and a thin laser scanning plane of focus. **(b)** Whole mounts of worms visualized using DIC microscopy reveals a ciliated epidermis along the ventral and lateral margins of the animal. **(c)** Only the exterior margins accumulate secondary antibody, and not the underlying ciliated columnar epithelial cells. **(d)** An overlay of the images from (b) and (c) show that the fluorescence is concentrated in regions on the surface of the specimen. Scale bars: 10 μm unless otherwise noted.

(a)



(b)



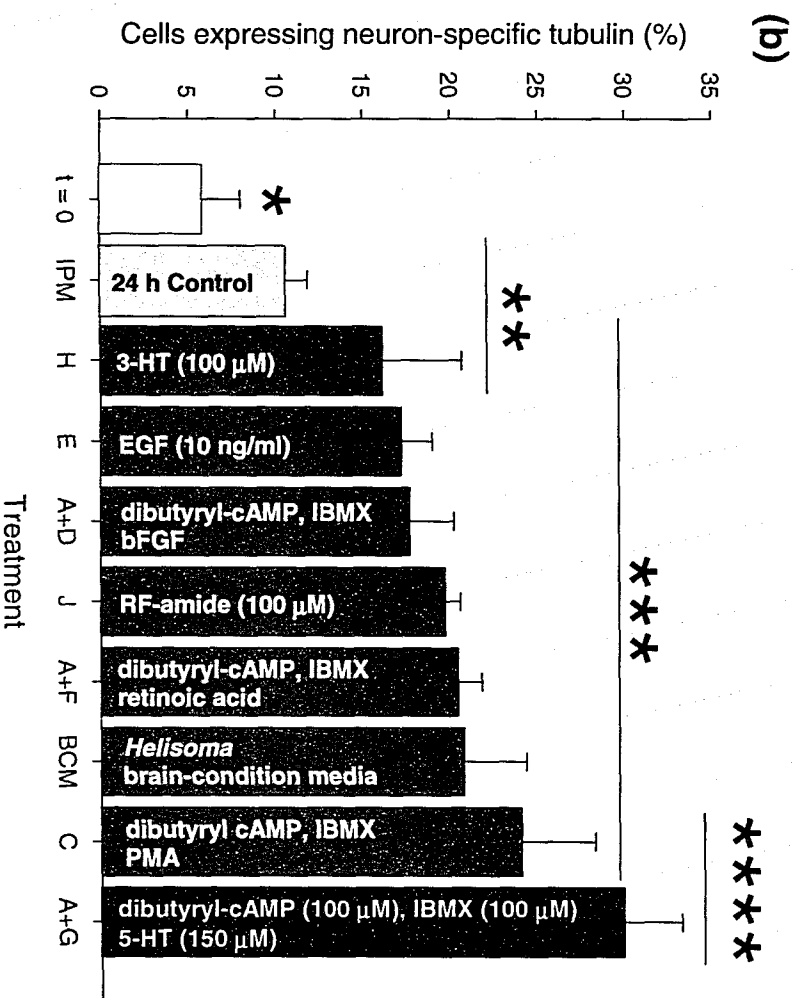
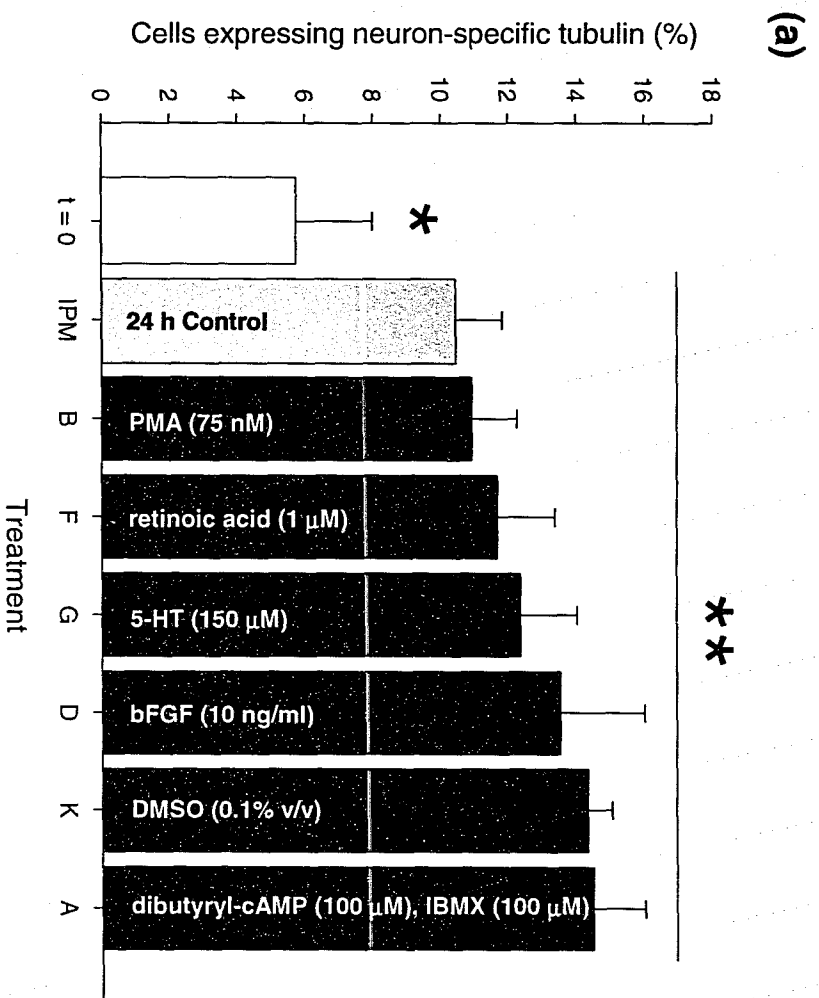
(c)



(d)



Figure 9. Effect of various putative morphogen treatments on the expression of a neuron-specific tubulin in neoblasts cultured for 24 h on 0.01% poly-L-lysine coated glass slides. The proportion of cells immunoreactive against the α -, β -tubulin Ab-4 antibody differed among treatments demonstrating their varying efficacy to induce morphological neuronal differentiation. **(a)** The proportion of cells expressing neuronal tubulin increases by approximately 2-fold under control conditions after 24 h, and several putative neurogenic agents were ineffective at inducing tubulin expression. When compared to cells immediately after dissociation, the percentage of cells expressing neuronal tubulin was statistically higher in cells cultured under control conditions and 6 additional treatments (ANOVA, $p < 0.001$, $n = 40$, Tukey multiple comparisons test, $p > 0.05$), however, there were no differences among the 6 treatments or with the 24 h control (ANOVA, $p > 0.05$, $n = 40$, Tukey multiple comparisons). White bar represents neoblasts immediately after dissociation, the grey bar represents neoblasts cultured for 24 h in control media, and the black bars represent the various putative neurogenic agents. **(b)** 8 treatments were effective in increasing the percentage of cultured neoblasts that express neuronal tubulin by up to 3 times control values (ANOVA, $p < 0.001$, $n = 50$). The 0 h and 24 h controls are the same as in the previous section. 7 treatments in dark grey increased the proportion of cells expressing tubulin by between 1.6-2.4 times when compared to the control media alone, but did not differ significantly from each other (Tukey multiple comparisons test, $p > 0.05$). The A+G treatment (black bar) induced a 3-fold increase in the percentage of neuronal tubulin expressing cells, and was significantly greater than both control, and 6 of the 7 experimental treatments (Tukey's multiple comparisons test, $p < 0.05$). Text within bars gives the morphogen and the concentration applied. Asterisks denote statistically different groups, and the horizontal lines denote treatments that did not differ significantly from each other. Error bars represent the S.E.M.



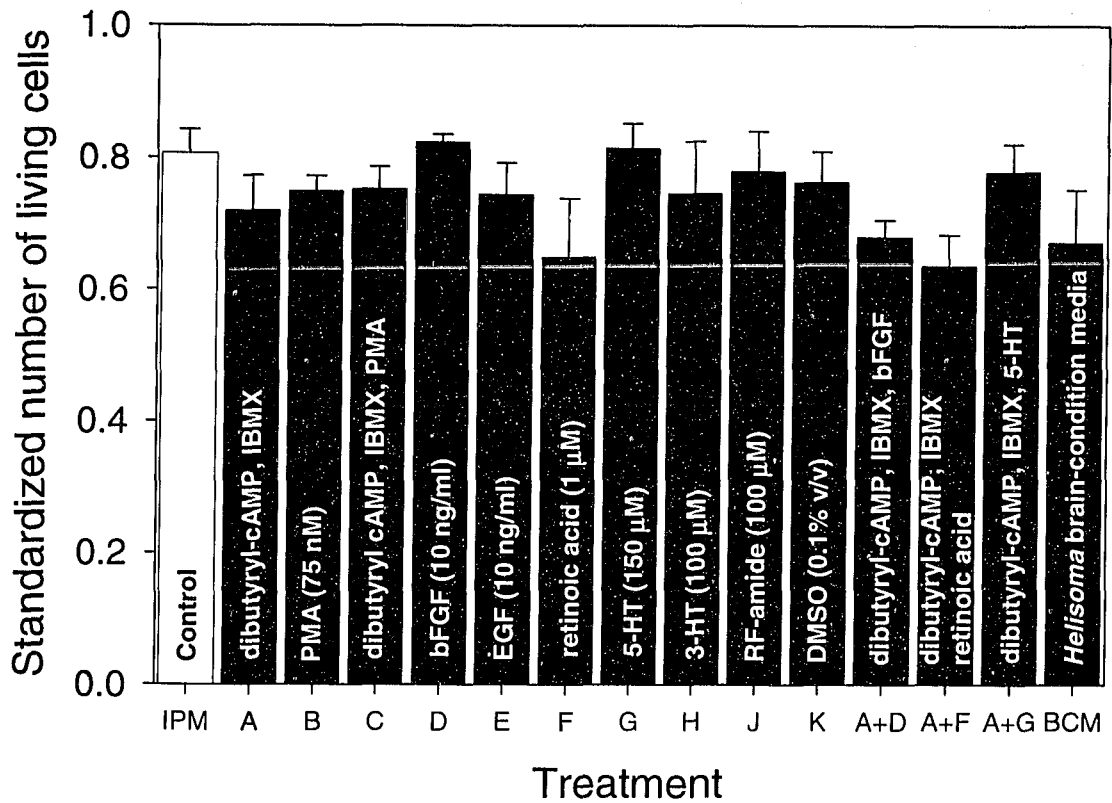
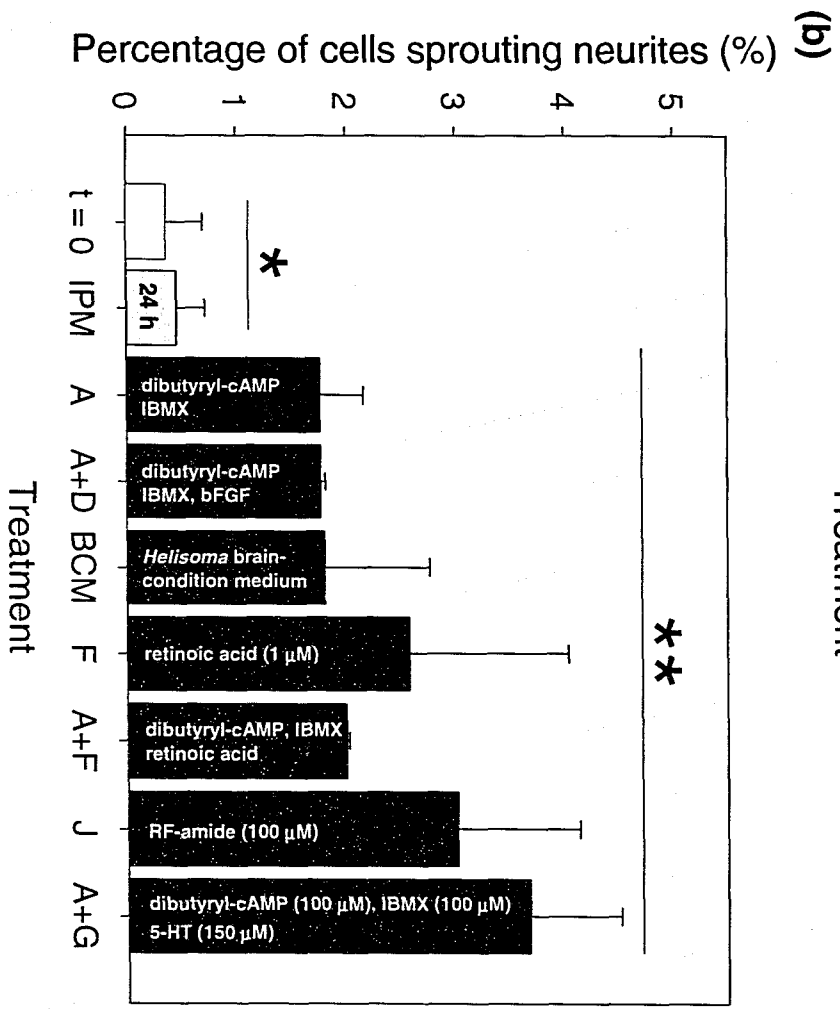
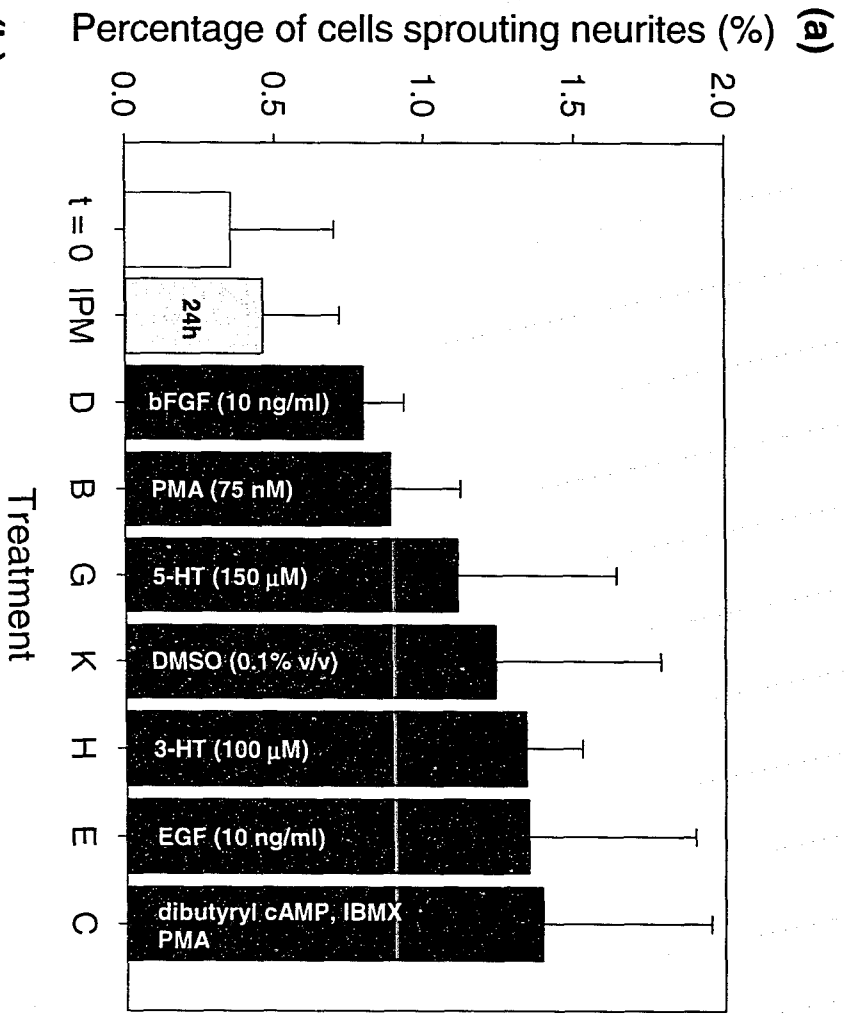


Figure 10. Effect of various morphogen treatments on viability of cultured cells after 24 h. After 24 h in culture in control isotonic media, approximately 80% of cells plated remained alive as determined by a Trypan Blue exclusion assay. The various morphogen treatments did not significantly affect the viability of cultures after 24 h in culture when compared to the control (ANOVA, $p > 0.05$, $n = 60$), and there were no differences among treatments (Tukey's multiple comparisons test, $p > 0.05$). Values are standardized to the number of living cells plated at 0 h. Error bars represent the S.E.M.

Figure 11. Treatment with morphogens induces differentiating neoblasts to develop neurite-like extensions. The percentage of cells immunoreactive against the α -, β -tubulin Ab-4 antibody, and sprouting extensions equal or greater than one soma diameter in length after a 24 h differed among treatments. **(a)** Immediately following dissociation (white bar), and after 24 h (grey bar) in control isotonic media, fewer than 0.5% of cells grew neurite-like extensions. Several treatments (7/14, black bars) had no effect on the percentage of cells sprouting extensions. (Kruskal-Wallis one-way analysis of variance, $p > 0.05$, $n = 120$). **(b)** Treatments that significantly increased the percentage of neoblasts expressing neuronal tubulin also increased the number of cells developing neurites (Kruskal-Wallis one-way analysis of variance, $p < 0.05$, $n = 120$). Treatment with A+G for 24 h induced the greatest percentage of cells ($3.68 \pm 0.84\%$, $n = 16$) to develop neurite-like extensions. Morphogen treatments are as described above. Asterisks denote statistically different groups, and the horizontal lines denote treatments that did not differ significantly from each other. Error bars represent the S.E.M.



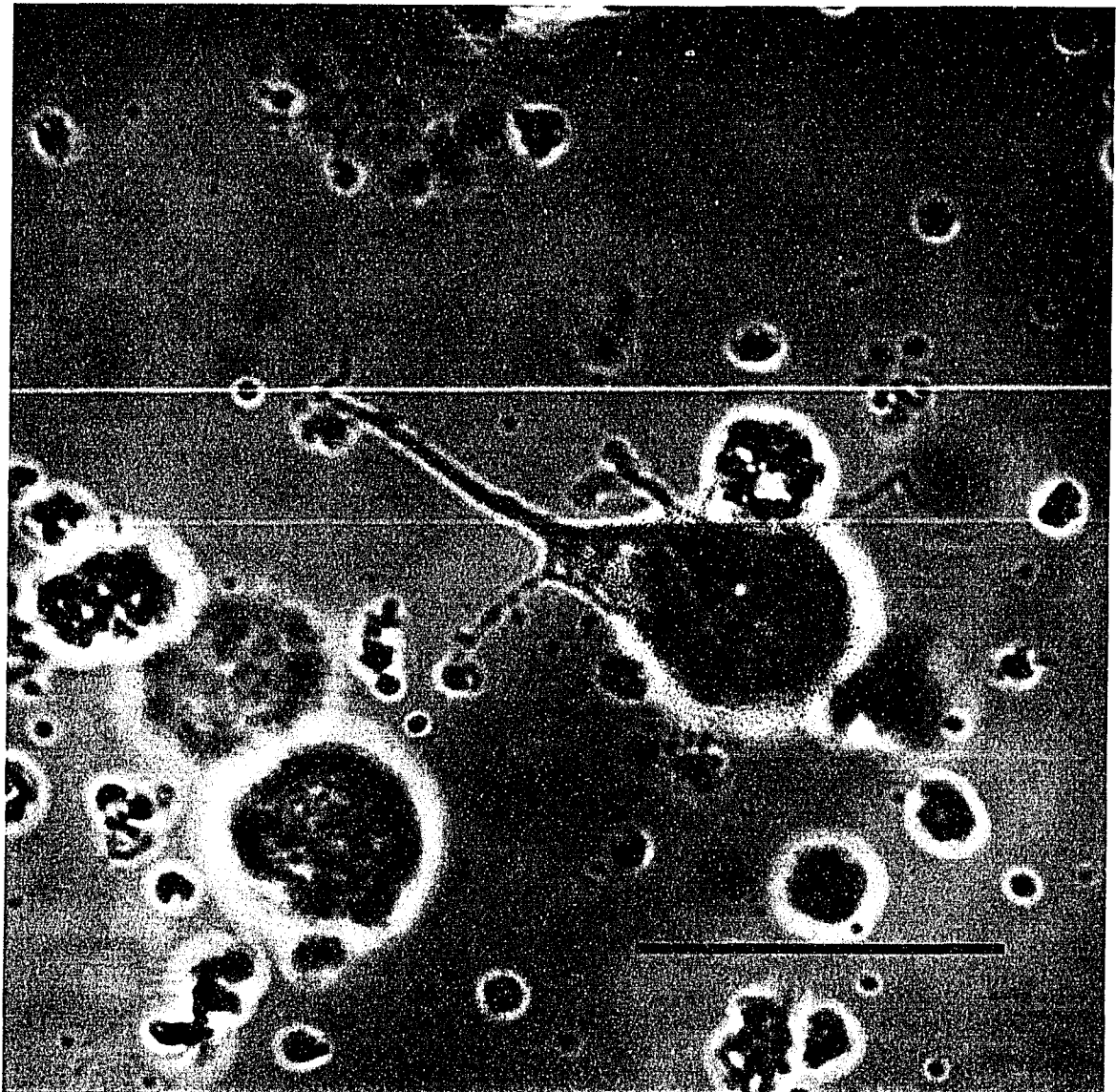


Figure 12. Differentiating neoblasts treated with A+G for 24 h develop neurite-like extensions. A small proportion of differentiating neoblasts expressing neuronal tubulin also grew neurite-like extensions. Developing cells differentiated into mono-, bi- and multipolar neurons. Only cells with extensions at least one soma diameter in length were considered as having extended neurite-like processes. Scalebar: 10 μ m.

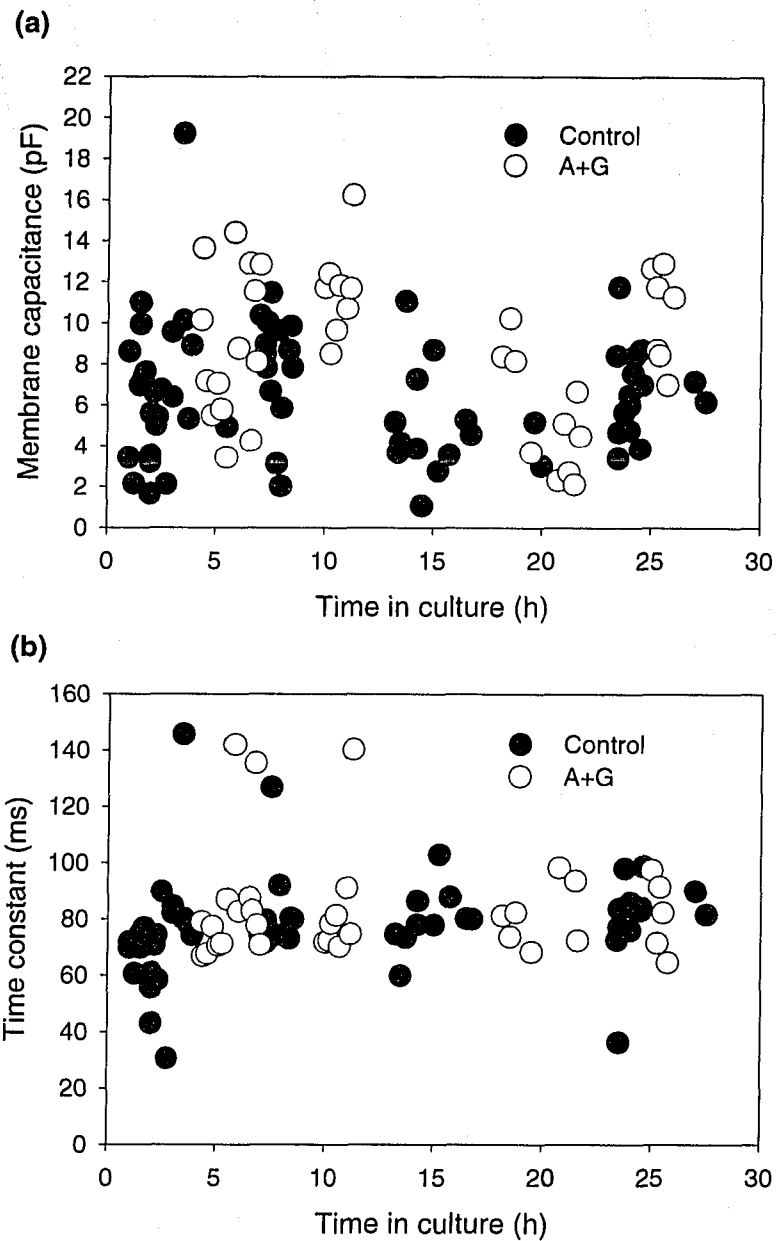


Figure 13. Membrane capacitance and time constant of differentiating neoblasts are unaffected by A+G treatment. **(a)** C_m of neoblasts ranged from 1.08 to 19.22 pF ($n=132$) and was unaffected by treatments inducing neuronal differentiation. **(b)** Membrane τ ranged between 30.6 to 145.7 ms ($n=115$) and was similarly unaffected by differentiation treatments. Differentiation treatments were: control (black) ($n=68$), A+G (white) ($n=39$). Both properties were unaffected by treatment and there was no effect by time in culture (ANCOVA, $p > 0.05$, (τ) $n = 115$, (C_m) $n = 132$).

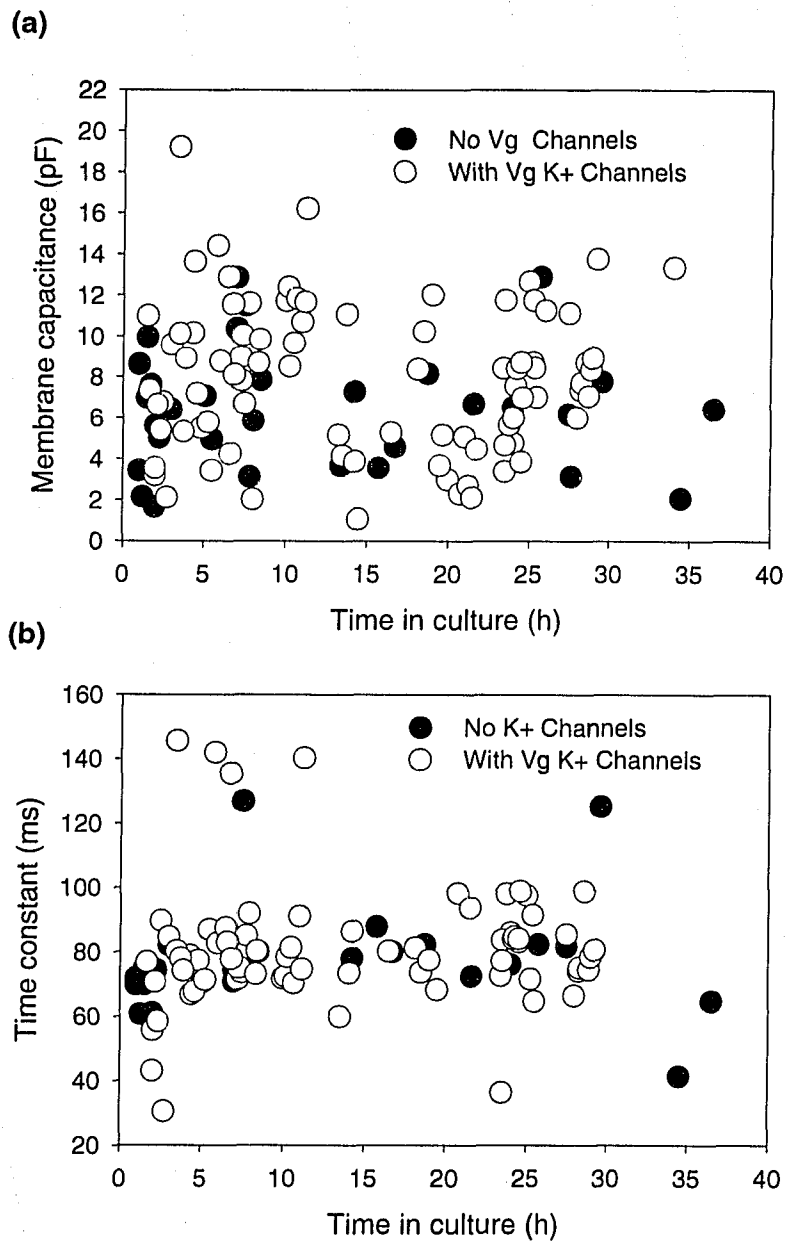


Figure 14. Membrane capacitance and time constant of differentiating neoblasts are unaffected by the presence of Vg-K⁺ channels. (a) Neoblasts (both undifferentiated and ones differentiating into neurons) with and without Vg-K⁺ channels had similar membrane capacitances ranging between 1.08 to 19.22 pF (n=132) and were unaffected by time in culture (ANCOVA, $p > 0.05$, $n = 132$). (b) Membrane time constants ranged between 30.6 to 145.7 ms (n=115) and were similarly unaffected by the presence or absence of Vg-K⁺ channels. (ANCOVA, $p > 0.05$, $n = 115$).

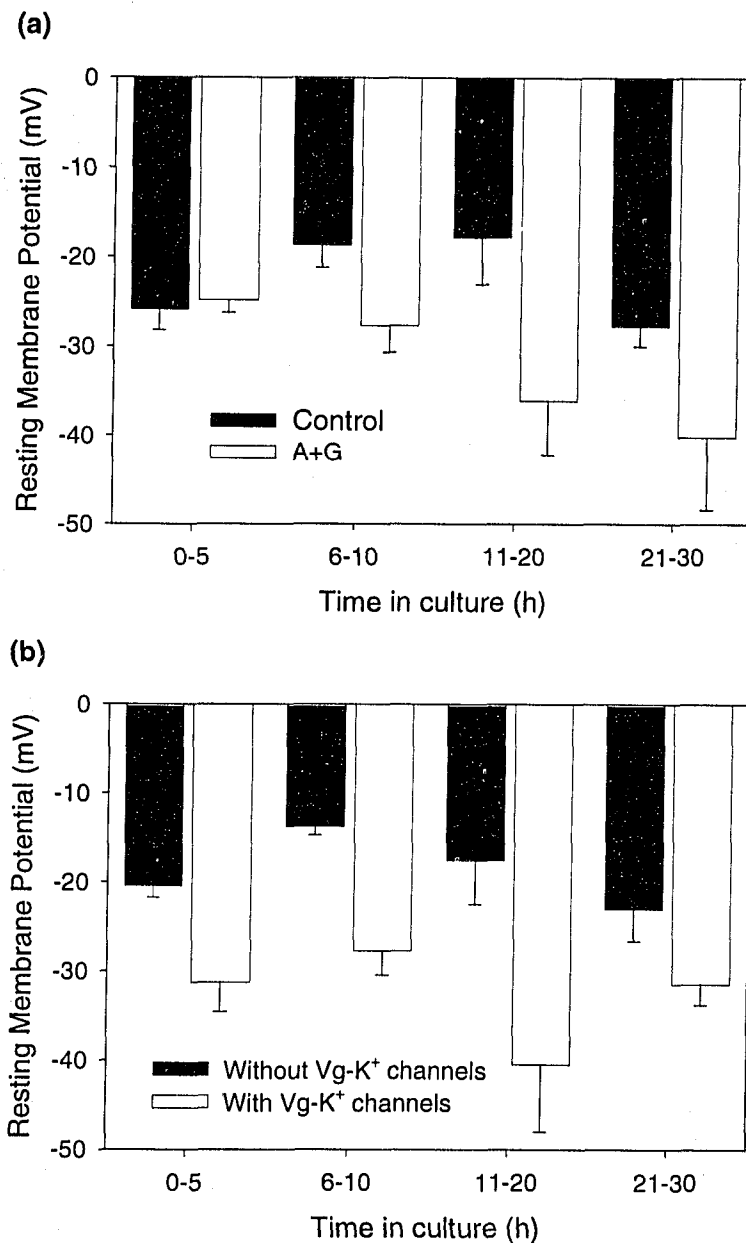


Figure 15. Resting V_m of differentiating neoblasts is affected by both treatment and the presence of $V_g\text{-K}^+$ channels. **(a)** Neoblasts treated with A+G develop more negative resting V_m after 10 h in culture whereas neoblasts treated with control media show no change at any time when compared to neoblasts immediately following dissociation (Two-way ANOVA, $p < 0.05$, $n = 69$). **(b)** Resting V_m of neoblasts were more negative in cells expressing a $V_g\text{-K}^+$ channel at all times compared with neoblasts lacking $V_g\text{-K}^+$ channels (Two-way ANOVA, $p < 0.05$, $n = 77$). Error bars represent the S.E.M.

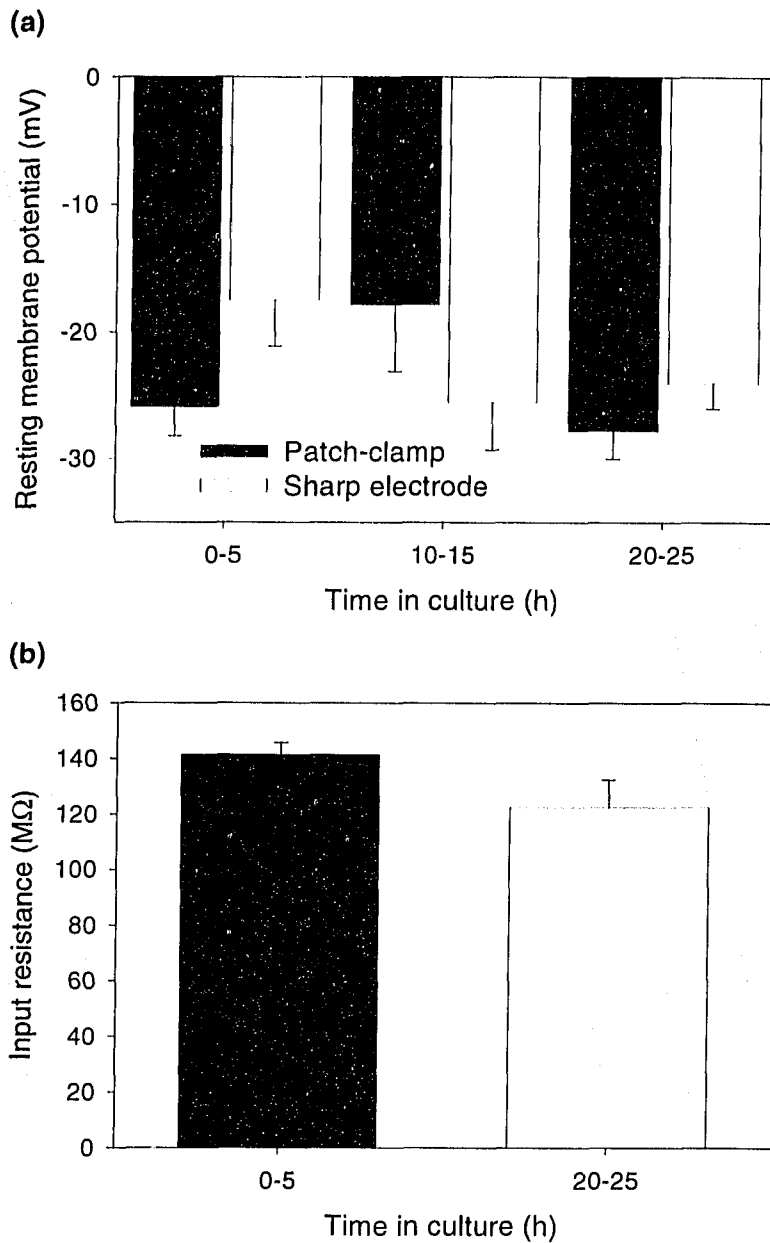


Figure 16. Resting V_m of control neoblasts are similar between whole-cell patch clamp and intracellular sharp electrode recordings. (a) Measurements of resting V_m using whole-cell patch clamp (black bars) were not different from recordings made using sharp electrodes (white bars). Neither the recording method nor time in culture had any effect on the resting V_m , nor was there an interaction between the two (Two-way ANOVA, $p > 0.05$, $n = 65$). (b) Input resistance of control neoblasts was relatively low at 0 h and 24 h. Time in culture had no effect on the R_i of cultured neoblasts (Unpaired t -test, $p > 0.05$, $n = 5$). Error bars represent the S.E.M.

Figure 17. K^+ currents recorded from cultured neoblasts. **(a)** A typical outward current recorded from a voltage-clamped neoblast. Currents were evoked by stepping the holding potential from -70 mV using 10 mV increments between -90 mV to +70 mV. The voltage waveform and scalebar are given below the current trace. **(b)** Current-voltage relationships of delayed rectifier currents recorded from neoblasts cultured in control media for 0 h and 24 h. Currents activate near -50 mV and are unaffected after 24 h in control culture media. Currents are standardized to the peak current. Data for 0 h control and 24 h represent 20 cells each. Error bars represent the S.E.M.

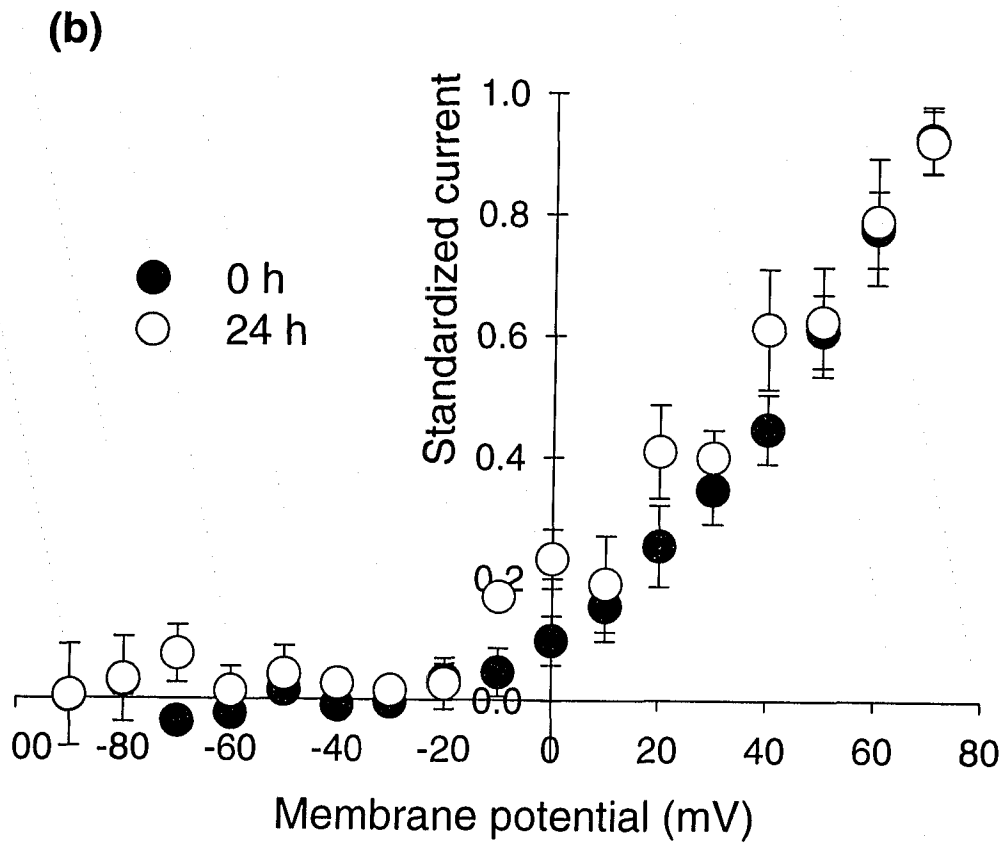
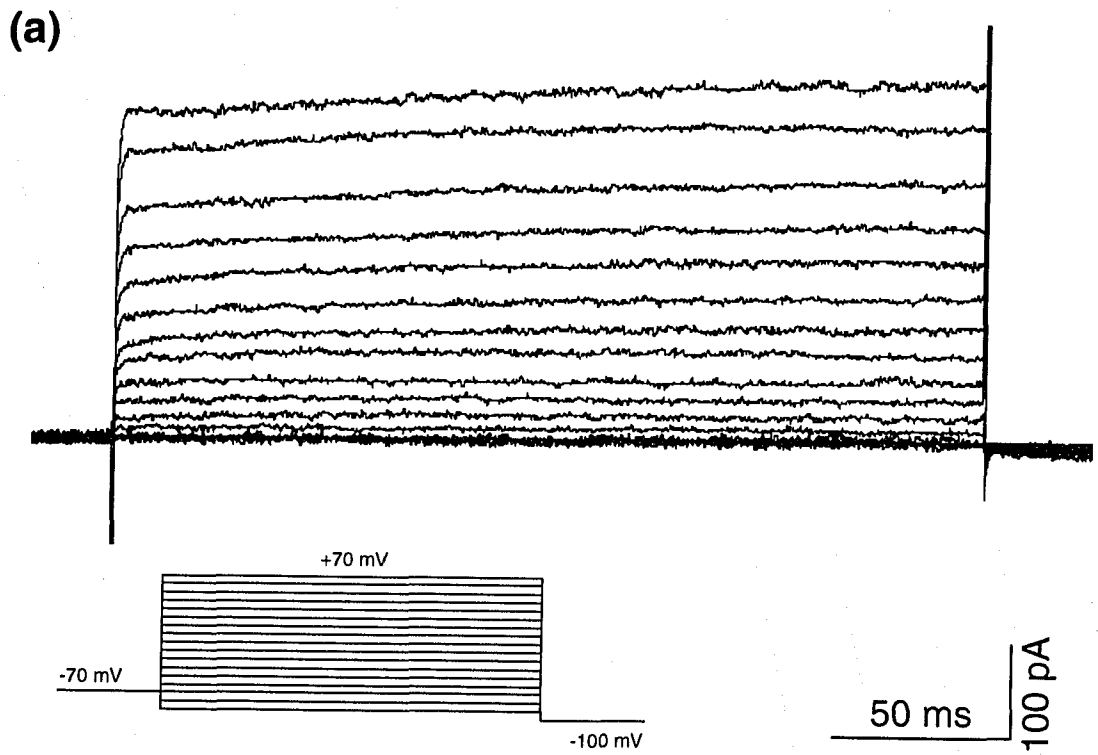
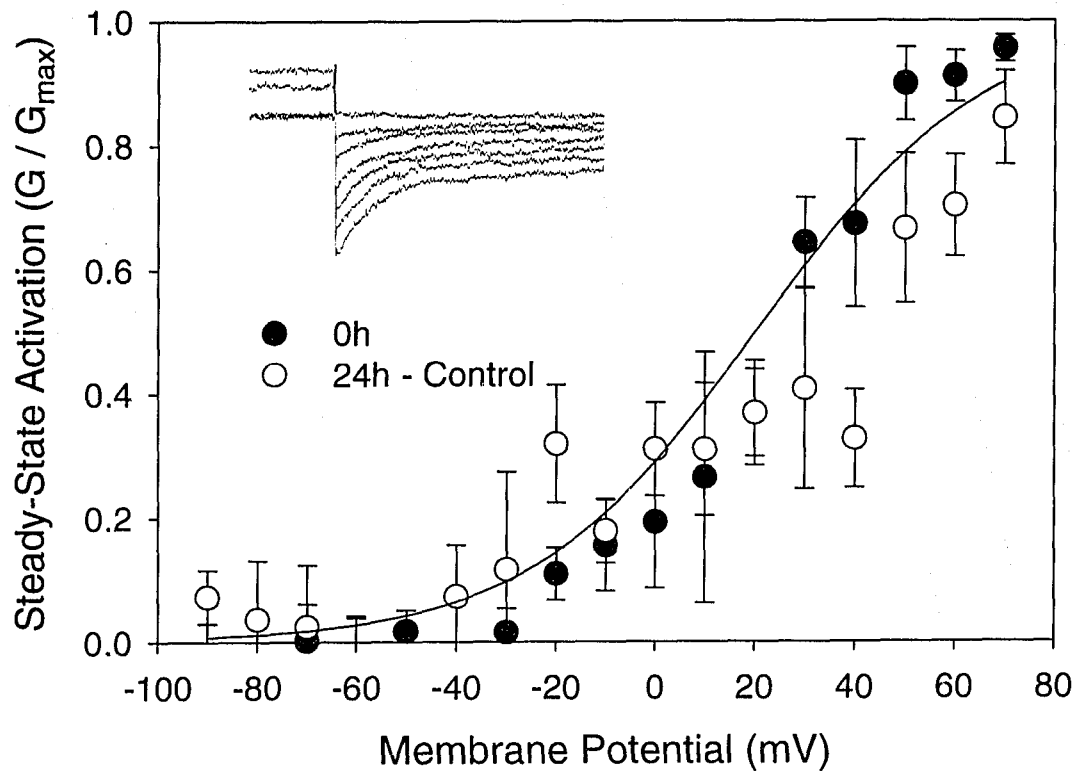
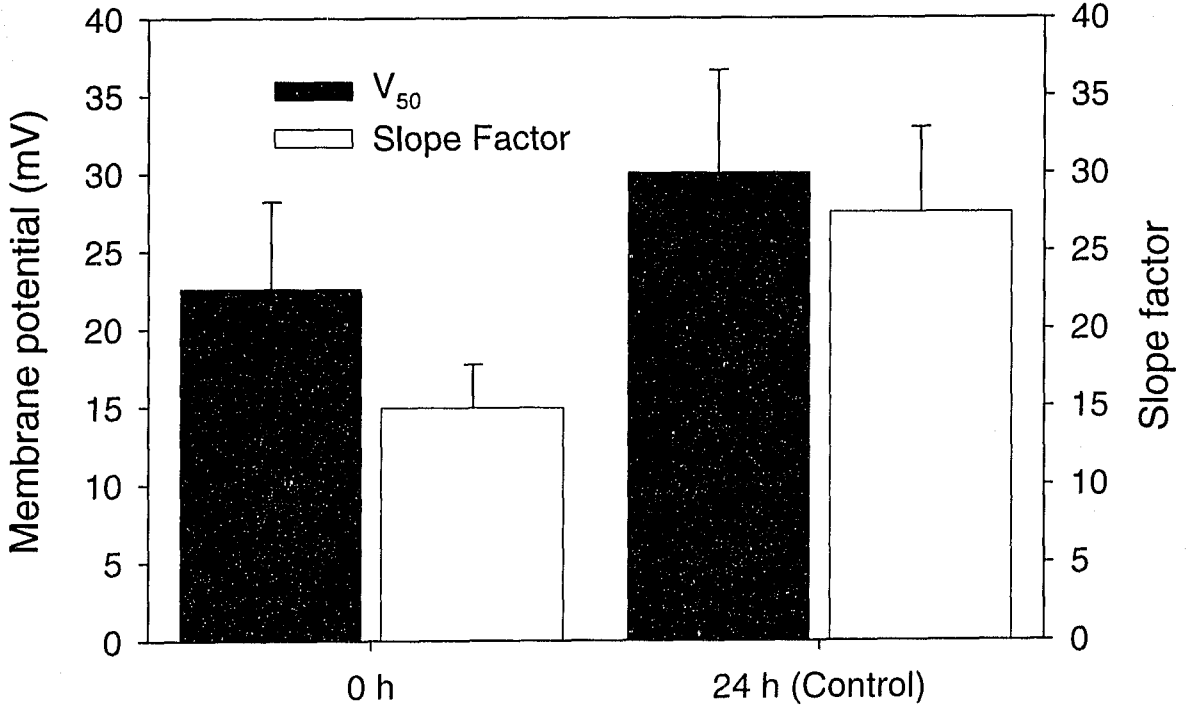


Figure 18. Activation properties of $V_g\text{-K}^+$ channels recorded from undifferentiated neoblasts. **(a)** Activation properties were measured by stepping the holding potential 10 mV from -70 mV to a series of values between -90 mV to +70 mV for 35 ms to reach steady-state activation, then stepped down to -100 mV to measure the tail currents. Tail currents (see inset) were fitted to a single exponential function to determine the peak amplitude. Currents were normalized to the maximal evoked current then plotted against the holding potential of the test pulse. Activation curves for individual cells were fitted to a multi-stage Boltzmann function to determine the voltage of half-activation and the slope factor. These values were used to generate mean steady-state Boltzmann curve (solid curve). Data for control are for 5 cells, and 8 cells for 24 h control. **(b)** Activation properties and kinetics of $V_g\text{-K}^+$ channels are unchanged under culture conditions. The parameters obtained from the Boltzmann function fits of steady-state activation (left scale) are similar between 0 h and 24 h control cells. The voltages of half-activation were markedly right-shifted at 22.6 ± 5.6 mV ($n = 5$) for 0 h control cells, and 30.0 ± 6.6 mV ($n = 8$) for cells cultured in control media for 24 h and did not differ statistically (ANOVA, $p > 0.05$, $n = 13$). The slope factor for the Boltzmann fit (right scale) did not differ significantly between different culture durations (ANOVA, $p > 0.05$, $n = 12$). The slope factor (given in arbitrary units) for 0 h control cells was 14.9 ± 2.8 ($n = 4$) and 27.5 ± 5.4 ($n = 8$) for 24 h control. Error bars represent the S.E.M.

(a)



(b)



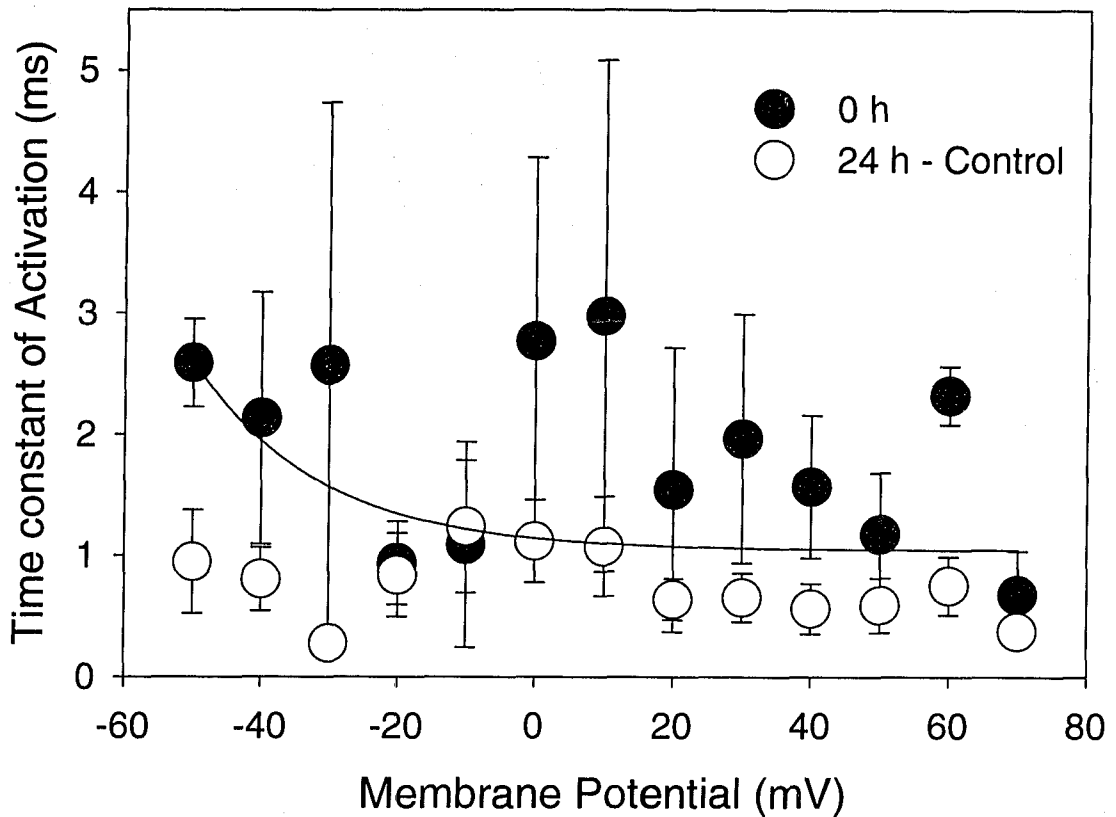


Figure 19. The time constant of activation was determined by evoking currents using 10 mV voltage steps from the holding potential of -70 mV to a series of values between -90 mV to +70 mV for 250 ms. The rising phase of outward currents was fitted to the four-stage Hodgkin-Huxley model of activation with first order kinetics. Mean values for τ_{a} are plotted for neoblasts cultured for 0 h in control media and 24 h control. The τ of activation was voltage-dependent and reached a maximum at voltages more positive than -20 mV of approximately 1 ms. Culturing in control media for 24 h did not affect the voltage-dependence, nor the three parameters of the exponential decay fit. The voltage-dependent τ of activation was similar to brain neurons (solid curve). Data for 0 h control represents 4 cells, and data for 24 h control represents 8 cells. Error bars represent the S.E.M.

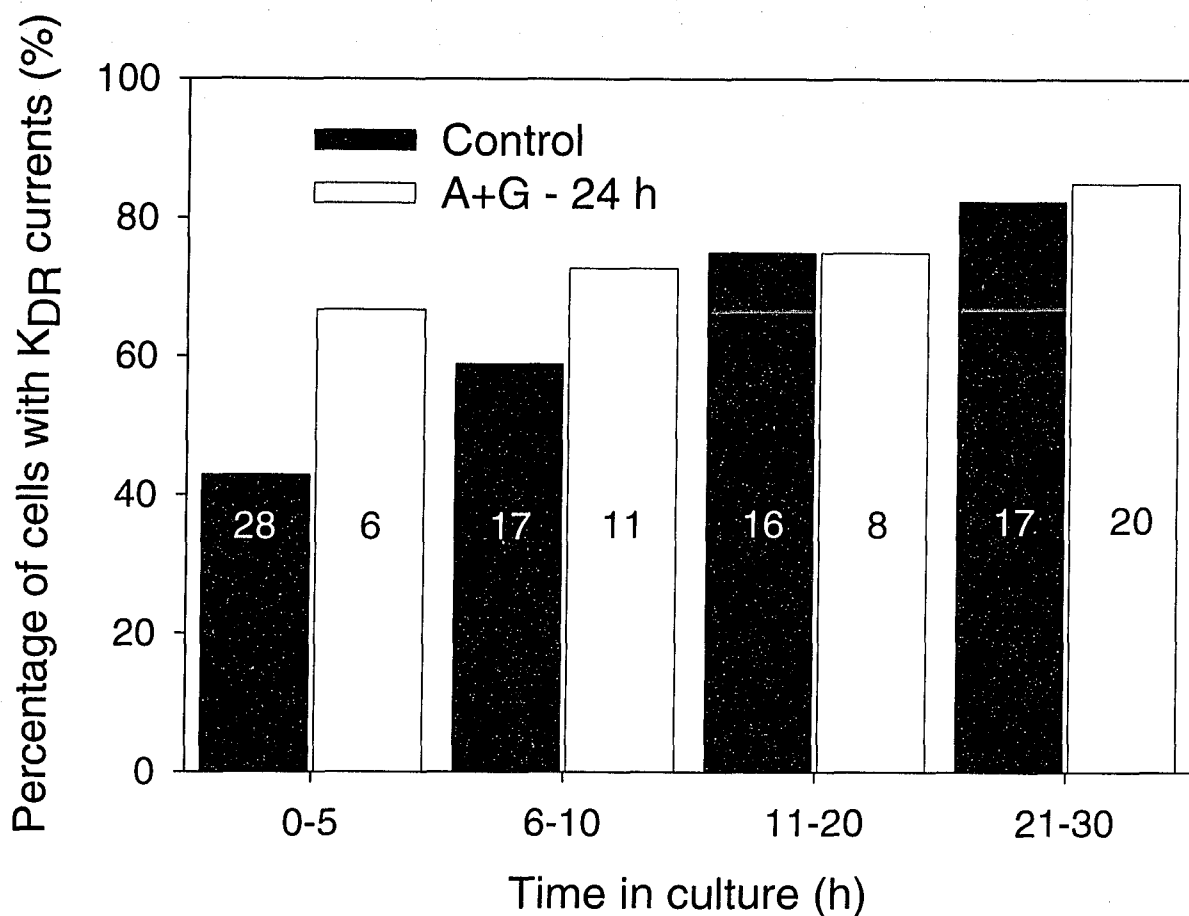


Figure 20. Appearance of $Vg-K^+$ currents in cultured neoblasts. Neoblasts expressed $Vg-K^+$ channels when cultured on 0.01% poly-L-lysine substrate alone and bathed in isotonic control media (black bars). Expression of $Vg-K^+$ channels increased gradually and peaked at 82.4% of cells after 21-30 h in culture. Treatment of neoblasts with A+G for 24 h (white bars) caused neoblasts to express $Vg-K^+$ channels sooner (66.7% of neoblasts had $Vg-K^+$ channels compared to only 42.9% of neoblasts in control media after 0-5 h in culture) (Chi-square test, $p < 0.05$, $n = 34$). Treatment did not affect the percentage of neoblasts expressing $Vg-K^+$ channels after 21-30 h in culture (Chi-square test, $p > 0.05$, $n = 37$). Numbers in within bars represents the sample size.

Figure 21. Maturation of a delayed rectifier K^+ current in differentiating neoblasts. K^+ currents were evoked by depolarizing neoblasts voltage clamped in the whole-cell configuration in K^+ isolating media. Cells were held at -70 mV, and then depolarized in 10 mV steps and the currents recorded. The currents recorded at various time intervals show that the magnitude of currents increases over the first 24 h in culture when neoblasts were exposed to the A+G treatment. The majority of cells recorded within the first 2 h after plating had no observable V_g - K^+ currents (top left panel). Currents became gradually larger when exposed to A+G for greater time periods. After 24 h treatment with A+G, currents ranged between 33.0 pA to 1077.1 pA ($n = 37$). Numbers below current traces represent the duration of treatment with A+G. The bottom panel shows the voltage waveform and the scalebar.

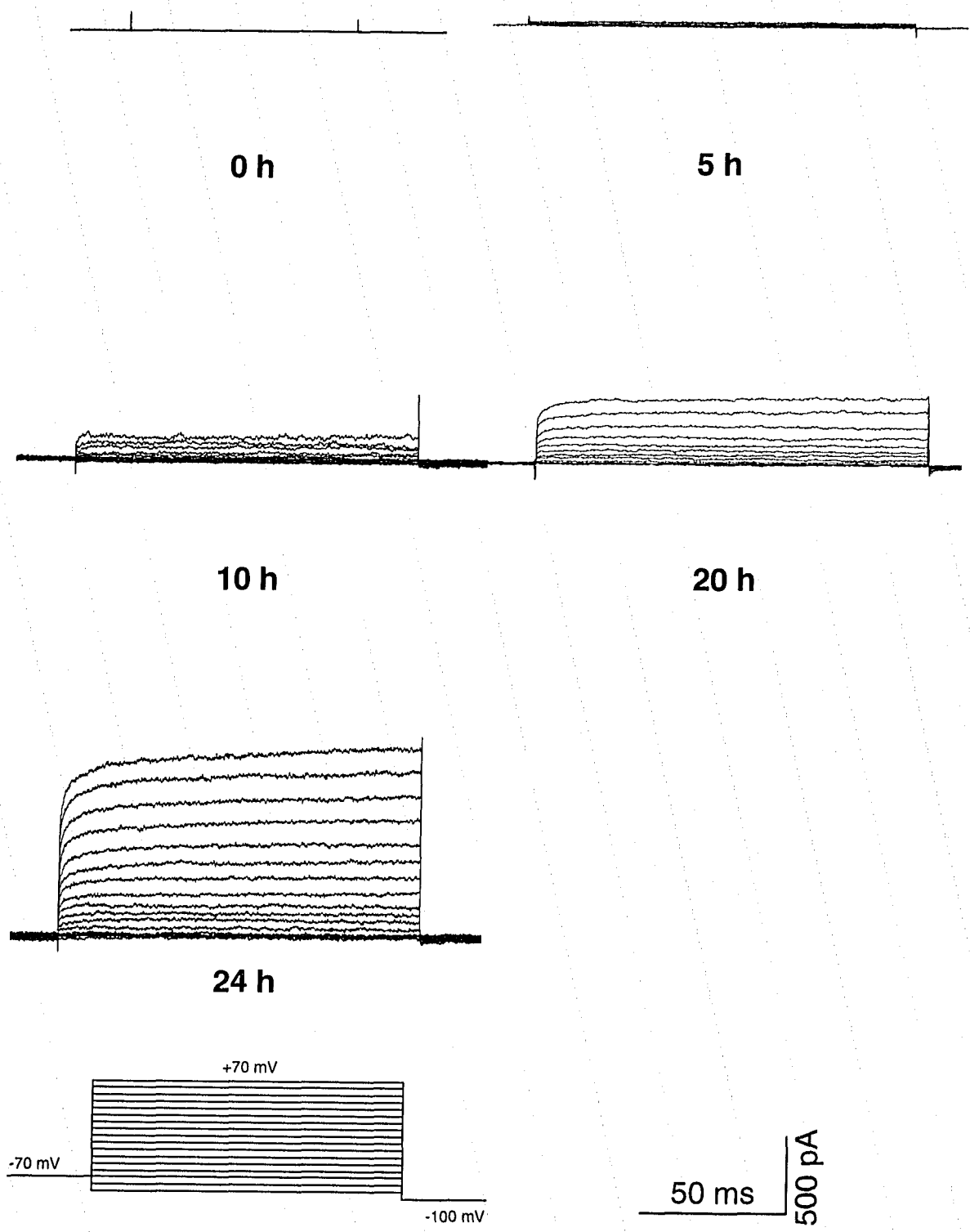
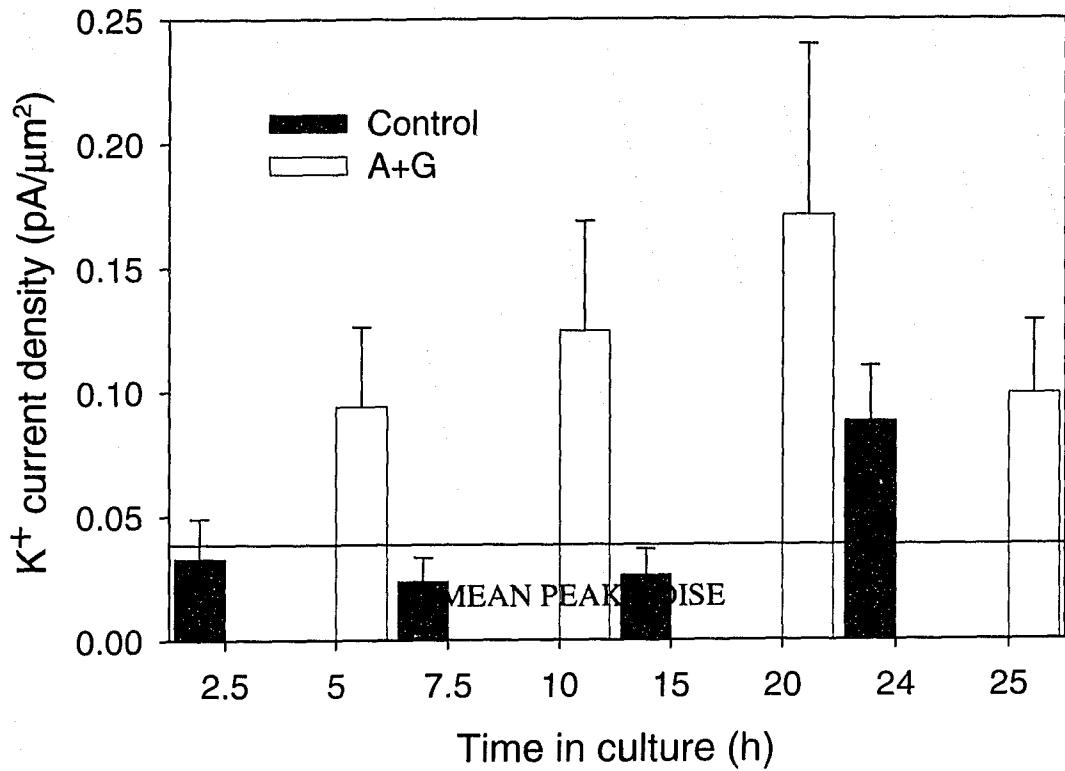


Figure 22. K^+ current density increases in differentiating neoblasts. K^+ currents were evoked by depolarizing neoblasts voltage clamped in the whole-cell configuration in K^+ isolating media. Cells were held at -70 mV, and then depolarized to (a) $+30$ mV, or (b) $+50$ mV. K^+ currents in differentiating neoblasts treated with A+G develop larger outward currents after 5 h in culture compared to controls after 2.5, 7.5 and 15 h (ANOVA, $p < 0.05$, $n = 32$). Neoblasts in controls only showed a change in the size of K^+ currents after 24 h cultured 0.01% poly-L-lysine (ANOVA, $p < 0.05$, $n = 55$). Treatments with A+G but not time nor their interaction influence K^+ current density (ANCOVA, $p < 0.05$, $n = 87$). Mean peak recording noise is denoted by the shaded bar. Error bars represent the S.E.M.

(a)



(b)

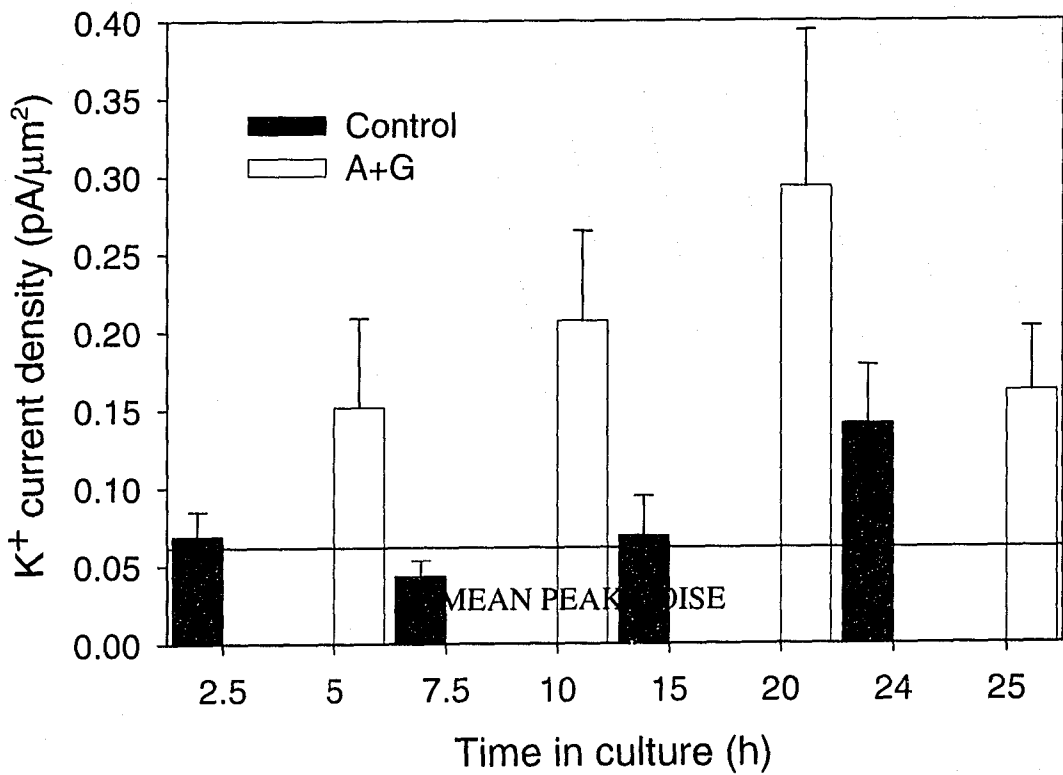
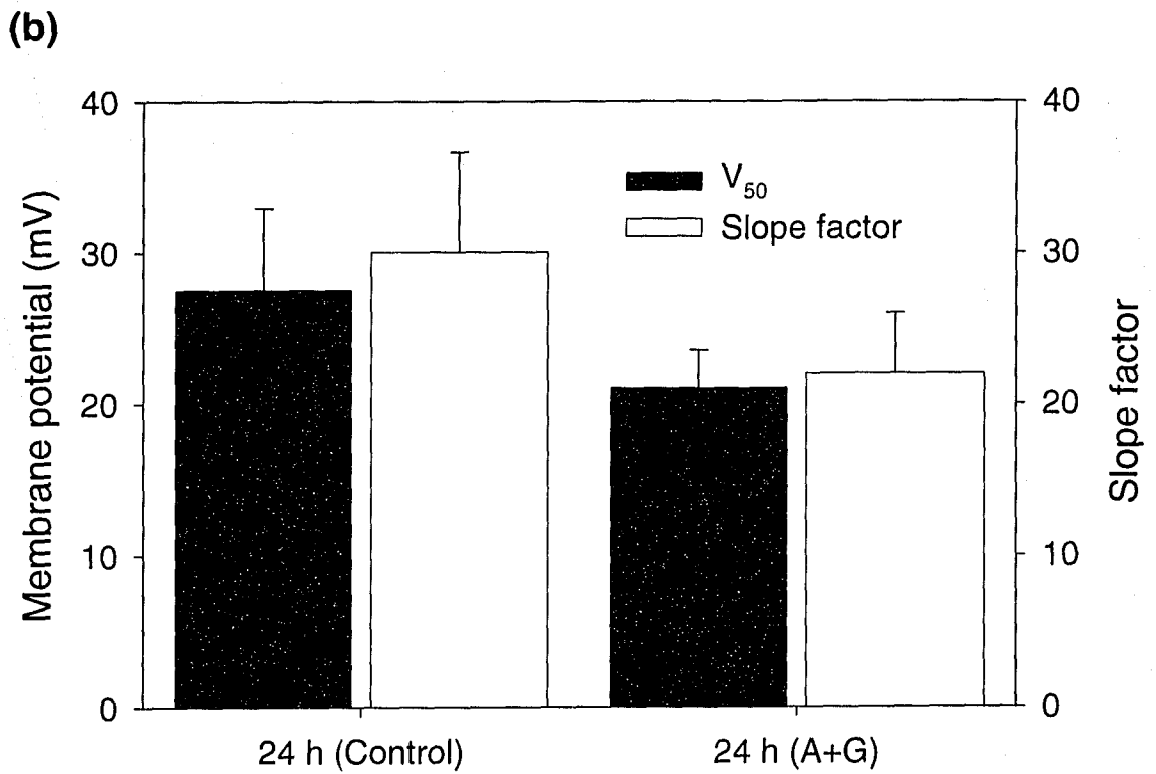
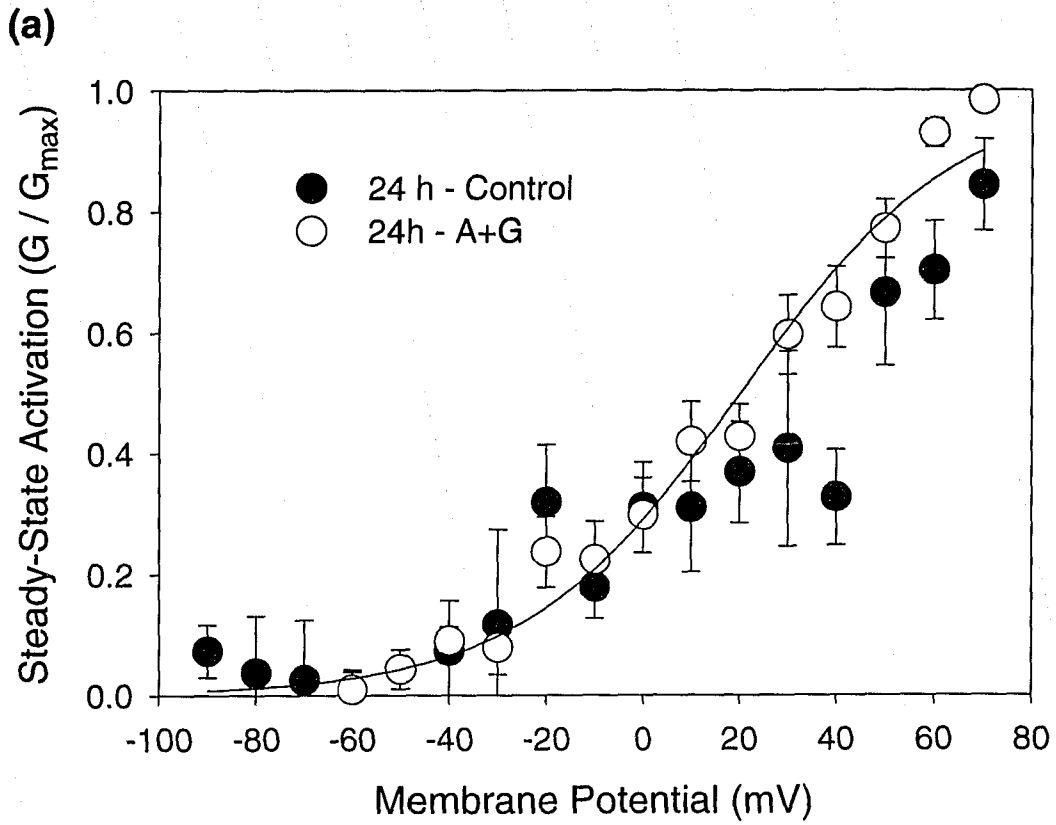


Figure 23. Activation properties of Vg-K⁺ channels from differentiating neoblasts. **(a)** Activation properties were measured as described before. Mean values for the Boltzmann fit of activation were used to generate a mean steady-state Boltzmann curve (solid curve). Data for control represent 8 cells and 9 cells for A+G. **(b)** Steady-state activation and τ of activation are unaffected by treatment with A+G. Activation properties and kinetics of Vg-K⁺ channels are unchanged under culture conditions. The parameters obtained from the Boltzmann function fit for steady-state activation are similar between 24 h control cells and cells treated with A+G for 24 h (ANOVA, $p > 0.05$, $n = 17$). The voltages of half-activation were markedly right-shifted at 27.5 ± 5.4 mV ($n = 8$) for 24 h control cells, and 22.0 ± 4.0 mV ($n = 9$) for cells cultured in A+G for 24 h. The slope factor for the Boltzmann fit did not differ significantly between different culture durations (ANOVA, $p > 0.05$, $n = 16$). The slope factor (given in arbitrary units) for 24 h control cells was 30.0 ± 6.6 ($n = 8$) and for 24 h in A+G, 21.0 ± 2.5 ($n = 8$). Error bars represent the S.E.M.



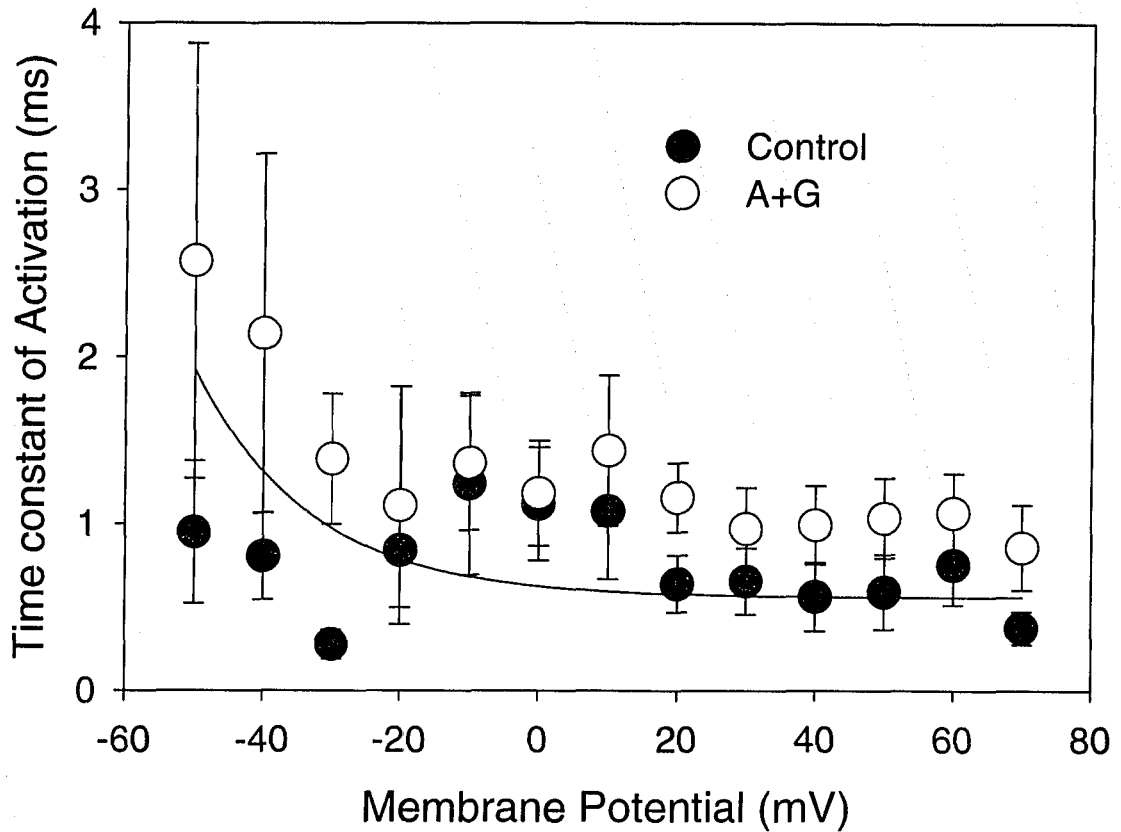
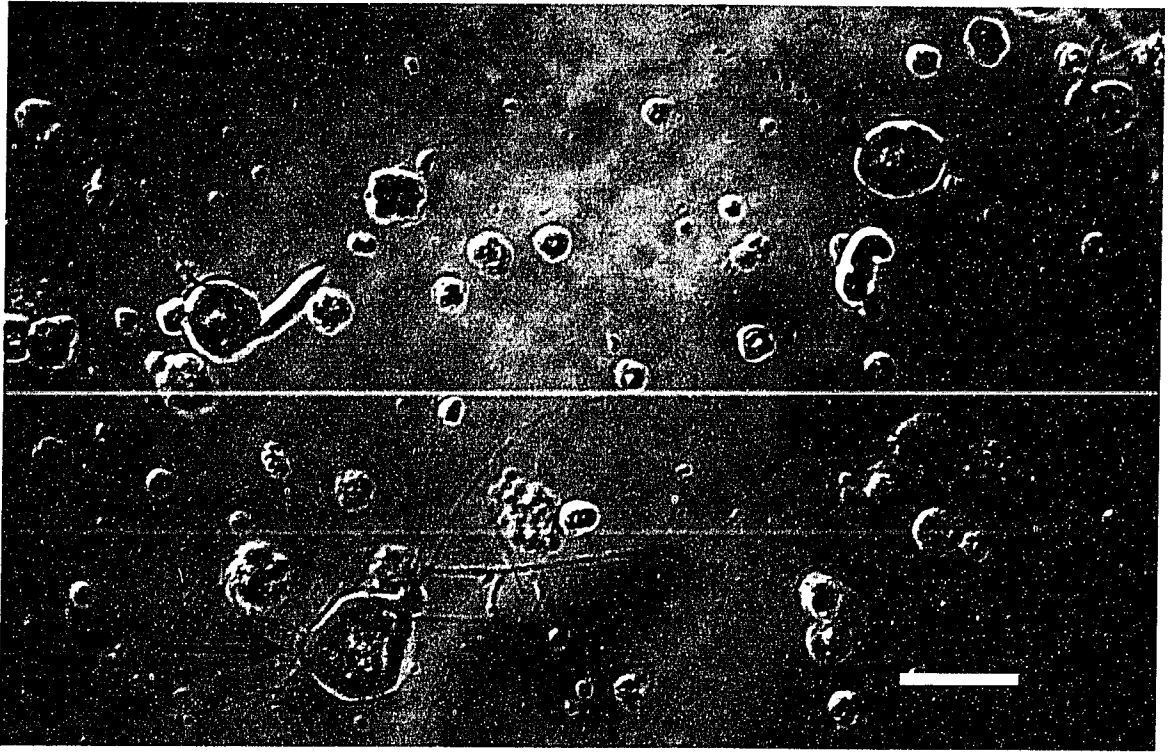


Figure 24. The time constant of activation of V_g -K⁺ channels from cells cultured for 24 h in control media and in the presence of A+G are similar and voltage-dependent. The τ of activation was voltage-dependent and reached a maximum at voltages more positive than -20 mV of approximately 1 ms. Treatment with A+G did not affect the voltage-dependence, nor the asymptote for the three-parameter exponential decay fit. The voltage-dependent τ of activation did not differ from that of brain neurons (solid curve). Data for control represents 6 cells, and data for A+G represents 9 cells. Error bars represent the S.E.M.

Figure 25. Developing neurons sprouting neurites had variable morphologies. A small proportion of neoblasts treated with A+G for 24 h ($3.7\pm 0.8\%$, $n = 5$) begin to develop neurite-like extensions. Cells were determined to have grown neurites if they possessed processes that were at least one soma diameter in length. Differentiating neoblasts varied in morphology, with monopolar (**a**), bipolar (**b**) and multipolar (**a**, solid arrow) cells. Most cells displayed a heteropolar arrangement of processes (**a**, solid arrow), but homopolar cells were also present (**b**). Contaminating neurons were distinguishable from differentiating neoblasts by the size of their nucleus, with neoblasts retaining their characteristically large nucleus, and fully differentiated neurons possessing a smaller nucleus to soma ratio (**a**, dashed arrow). Scalebar: 10 μm .

(a)



(b)

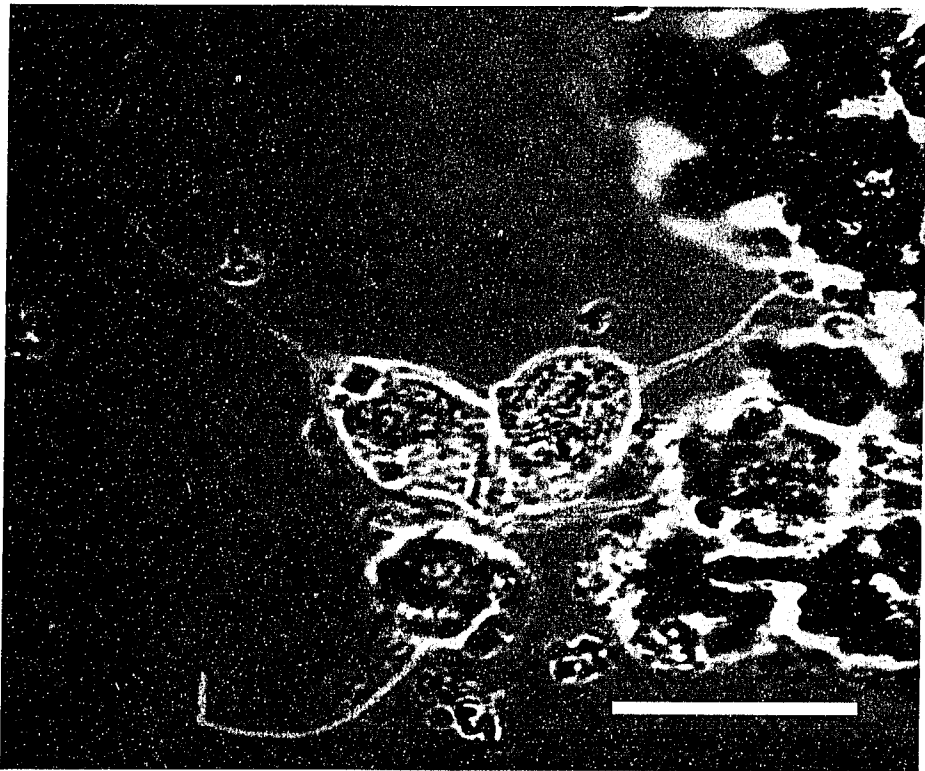
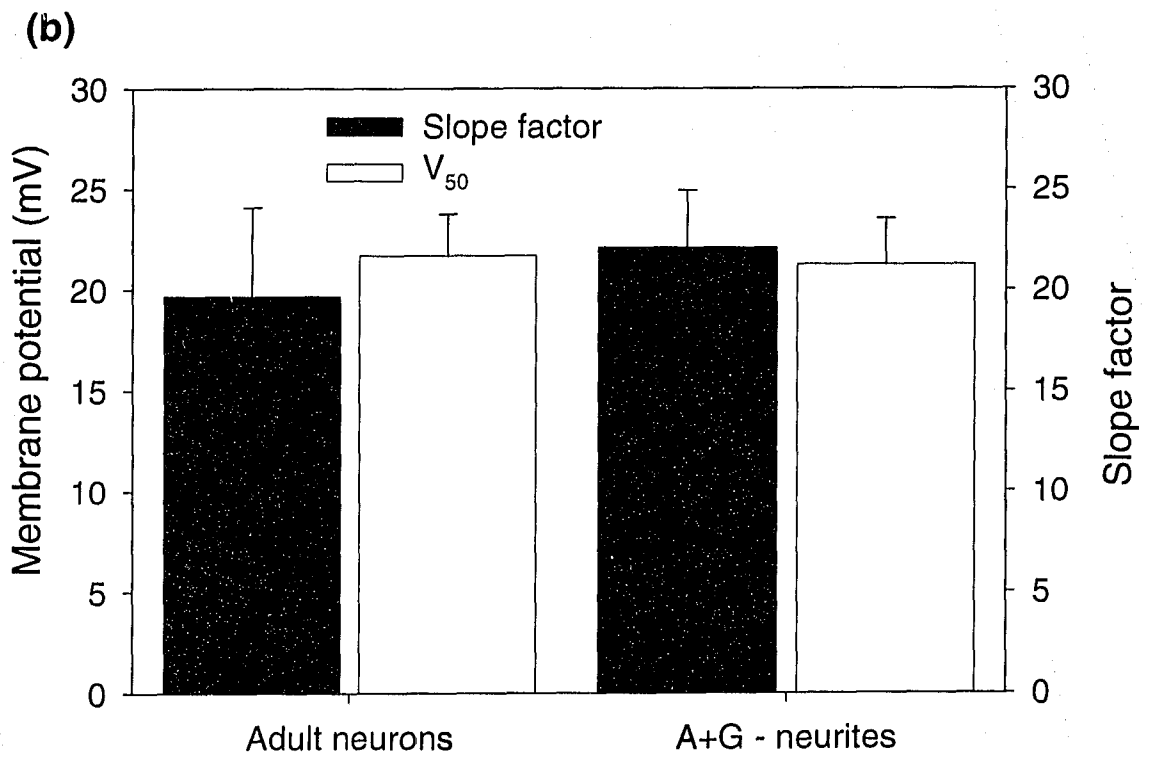
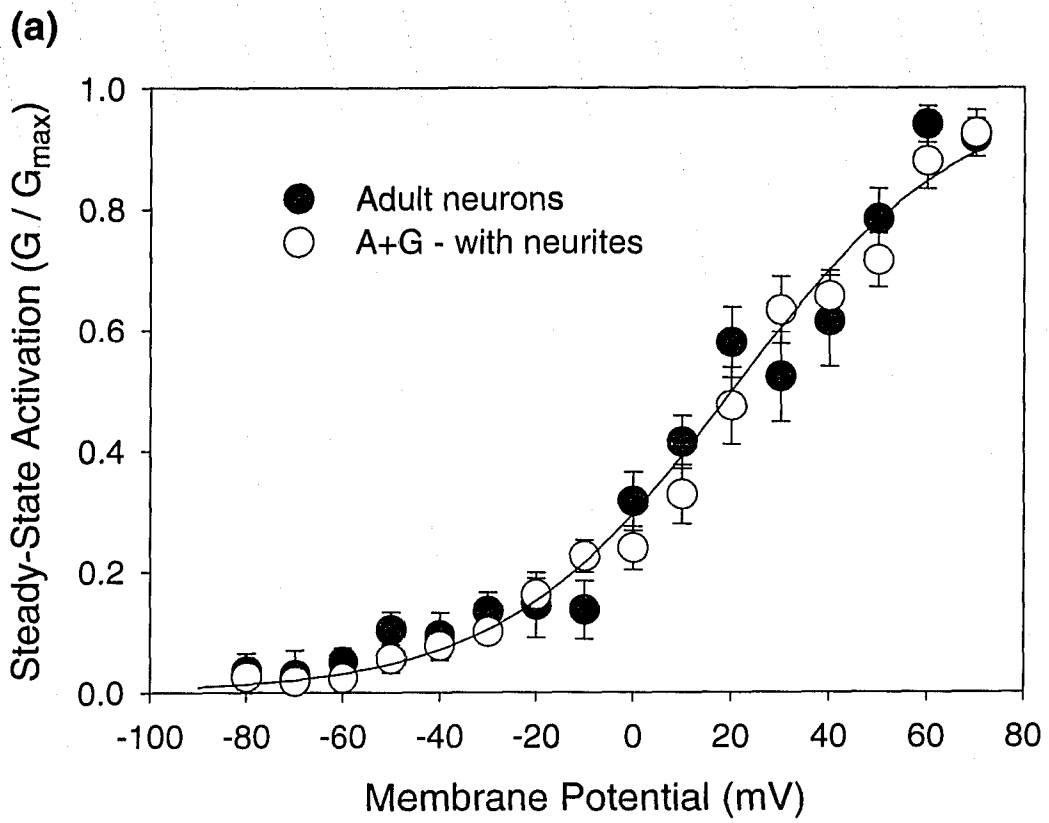


Figure 26. Developing neurons extending neurites express delayed rectifier K^+ channels with the same activation properties as those in adult brain neurons. Steady-state activation and activation τ were compared between differentiating neoblasts and brain neurons isolated from adult animals. **(a)** Steady-state activation properties were measured by fitting data to a Boltzmann function as described previously. The delayed rectifier channels activated near -50 mV and had a voltage of half-activation of 19.7 ± 4.4 mV ($n = 10$) and 22.1 ± 2.9 mV ($n = 10$) for the adult neurons and the neoblasts treated with A+G respectively. The slope factor was 21.7 ± 2.1 ($n = 10$) and 21.2 ± 2.3 ($n = 10$) for the adult neurons and A+G treated cells respectively. The mean Boltzmann fit for adult neuron data is shown (solid curve). **(b)** The activation properties of V_g - K^+ channels from adult neurons and developing neoblasts are not statistically different. **(a)** Parameters describing the voltage of half-activation and the slope factor for the Boltzmann function fit are not significantly different among adult neurons and neoblasts treated with A+G that extend neurites (ANOVA, $p > 0.05$, $n = 20$). Error bars represent the S.E.M.



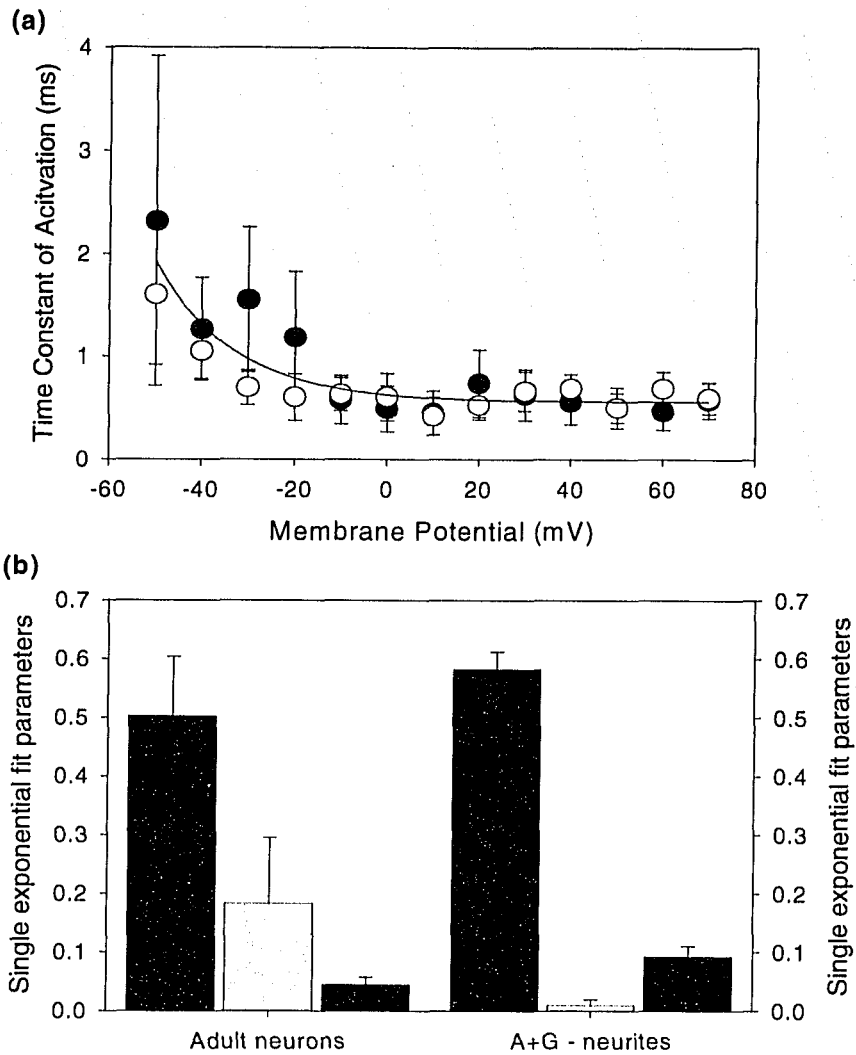
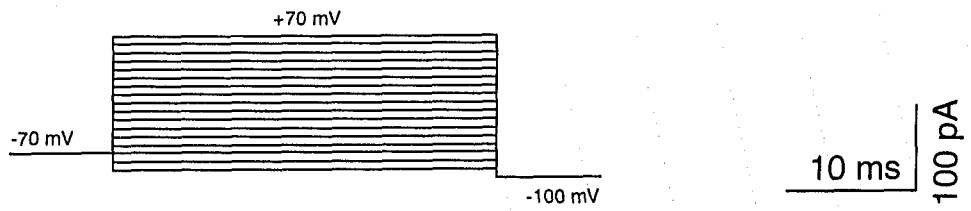
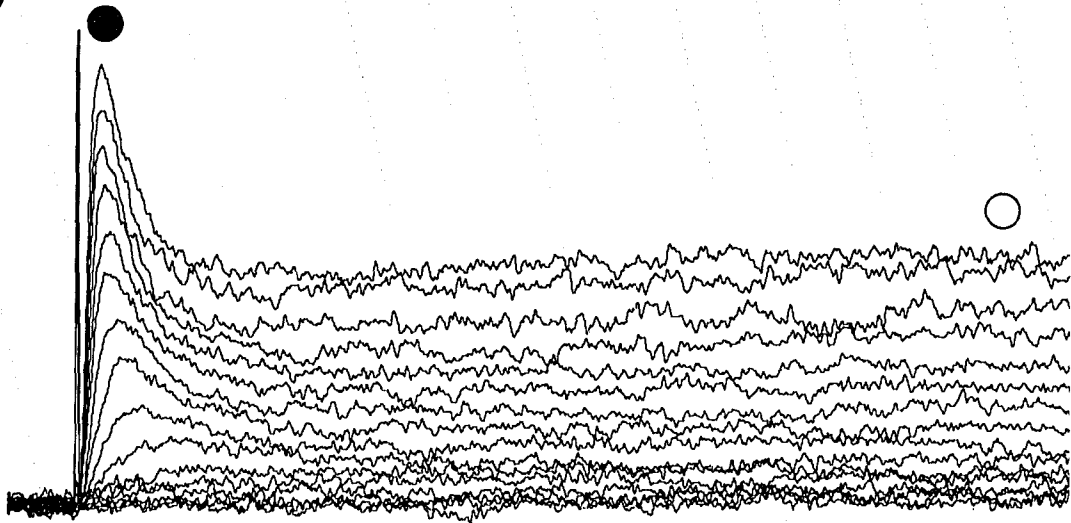


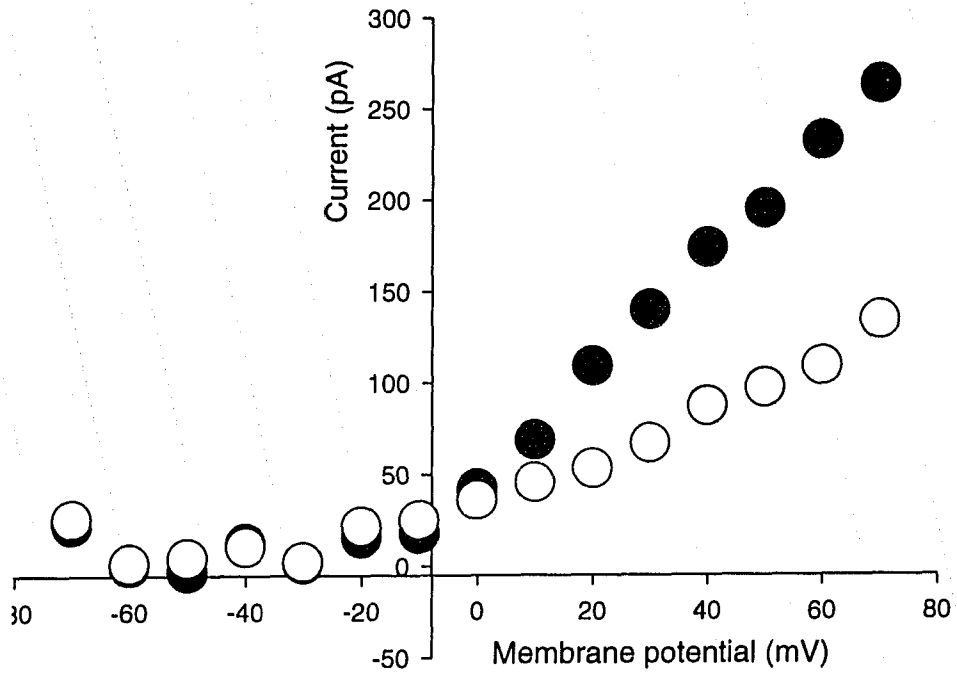
Figure 27. The time constant of activation from K^+ channels in differentiating neuroblasts and adult neurons is similar and voltage-dependent. **(a)** The rate of activation was voltage-dependent, and showed similar values for the three-parameter exponential decay fit. At -50 mV, the τ of activation was near 2 ms, and reached a maximal rate near -20 mV where the time constant approached 0.5 ± 0.1 ms and 0.58 ± 0.03 ms for the adult neurons and differentiating neuroblasts respectively. Data for both treatments represent 10 cells each. **(b)** Coefficients for the three parameter exponential decay function used to describe the voltage-dependency of the rate of activation of K^+ channels are not statistically different among adult neurons and differentiating neuroblasts that extend neurites (Kruskal-Wallis one-way analysis of variance, $p > 0.05$, $n = 20$). Error bars represent the S.E.M.

Figure 28. Whole-cell patch clamp recordings in solutions isolating for K^+ currents reveal that neoblasts sprouting neurites possess both an inactivating and non-inactivating component. All cells sprouting neurites ($n = 8$) expressed a K_{DR} current, and 50.0% ($n = 8$) of cells also expressed K_A currents. **(a)** A representative whole-cell recording of a differentiating neoblast that sprouted processes. Whole-cell currents were evoked by depolarizing cells held at -70 mV through a series of 10 mV steps. The transient component of K^+ currents peaked within 2 ms of the test pulse and the rate of activation was voltage dependent. The stimulus waveform and scalebar are shown below the current traces. **(b)** The $I-V$ relationship of the currents from (a) comparing peak (filled circles) and steady-state (open circles) currents. K^+ currents appeared at potentials positive of approximately -50 mV. The ratio of peak to steady-state current was voltage dependent and largest at ratio at more positive potentials.

(a)



(b)



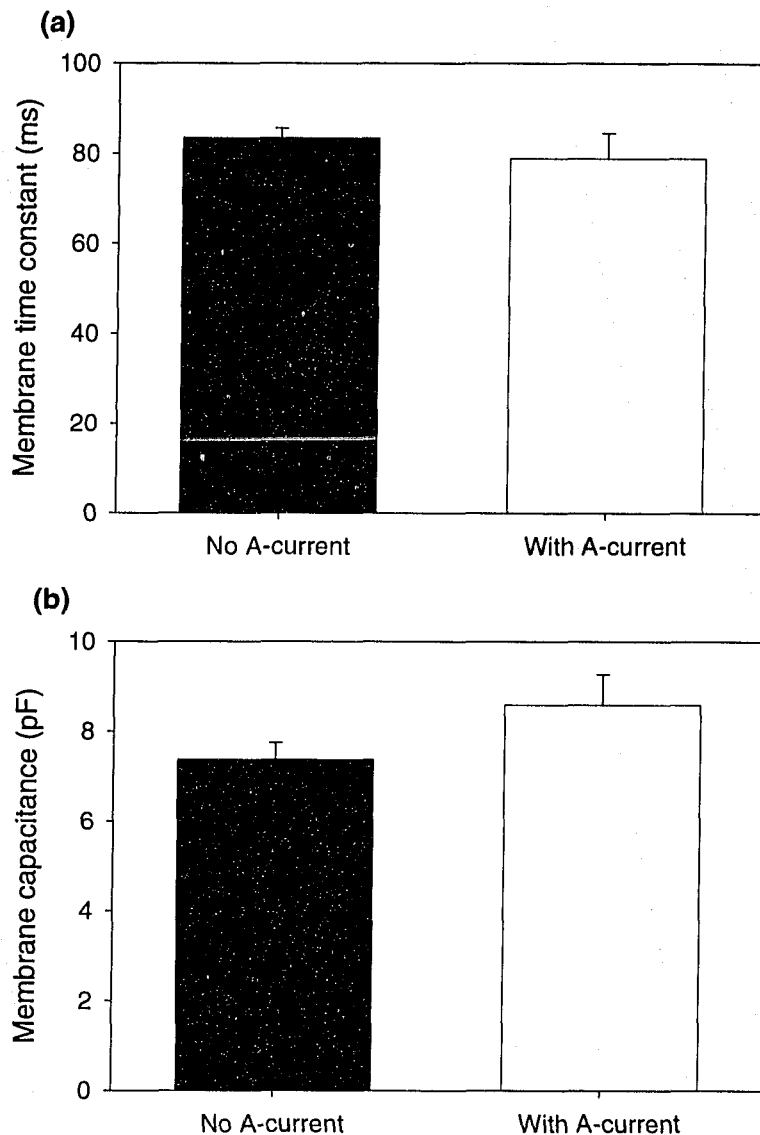


Figure 29. Resting membrane properties of differentiating neurons expressing an A-type V_g - K^+ current. Treatment with A+G for 24 h induced some cells to sprout neurites and express an A-type K^+ current (white bars). (a) Cells expressing both a delayed rectifier K^+ current and an A-type K^+ current had a mean membrane τ of 78.9 ± 5.7 ms ($n = 6$) and did not differ significantly from cells expressing only a K_{DR} current (83.5 ± 2.2 ms, $n = 45$, black bars) (unpaired t -test, $p > 0.05$, $n = 51$). (b) The C_m measured from cells with neurites expressing both currents was larger (8.8 ± 0.7 pF, $n = 7$) than in cells without (7.4 ± 0.4 pF, $n = 67$), but not statistically different (unpaired t -test, $p = 0.07$, $n = 74$). Error bars represent the S.E.M.

Figure 30. Delayed rectifier currents from differentiating neoblasts are smaller than those observed in adult brain neurons. **(a)** Delayed rectifier currents recorded from a differentiating neoblast treated with A+G for 24 h in solutions isolating for K^+ currents ranged between 33.0 pA to 1077.1 pA ($n = 37$) when a +70 mV depolarizing pulse was applied. **(b)** Delayed rectifier currents recorded using the same solutions as in (a), but from adult brain neurons. Peak steady-state currents ranged between 76.0 pA and 3704.8 pA ($n = 13$) when a +70 mV depolarizing pulse was applied. **(c)** The voltage-clamp waveform used to evoke delayed rectifier currents and the scalebar for both (a) and (b) are shown. **(d)** Mean K^+ current densities were consistently 3.3 times and significantly larger when recorded from adult brain neurons when compared to differentiating neoblasts treated with A+G for 24 h (Kruskal-Wallis one-way test of analysis, $p < 0.05$, $n = 62$). Error bars represent the S.E.M.

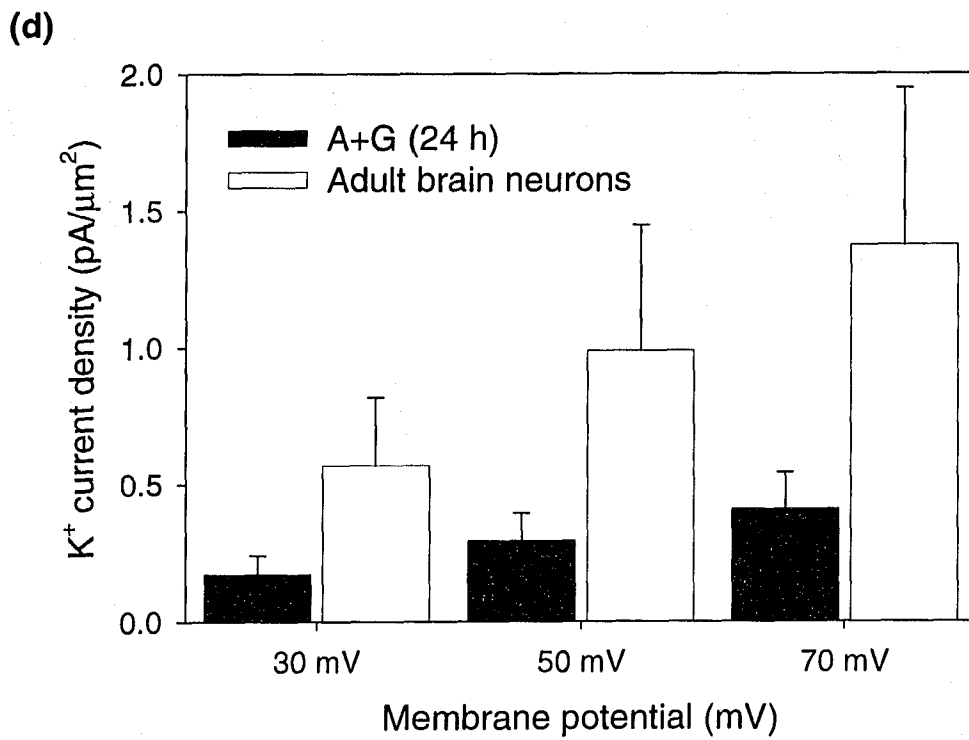
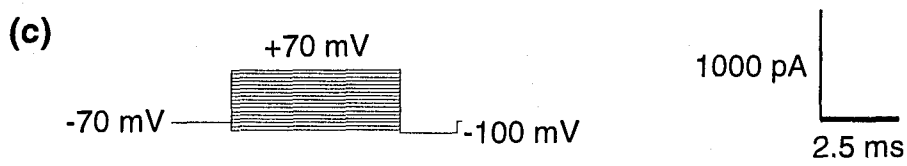
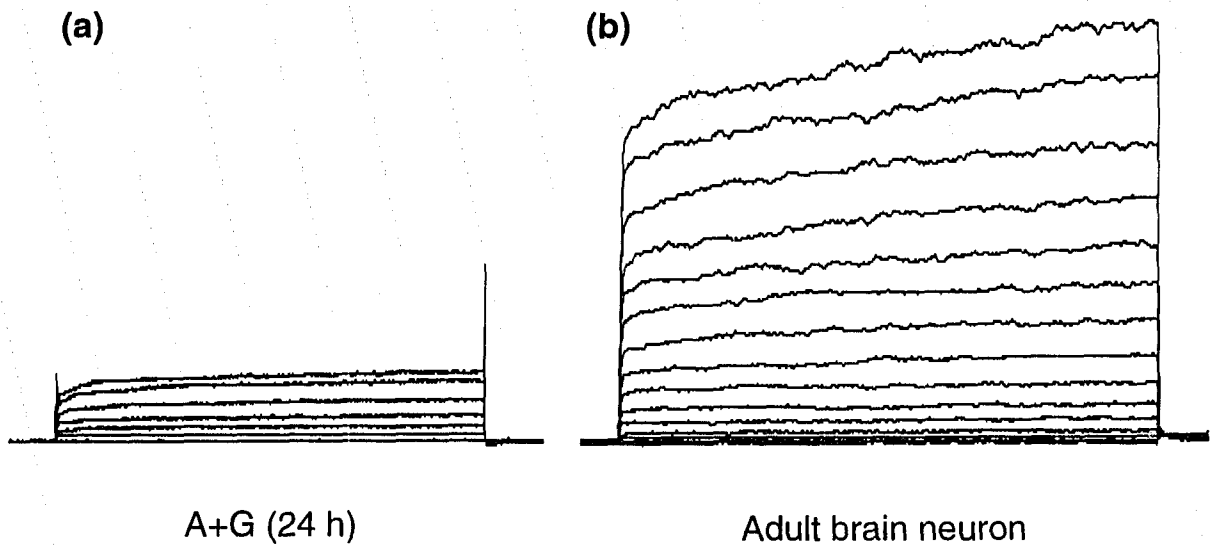


Table 1 – Early expression of Vg-ion channels during development – phylogenetic and cell lineage comparisons.

Phylum	Species	Cell Type / Lineage	Sequence of Vg-channel expression	Kv 1st	Electrical before morphological differentiation	Ionic dependence of AP	Ref. (next page)
Protostomes							
Nematoda	<i>C. elegans</i>	Oocytes	VgCl ⁻	N	?	—	1
		Muscle / mesoderm	Ca ²⁺ → K _{Ca} → K _{DR} → K _A	N	?	Ca ²⁺ & Na ⁺	2
Arthropoda	<i>D. melanogaster</i>	Embryonic muscle	Ca ²⁺ → K _A → K _{DR} → K _{Ca}	N	?	Ca ²⁺	3
		Pupal muscle			?	Ca ²⁺	4
Nematoda	<i>C. elegans</i>	Neuroblasts / ectoderm	VgCl ⁻	?	?	Ca ²⁺ & Na ⁺	11
Annelida	<i>Hirudo medicinalis</i>	Neurons		Y	?	Na ⁺	12,13
Arthropoda	<i>D. melanogaster</i>	Neurons (ganglionic)	K _{DR} → Ca ²⁺ → Na ⁺ → K _A	Y	?	Na ⁺	14
		Neurons (photoreceptors)	K _{DR} → K _A	Y	?	Na ⁺	15
	<i>Schistocerca nitens</i>	Neurons (DUM neuroblasts)	K _{DR} → K _A	Y	?	Ca ²⁺ & Na ⁺	16

Deuterostomes

Chordata	<i>Boltenia sp.</i>	Muscle	$K_{ir} \rightarrow K_{DR} \rightarrow K_{ir} \rightarrow Ca^{2+} \rightarrow K_v \text{ \& } K_{Ca}$ & Ca^{2+}	Y	?	$Ca^{2+} \text{ \& } Na^+$ $\rightarrow Ca^{2+}$ only	5,6
	<i>Halocynthia sp.</i>	Muscle					7,8
	<i>Xenopus laevis</i>	Muscle	$K_{ir} \rightarrow K_{DR} \rightarrow Na^+ \rightarrow Ca^{2+}$	Y	N	Na^+	9,10

	<i>Boltenia sp.</i>						
	Fish	Sensory neurons					17
	<i>X. laevis</i>	Motoneurons	$K^+ \text{ \& } Na^+ \text{ \& } Ca^{2+} \rightarrow K_{Ca} \rightarrow K_A$	N	N	$Ca^{2+} \rightarrow Na^+$	18,19
	<i>Ambystoma</i>	Motoneurons	$K^+ \text{ \& } Na^+ \text{ \& } Ca^{2+}$ concurrently	N	N		20
	Chick	Motoneurons	$K^+ \rightarrow Ca^{2+} \rightarrow Na^+ \text{ \& } K_{Ca}$	Y	?	Na^+	21, 22
		Sensory neurons				Both	22
	Quail	Sensory neurons	$K_{DR} \text{ \& } K_A$	Y	N	Na^+	23
	Mouse	Interneurons	$K_{DR} \text{ \& } Na^+$ concurrently	Y	N	Na^+	24
	Rat	Motoneurons				Na^+	25, 26, 27

Lightly shaded cells represent excitable cells derived from mesoderm.
Darkly shaded cells represent excitable cells derived from ectoderm.

References on the following page.

1. Rutledge *et al.* (2001)
2. Santi *et al.* (2003)
3. Broadie & Bate (1993b)
4. Salkoff & Wyman (1981)
5. Davis *et al.* (1995)
6. Block & Moody (1987)
7. Takahashi *et al.* (1971)
8. Miyazaki *et al.* (1972)
9. Ribera & Spitzer (1991)
10. Spruce & Moody (1992)
11. Christensen & Strange (2001)
12. Schirrmacher & Deitmer (1989)
13. Schirrmacher & Deitmer (1991)
14. Baines & Bate (1998)
15. Hardie (1991)
16. Goodman *et al.* (1980)
17. Olson *et al.* (2000)
18. Olson (1996)
19. Spitzer *et al.* (2000)
20. Barish (1986)
21. Bader *et al.* (1983)
22. Gottmann *et al.* (1988)
23. Bader *et al.* (1986)
24. Bahrey & Moody (2003)
25. Ziskind-Conhaim (1988a)
26. Gao & Ziskind-Conhaim (1998)
27. Martin-Caraballo & Greer (2000)

Table 2 - Composition of neurogenic treatments applied to neoblasts.

	Treatment													
	Control	A	B	C	D	E	F	G	H	J	K	A+D	A+F	A+G
dibutyryl-cAMP	—	100µM	—	100µM	—	—	—	—	—	—	—	100µM	100µM	100µM
IBMX	—	100µM	—	100µM	—	—	—	—	—	—	—	100µM	100µM	100µM
PMA	—	—	100nM	100nM	—	—	—	—	—	—	—	—	—	—
bFGF	—	—	—	—	10ng/ml	—	—	—	—	—	—	10ng/ml	—	—
EGF	—	—	—	—	—	10ng/ml	—	—	—	—	—	—	—	—
RA	—	—	—	—	—	—	1µM	—	—	—	—	—	1µM	—
5-HT	—	—	—	—	—	—	—	150µM	—	—	—	—	—	150µM
3-HT	—	—	—	—	—	—	—	—	100µM	—	—	—	—	—
RF-amide	—	—	—	—	—	—	—	—	—	100µM	—	—	—	—
DMSO(v/v)	—	0.005	0.01	0	0	0.05	0	0	0	0	0.1	0.005	0.015	0.005

IBMX – iso-butyl-methylxanthine

PMA – phorbol 12-myristate 13-acetate

bFGF – basic fibroblast growth factor

EGF – epidermal growth factor

RA – retinoic acid

5-HT – 5-hydroxytryptamine (serotonin)

3-HT – 3-hydroxytryptamine (dopamine)

RF-amide – Arg-Phe-NH₂ isolated from tissues of *P. penicillatus*

DMSO – dimethyl sulfoxide

Table 3 - Composition of the different extracellular and intracellular solutions used to determine resting membrane properties and identify voltage-gated ion channels in neoblasts from *Girardia tigrina*. All values are expressed in mM concentrations.

	K ⁺ extracellular	K ⁺ pipette	K ⁺ pipette - with ATP	Ca ²⁺ extracellular	Ba ²⁺ extracellular	Ca ²⁺ pipette
Choline chloride	130	—	—	130	130	—
KCl	5	135	135	—	—	—
MgCl ₂	1	—	—	1	1	—
CoCl ₂	2	—	—	—	—	—
CsCl	—	—	—	5	5	135
CaCl ₂	—	—	—	2	—	—
BaCl ₂	—	—	—	—	2	—
HEPES	10	10	10	10	10	10
EGTA	—	—	—	—	—	10
D-glucose	—	10	10	—	—	10
Mg-ATP	—	—	2	—	—	2
GTP	—	—	0.1	—	—	0.1
pH	7.3 w/ KOH	7.3 w/ KOH	7.3 w/ KOH	7.4 w/ CsOH	7.4 w/ CsOH	7.4 w/ CsOH

Table 4 – Summary of neuropeptides, neurotransmitters, and second messenger pathways involved in regulating neurogenesis

Morphogenic Agent	Tubulin expression	Neurite outgrowth
Retinoic acid	No effect	+++
Neuropeptides		
RF-amide	++	+++
Epidermal growth factor	++	No effect
Basic fibroblast growth factor	No effect	No effect
Biogenic amines		
Dopamine	++	No effect
Serotonin	No effect	No effect
Intracellular messengers		
Phorbol esters (PMA)	No effect	No effect
↑ cAMP (DBcAMP, IBMX)	No effect	++
Cocktail treatments		
Phorbol esters + ↑ cAMP	++	No effect
Basic fibroblast growth factor + ↑ cAMP	++	++
Serotonin + ↑ cAMP	+++	+++
<i>Helisoma</i> BCM (growth & neurotrophic factors, 5-HT)	++	++

++ increased by 2-fold compared to control - Statistically different from 24 h control, $p < 0.05$

+++ increased by 3-fold compared to control - Statistically different from (++) , $p < 0.05$

Table 5 – Review table of changes in occurring in differentiation neurons (A+G treated) from *G. tigrina*

Time in culture	% neurons	% with neurites	C _m (pF)	Tau (ms)	Resting V _m (mV)	% with K _{DR}	Peak / density (pA/μm ²)	% with K _A
0 h	5.7±2.3 (5)	0.35±0.4 (5)	8.41±1.4 (8)	82.8±8.8 (8)	-24.8±1.4 (5)	66.7 (6)	0.20±0.06 (15)	0 (6)
24 h – Control	10.4±1.4 [†] (5)	0.46±0.3 (5)	8.24±0.6 (15)	81.2±4.0 (14)	-27.8±2.2 (11)	82.4 [†] (17)	0.20±0.05 (10)	0 (n=17)
12 h – A+G	—	—	8.93±1.6 (8)	88.8±8.1 (8)		72.7 to 75.0 [†] (19)		—
24 h – A+G			7.82±1.1 (12)	81.2±4.0 (7)		85.0 [†] (20)		

Values are means ± SEM; sample size is in parentheses. Membrane capacitance (C_m), membrane time constant (Tau), and resting membrane potential (V_m) were measured in the whole-cell patch clamp configuration

K_{DR} – delayed rectifier K⁺ channels

K_A – A-type like K⁺ channels

[†] Statistically different from 0 h control, p < 0.05 (light grey cells)

[‡] Statistically different from 24 h control, p < 0.05 (dark grey cells)

Literature cited

- Achee, N.L., & Zoran, M.J. (1996). Short-term and long-term alterations in neuronal excitability during injury-induced axonal regeneration in galglia and cell culture. *Invertebrate Neuroscience*, 2:189-198
- Adoutte, A., Balavoine, G., Lartillot, N., de Rosa, R. (1999). Animal evolution: the end of the intermediate taxa?. *Trends in Genetics*, 15:104-108
- Adoutte, A., Balavoine, G., Lartillot, N., Lespinet, O., Prud'homme, B., & de Rosa, R. (2000). The new animal phylogeny: Reliability and implications. *Proceedings of the National Academy of Sciences, USA*, 97:4453-4456
- Agata, K., & Watanabe, K. (1999). Molecular and cellular aspects of planarian regeneration. *Seminars in Cell and Developmental Biology*, 10:377-383
- Agata, K., Soejima, Y., Kato, K., Kobayahis, C., Umesono, Y., Watanabe, K. (1998). Structure of the planarian central nervous system (CNS) revealed by neuronal cell markers. *Zoological Science*, 15:433-440
- Agata, K., Tanaka, T., Kobayashi, C., Kato, K., & Saitoh, Y. (2003). Intercalary regeneration in planarians. *Developmental Dynamics*, 226:308-316
- Alegri, S., Carolei, A., Ferretti, P., Gallone, C., Palladini, G., & Venturini, G. (1983). Effects of depaminergic agents on monoamine levels and motor behaviour in planaria. *Comparative Biochemistry and Physiology, C*, 74:27-29
- Amagai, Y., Iijima, M., & Kasai, S. (1983). Development of excitability during the *in vitro* differentiation of a newly established myogenic cell line. *Japanese Journal of Physiology*, 33:547-557
- Anderson, P.A.V., & Mackie, G.O. (1977). Electrically coupled, photosensitive neurons control swimming in a jellyfish. *Science*, 197:186-188
- Arakawa, Y., Sendtner, M., & Thoenen, H. (1990) Survival effect of ciliary neurotrophic factor (CNTF) on chick embryonic motoneurons in culture-comparison with other neurotrophic factors and cytokines. *The Journal of Neuroscience*, 10:3507-3515
- Arkett, S.A., & Spencer, A.N. (1986). Neuronal mechanisms of a hydromedusan shadow reflex. II. Graded response of reflex components, possible mechanisms of photic integrations, and functional significance. *Journal of Comparative Physiology, A*, 159:215-225

Asami, M., Nakatsuka, T., Hayashi, T., Kou, K., Kagawa, H., & Agata, K. (2002). Cultivation and characterization of planarian neuronal cells isolated by fluorescence activated cell sorting (FACS). *Zoological Science*, 19:1257-1265

Ax, P. (1987). *The phylogenetic system: the systematization of organisms on the basis of their phylogenesis*. Wiley Interscience. New York, NY

Bader, C.R., Bertrand, D., & Kato, A.C. (1983). Membrane currents in a developing parasympathetic ganglion. *Developmental Biology*, 98:515-519

Bader, C.R., Bertrand, D., & Dupin, E. (1985). Voltage-dependent potassium currents in developing neurones from quail mesencephalic neural crest. *Journal of Physiology*, 366:129-151

Bahrey, H.L., & Moody, W.J. (2003). Early development of voltage-gated ion currents and firing properties in neurons of the mouse cerebral cortex. *Journal of Neurophysiology*, 89:1761-1773

Baguna, J. (1974). Dramatic mitotic response in planarians after feeding, and a hypothesis for the control mechanism. *Journal of Experimental Zoology*, 190:117-122

Baguna, J. (1976a). Mitosis in the intact and regenerating planarian *Dugesia mediterranea* n.sp.: I. Mitotic studies during growth, feeding and starvation. *Journal of Experimental Zoology*, 195:53-64

Baguna, J. (1976b). Mitosis in the intact and regenerating planarian *Dugesia mediterranea* n.sp.: II. Mitotic studies during regeneration, and a possible mechanism of blastema formation. *Journal of Experimental Zoology*, 195:65-80

Baguna, J. (1998). Planarians. *In Cellular and molecular basis of regeneration: from invertebrates to humans*, Ferretti, P., & Geraudie, J. *ed.* John Wiley & Sons Ltd. Chichester, pp:135-165

Baguna, J., & Romero, R. (1981). Quantitative analysis of cell types during growth, degrowth and regeneration in the planarians *Dugesia mediterranea* and *Dugesia tigrina*. *Hydrobiologia*, 84:181-194

Baguna, J., & Boyer, B.C. (1990). Descriptive and experimental embryology of the Turbellaria: Present knowledge, open questions and future trends. *In Experimental Embryology in Aquatic Plants and Animals*, Marthy, H.-J., *ed.* Plenum Press, New York, NY, pp:95-128

Baguna, J., Salo, E., Collet, J., Auladell, M.C., & Ribas, M. (1988). Cellular, molecular and genetic approaches to regeneration and pattern formation in planarians. *Fortschritte der Zoologie*, 36:65-78

- Baguna, J., Salo, E., & Auladell, C. (1989). Regeneration and pattern formation in planarians. III. Evidence that neoblasts are totipotent stem cells and the source of blastema cells. *Development*, 107:77-86
- Baguna, J., Romero, Salo, E., Collet, C.A., Ribas, M., Riutort, M., J., Garcia-Fernandez, J., Burgaya, F., & Bueno, D. (1990). Growth, degrowth and regeneration as developmental phenomena in adult freshwater planarians. *In Experimental Embryology in Aquatic Plants and Animals*, Marthy, H.-J., *ed*, Plenum Press, New York, NY, pp:129-162
- Baguna, J., Salo, E., Romero, R., Garcia-Fernandez, J., Bueno, D., Munoz-Marmoi, A.M., Bayascas-Ramirez, J.R., & Casali, A. (1994). Regeneration and pattern formation in planarians: Cells, molecules and genes. *Zoological Science*, 11:781-795
- Bain, G., Kitchens, D., Yao, M., Huettner, J.E., & Gottlieb, D.I. (1995). Embryonic stem cells express neuronal properties *in vitro*. *Developmental Biology*, 168:342-357
- Baines, R.A., & Bate, M. (1998). Electrophysiological development of central neurons in the *Drosophila* embryo. *The Journal of Neuroscience*, 18(12):4673-4683
- Bargmann, C.I. (1998). Neurobiology of the *Caenorhabditis elegans* genome. *Science*, 282:2028-2033
- Becker, E., Soler, R.M., Yuste, V.J., Gine, E., Sanz-Rodriguez, C., Egea, J., Martin-Zanca, D., & Comella, J.X. (1998). Development of survival responsiveness to brain-derived neurotrophic factor, neurotrophin 3 and neurotrophin 4/5, but not to nerve growth factor, in cultured motoneurons from chick embryo spinal cord. *The Journal of Neuroscience*, 18(19):7903-7911
- Benquet, P., Guen, J., Pichon, Y., & Tiaho, F. (2001). Differential involvement of Ca²⁺ channels in survival and neurite outgrowth of cultured embryonic cockroach brain neurons. *Journal of Neurophysiology*, 88:1475-1490
- Bertrand, N., Castro, D.S., & Guillemot, F. (2002). Proneural genes and the specification of neural cell types. *Nature Reviews Neuroscience*, 3:517-530
- Betchaku, T. (1967). Isolation of planarian neoblasts and their behaviour *in vitro* with some aspects of the mechanism of the formation of regeneration blastema. *The Journal of Experimental Zoology*, 164:407-434
- Biser, P.S., Thayne, K.A., Kong, J.Q., Fleming, W.W., & Taylor, D.A. (2000). Quantification of the α -subunit of the Na⁺/K⁺-ATPase in developing rat cerebellum. *Developmental Brain Research*, 123:165-172

- Bixby, J.L., & Spitzer, N.C. (1984). The appearance and development of neurotransmitter sensitivity in *Xenopus* embryonic spinal neurones *in vitro*. *Journal of Physiology*, 353:143-155
- Block, M.L., & Moody, W.J. (1987). Changes in sodium, calcium and potassium currents during early embryonic development of the ascidian *Boltenia villosa*. *The Journal of Physiology*, 393:619-634
- Bode, H., Berking, S., David, C.N., Gierer, A., Schaller, H., & Trenkner, E. (1973). Quantitative analysis of cell types during growth and morphogenesis in *Hydra*. *Wilhelm Roux' Archiv fur Entwicklungsmechanik der Organismen*, 171:269-285
- Bogler, O., Wren, D., Barnett, S.C., Land, H., & Nobel, M. (1990). Cooperation between two growth factors promotes extended self-renewal and inhibits differentiation of oligodendrocyte-type-2 astrocyte (O-2A) progenitor cells. *Proceedings of the National Academy of Sciences, USA*, 87:6368-6372
- Borges, K., Wolswijk, G., Ohlemeyer, C., & Kettenmann, H. (1995). Adult rat optic nerve oligodendrocyte progenitor cells express a distinct repertoire of voltage- and ligand-gated ion channels. *Journal of Neuroscience Research*, 40:591-605
- Borodinsky, L.N., Root, C.M., Cronin, J.A., Sann, S.B., Gu, X., Spitzer, N.C. (2004). Activity-dependent homeostatic specification of transmitter expression in embryonic neurons. *Nature*, 429:523-530
- Boyer, B.C. (1971). Regulative development in a spiralian embryo as shown by cell deletion experiments on the acoel *Childia*. *The Journal of Experimental Zoology*, 176:97-106
- Boyer, B.C. (1987). Development of *in vitro* fertilized embryos of the polyclad flatworm *Hoplana inquilina* following blastomere separation and deletion. *Roux's Archives of Developmental Biology*, 196:158-164
- Boyer, B.C. (1989). The role of the first quartet micromers in the development of the polyclad *Hoplana inquilina*. *Biological Bulletin*, 177:338-343
- Boyer, B.C. (1992) The effect of deleting opposite first quartet micromeres on the development of the polyclad *Hoplana*. *Biological Bulletin*, 183:374-375
- Boyer, B.C., Henry, J.J., & Martindale, M.Q. (1996). Dual origins of mesoderm in a basal bilaterian: Cell lineage analyses in the Polyclad Turbellarian *Hoplana inquilina*. *Developmental Biology*, 179:329-338
- Boyer, B.C., Henry, J.J., & Martindale, M.Q. (1998) The cell lineage of a Polyclad Turbellarian embryo reveals close similarity to Coelomate Spiralian. *Developmental Biology*, 204:111-123

- Brismar, T., & Gilly, W.F. (1987). Synthesis of sodium channels in the cell bodies of squid giant axons. *Proceedings of the National Academy of Sciences, USA*, 84:1459-1463
- Broadie, C., & Sampson, S.R. (1986). Influence of various growth factors and conditions on development of resting membrane potential and its electrogenic pump component of cultured rat skeletal myotubes. *International Journal of Developmental Neuroscience*, 4:327-337
- Broadie, K., & Bate, M. (1993b). Activity-dependent development of the neuromuscular synapse during *Drosophila* embryogenesis. *Neuron*, 11:607-619
- Brondsted, H.V. (1955). Planarian regeneration. *Biological Review*, 30:65-126
- Brusca, R.C., & Brusca, G.J. (1990). *Invertebrates*. Sinauer Associates, Inc. Sunderland, MA
- Buckingham, S.D., & Spencer, A.N. (2000). K^+ currents in cultured neurones from a polyclad flatworm. *The Journal of Experimental Biology*, 203:3189-3198
- Buckingham, S.D., & Spencer, A.N. (2002) The role of high-voltage activated potassium currents in high-frequency neuronal firing: evidence from a basal metazoan. *Journal of Neurophysiology*, 88:861-868.
- Bueno, D., Espinosa, L., Soriano, M.A., Batlle, E., Baguna, J., & Romero, R. (1995). TCEN-49, a monoclonal antibody that identifies a central body antigen in the planarian *Dugesia (Girardia) tigrina*. Implications for pattern formation and positional signalling mechanisms. *Hydrobiologia*, 305:235-240
- Bueno, D., Baguna, J., & Romero, R. (1997). Cell-, tissue-, and position-specific monoclonal antibodies against the planarian *Dugesia (Girardia) tigrina*. *Histochemistry and Cell Biology*, 107:139-149
- Bullock, T.H., & Horridge, G.A. (1965). *Structure and function in the nervous systems of invertebrates*, Vol. I. W H Freeman and Co., San Francisco
- Buonanno, A., & Fields, R.D. (1999). Gene regulation by patterned electrical activity during neural and skeletal muscle development. *Current Opinion in Neurobiology*, 9:110-120
- Burke, R.D., Myers, R.L, Sexton, T.L., & Jackson, C. (1991). Cell movements during the initial phase of gastrulation in the sea urchin embryo. *Developmental Biology*, 146:542-557

- Cameron, H.A., Hazel, T.G., & McKay, D.G. (1998a). Regulation of neurogenesis by growth factors and neurotransmitters. *Journal of Neurobiology*, 36:287-306
- Campanot, R.B. (1977). Local control of neurite development by nerve growth factor. *Proceedings of the National Academy of Sciences, USA*, 74:4516-4519
- Carranza, S., Baguna, J., & Riutort, M. (1997). Are the Platyhelminthes a monophyletic primitive group? An assessment using 18S rDNA sequences. *Molecular Biology and Evolution*, 14:485-497
- Cayouette, M., & Raff, M. (2002). Asymmetric segregation of Numb: a mechanism for neural specification from *Drosophila* to mammals. *Nature Neuroscience*, 5:1265-1269
- Cebria, F., Kobayashi, C., Umesono, Y., Nakazawa, M., Mineta, K., Ikeo, K., Gojobori, T., Itoh, M., Taira, M., Sanchez Alvarado, A., & Agata, K. (2002a). FGFR-related gene *nou-darake* restricts brain tissues to the head region of planarians. *Nature*, 419:620-624
- Cebria, F., Kudome, T., Nakazawa, M., Mineta, K., Ideo, K., Gojobori, T., & Agata, K. (2002b). The expression of neural-specific genes reveals the structural and molecular complexity of the planarian central nervous system. *Mechanisms of Development*, 116:199-204
- Cebria, F., Nakazawa, M., Mineta, K., Ideo, K., Gojobori, T., & Agata, K. (2002c). Dissecting planarian central nervous system regeneration by the expression of neural-specific genes. *Development Growth and Differentiation*, 44:135-146
- Cepko, C.L. (1999). The roles of intrinsic and extrinsic cues and bHLH genes in the determination of retinal cell fates. *Current Opinion in Neurobiology*, 9:37-46
- Chia, W., & Yang, X. (2002). Asymmetric division of *Drosophila* neural progenitors. *Current Opinion in Genetics and Development*, 12:459-464
- Chitnis, A.B. (1999). Control of neurogenesis. *Current Opinion of Neurobiology*, 9:18-25
- Christensen, M., Strange, K. (2001). Developmental regulation of a novel outwardly rectifying mechanosensitive anion channel in *Caenorhabditis elegans*. *The Journal of Biological Chemistry*, 276(48):45024-45030
- Cloues, R.K., & Sather, W.A. (2003). Afterhyperpolarization regulates firing rate in neurons of the suprachiasmatic nucleus. *The Journal of Neuroscience*, 23(5):1593-604
- Cohan, C.S., Connor, J.A., Kater, S.B. (1987). Electrically and chemically mediated increases in intracellular calcium in neuronal growth cones. *The Journal of Neuroscience*, 7(11):3588-3599

- Cohan, C.S., & Kater, S.B. (1986). Suppression of neurite elongation and growth cone motility by electrical activity. *Science*, 232:1638-1640
- Collins, F., Schmidt, M.F., Guthrie, P.B., & Kater, S.B. (1991). Sustained increase in intracellular calcium promotes neuronal survival. *The Journal of Neuroscience*, 11(8):2582-2587
- Connor, J. A., & Stevens, C. F. (1971b). Voltage clamp studies of a transient outward membrane current in gastropod neural somata. *Journal of Physiology*, 213:21-30
- Constantine-Paton, M. Cline, H.T. & Debski, E.A. (1990). Patterned activity, synaptic convergence and the NMDA receptor in developing visual pathways. *Annual Review of Neuroscience*, 13:129-154
- Crair, M.C. (1999). Neuronal activity during development: permissive or instructive? *Current Opinion in Neurobiology*, 9:88-93
- Curry, W.J., Shaw, C., Johnston, C.F., Thim, L., & Buchanan, K.D. (1992). Neuropeptide F: primary structure from the turbellarian, *Artioposthia triangulate*. *Comparative Biochemistry and Physiology, C*, 101:269-274
- Dallman, J.E., Davis, A.K., & Moody, W.J. (1998). Spontaneous activity regulates calcium-dependent K⁺ current expression in developing ascidian muscle. *Journal of Physiology*, 511:683-693
- Dallman, J.E., Dorman, J.B., & Moody, W.J. (2000). Action potential waveform voltage clamp shows significance of different Ca²⁺ channel types in developing ascidian muscle. *Journal of Physiology*, 524:375-386
- Damen, P., & Dictus, W.J.A.G. (1994). Cell lineage of the prototroch of *Patella vulgata* (Gastropoda, Mollusca). *Developmental Biology*, 162:364-383
- Davidson, E.H. (1990). How embryos work: a comparative view of diverse modes of cell fate specification. *Development*, 108:365-389
- Davidson, E.H. (1991). Spatial mechanisms of gene regulation in metazoan embryos. *Development*, 113:1-26
- Davidson, E.H. (2001). Genomic regulatory systems. Academic Press, San Diego, CA
- Davis, A.K., Greaves, A.A., Dallman, J.E., & Moody, W.J. (1995). Comparison of ionic currents expressed in immature and mature muscle cells of an ascidian larva. *The Journal of Neuroscience*, 15(7):4875-4884
- Day, T.A., & Maule, A.G. (1999). Parasitic peptides! The structure and function of neuropeptides in parasitic worms. *Peptides*, 20:999-1019

- Day, T.A., Maule, A.G., Shaw, C., Halton, D.W., Moore, S., Bennett, J.L., & Pax, R.A. (1994). Platyhelminth FMRFamide-related peptides (FaRPs) contract *Schistosoma mansoni* (Trematoda: Digenea) muscle fibres *in vitro*. *Parasitology*, 109:455-459
- Day, T.A., Chen, G.-Z., Miller, C., Ming, T., Bennett, J.L., & Pax, R.A. (1996). Cholinergic inhibition of muscle fibres isolated from *Schistosoma mansoni* (Trematoda: Digenea). *Parasitology*, 1013:55-61
- Day, T.A., Maule, A.G., Shaw, C., & Pax, R.A. (1997). Structure-activity relationships of FMRFamide-related peptide induced contractions of *Schistosoma mansoni* muscle. *Peptides*, 18:917-921
- Dicarprio, R.A. (1989). Non-spiking interneurons in the ventilatory central pattern generator of the shore crab, *Carcinus maenas*. *Journal of Comparative Neurology*, 285:83-106
- Dodson, P.D., Barker, M.C., & Forsythe, I.D. (2002). Two heteromeric Kv1 potassium channels differentially regulate action potential firing. *The Journal of Neuroscience*, 22:6953-6961
- Drobysheva, I.M. (1986). Physiological regeneration of the digestive parenchyma in *Convoluta convolute* and *Oxyposthia praedator* (Turbellaria, Acoela). *Hydrobiologia*, 132:189-193
- Drobysheva, I.M. (1997). Characteristics of cell proliferation in *Notoplana humilis* (Polycladida, Plathelminthes). *Doklady Biological Sciences*, 353:135-137
- Drobysheva, I.M., & Mamkaev, Y.V. (2001). On mitosis in embryos and larvae of polyclads (Platyhelminthes). *Belgian Journal of Zoology*, 131(Supplement 1):65-66
- Duzhyy, D.E., Sakai, Y., & Sokolowski, B.H. (2004). Cloning and developmental expression of Shaker potassium channels in the cochlea of the chicken. *Molecular Brain Research*, 121:70-85
- Easter, S.S. Jr., Purves, D., Rakic, P., & Spitzer, N.C. (1985). The changing view of neural specificity. *Science*, 230:507-511
- Edlund, T., & Jessell, T.M. (1999). Progression from extrinsic to intrinsic signalling in cell fate specification: A view from the nervous system. *Cell*, 96:211-224
- Ehlers, U. (1985). *Das phylogenetische system der Plathelminthes*. Gustav Fischer, Stuttgart, New York. 317 pp
- Ehlers, U. (1986). Comments on a phylogenetic system of the Platyhelminthes. *Hydrobiologia*, 132:1-12

- Ehlers, U. (1995). The basic organization of the Plathelminthes, *Hydrobiologia*, 305:21-26
- Faber, E.S.L., & Sah, P. (2004). Opioids Inhibit Lateral Amygdala Pyramidal Neurons by Enhancing a Dendritic Potassium Current. *The Journal of Neuroscience*, :24:3031-3039
- Fairweather, I., & Skuce, P.J. (1995). Flatworm neuropeptides – present status, future directions. *Hydrobiologia*, 305:309-316
- Fernandez-Rodriguez, J., Cardona, A., Hernandez, V., Romero, R., Bueno, D. (2001). TNEX59, a planarian regional nuclear factor differentially expressed during regeneration. *International Journal of Developmental Biology*, 45(Supplement 1):S125-S126
- Ferrari, M.B., Rohrbough, J., Spitzer, N.C. (1996). Spontaneous calcium transients regulate myofibrillogenesis in embryonic *Xenopus* myocytes. *Developmental Biology*, 178:484-497
- Francis, M.M., Mellem, J.E., & Maricq, A.V. (2003). Bridging the gap between genes and behaviour: Recent advances in the electrophysiological analysis of neural function in *Caenorhabditis elegans*. *Trends in Neurosciences*, 26(2):90-99
- Frankfurter, A., Binder, L.I., & Rebhun, L. (1986). Limited tissue distribution of a novel β -tubulin isoform. *Journal of Cell Biology*, 103:273A
- Franks, C.J., Pemberton, D., Vinogradova, I., Cook, A., Walker, R.J., & Holden-Dye, L. (2002). Ionic basis of the resting membrane potential and action potential in the pharyngeal muscle of *Caenorhabditis elegans*. *Journal of Neurophysiology*, 87:954-961
- Franquinet, R. (1979). Role de la serotonine et des catecholamines dans la regeneration de la planaire *Polycelis tenuis*. *Journal of Embryology and Experimental Morphology*, 51:85-95
- Franquinet, R. (1981). Synthese d'ADN dans les cellules de planaires cultivees in vitro. Role de la serotonine. *Biologie Cellulaire*, 40:41-46
- Friedel, T., & Webb, R.A. (1979). Stimulation of mitosis in *Dugesia tigrina* by a neurosecretory fraction. *Canadian Journal of Zoology*, 57:1818-1819
- Fujisawa, T. (1989). Role of interstitial cell migration in generating position-dependent patterns of nerve cell differentiation in *Hydra*. *Developmental Biology*, 133:77-82
- Galcheva-Gargova, Z., Derijard, B, Wu, I-H., & Davis, R.J. (1994). An osmosensing signal transduction pathway in mammalian cells. *Science*, 265:806-808

- Garnovskaya, M.N., Mukhin, Y.V., Vlasova, T.M., & Raymond, J.R. (2003). Hypertonicity activates Na^+/H^+ exchange through Janus kinase 2 and calmodulin. *Journal of Biological Chemistry*, 278:16908-16915
- Gilbert, S.F. (1997). *Developmental Biology*. 5th ed. Sinauer Associates, Inc. Sunderland, MA
- Giribet, G., & Wheeler, W.C. (1999). The position of arthropods in the animal kingdom: Ecdysozoa, islands, trees, and the "parsimony ratchet". *Molecular Phylogenetics and Evolution*, 13:619-623
- Giribet, G., Distel, D.L., Polz, M., Sterrer, W., Wheeler, W.C. (2000). Triploblastic relationships with emphasis on the acoelomates and the position of Gnathostomulida, Cycliophora, Plathelminthes, and Chaetognatha: A combined approach of 18S rDNA sequences and morphology. *Systematic Biology*, 49:539-562
- Goldberg, J.I., Mills, L.R., & Kater, S.B. (1992). Effects of serotonin on intracellular calcium in embryonic and adult *Helisoma* neurons. *International Journal of Developmental Neuroscience*, 10:255-264
- Goldstein, L. (1950). An experimental study of maturation in *Chaetopterus* eggs. *Biological Bulletin*, 99:341
- Gomez, T.M., Robles, E., Poo, M., & Spitzer, N.C. (2001). Filopodial calcium transients promote substrate-dependent growth cone turning. *Science*, 291:1983-1987
- Goodman, C.S., & Spitzer, N.C. (1979). Embryonic development of identified neurones: differentiation from neuroblasts to neurone. *Nature*, 280:208-214
- Goodman, C.S., O'Shea, M., McCaman, R., & Spitzer, N.C. (1979). Embryonic development of identified neurons: Temporal pattern of morphological and biochemical differentiation. *Science*, 204:1219-1222
- Goodman, C.S., & Spitzer, N.C. (1981a). The mature electrical properties of identified neurones in grasshopper embryos. *Journal of Physiology*, 313:369-384
- Goodman, C.S. & Spitzer, N.C. (1981b). The development of electrical properties of identified neurones in grasshopper embryos. *Journal of Physiology*, 313:385-403
- Goodman, C.S., O'Shea, M., McCaman, R., & Spitzer, N.C. (1979). Embryonic development of identified neurons: Temporal pattern of morphological and biochemical differentiation. *Science*, 204:1219-1222
- Goodman, C.S., Pearson, K.G., & Spitzer, N.C. (1980). Electrical excitability: A spectrum of properties in the progeny of a single embryonic neuroblasts. *Proceedings of the National Academy of Sciences, USA*, 77(3):1676-1680

- Gomez, T.M., & Spitzer, N.C. (1999). In vivo regulation of axon extension and pathfinding by growth-cone calcium transients. *Nature*, 397:350-355
- Goridis, C., & Rohrer, H. (2002). Specification of catecholaminergic and serotonergic neurons. *Nature Reviews Neuroscience*, 3:531-541
- Goss, G.G., Jiang, L., Vandorpe, D.H., Kieller, D., Chernova, M.N., Roberston, M., & Alper, S.L. (2001). Role of JNK in hypertonic activation of Cl⁻ dependent Na⁺/H⁺ exchange in *Xenopus* oocytes. *American Journal of Cell Physiology*, 281:1978-1990
- Gottmann, K., Dietzel, I.D., Lux, H.D., Huck, S., & Rohrer, H. (1988). Development of inward currents in chick sensory and autonomic neuronal precursor cells in culture. *The Journal of Neuroscience*, 8:3722-3732
- Greene, L.A., & Kaplan, D.R. (1995). Early events in neurotrophin signalling via Trk and p75 receptors. *Current Opinion in Neurobiology*, 5:579-587
- Grewel, S.S., York, R.D., & Stork, P.J.S. (1999). Extracellular-signal-regulated kinase signalling in neurons. *Current Opinion in Neurobiology*, 9:544-553
- Grigaliuna, A., Bradley, R.M., MacCallum, D.K., & Mistretta, C.M. (2002). Distinctive neurophysiological properties of embryonic trigeminal and geniculate neurons in culture. *Journal of Neurophysiology*, 88:2058-2078
- Gritti, A., Parati, E.A., Cova, L., Frolichsthal, P., Galli, R., Wanke, E., Faravelli, L., Morassutti, D.J., Roisen, F., Nickel, D.D., & Vescovi, A.L. (1996). Multipotential stem-like cells from the adult mouse brain proliferate and self-renew in response to basic fibroblast growth factor. *The Journal of Neuroscience*, 16:1091-1100
- Gritti, A., Frolichsthal-Schoeller, P., Galli, R., Parati, E.A., Cova, L., Pagano, S.F., Bjornson, C.R., & Vescovi, A.L. (1999). Epidermal and fibroblast growth factors behave as mitogenic regulators for a single multipotent stem cell-like population from the subventricular region of the adult mouse forebrain. *The Journal of Neuroscience*, 19:3287-3297
- Gschwentner, R., Ladurner, P., Nimeth, K., & Rieger, R. (2001). Stem cells in a basal bilaterian: S-phase and mitotic cells in *Convolutriloba longifissura* (Acoela, Platyhelminthes). *Cell and Tissue Research*, 304:401-408
- Gu, X., & Spitzer, N.C. (1995). Distinct aspects of neuronal differentiation encoded by frequency of spontaneous Ca²⁺ transients. *Nature*, 375:784-787
- Gustaffson, M.K.S., Eriksson, K., & Hyden, A. (1995). Never ending growth and a growth factor. II. Immunocytochemical evidence for the presence of epidermal growth factor in a tapeworm. *Hydrobiologia*, 305:229-233

- Guyton, A.C., & Hall, J.E. (2000). Textbook of medical physiology, 10th ed. Saunders, Toronto, ON.
- Hall, F., Morita, M., & Best, J.B. (1986a). Neoplastic transformation in the planarian: I. Cocarcinogenesis and histopathology. *Journal of Experimental Zoology*, 240:211-227
- Hall, F., Morita, M., & Best, J.B. (1986b). Neoplastic transformation in the planarian: II. Ultrastructure of malignant reticuloma. *Journal of Experimental Zoology*, 240:229-244
- Halton, D.W., & Maule, A.G. (2004). Flatworm nerve-muscle: structural and functional analysis. *Canadian Journal of Zoology*, 82:316-333
- Harbers, E., Burst, R., & Notbohm, H. (1982). Structural arrangement of chromatin. *Klinische Wochenschrift*, 60:51-59
- Hardie, R.C. (1991). Voltage-sensitive potassium channels in *Drosophila* photoreceptors. *The Journal of Neuroscience*, 11(10):3079-3095
- Harris, K.M., Jensen, F.E., & Tsao, B. (1992). Three-dimensional structure of dendritic spines and synapses in rat hippocampus at postnatal day 15 and adult ages: implications for the maturation of synaptic physiology and long-term potentiation. *The Journal of Neuroscience*, 12:2685-2705
- Harris-Warrick, R.M., Flamm, R.E., Johnson, B.R., & Katz, P.S. Modulation of neural circuits in Crustacea. *American Zoologist*, 29:1305-1320
- Hartenstein, V., & Ehlers, U. (2000). The embryonic development of the rhabdocoel flatworm *Mesostoma lingua* (Abildgaard, 1789). *Development Genes and Evolution*, 210:399-415
- Hartline, D.K., & Maynard, D.M. (1975). Motor patterns in the stomatogastric ganglion of the lobster *Panulirus argus*. *Journal of Experimental Biology*. 62:405-420
- Hay, E.D., & Coward, S.J. (1975). Fine structure studies on the Planarian, *Dugesia*: I. Nature of the "Neoblast" and other cell types in noninjured worms. *Journal of Ultrastructure Research*, 50:1-21
- Haydon, P.G., McCobb, D.P., & Kater, S.B. (1984). Serotonin selectively inhibits growth cone motility and synaptogenesis of specific identified neurons. *Science*, 226:561-564
- Haydon, P.G., McCobb, P., & Kater, S.B. (1987). The regulation of neurite outgrowth, growth cone motility, and electrical synaptogenesis by serotonin. *Journal of Neurobiology*, 18:197-215

- Henry, J.J., & Martindale, M.Q. (1999). Conservation and innovation in spiralian development. *Hydrobiologia*, 402:255-265
- Hernandez, R.J. (1992). Na⁺/K⁺-ATPase regulation by neurotransmitters. *Neurochemistry International*, 20:1-10
- Hille, B. (2001). Ion channels of excitable membranes. 3rd ed. Sinauer Associates, Inc. Sunderland, MA
- Hodgkin, A.L., & Huxley, A.F. (1952a). Currents carried by sodium and potassium ions through the membrane of the giant axon of *Loligo*. *Journal of Physiology*, 116:449-472.
- Hodgkin, A.L., & Huxley, A.F. (1952b). The components of membrane conductance in the giant axon of *Loligo*. *Journal of Physiology*, 116:473-496.
- Hodgkin, A.L., & Huxley, A.F. (1952d). Quantitative description of membrane current its application to conduction and excitation in nerve. *Journal of Physiology*, 117:500-544.
- Hogg, R.C., Chipperfield, H., Whyte, K.A., Stafford, M.R., Hansen, M.A., Cool, S.M., Nurcombe, V., & Adams, D.J. Functional maturation of isolated neural progenitor cells from the adult rat hippocampus. *European Journal of Neuroscience*, 19:2410-2420
- Hopker, V.H., Shewan, D., Tessier-Lavigne, M., Poo, M.M., & Holt, C. (1999). Growth-cone attraction to netrin-1 is converted to repulsion by laminin-1. *Nature*, 401:69-73
- Hribar, M., Bloc, A., Medilanski, J., Nusch, L., & Eder-Colli, L. (2004). Voltage-gated K⁺ current: a marker for apoptosis in differentiating neuronal progenitor cells? *European Journal of Neuroscience*, 20:635-648
- Hubel, D., & Wiesel, T. (1962). Receptive fields, binocular interaction and functional architecture in the cat's visual cortex. *Journal of Physiology*, 160:106-154
- Hubel, D., & Wiesel, T. (1963). Receptive fields of cells in striate cortex of very young, visually inexperienced kittens. *Journal of Neurophysiology*, 26:994-1002
- Huff, R., Furst, A., & Mahowald, A.P. (1989). *Drosophila* embryonic neuroblasts in culture: Autonomous differentiation of specific neurotransmitters. *Developmental Biology*, 134:146-157
- Hyman, L.H. (1951). The invertebrates: Platyhelminthes and Rhynchocoela, vol. II. 2nd ed. McGraw-Hill Book Company, Inc. New York, NY
- Ishii, S. (1995). Cellular succession in the epithelium lining the pharyngeal cavity of planarians. *Hydrobiologia*, 305:223-224

- Jan, Y.N., & Jan, L.Y. (2000). Asymmetric cell division in the *Drosophila* nervous system. *Nature Review*
- Jeffery, W.R. (1985). The spatial distribution of maternal mRNA is determined by a cortical cytoskeletal domain in *Chaetopterus* eggs. *Developmental Biology*, 110:217-229
- Jensen, L.M. (1987). Phenotypic differentiation of aphidicolin-selected human neuroblastoma cultures after long-term exposure to nerve growth factor. *Developmental Biology*, 120:56-64
- Jessell, T.M. (2000). Neuronal specification in the spinal cord: Inductive signals and transcriptional codes. *Nature Reviews Genetics*, 1:20-28
- Johnston, R.N., Shaw, C., Halton, D.W., Verhaert, P., & Baguna, J. (1995). GYIRFamide: a novel FMRFamide-related peptide (FaRP) from the triclad turbellarian, *Dugesia tigrina*. *Biochemical and Biophysical Research Communications*, 209:689-697
- Johnston, R.N., Shaw, C., Halton, D.W., Verhaert, P., Blair, K.L., Brennan, G.P., Price, D., & Anderson, P.A.V. (1996). Isolation, localization and bioactivity of the FMRFamide related neuropeptides GYIRFamide and YIRFamide from the marine turbellarian, *Bdelloura candida*. *Journa of Neurochemistry*, 67:814-821
- Junge, D. (1992). *Nerve and muscle excitation*. 3rd ed. Sinauer, Sunderland, MA
- Kamb, A., Iverson, L.E., & Tanouye, M.A. (1987). Molecular characterization of *Shaker*, a *Drosophila* gene that encodes a potassium channel. *Cell*, 50:405-413
- Kandel, E.R., Schwartz, J.H., & Jessell, T.M. (2000). *Principles of neural science*, 4th ed. McGraw Hill, New York, NY
- Kapus, A., Szaszi, K., Sun, J., Rizoli, S., & Rolstein, O.R. (1999). Cell shrinkage regulates Src kinases and induces tyrosine phosphorylation of cartactin, independent of the osmotic regulation of Na⁺/H⁺ exchangers. *Journal of Biological Chemistry*, 274:8093-8102
- Karling, T.G. (1974). On the anatomy and affinities of the Turbellarian orders. *In* *Biology of the Turbellaria*, ed. Riser, N.W, & Morse, M.P. pp:1-16, McGraw-Hill, New York, NY
- Kato, K., Orii, H., Watanabe, K., & Agata, K. (2001). Dorsal and ventral positional cues required for the onset of planarian regeneration may reside in differentiated cells. *Developmental Biology*, 233:109-121
- Katz, P.S. (1991). Neuromodulation and the evolution of a simple motor system. *Seminars in the Neurosciences*, 3:379-389

- Kimpinski, K., Campenot, R.B., & Mearow, K. (1997). Effects of the neurotrophins nerve growth factor, neurotrophin-3, and brain-derived Neurotrophic factor (BDNF) on neurite outgrowth from adult sensory neurons in compartmented cultures. *Journal of Neurobiology*, 33:395-410
- Knoll, A.H., & Carroll, S.B. (1999). Early animal evolution: emerging views from comparative biology and geology. *Science*, 284:2129-2137
- Komuro, H., & Rakic, P. (1992). Selective role of N-type calcium channels in neuronal migration. *Science*, 257:806-809
- Komuro, H., & Rakic, P. (1996). Intracellular Ca²⁺ fluctuations modulate the rate of neuronal migration. *Neuron*, 17:275-285
- Komuro, H., & Rakic, P. (1998b). Orchestration of neuronal migration by activity of ion channels, neurotransmitter receptors, and intracellular Ca²⁺ fluctuations. *Journal of Neurobiology*, 37:110-130
- Koos, R.D., & Seidel, R.H. (1989). Detection of acidic fibroblast growth factor mRNA in the rat ovary using reverse transcription-polymerase chain reaction amplification. *Biochemical Biophysical Research Communications*, 165:82-88
- Kornblum, H.I., Hussain, R.J., Bronstein, J.M., Gall, C.M., Lee, D.C., & Seroogy, K.B. (1997). Prenatal ontogeny of the epidermal growth factor receptor and its ligand, transforming growth factor receptor and its ligand, transforming growth factor alpha, in the rat brain. *Journal of Comparative Neurology*, 380:243-261
- Kreshchenko, N.D., Reuter, M., Sheiman, I.M., Halton, D.W., Johnston, R.N., Shaw, C., & Gustafsson, M.K.S. (1999). Relationship between musculature and nervous system in the regenerating pharynx in *Girardia tigrina* (Plathelminthes). *Invertebrate Reproduction and Development*, 35(2):109-125
- Kuang, S., Doran, S.A., Wilson, R.J.A., Goss, G.G., & Goldberg, J.I. (2002). Serotonergic sensory-motor neurons mediate a behavioral response to hypoxia in pond snail embryos. *Journal of Neurobiology*, 52:73-83
- Kuo, J.J., Siddique, T., Fu, R., & Heckman, C.J. (2005). Increased persistent Na⁺ current and its effect on excitability in motoneurons cultured from mutant SOD1 mice. *Journal of Physiology*, 563:843-854
- Ladurner, P., Rieger, R., & Baguna, J. (2000). Spatial distribution and differentiation potential of stem cells in hatchlings and adults in the marine Platyhelminth *Macrostomum* sp.: A Bromodeoxyuridine analysis. *Developmental Biology*, 226:231-241

- Laferriere, N.B., MacRae, T.H., & Brown, D.L. (1997). Tubulin synthesis and assembly in differentiating neurons. *Biochemistry and Cell Biology*, 75:103-117
- Lang, F., Busch, G.L., Ritter, M., Volkl, H., Waldegger, S., Gulbins, E., & Haussinger, D. (1998). Functional significance of cell volume regulatory mechanisms. *Physiological Reviews*, 78:247-306
- Lankford, K.L., DeMello, F.G., & Klein, W.L. (1988). D₁-type dopamine receptors inhibit growth cone motility in cultured retina neurons: Evidence that neurotransmitters act as morphogenic growth regulators in the developing central nervous system. *Proceedings of the National Academy of Sciences, USA*, 85:2839-2843
- Leber, S.M., & Sanes, J.R. (1995). Migratory paths of neurons and glia in the embryonic chick spinal cord. *The Journal of Neuroscience*, 15(2):1236-1248
- Lender, T.H. (1960). L'inhibition spécifique de la différenciation du cerveau des planaires d'eau douce en régénération. *Journal of Embryological and Experimental Morphology*, 8(3):291-301
- Levetzow, K.G.V. (1939). Die regeneration der polycladen turbellarien. *Archiv Entwicklung Mechanik Organismen*, 139:780-818
- Levi-Montalcini, R., & Cohen, S. (1956). *In vitro* and *in vivo* effects of a nerve growth-stimulating agent isolated from snake venom. *Proceedings of the National Academy of Sciences, USA*, 42(9):695-699
- Levi-Montalcini, R., & Booker, B. (1960). Excessive growth of the sympathetic ganglia evoked by a protein isolated from mouse salivary glands. *Proceedings of the National Academy of Sciences, USA*, 46:373-384
- Levi-Montalcini, R., & Angeletti, P.U. (1968). Nerve growth factor. *Physiological Reviews*, 48:534-569
- Levitan, I.B., & Kaczmarek, L.K. (2002). *The neuron: cell and molecular biology*. 3rd ed. Oxford University Press, New York, NY
- Liebl, D.J., & Koo, P.H. (1993). Serotonin-activated α_2 -macroglobulin inhibits neurite outgrowth and survival of embryonic sensory and cerebral cortical neurons. *Journal of Neuroscience Research*, 35:170-182
- Liem, K.F., Jr., Tremml, ., & Jessell, T.M. (1997). A role for the roof plate and its resident TGF β -related proteins in neuronal patterning in the dorsal spinal cord. *Cell*, 91:127-138

- Lieske, V., Bennett-Clarke, C.A., & Rhoades, R.W. (1999). Effects of serotonin on neurite outgrowth from thalamic neurons *in vitro*. *Neuroscience*, 90:967-974
- Lillien, L. (1998). Neural progenitors and stem cells: mechanisms of progenitor heterogeneity. *Current Opinion in Neurobiology*, 8:37-44
- Lillien, L., & Cepko, C. (1992). Control of proliferation in the retina: temporal changes in responsiveness to FGF and TGF α . *Development*, 115:253-266
- Lima, L., Matus, P., & Urbina, M. (1994). Serotonin inhibits outgrowth of goldfish retina and impairs the trophic effect of taurine. *Journal of Neuroscience Research*, 38:444-450
- Lin, Y.C.J., Grigoriev, N.G., & Spencer, A.N. (2000). Wound healing in jellyfish striated muscle involves rapid switching between two modes of cell motility and a change in the source of regulatory calcium. *Developmental Biology*, 225:87-100
- Linsdell, P., & Moody, W.J. (1995). Electrical activity and calcium influx regulate ion channel development in embryonic *Xenopus* skeletal muscle. *The Journal of Neuroscience*, 15(6):4507-4514
- Littlewood, D.T.J., Rohde, K., & Clough, K.A. (1999). The interrelationships of all major groups of Platyhelminthes: Phylogenetic evidence from morphology and molecules. *Biological Journal of the Linnaean Society*, 66:75-114
- Liu, S.-Q., J., & Kaczmarek, L.K. (1998). Depolarization selectively increases the expression of the Kv3.1 potassium channel in developing inferior colliculus neurons. *The Journal of Neuroscience*, 18(21):8758-8769
- Lnenicka, G.A., & Atwood, H.L. (1985a). Age-dependent long-term adaptation of crayfish phasic motor axon synapses to altered activity. *The Journal of Neuroscience*, 5:459-467
- Lockery, S.R., & Spitzer, N.C. (1992). Reconstruction of action potential development from whole-cell currents of differentiating spinal neurons. *The Journal of Neuroscience*, 12(6):2268-2287
- Loken, M.R. (1980). Simultaneous quantitation of Hoechst 3342 and immunofluorescence on viable cells using a fluorescence activated cell sorter. *Cytometry*, 1:136-142
- Lotto, B., Upton, L., Price, D.J., & Gaspar, P. (1999). Serotonin receptor activation enhances neurite outgrowth of thalamic neurones in rodents. *Neuroscience Letters*, 269:87-90

- Luskin, M.B., Zigova, T., Soteres, B.J., & Stewart, R.R. (1999). Neuronal progenitor cells derived from the anterior subventricular zone of the neonatal rat forebrain continue to proliferate *in vitro* and express a neuronal phenotype. *Molecular Cellular Neuroscience*, 8:351-366
- Machaca, K., DeFelice, L.J., L'Hernault, S.W. (1996). A novel chloride channel localizes to *Caenorhabditis elegans* spermatids and chloride channel blockers induce spermatid differentiation. *Developmental Biology*, 176:1-16
- Macica, C.M., von Hehn, C.A.A., Wang, L-Y., Ho, C-S., Yokoyama, S., Joho, R.H., & Kaczmarek, L.K. (2003). Modulation of the Kv3.1b potassium channel isoform adjusts the fidelity of the firing pattern of auditory neurons. *The Journal of Neuroscience*, 23(4):1133-1141
- Mackie, G.O., & Meech, R.W. (1985). Separate sodium and calcium spikes in the same axon. *Nature*, 313:791-793
- Magistretti, J., Mantegazza, M., Guatteo, E., & Wanke, E. (1996). Action potentials recorded with patch-clamp amplifiers: are they genuine? *Trends in Neuroscience*, 19:530-534
- Marois, R., & Carew, T.J. (1997b). Ontogeny of serotonergic neurons in *Aplysia californica*. *Journal of Comparative Neurology*, 386:477-490
- Marsal, M., Pineda, D., & Salo, E. (2003). *Gtwnt-5*, a member of the *wnt* family expressed in a subpopulation of the nervous system of the planarian *Girardia tigrina*. *Gene Expression Patterns*, 3:489-495
- Martelly, I. (1984b). Calcium thresholds in the activation of DNA and RNA synthesis in cultured planarian cells: relationship with hormonal and DB cAMP effects. *Cellular Differentiation*, 15:25-36
- Martelly, I., & Franquinet, R. (1984). Planarian regeneration as a model for cellular activation studies. *Trends in Biochemical Sciences*,
- Martelly, I., Franquinet, R., & Le Moigne, A. (1981). Relationship between variations of cAMP, neuromediators and the stimulation of nucleic acid synthesis during planarian (*Polycelis tenuis*) regeneration. *Hydrobiologia*, 84:195-201
- Mathias, R.T., Cohen, I.S., & Oliva, C. (1990). Limitations of the whole cell patch clamp technique in the control of intracellular concentrations. *Biophysical Journal*, 58:759-770
- Matsuda, S., Kawasaki, H., Moriguchi, T., Gotoh, Y., & Nishida, E. (1995). Activation of protein kinase cascades by osmotic shock. *Journal of Biological Chemistry*, 270:12781-12786

- Mattson, M.P., & Kater, S.B. (1987). Calcium regulation of neurite elongation and growth cone motility. *The Journal of Neuroscience*, 7(12):4034-4043
- Maule, A.G., Halton, D.W., Johnston, C.F., Shaw, C., & Fairweather, I. (1990). The serotonergic, cholinergic and peptidergic components of the nervous system in the monogenean parasite, *Diclidophora merlangi*: a cytochemical study. *Parasitology*, 100:255-273
- Maule, A.G., Shaw, C., Halton, D.W., Thim, L., Johnston, C.F., Fairweather, I., & Buchanan, K.D. (1991). Neuropeptide F: a novel parasitic flatworm regulatory peptide from *Moniezia expansa* (Cestoda: Cyclophyllidea). *Parasitology*, 102:309-316
- Maule, A.G., Shaw, C., Halton, D.W., & Thim, L. (1993b). GNFFRFamide: a novel FMRFamide-immunoreactive peptide isolated from the sheep tapeworm, *Moniezia expansa*. *Biochemical and Biophysical Research Communications*, 193:1054-1060
- Maule, A.G., Shaw, C., Halton, D.W., Curry, W.J., & Thim, L. (1994). RYIRFamide: a turbellarian FMRFamide-related peptide (FaRP). *Regulatory Peptides*, 50:37-43
- McCobb, Cohan, C.S., Connor, J.A., & Kater, S.B. (1988). Interactive effects of serotonin and acetylcholine on neurite elongation. *Neuron*, 1:377-385
- McCobb, D.P., Haydon, P.G., & Kater, S.B. (1988). Dopamine and serotonin inhibition of neurite elongation of different identified neurons. *Journal of Neuroscience Research*, 19:19-26
- McFarlane, S., Pollock, N.S. (2000). A role for voltage-gated potassium channels in the outgrowth of retinal axons in the developing visual system. *The Journal of Neuroscience*, 20(3):1020-1029
- McKinnon, R.D., Matsui, T., Dubois-Dalcq, M., & Aaronson, S.A. (1990). FGF modulates the PDGF-driven pathway of oligodendrocyte development. *Neuron*, 5:603-614
- Meininger, V., & Binet, S. (1989). Characteristics of microtubules at the different stages of neuronal differentiation and maturation. *International Review of Cytology*, 114:21-80
- Memberg, S.P., & Hall, A.K. (1995). Dividing neuron precursors express neuron-specific tubulin. *Journal of Neurobiology*, 27:26-43
- Meis, S., & Deitmer, J.W. (1997). Developmental changes of potassium currents of embryonic leech ganglion cells in primary culture. *Journal of Neuroscience Research*, 50:967-978

- Millar, A.G., & Atwood, H.L. (2004). Crustacean phasic and tonic motor neurons. *Integrative and Comparative Biology*, 44:4-13
- Miller, C.M. (2000). An overview of the potassium channel family. *Genome Biology*, 1(4):1-5
- Miller, F.D., Naus, C.C.G., Durand, M., Bloom, F.E., & Milner, R.J. (1987). Isotypes of α -tubulin are differentially regulated during neuronal maturation. *Journal of Cell Biology*, 105:3065-3073
- Miller, J.D., & Hadley, R.D. (1991). Laminin-like immunoreactivity in the snail *Helisoma*: Involvement of a ~300 kD extracellular matrix protein in promoting outgrowth from identified neurons. *Journal of Neurobiology*, 22:431-442
- Minichev, Y.S., & Pugovkin, A.P. (1979). Nervous system of the polyclad flatworm *Notoplana atomata* (O.F. Muller). *Cahiers de Biologie Marine*, 181-188
- Ming, G., Henley, J., Tessier-Lavigne, M., Song, H., Poo, M. (2001). Electrical activity modulates growth cone guidance by diffusible factors. *Neuron*, 29:441-452
- Miyazaki, S., Takahashi, K., & Tsuda, K. (1972). Calcium and sodium contributions to regenerative response in the embryonic excitable cell membrane. *Science*, 176:1441-1443
- Molnar, L.R., Thayne, K.A., Fleming, W.W., & Taylor, D.A. (1999). The role of the sodium pump in the developmental regulation of membrane electrical properties of cerebellar Purkinje neurons of the rat. *Developmental Brain Research*, 112:287-291
- Moody, W.J. (1998). Control of spontaneous activity during development. *Journal of Neurobiology*, 37:97-109
- Moraczewski, J. (1981). Cell activation during regeneration of planarians. *Hydrobiologia*, 84:203-207
- Moraczewski, J., Martelly, I., & Franquinet, R. (1986). Protein phosphorylation and the role of Ca^{2+} in planarian turbellarian regeneration. *Hydrobiologia*, 132:223-227
- Morgan, T.H. (1898). Experimental studies of the regeneration of *Planaria maculata*. *Wilhelm Roux' Archiv fur Entwicklungsmechanik der Organismen*, 7:364-397
- Morita, M., & Best, J.B. (1984a). Electron microscopic studies of planarian regeneration. III. Degeneration and differentiation of muscles. *The Journal of Experimental Zoology*, 229:413-424

- Morita, M., & Best, J.B. (1984b). Electron microscopic studies of planarian regeneration. IV. Cell division of neoblasts in *Dugesia dorotocephala*. *The Journal of Experimental Zoology*, 229:425-436
- Morita, M., & Best, J.B. (1984c). Effects of photoperiods and melatonin on planarian asexual reproduction. *The Journal of Experimental Zoology*, 231:273-283
- Morawska, E., Moraczewski, J., Malczewska, M., & Duma, A. (1981). Adenylate cyclase in regenerating tissues of the planarian *Dugesia lugubris* (O. Schmidt). *Hydrobiologia*, 84:209-212
- Murphy, M, Reid, K., Ford, M., Funes, J.B., & Bartlett, P.F. (1994). FGF2 regulates proliferation of neural crest cells, with subsequent neuronal differentiation regulated by LIF or related factors. *Development*, 120:3519-3528
- Murray, M.R. (1927). The cultivation of planarian tissues in vitro. *The Journal of Experimental Zoology*, 47:467-505
- Murrain, M., Murphy, D., Mills, L.R., & Kater, S.B. (1990). Neuron-specific modulation by serotonin of regenerative outgrowth and intracellular calcium within the CNS of *Helisoma trivolvis*. *Journal of Neurobiology*, 21:611-618
- Nakajo, K., & Okamura, Y. (2004). Development of transient outward currents coupled with Ca^{2+} -induced Ca^{2+} release mediates oscillatory membrane potential in ascidian muscle cells. *Journal of Neurophysiology*, 92:1056-1066
- Nerbonne, J.M., & Gurney, A.M. (1989). Development of excitable membrane properties in mammalian sympathetic neurons. *The Journal of Neuroscience*, 9(9):3272-3286
- Newmark, P.A., & Sanchez Alvarado, A. (2000). Bromodeoxyuridine specifically labels the regenerative stem cells of planarians. *Developmental Biology*, 220:142-153
- Nimeth, K.T., Mahlke, M., Mezzanato, A., Peter, R., Rieger, R., & Ladurner, P. (2004). Stem cell dynamics during growth, feeding, and starvation in the basal flatworm *Macrostomum* sp. (Platyhelminthes). *Developmental Dynamics*, 230:91-99
- Nishizuka, Y. (1984). The role of protein kinase C in cell surface signal transduction and tumour promotion. *Nature*, 308:693-698
- Ogawa, K., Kobayashi, C., Hayashi, T., Orii, H., Watanabe, K., & Agata, K. (2002). Planarian fibroblast growth factor receptor homologs expressed in stem cells and cephalic ganglions. *Development Growth and Differentiation*, 44:191-204
- Olmsted, J.M.D. (1922). The role of the nervous system in the regeneration of polyclad Turbellaria, 25:157-176

- O'Dowd, D.K., Ribera, A.B., & Spitzer, N.C. (1988). Development of voltage-dependent calcium, sodium, and potassium currents in *Xenopus* spinal neurons. *The Journal of Neuroscience*, 8(3):792-805
- Olson, E.C.E. (1996). Onset of electrical excitability during a period of circus plasma membrane movements in differentiating *Xenopus* neurons. *The Journal of Neuroscience*, 16(16):5117-5129
- Olsen, A.J., Picones, A., & Korenbrot, J.I. (2000). Developmental switch in excitability, Ca²⁺ and K⁺ currents of retinal ganglion cells and their dendritic structure. *Journal of Neurophysiology*, 84:2063-2077
- Ono, F., Katsuyama, Y., Nakajo, K., & Okamura, Y. (1999). Subfamily-specific posttranscriptional mechanism underlies K⁺ channel expression in a developing neuronal blastomeres. *The Journal of Neuroscience*, 16(16):6874-6886
- Oppenheim, R.W., Quinwei, Y., Prevet, D., & Yan, Q. (1992). Brain-derived neurotrophic factor rescues developing avian motoneurons from cell death. *Nature*, 360:755-757
- Palladini, G., Medolago-Albani, L., Gallo, V.P., Lauro, G.M., Diana, G., Scorsini, D., & Margotta, V. (1988). The answer of the planarian *Dugesia gonocephala* neurons to nerve growth factor. *Cellular and Molecular Biology*, 34:53-63
- Palmberg, I.E. (1986). Cell migration and differentiation during wound healing and regeneration in *Microstomum lineare* (Turbellaria). *Hydrobiologia*, 132:181-188
- Palmberg, I.E. (1990). Differentiation in free-living flatworms. *Acta Academiae Aboensis, Ser. B.*, 50(8):6-50
- Palmberg, I.E., & Reuter, M. (1990). Neuronal subsets in regenerating *Microstomum lineare*. Immunocytochemistry of FMRF/RF-amide and 5-HT. In Gustafsson, M.K.S. & Reuter, M. Eds., *The early brain*, Academiae Aboensis, Ser. B., 50(8):147-160
- Pax, R.A., Siefker, C., & Bennett, J.L. (1984). *Schistosoma mansoni*: differences in acetylcholine, dopamine, and serotonin control of circular and longitudinal parasite muscles. *Experimental Parasitology*, 58:314-324
- Pedersen, K.J. (1959a). Some features of the fine structure and histochemistry of planarian subepidermal gland cells. *Zeitschrift für Zellforschung*, 50:121-142
- Pedersen, K.J. (1959b). Cytological studies on the planarian neoblast. *Zeitschrift für Zellforschung*, 50:799-817
- Pedersen, K.J. (1961). Studies on the nature of planarian connective tissue. *Zeitschrift für Zellforschung*, 53:569-608

Perrier JF, Noraberg J, Simon M & Hounsgaard J (2000). Dedifferentiation of intrinsic response properties of motoneurons in organotypic cultures of the spinal cord of the adult turtle. *Eur J Neurosci* **12** , 2397-2404

Petersen, O.H., & Cancela, J.M. (2000). Attraction or repulsion by local Ca²⁺ signals. *Current Biology*, 10:311-314

Piper, D.R., Mujtaba, T., Rao, M.S., & Lucero, M.T. (2000). Immunocytochemical and physiological characterization of a population of cultured human neural precursors. *Journal of Neurophysiology*, 84:534-548

Purves, D., Riddle, D.R., White, L.E., & Guitierrez-Ospina, G. (1994). Neural activity and the development of the somatic sensory system. *Current Opinion in Neurobiology*, 4:120-123

Rakic, P. (1972). Mode of cell migration to the superficial layers of fetal monkey neocortex. *Journal of comparative neurology*. 145:61-83

Reiff, D.F., & Guenther, E. (1999). Developmental changes in voltage-activated potassium currents of rat retinal ganglion cells. *Neuroscience*, 92:1103-1117

Render, J. (1991). Fate maps of the first quartet micromeres in the gastropod *Ilyanassa* obsolete. *Development*, 113:495-501

Reuter, M., & Palmberg, I.M. (1989). Development and differentiation of neuronal subsets in asexually reproducing *Microstromum lineare*. Immunocytochemistry of 5-HT, RF-amide, and SCP. *Histochemistry*, 91:123-131

Reuter, M., Gustafsson, M.K.S., Sheiman, I., Terenina, N., Halton, D.W., Maule, A.G., & Shaw, C. (1995c). The nervous system of Tricaladia. II. Neuroanatomy of *Dugesia tigrina* (Paludicola, Dugesidae): an immunocytochemical study. *Invertebrate Neuroscience*, 1:133-143

Reuter, M., & Gustafsson, M.K.S. (1996). Neuronal signal substances in asexual multiplication and development in flatworms. *Cellular and Molecular Neurobiology*, 16(5):591-616

Reuter, M., Mantyla, K., & Gustafsson, M.K.S. (1998). Organization of the orthogon – main and minor nerve cords. *Hydrobiologia*, 383:175-182

Reuter, M., Raikova, O.I., & Gustafsson, M.K.S. (2001). Patterns in the nervous and muscle systems in lower flatworms. *Belgian Journal of Zoology*, 131 (Supplement 1):47-53

- Reynolds, B.A., & Weiss, S. (1992). Generation of neurons and astrocytes from isolated cells of the adult mammalian central nervous system. *Science*, 255:1707-1710
- Ribera, A.B., & Spitzer, N.C. (1990). Differentiation of I_{K_A} in amphibian spinal neurons. *The Journal of Neuroscience*, 10(6):1886-1891
- Ribera, A.B., & Spitzer, N.C. (1991). Differentiation of delayed rectifier potassium current in embryonic amphibian myocytes. *Developmental Biology*, 144:119-128
- Ribera, A.B., & Spitzer, N.C. (1992). Developmental regulation of potassium channels and the impact on neuronal differentiation, *In Ion Channels*, vol. 3, Narahashi, T., ed., Plenum Press, NY, pp:1-38
- Rieger, R.M. (1998). 100 years research on "Turbellaria". *Hydrobiologia*, 383:1-27
- Rieger, R.M., Legniti, A., Ladurner, P., Reiter, D., Asch, E., Salvenmoser, W., Schurmann, W., & Peter, R. (1999). Ultrastructure of neoblasts in microturbellaria: significance for understanding stem cells in free-living Platyhelminthes. *Invertebrate Reproduction and Development*, 35(2):127-140
- Rieger, R.M., & Ladurner, P. (2001). Searching for the stem species of the Bilateria. *Belgian Journal of Zoology*, 131 (Supplement 1):27-34.
- Robb, S.M.C., & Sanchez Alvarado, A. (2002). Identification of immunological reagents for use in the study of freshwater planarians by means of whole-mount immunofluorescence and confocal microscopy. *Genesis*, 32:293-298
- Ribera, A.B., & Spitzer, N.C. (1991). Differentiation of delayed rectifier potassium current in embryonic amphibian myocytes. *Developmental Biology*, 144:119-128
- Ridgeway, R.L., Syed, N.I., Lukowiak, K., & Bulloch, A.G.M. (1991). Nerve growth factor (NGF) induces sprouting of specific neurons of the snail, *Lymnaea stagnalis*. *Journal of Neurobiology*, 22:377-390
- Robinson, M.J., & Cobb, M.H. (1997). Mitogen-activated protein kinase pathways. *Current Opinion in Cell Biology*, 9:180-186
- Rodriguez, O.C., Schaefer, A.W., Mandato, C.A., Forscher, P., Bement, W.M., & Waterman-Storer, C.M. (2003). Conserved microtubule-actin interactions in cell movement and morphogenesis. *Nature Cell Biology*, 5:599-609
- Romero, R., & Baguna, J. (1991). Quantitative cellular analysis of growth and reproduction in freshwater planarians (Turbellaria; Tricladida). I. A cellular description of the intact organism. *Invertebrate Reproduction and Development*, 19(2):157-165
- Rudy, B. (1988). Diversity and ubiquity of K channels. *Neuroscience*, 25:729-749

- Ruiz-Trillo, I., Riutort, M., Littlewood, D.T.J., Herniou, E.A., & Baguna, J. (1999). Acoel flatworms: Earliest extant bilaterian metazoans, not members of Platyhelminthes. *Science*, 283:1919-1923
- Russell, D.F., & Hartline, D.K. (1978). Bursting neural networks: a re-examination. *Science*, 200:453-456
- Rutledge, E., Bianchi, L., Christensen, M., Boehmer, C., Morrison, R., Broslat, A., Beld, A.M., George, A.L. Jr., Greenstein, D., Strange, K. (2001). CLH-3, a CIC-2 anion channel ortholog activated during meiotic maturation in *C. elegans* oocytes. *Current Biology*, 11:161-170
- Saitoh, O., Yuruzume, E., Watanebe, K., & Nakata, H. (1997). Molecular identification of a G protein-coupled receptor family which is expressed in planarians. *Gene*, 195:55-61
- Salkoff, L. (1985). Development of ion channels in the flight muscle of *Drosophila*. *Journal of Physiology (Paris)*. 80:275-282
- Salkoff, L., & Wyman, R. (1981). Outward currents in developing *Drosophila* flight muscle. *Science*, 212:461-463
- Salkoff, L., & Wyman, R. (1983). Ion currents in *Drosophila* flight muscles. *Journal of Physiology (London)*, 337:687-709
- Salo, E., & Baguna, J. (1986). Stimulation of cellular proliferation and differentiation in the intact and regenerating planarian *Dugesia (G) tigrina* by the neuropeptides Substance P. *The Journal of Experimental Zoology*, 237:129-135
- Salo, E., & Baguna, J. (1989a). Regeneration and pattern formation in planarians. II. Local origin and role of cell movements in blastema formation. *Development*, 107:69-76
- Salo, E., & Baguna, J. (1989b). Changes in ornithine decarboxylase activity and polyamine content and effects of polyamine inhibitors in the regenerating planarian *Dugesia (G) tigrina*. *The Journal of Experimental Zoology*, 250:150-161
- Salo, E., & Baguna, J. (2002). Regeneration in planarians and other worms: New findings, new tools, and new perspectives. *The Journal of Experimental Zoology*, 292:528-539
- Sanchez Alvarado, A. (2000). Regeneration in the metazoans: Why does it happen? *BioEssays*, 22:578-590

- Sanchez Alvarado, A. (2003). The freshwater planarian *Scmidtea mediterranea*: embryogenesis, stem cells and regeneration. *Current Opinion in Genetics and Development*, 13:438-444
- Sanes, J.R. (1989). Extracellular matrix molecules that influence neural development. *Annual Review in Neuroscience*, 12:491-516
- Santi, C.M., Yuan, A., Fawcett, G., Wang, Z.-W., Butler, A., Nonet, M.L., Wei, A., Rojas, P., & Salkoff, L. (2003). Dissection of K⁺ currents in *Caenorhabditis elegans* muscle cells by genetics and RNA interference. *Proceedings of the National Academy of Sciences, USA*, 100(24):14391-14396
- Sanguinetti, M.C., Curran, M.E., Spector, P.S., & Keating, M. (1996). Spectrum of *HERG* K⁺-channel dysfunction in an inherited cardiac arrhythmia. *Proceedings of the National Academy of Sciences, USA*, 93:2208-2212
- Schirmmacher, K., & Deitmer, J.W. (1989). Membrane properties of identified embryonic nerve and glial cells of the leech central nervous system. *Journal of Comparative Physiology A*, 164:645-653
- Schirmmacher, K., & Deitmer, J.W. (1991). Sodium- and calcium-dependent excitability of embryonic leech ganglion cells in culture. *Journal of Experimental Biology*, 155:435-453
- Schmid, V. (1992). Transdifferentiation in medusae. *International Review of Cytology*, 142:213-259
- Schuldiner, M., Yanuk, O., Itskovitz-Eldor, J., Melton, D.A., & Benvenisty, N. (2000). Effects of eight growth factors on the differentiation of cells derived from human embryonic stem cells. *Proceedings of the National Academy of Sciences, USA*, 97:11307-11312
- Schurmann, W., & Peter, R. (1988). Isolation and cultivation of planarian neoblasts by a novel combination of methods. *Fortschritte der Zoologie*, 36:111-114
- Schurmann, W., & Peter, R. (1993). Primarkulturen von Neoblasten (Stammzellen) aus *Dugesia polychroa* (Turbellarien: Tricladida paludicola). *Verhandlungen der Deutschen Zoologischen Gesellschaft (Stuttgart)*, 86.1:208
- Schurmann, W., & Peter, R. (2001). Planarian cell culture: A comparative review of methods and an improved protocol for primary cultures of neoblasts. *Belgian Journal of Zoology*, 131(Supplement 1):123-130
- Schurmann, W., Betz, S., & Peter, R. (1998). Separation and subtyping of planarian neoblasts by density-gradient centrifugation and staining. *Hydrobiologia*, 383:117-124

- Schwartz, T.L., Tempel, B.L., Papzian, D.M., Jan, Y.N., & Jan, L.Y. (1988). Multiple potassium-channel components are produced by alternative splicing at the Shaker locus in *Drosophila*. *Nature*, 331:137-142
- Shankland, M. (1987). Cell lineage in leech embryogenesis. *Trends in Genetics*, 3:314-319
- Shatz, C.J. (1990). Impulse activity and the patterning of connections during CNS development. *Neuron*, 5:745-756
- Shatz, C.J. & Katz, L.C. (1996). Synaptic activity and the construction of cortical circuits. *Science*, 274:1133-1138
- Sheikh-Hamad, D., & Gustin, M.C. (2004). MAP kinases and the adaptive response to hypertonicity: functional preservation from yeast to mammals. *American Journal of Physiology*, 287:1102-1110
- Shen, Q., Zhong, W., Jan, Y.N., & Temple, S. (2002). Asymmetric Numb distribution is critical for asymmetric cell division of mouse cerebral cortical stem cells and neuroblasts. *Development*, 129:4843-4853
- Shinozawa, T., Kawarada, H., Takezaki, K., Tanaka, H., & Inoue, K. (1995). Preparation of monoclonal antibodies against planarian organs and the effect of fixatives. *Hydrobiologia*, 305:255-257
- Simonneau, M., Distasi, C., Tauc, L., & Poujeol, C. (1985). Development of ionic channels during mouse neuronal differentiation. *Journal of Physiology (Paris)*, 80:312-320
- Skaliora, I., Scobey, R.P., & Chalupa, L.M. (1993). Prenatal development of excitability in cat retinal ganglion cells: action potentials and sodium currents. *The Journal of Neuroscience*, 13:313-323
- Smith, C.M., & Weisblat, D.A. (1994). Micromere fate maps in leech embryos: lineage-specific differences in rates of cell proliferation. *Development*, 120:3427-3438
- Smith, J.P.S. III, & Tyler, S. (1985b). Frontal organs in the Acoelomorpha: ultrastructure and phylogenetic significance. *Hydrobiologia*, 132:71-78
- Song, H.-J., & Poo, M.-M. (1999). Signal transduction underlying growth cone guidance by diffusible factors. *Current Opinion in Neurobiology*, 9:355-363
- Spencer, A.N. (1978). Neurobiology of *Polyorchis* I. Function of effector systems. *Journal of Neurobiology*, 9:143-157

Spencer, A.N. (1981). The parameters and properties of a group of electrically coupled neurones in the central nervous system of a hydrozoan jellyfish. *Journal of Experimental Biology*, 93:33-50

Spencer, A.N., Przysieznik, J., Acosta-Urquidi, J., & Basarsky, T.A. (1989). Presynaptic spike broadening reduces junctional potential amplitude. *Nature*, 340:636-638.

Spitzer, N.C. (1979). Ion channels in development. *Annual Review of Neuroscience*, 2:363-395

Spitzer, N.C., & Lamborghini, J.E. (1976). The development of the action potential mechanism of amphibian neurons isolated in culture. *Proceedings of the National Academy of Sciences, USA*, 73(5):1641-1645

Spitzer, N.C., & Ribera, A.B. (1998). Development of electrical excitability in embryonic neurons: Mechanisms and roles. *Journal of Neurobiology*, 37:190-197

Spitzer, N.C., Vincent, A., & Lautermilch, N.J. (2000). Differentiation of electrical excitability in motoneurons. *Brain Research Bulletin*, 53(5):547-552

Spitzer, N.C., Root, C.M., & Borodinsky, L.N. (2004). Orchestrating neuronal differentiation: patterns of Ca²⁺ spikes specify transmitter choice. *Trends in Neurosciences*, 27(7):415-421

Spruce, A.E., & Moody, W.J. (1992). Developmental sequence of expression of voltage-dependent currents in embryonic *Xenopus laevis* myocytes. *Developmental Biology*, 154:11-22

Stariha, R.L., & Kim, S.U. (2001). Mitogen-activated protein kinase signalling in oligodendrocytes: a comparison of primary cultures and CG-4. *International Journal of Developmental Neuroscience*, 427-437

Stossel, T.P. (1993). On the crawling of animal cells. *Science*, 260:1086-1094

Stryker, M.P., & Harris, W.A. (1986). Binocular impulse blockade prevents the formation of ocular dominance columns in cat visual cortex. *The Journal of Neuroscience*, 6(8):2117-2133

Strange, K. (2003). From genes to integrative physiology: Ion channel and transporter biology in *Caenorhabditis elegans*. *Physiological Review*, 83:377-415

Sudlow, L.C., & Gillette, R. (1997). Cyclic AMP levels, adenylyl cyclase activity, and their stimulation by serotonin quantified in intact neurons. *Journal of General Physiology*, 110:243-255

- Sulston, J.E., Schierenberg, E., White, J.G., Thomson, J.N. (1983). The embryonic cell lineage of the nematode *Caenorhabditis elegans*. *Developmental Biology* 100(1):64-119
- Sun, Q.Q., & Dale, N. (1998). Developmental changes in expression of ion currents accompany maturation of locomotor pattern in frog tadpoles. *Journal of Physiology*, 507:257-264
- Sulston, J.E., Schierenberg, E., White, J.G., & Thomson, J.N. (1983). The embryonic cell lineage of the nematode *Caenorhabditis elegans*. *Developmental Biology*, 100:64-119
- Suter, D.M., & Forscher, P. (2000). Substrate-cytoskeletal coupling as a mechanism for the regulation of growth cone motility and guidance. *Journal of Neurobiology*, 44:97-113
- Sutherland, M.L., Williams, S.H., Abedi, R., Overbeek, R.A., Pfaffinger, P.J., & Noebels, J.L. (1999). Overexpression of a Shaker-type potassium channel in mammalian central nervous system dysregulates native potassium channel gene expression. *Proceedings of the National Academy of the Sciences, USA*, 96:2451-2455
- Syntichaki, P., & Tavernarakis, N. (2003). Genetic models of mechanotransduction: The nematode *Caenorhabditis elegans*. *Physiological Reviews*, 84:1097-1153
- Taghert P.H., Doe, C.Q., & Goodman, C.S. (1984). Cell determination and regulation during development of neuroblasts and neurones in grasshopper embryo. *Nature*, 307:163-165
- Takahashi, K., Miyazaki, S., & Kidokoro, Y. (1971). Development of excitability in embryonic muscle cell membranes in certain tunicates. *Science*, 171:415-418
- Takahashi, K., & Tanaka-Kunishima, M. (1998). Monitoring early neuronal differentiation by ion channels in ascidian embryos. *Journal of Neurobiology*, 37:3-22
- Tang, D., & Goldberg, D.J. (2000). Bundling of microtubules in the growth cone induced by laminin. *Molecular and Cellular Neuroscience*, 15:303-313
- Tazaki, A., Gaudieri, S., Ikeo, K., Gojobori, T., Watanabe, K., & Agata, K. (1999). Neural network in planarian revealed by an antibody against planarian synaptotagmin homologue. *Biochemical and Biophysical Research Communications*, 260:426-432
- Tekaya, S., Dhainaut-Courtois, N., & Zghal, F. (1996). Intervention d'un materiel immunologiquement apparente a la tubuline lors de la regeneration de la planaire marine *Sabussowia dioica* (Claparede, 1863) (Plathelminthes, Tricladida). *Bulletin of the Zoological Society of France*, 121:269-278
- Teragawa, C.K., & Bode, H.R. (1990). Spatial and temporal patterns of interstitial cell migration in *Hydra vulgaris*. *Developmental Biology*, 138:63-81

- Teshirogi, W., & Tohya, K. (1988). Primary tissue culture of freshwater planarians in a newly devised medium. *Fortschritte der Zoologie*, 36:91-96
- Thompson, S. H. (1977). Three pharmacologically distinct potassium channels in molluscan neurones. *Journal of Physiology*, 265:465-488
- Totten, M.I.J., Kreshenko, N.D., Day, T.A., Marks, N.J., Halton, D.W., & Maule, A.G. (2002). Signal transduction mechanisms mediating muscle contraction in platyhelminths. *In the Proceedings of the Tenth International Congress of Parasitology, Vancouver, British Columbia, 4-9 August 2002. Monduzzi Editore, Bologna, Italy. Pp.117-120*
- Tribut, F., Calabrese, B., & Pellegrino, M. (1999). The A-like potassium current of a leech neuron increases with age in cell culture. *Invertebrate Neuroscience*, 4:25-31
- Trotier, D., & Doving, K.B. (1996). Direct influence of the sodium pump on the membrane potential of vomeronasal chemoreceptor neurones in frog. *Journal of Physiology*, 490:611-621
- Truman, J.W. (1983). Programmed cell death in the nervous system of an adult insect. *Journal of Comparative Neurology*, 216:445-452
- Truman, J.W. (1984). Cell death in invertebrate nervous systems. *Annual Review of Neuroscience*, 7:171-188
- Tojima, T., Kobayashi, S., & Ito, E. (2003). Dual role of cyclic AMP-dependent protein kinase in neuritogenesis and synaptogenesis during neuronal differentiation. *Journal of Neuroscience Research*, 74:829-837
- Tyler, S., & Rieger, R.M. (1977). Ultrastructural evidence for the systematic position of the Nemertodermatida (Turbellaria). *ACTA Zoologica*, 154:193-207
- Tyler, S., & Hooge, M. (2004). Comparative morphology of the body wall in flatworms (Platyhelminthes). *Canadian Journal of Zoology*, 82:194-210
- Tyzio, R., Ivanov, A., Bernard, C., Holmes, G.L., Ben-Ari, Y., & Khazipov, R. (2003). Membrane potential of CA3 hippocampal pyramidal cells during postnatal development. *Journal of Neurophysiology*, 90:264-2972
- Vincent, A., Lautermilch, J., & Spitzer, N.C. (2000). Antisense suppression of potassium channel expression demonstrates its role in maturation of the action potential. *The Journal of Neuroscience*, 20(16):6087-6094
- Volkov, E.M., Nurullin, L.F., Svandova, I., Nikolsky, E.E., & Vyskocil, F. (2000). Participation of electrogenic Na⁺-K⁺-ATPase in the membrane potential of earthworm body wall muscles. *Physiological Research*, 49:481-484

- Wanaka, A., Johnson, E.M., & Milbrandt, J. (1990). Localization of FGF receptor mRNA in the adult rat central nervous system by *in situ* hybridization. *Neuron*, 5:267-281
- Wanaka, A., Milbrandt, J., & Johnson, E.M. (1991). Expression of FGF receptor gene in rat development. *Development*, 111:455-468
- Wang, L.Y., Gan, L., Forsythe, I.D., & Kaczmarek, L.K. (1998). Contribution of the Kv3.1 potassium channel to high-frequency firing in mouse auditory neurones. *Journal of Physiology (London)*, 509:183-194
- Watt, S.D., Gu, X., Smith, R.D., & Spitzer, N.C. (2000). Specific frequencies of spontaneous Ca²⁺ transients upregulate GAD 67 transcripts in embryonic spinal neurons. *Molecular and Cellular Neuroscience*, 16:376-387
- Wei, A., Covarrubias, M., Butler, A., Baker, K., Pak, M., & Salkoff, L. (1990). K⁺ current diversity is produced by an extended gene family conserved in *Drosophila* and mouse. *Science*, 248:599-603
- Weisblat, D.A., Kim, S.Y., & Stent, G.S. Embryonic origins of cells in the leech *Helobdella triserialis*. *Developmental Biology*, 104:65-85
- Wiens, T.J., & Atwood, H.L. (1978). Motoneuron interactions in crayfish claw control: Evidence from intracellular recording. *Journal of Comparative Physiology*, 124:237-247
- Wildering, W.C., Hermann, P.M., & Bulloch, A.G.M. (1998). Neurite outgrowth, RGD-dependent, and RGD-independent adhesion of identified molluscan motoneurons on selected substrates. *Journal of Neurobiology*, 35:37-52
- Wilkgren, M., Reuter, M., & Gustafsson, M. (1985). Neuropeptides in free-living and parasitic flatworms (Platyhelminthes). An immunocytochemical study. *Hydrobiologia*, 132:93-99
- Willmer, P. (1990). *Invertebrate relationships: patterns in animal evolution*. Cambridge University Press, New York, NY
- Wolf, Y.I., Rogozin, I.R., & Koonin, E.V. (2004). Coelomata and not Ecdysozoa: Evidence from genome-wide phylogenetic analysis. *Genome Research*, 14:29-36
- Wolff, E. (1962). Recent researches on the regeneration of planaria. *In* *Regeneration*. Rudnick, D. *ed.* The Ronald Press, NY, pp:53-8
- Wong, R.G., Hadley, R.D., Kater, S.B., & Hauser, G.C. (1981). Neurite outgrowth in molluscan organ and cell cultures: the role of conditioning factors. *The Journal of Neuroscience*, 1:1008-1021

- Wong, R.G., Barker, D.L., Kater, S.B., & Bodnar, D.A. (1984). Nerve growth-promoting factor produced in culture media conditioned by specific CNS tissues of the snail *Helisoma*. *Brain Research*, 292:81-91
- Wu, R.-L., & Barish, M.E. (1992). Two pharmacologically and kinetically distinct transient potassium currents in cultured mouse hippocampal neurons. *The Journal of Neuroscience*, 12:2235-2246
- Wu, R., -L., Butler, D.M., & Barish, M.E. (1998). Potassium current development and its linkage to membrane expansion during growth of cultured embryonic mouse hippocampal neurons: Sensitivity to inhibitors of phosphatidylinositol 3-kinase and other protein kinases. *The Journal of Neuroscience*, 18:6261-6278
- Yedvobnick, B., Kumar, A., Chaudhury, P., Opraseuth, Mortimer, N., & Bhat, K.M. (2004). Differential effects of *Drosophila* mastermind on asymmetric cell fate specification and neuroblasts formation. *Genetics*, 166:1281-1289
- Younossi-Hartenstein, A., & Hartenstein, V. (2000). The embryonic development of the polyclad flatworm *Imogine mcgrathi*. *Development Genes and Evolution*, 210:383-398
- Younossi-Hartenstein, A., Ehlers, U., & Hartenstein, V. (2000). Embryonic development of the nervous system of the rhabdocoel flatworm *Mesostoma lingua* (Abildgaard, 1789). *The Journal of Comparative Neurology*, 416:461-474
- Younossi-Hartenstein, A., Jones, M., & Hartenstein, V. (2001). Embryonic development of the nervous system of the Temnocephalid flatworm *Craspedella pedum*. *Journal of Comparative Neurology*, 434:56-68
- Ziskind-Conhaim, L. (1987). Electrical properties of motoneurons in the spinal cord of rat embryos. *Developmental Biology*, 128:21-29
- Zrzavy, J., Mihulka, S., Kepka, P., Bazdek, A., & Tietz, D. (1998). Phylogeny of the Metazoa based on morphological and 18S ribosomal DNA evidence. *Cladistics*, 14:249-285

Appendix 1. Properties of cultured brain neurons and neuroblasts in the marine polyclad *Notoplana atomata*.

The initial goal of the thesis to induce stem cells from the flatworms and monitored changes in electrophysiological properties was achieved; however, the test organism was not the first choice. Due to the importance of drawing a general answer to an evolutionary process, *Girardia tigrina* may not have been the most suitable flatworm since the order tricladida is considered an evolutionarily derived group among the *Platyhelminthes*. Initially, experiments had been performed on the marine flatworm *Notoplana atomata*. The polyclads are still considered as one of the most basal groups among the flatworms having retained many ancestral characteristics. Worms from this genus had been the only group where patch-clamp methods were developed (Buckingham & Spencer, 2000). There had been moderate success trying to isolating and culturing stem cells from this animal, however, the reproducibility and success was near as high as with *Girardia*.

Three basic groups of experiments were performed using *N. atomata*. First, was a need to determine and identify potential morphogens capable of inducing neurogenesis. Also, it would be important to compare changes occurring in newly differentiating neurons with regenerating neurons, where we were using dissociated brain neurons as a model of changes in Vg expression during neurite extension. In these experiments, mass dissociations were performed on hemi-ganglia, and distinct populations were revealed based on their morphology, and response to both bFGF and serotonin. These experiments focused on the characteristics of neurite regeneration, and on the expression of Vg-Ca²⁺ channels during neurite extension.

The second set of experiments focused on isolating and purifying neuroblasts using discontinuous Percoll gradients. There was much less success with these experiments, since it proved difficult to obtain viable neuroblasts at a sufficient viability to perform

subsequent electrophysiological experiments. It appeared that the main problem was the thick layer of mucous these worms produce whenever they are handled. We had attempted to reduce the expulsion of mucous by first anaesthetizing the animals, but it appears that mucous production is not voluntary and there is a large response to tissue damage. We also tried reducing mucosal loads enzymatically in cell suspensions, but there was not much success. Neoblasts were recovered and some attempts were made to induce neuronal differentiation in these cultures.

The last set of experiments was an attempt to find a simple marker for neuronal phenotype. Combining immunocytochemistry and Confocal microscopy, two tubulin antibodies were screened to determine whether either showed specific cross-reactivity towards nervous tissue. It was shown that the commercially purchased tubulin antibody (Tub Ab-4, NeoMarkers) was relatively neuron specific when compared to antibodies against acetylated- α -tubulin that labeled both nervous tissues and ciliated cells.

These experiments are outline in brief below, focusing mainly on the methods used, and the results observed.

1. Effects of substrate, and exogenous diffusible factors on neurite outgrowth in cultured brain neurons from *Notoplana atomata*.

A. Methods and Materials

The following describe a procedure adapted from Wong *et al.* (1981) and Wong *et al.* (1984) for developing culture media conditioned by tissue from the CNS of *Notoplana atomata*. This method is used to determine whether (a) flatworm brains produce nerve growth-promoting factors (and if so, an optimization assay to screen for the dose-dependent efficacy of nerve growth-promoting ability) and (b) whether various substrata influence neurite outgrowth.

Remove brains as described in Brain Dissection / Dissociation Protocol (1.0). Excise brains and place in *Notoplana* Defined Media (DM) under sterile conditions. Remove the sheath surrounding the ganglia with enzymatic digestion and tungsten microknives. Rinse ganglia in either 70% EtOH or 10% Lysterine in ASW. Conditioned medium (CM) is prepared by placing the dissected, desheathed central ganglia in normal DM for specified time. Assay for time dependency of CM factor production. Control the number of ganglia / ml of DM. Determine if factors can be sterile-filtered.

Preparing culture substrata

Substrata	Method of Preparation
untreated plastic	35 x 10 mm polystyrene Falcon 'Easy Grip' culture dish (No. 353001)
untreated glass	22 mm ² glass coverslips, acid-washed
(0.1%) poly-L-lysine coated plastic	incubate 35 mm Falcon dish with 2 or 3 ml of 0.1% poly-L-lysine (vary incubation times 6 h, 12 h, 24 h), wash with dH ₂ O, rinse in ASW 20 min, store at room temp. in dry, dark location
(0.1%) poly-L-lysine coated glass	as above, but line bottom of 35 mm dish with 22 mm ² glass coverslips, acid-washed

Try pretreating dishes by exposing substrate-lined surface to 2.0 ml of DM or CM at room temperature for 24 h or by shaking dishes continuously for 2 h.

The assay will determine effects of factors on:

1. time dependency of cell viability / survivorship – measured comparing the number of viable cells (cells with phase-bright somas) immediately, and at various subsequent times (2 h, 6 h, 12 h, 24 h, 2 d, 3 d, 4 d, 5 d, 6 d, 7 d)

2. nerve-growth promoting ability – measured by comparing proportion of cells that have ‘grown’ (extended neurites greater than 1 soma in diameter) over time (2 h, 6 h, 12 h, 24 h, 2 d, 3 d, 4 d, 5 d, 6 d, 7 d)
3. electrical phenotype – measured by comparing the proportion of excitable vs. inexcitable cells, the individual electrical properties of ‘specific’ cell phenotypes (e.g. small soma vs. large, etc.)

Dissociate one hemi- ganglion per culture dish following Buckingham & Spencer (2000). Immediately count the number of cells in the dish and record cell sizes.

B. Results

B.1. Neurite outgrowth is initiated early after plating and is unaffected by substrate.

The effects of substrate would ideally be monitored on single identified neurons, however, since this technique has not yet been developed in brain cell cultures from *Notoplana*, important characteristics of neurite outgrowth very studied in populations of brain neurons. Specifically, development of growth cones, the length of primary neurites, and the number of primary neurites was examined to determine whether either substrate or the presence of serotonin or basic fibroblast growth factor had any influence on the behaviour of cultured brain neurons. In the mass dissociations, cells other than neurons were always present, the majority of which were glial-like cells. These cells had distinct morphologies, with all these cells developing a halo-like arrangement of lamellopodia.

Primary cultures of brain neurons isolated by dissociating hemi-ganglia into suspensions using both enzymatic and mechanical treatments produced the most healthy and viable cells. Most cells attached to the substrate firmly within thirty minutes following plating. After 7 days in culture, a variety of neuronal morphologies was observed (**Fig. A.1**). Almost immediately after plating, neurons plated on both untreated polystyrene and polystyrene coated with 0.1% poly-L-lysine developed growth cones (**Fig. A.2**). The

proportion of cells with obvious growth cones increased and peaked during the first 24 h in culture with 16.5% (n=134) and 11.3% (n=195) when culture on polystyrene and 0.1% poly-L-lysine respectively. The proportion decreased gradually over 7 days to levels below those immediately after plating with 1.6% (n=64) and 3.4% (n=175) of neurons with growth cones when plated on polystyrene and 0.1% poly-L-lysine respectively. Substrate showed little if any effect on the peak after 24 h and the gradual decline of neurons with growth cones (**Fig. A.2**).

A small proportion of dissociated cells retained short (with neurites equal to 1 soma diameter in length) and/or long neurites (with neurites longer than 2 soma diameters in length), with 30.2% (n=126) and 33.0% (n=185) when plated on polystyrene alone and 0.1% poly-L-lysine respectively (**Fig. A.3a**). The proportion of neurons extending short neurites increased gradually and peak after about 4 days in culture when plated on both polystyrene and 0.1% poly-L-lysine (**Fig. A.3a**). This trend was similar with respect to the proportion of cells extending long neurites (**Fig. A.3b**). Fewer cells retained long neurites immediately after dissociation, but the proportion increased and peaked after 4 days on either substrate. There appeared to be no effect of substrate on the length on neurites extended.

Substrate also had little effect on the number of neurites developed by cultured neurons (**Fig. A.4**). The majority of neurons developed monopolar morphologies after 7 days in culture with the proportion increasing from 5.6% (n=126) to 54.7% (n=64) and 17.8% (n=185) to 47.4% (n=175) when cells were plated on polystyrene and 0.1% poly-L-lysine respectively (**Fig. A.4a**). The proportion of monopolar neurons increased during the first 2 days in culture and peaked after 3 days (**Fig. A4b**). The proportion of multipolar neurons showed a similar trend with few cells retained multiple neurites immediately after plating, then increasing gradually and peaking after about 3 days in culture (**Fig.A.4b**). When neurons were plated on 0.1% poly-L-lysine, the proportion of neurons developing several neurites was slightly higher than in control cultures. A small proportion of cells did not develop neurites at all, although the majority of these cells appeared to be glial-like cells, determined by their distinct morphology.

B.2. Effects of diffusible factors on neurite initiation and outgrowth.

The effects two diffusible factors found in the CNS of flatworms (basic fibroblast growth factor and serotonin) were tested to determine if they might act as signals directing the initiation and growth of neurites, as well as the number of neurites developed. The same measurements of neurite outgrowth were measured as before and cells were plated on 0.1% poly-L-lysine as a control.

Basic fibroblast growth factor had a slight effect by increasing the proportion of cells developing growth cones (**Fig. A.5**). In a dose dependent manner, a greater proportion of neurons in developed growth cones in cultures treated with bFGF. Higher concentrations of bFGF (100 ng/ml) showed the largest effect, but there was only a small difference between bFGF treated cultures and the control. The proportion of cells with growth cones increased and peaked during the first 24 h in culture and began to decline gradually afterwards under all concentrations tested (**Fig. A.5**).

The effect of bFGF on the length of neurites appeared consistent between neurons extending short neurites and neurites developing long neurites (**Fig. A.6**). The proportion of cells extending short neurites increased gradually and peaked after 3 days in culture and there appeared to be a moderate inhibitory effect due to treatment with bFGF (**Fig. A.6a**). This effect was more pronounced in inhibiting neurons from sprouting long neurites and the effect was dose-dependent (**Fig. A.6b**). The fewest proportion of cells sprouting long neurites was observed in cultures treated with the highest concentration of bFGF (100 ng/ml), and there was only a slight difference between low concentrations (1 ng/ml) of bFGF and the control. The proportion of cells developing long neurites increased gradually over 5 days in culture.

There appeared to be no effect on the proportion monopolar or multipolar neurons when bFGF was applied to cultures (**Fig. A.7**). Application of bFGF appeared to only delay the establishment of either the monopolar or multipolar morphology in cultured brain

neurons. After 3 days in culture, the bFGF appeared to inhibit the number of monopolar (**Fig. A.7a**) and multipolar neurons (**Fig. A.7b**). however, there was no difference when compared to the control after 5 days in culture.

Cultures of brain cells grown in the presence of serotonin tended to have a higher proportion of cells developing growth cones (**Fig. A.8**). The response of cells to 5-HT depended on the concentration of 5-HT applied. Immediately after plating, cells began to respond to moderated levels of 5-HT and the proportion of cells with growth cones was nearly double that of the control. The proportion of cells developing growth cones was 21.9% (n=105) and 17.4% (n=86) immediately after plating, then increased and peaked after 24 h to 24.6% (n=126) and 25.3% (n=99) in cultures exposed to 1 μ M and 1 nM 5-HT respectively (**Fig. A.8**). No effect was observed when higher levels of 5-HT (1 mM) were applied. The proportion of cells with growth cones decreased gradually over the next 4 days in culture, however, cells exposed to 1 μ M and 1 nM 5-HT retained proportions greater than 4 times those of the control.

Although 5-HT applied exogenously increased the proportion of cells developing growth cones, 5-HT inhibited the proportion of cells sprouting both short and long neurites (**Fig. A.9**). The inhibition of cells developing short neurites was greatest when the highest concentrations of 5-HT (1 mM) were applied and a smaller effect was observed at lower concentrations. In both control and 5-HT treated cultures, the proportion of cells developing short neurites increased steadily during 5 days in culture. The proportion of cells with short neurites was nearly half the control in 5-HT treated cultures. When 1 mM and 1 μ M 5-HT was applied, there was only a slight increase in the proportion of cells with short neurites from 19.1% (n=68) to 32.5% (n=40) and 19.0% (n=105) to 44.4% (n=45) respectively (**Fig. A.9a**). There was a reduced effect with 1 nM 5-HT, however, the proportion of cells with short neurites was always smaller than the control. A similar effect was observed in the proportion of cells extending long neurites, but the effect was more pronounced, with a much larger level of inhibition observed when 1 mM and 1 μ M 5-HT were applied (**Fig. A.9b**). After 5 days in culture, the proportion of

neurons extending long neurites in control cultures was 71.6% (n=201), but inhibited to 15.0% (n=40) and 22.2% (n=45) in 1 mM and 1 μ M 5-HT treated cultures respectively.

Serotonin also appeared to inhibit monopolar and multipolar neurons from sprouting neurites (**Fig. A.10**). Treatment with serotonin at 1 mM for 5 days resulted in only a small change (8.8% to 17.5%, n=68 and 40) in the proportion of cells developing a monopolar morphology when compared to the control (5.6% to 50.6%, n=126 and 201), and treatment with 1 mM 5-HT resulted in virtually no change in the proportion (30.5% to 28.9%, n=105 and 45) (**Fig. A.10a**). Serotonin had a more dramatic effect on the proportion of multipolar neurons. Inhibition was greatest at high concentrations of 5-HT, and low concentrations had little effect (**Fig. 10b**). In cultures exposed to 1 mM 5-HT, the small proportion of multipolar neurons present after 24 h (1.3%, n=43) appeared to retract their neurites since no multipolar cells were observed after 3 days in culture. Cultures with 1 mM 5-HT also showed a reduction in the proportion of multipolar neurons (3.6% to 2.2%, n=105 and 45, after 5 days). The effect of 5-HT on the number of neurites sprouted appeared to be dose-dependent, but 1 nM 5-HT had almost no effect when compared to the control where 19.3% (n=201) of cells developed multipolar morphologies after 5 days in culture.

B.3. Neurite outgrowth is correlated with changes in expression of Vg channels

It was an important goal to determine the electrophysiological changes occurring during major events associated with neuronal differentiation and development. Thus, it was important to determine the suite of Vg channels expressed and possibly involved in development. Calcium channels seem particularly important during neurite initiation and outgrowth, thus, the proportion of neurons expressing Ca^{2+} currents was determined in cultures of different ages, and when cultures were exposed to both basic fibroblast growth factor and serotonin.

Immediately after plating, 33.0% (n=12) of cells possessed at least one type of Ca^{2+} channel. The proportion of cells with Ca^{2+} currents increased and peaked at 24 h when

100.0% (n=10) of cells had measurable Ca^{2+} currents (**Fig. A.11**). This coincided with the peak in cells developing growth cones, and with the largest change in the proportion of cells extending long extensions (**Fig. A.2, A.3a**). After the peak at 24 h, the proportion of cells expressing Ca^{2+} channels decreased and returned to similar levels as immediately following dissociation. After 7 days in culture, only 28.6% (n=7) of cells retained Ca^{2+} currents. Expression of Ca^{2+} channels required *de novo* protein synthesis since application of the protein transcription inhibitor cyclohexamide at 30 $\mu\text{g}/\text{ml}$ prevented the increase in cells expressing Ca^{2+} channels after 12 h (**Fig. A.12**).

If Ca^{2+} channel expression was important and required during neurite outgrowth, then treatments inhibiting growth cone development and neurite extension should also inhibit Ca^{2+} channel expression. Treatment with bFGF slightly increased the proportion of cells developing growth cones (**Fig. A.5**), and a larger increase was observed in cultures treated with 5-HT (**Fig. A.8**), but surprisingly, both treatments resulted in a significant decrease in the proportion of neurons expressing Ca^{2+} channels (**Fig. A.13**). After 5 day treatments with bFGF and serotonin, the proportion of cells expressing Vg- Ca^{2+} channels decreased to 21.4% (n=14) and 43.8% (n=16) respectively. However, the decrease in cells expressing Ca^{2+} induced by diffusible factors (bFGF; **Fig. A.6** and 5-HT; **Fig. A.9**) was correlated with a decrease in the proportion of cells extending neurites.

The proportion of cells expressing K^{+} channels was also examined. Brain neurons expressed at least two types of K^{+} channels, a delayed rectifier-like (K_{DR}) and a rapidly inactivating A-type like (K_{A}) channel. Immediately after plating, 16.7% (n=12) of cells expressed a K_{DR} channel, which increased to 100.0% (n=14) after 3 days in culture (**Fig. A.14**). The proportion of cells expressing a K_{DR} channel decreased slightly after treatment with 10 ng/ml bFGF and 1 μM 5-HT to 71.4% (n=14) and 87.5% (n=9) respectively, but the difference was not statistically significant (Chi-Square test, $p > 0.05$, n = 37). In control conditions the proportion of cells expressing K_{A} channels increases from 8.3% (n=12) to 42.9% (n=7) (**Fig. A.15**). A slightly larger increase is observed when 1 μM 5-HT was applied, where 50.0% (n=16) of cells had a K_{A} channel, but the difference was not statistically significant (Chi-Square test, $p > 0.05$, n=23). A decrease in

cells expressing K_A channels was significantly reduced in cultures treated with 10 ng/ml bFGF where 21.4% (n=14) of cells had the currents (Chi-Square test, $p < 0.05$, n=21).

B.4. Electrophysiological properties of calcium channels involved in neurite outgrowth.

The activation kinetics of Ca^{2+} channels were measured from brain neurons after 24 h in culture. Under these conditions, 100% of cells had at least one type of Ca^{2+} channel and in some cells, at least two components could be observed. Cells were bathed in Ca^{2+} current isolating medium, and measured using whole-cell patch clamp. All cells possessed a sustained, non-inactivating component, but many had both transient inactivating and non-inactivating currents (**Fig. 16a**). Current-voltage relationships were determined and show that channels activate at a similar potential, near -30 mV, and reach a peak current at +10 mV and the mean reversal potential was $+45.7 \pm 3.2$ mV (n=17) (**Fig. 16b**).

The inactivating component appeared to be completely inactivated after 400 ms, so isolation of the two components was achieved by applying a 450 ms prepulse followed by a test pulse to +10 mV that only stimulated the non-inactivating component (**Fig. 17a**). Both components appeared to activate at similar rates and were fully activated at +20 mV. The voltage of half-activation was 7.4 ± 1.1 mV (n=10), and the slope factor of the curve derived from fitting the data to a Boltzmann function was 6.3 ± 1.2 (n=10). Channels mediating the transient current began to inactivate at -60 mV and were fully inactivated at potentials positive of +20 mV (**Fig. 17b**). The voltage of half-inactivation was -26.6 ± 1.5 mV (n=10) and the slope factor was -12.0 ± 1.3 (n=10).

The current density changed with the time neurons had been in culture. Immediately after plating, cells with Ca^{2+} currents had a peak current density of -0.021 ± 0.004 pA/ μm^2 (n=7), but following 24 h in culture, the peak current density increased to -0.095 ± 0.005 pA/ μm^2 (n=7) (**Fig. 18**). The peak Ca^{2+} current density decreased gradually after 24 h and returned to similar levels as immediately after plating following 72 h in culture. The increase in current density was dependent upon *de novo* protein synthesis as application

of 30 µg/ml of the protein transcription inhibitor for 12 h prevented the increase in peak current density. This suggests that the increase in current density was due to changes in membrane channel density and not due to changes in single channel conductance.

2. Neoblasts from the flatworm *Notoplana atomata*

A. Methods and Materials

The following describe a procedure adapted from Schurmann *et al.* (1998) and Schurmann and Peter (2001), and primary cultures of neoblasts. This method disaggregates tissue from whole worms using both enzymatically and mechanically to produce a single cell suspension. Whole-worm cell suspensions are first passed through filters with progressively smaller clearances to yield neoblasts (10-15 µm in diameter), then run through a discontinuous Percoll gradient by isopycnic centrifugation for optimal separation. The protocol is meant to obtain primary cultures of neoblast of greater than 80% purity that are viable for at least one week.

Formation of a single cell suspension

Notoplana are pre-incubated in ASW containing 0.05 mg/ml gentamycin sulfate for at least 24 hr prior to dissociation to reduce bacterial contamination found within the mucous layer covering the worms. Worms are anaesthetized in SW with elevated Mg²⁺ (1:1 mix of 0.33 MgCl₂:ASW) for at least 45 min prior to dissociation. Worms are placed into a Dounce Tissue Grinder with a large clearance pestle (~50 µm), and 10 ml of Dissociation Solution (0.05% type III trypsin, 0.0005% dithiothreitol, 0.5 mM EDTA; in Ca²⁺-free ASW) and dissociated using ~20-30 gentle strokes.

Trypsin – used to digest intercellular proteins holding cells together

Dithiothreitol – used to break sulfide bonds found within mucosal substances –
this agent greatly reduces viscosity, and ensures that cell

clumps/aggregates do not form in latter stages, specifically during the Percoll separation steps

Ca²⁺-free ASW / EDTA – prevents Ca²⁺-dependent CAM's from causing cell aggregate formation

The resulting suspension is incubated at room temperature for 15 min on a shaker table to allow trypsinization to occur. The enzymatic reaction is stopped by adding 1 ml of soybean trypsin inhibitor (SBTI, 2.55 mg/ml). DNase (164 U) is added to digest DNA that may be released from ruptured cells during the 'grinding' step. Long strands of DNA may interfere with the Percoll separation. The solution is incubated at 37°C for 10 min. Cellular debris is removed by a centrifugation step, 5 min at 200 x g at 12°C. The pelleted cells are washed 3 times by adding 5 ml of *Notoplana* L-15 defined medium (NL-15), and the centrifugation is repeated. The resulting pellet is resuspended in a 1:1 mixture of NL-15:SBTI-DNase solution. The cell suspension is then triturated gently through a series of progressively smaller sterile needles, 5 –10 times gently to avoid introduction of air bubbles. 19½-G, 23-G, 26½-G needles are used. An additional step can be added (serial filtration through nylon mesh, with exclusion sizes of 126 µm, 64 µm, and 25 µm) to further reduce the presence of larger unwanted cells. Cells passing through the size-exclusion step are then washed by centrifugation (as above), and resuspended in a small volume of Ca²⁺-ASW. This mixture is then layered on top of a preformed Percoll gradient of the following composition:

Top layer – dissociated cells

2nd layer – 20% Percoll

3rd layer – 35% Percoll

4th layer – 37.5% Percoll

5th layer – 40% Percoll

6th layer – 50% Percoll

This gradient is centrifuged for at least 30 min at 2000 x g at 12°C. After centrifugation, layers are gently aspirated from the top using a fire-polished Pasteur pipette. Neoblasts can be harvested from the 3rd through 5th layers, with 37.5% Percoll yielding the greatest

concentration. Cells are washed by diluting the fractions with 5 X the volume with NL-15 defined media. The washing step is repeated 3 times by centrifugation. The final cell pellet is resuspended using a 26-G needle and plated in 3 ml of NL-15 defined media onto 35mm Falcon dishes (35001), with poly-L-lysine coated glass coverslips (22 mm², No. 1 thickness).

B. Results

B.1. Isolation and purification of neoblasts in *N. atomata*.

When whole organisms were dissociated mechanically and enzymatically, the proportion of neoblasts recovered was relatively small when compared to other cell types. There were 5-10 cell phenotypes readily identifiable in culture, including; ciliated epidermal cells, rhabdite-forming cells, pigment-forming cells, flame cells, muscle cells, neurons, and neoblasts. Muscle cells were a very common cell type found in all cell suspensions and represented approximately $3.3 \pm 0.5\%$ (n=10) of the total cells recovered. Neoblasts were found to comprise $4.4 \pm 0.8\%$ (n=10) of all cells in whole worm suspensions (**Fig. 19a**). Discontinuous Percoll gradients were used in an attempt to purify neoblasts based on density. When a discontinuous gradient with four layers (20%, 30%, 40%, and 50%) was used, neoblasts comprised a higher proportion of the plated cells. Neoblasts could be found most concentrated at the boundary between the 20% and 30% Percoll layers (**Fig. 19b**). The concentration of neoblasts at this density was $33.0 \pm 7.8\%$ (n=2), and nearly three times larger than in any other location. Neoblasts could be readily identified using azure-A and eosin-B staining. Neoblasts stained specifically and were dark blue, whereas other cells stained pink (**Fig. 20**). Neoblasts from *N. atomata* possessed the same morphological features as stem cells from other flatworms. They had an extremely high nucleus to cytoplasm ratio, and were approximately 10 μm in diameter.

Neoblasts recovered from various Percoll layers were tested for a response to potential morphogens to induce neuronal differentiation. The effect of substrate, activators of second messenger systems, bFGF, and serotonin were tested. In control conditions, when neoblasts were plated on 0.1% poly-L-lysine coated glass for 7 days, the effect on the

proportion of cells expressing neuronal tubulin was dependent upon the Percoll layer from which they were recovered. The proportion of tubulin expressing cells increased in neoblasts cultures recovered from 60% and 70% Percoll (**Fig. 21a**). In cultures from the other densities, the proportion of tubulin expressing cells decreased after 7 days compared to immediately after plating. Treatment of neoblast cultures had little or no effect on the proportion of cells expressing neuronal tubulin (**Fig. 21b**). In general, 10 ng/ml bFGF tended to slightly increase the proportion of cells expressing tubulin, with the exception of cells recovered from the 40% Percoll layer where the number of tubulin expressing cells decreased. When 1 μ M serotonin was added to the culture medium, there was a decrease the proportion of cells expressing neuronal tubulin.

B.2. Neoblasts express a delayed rectifier-like K^+ channel.

It was important to determine the complement of Vg channels already present in undifferentiated neoblasts to determine if the morphogen treatments could alter the suite of Vg channels expressed during differentiation. When plated on 0.1% poly-L-lysine coated glass cover slips, a small proportion of neoblasts expressed a delayed rectifier like current (**Fig. 22a**). These currents were recorded in 30.0% (n=10) of neoblasts immediately after plating. Currents were recorded by using the whole-cell patch clamp method by stepping the membrane potential from a holding potential of -70 mV through a series of test pulses between -70 mV and +50 mV. The current-voltage relationship from a typical recording shows that channels begin to activate at -30 mV and the current increases proportionally to the depolarizing test pulse (**Fig. 22b**). Steady state activation curves that plotted the standardized current against the membrane potential reveal that channels activate near -40 mV, have a half-activation of $+16.2 \pm 3.0$ mV (n=3), and a slope factor of $+15.7 \pm 1.1$ (n=3) (**Fig. 22c**). Channels become fully activated at potentials near +40 mV. No other voltage-activated currents were observed in neoblasts immediately after plating.

3. The architecture of the nervous system of *N. atomata* revealed by tubulin immunohistochemistry.

A. Methods and Materials

An adult *Notoplana* was relaxed in anaesthetic, placed between two glass coverslips to ensure the worm would not contract, then fixed in 4% paraformaldehyde in ASW. The worm was dehydrated, and cleared in xylene before embedding into Paraffin. The worm was subsequently serially sectioned, sections were mounted on pre-cleaned, charged slides, deparaffinized and rehydrated through a series of ethanol steps, then rinsed in 0.1M PBS. Tissues were permeabilized using Triton X-100, then incubated with primary anti-sera against the above-mentioned molecules. Sections were then blocked against non-specific binding, and then treated with a secondary antibody conjugated to an Alexa fluorescent dye (Molecular Probes). Slides were rinsed in 0.1M PBS, then mounted in a 1:9 0.1M PBS:Glycerol solution and viewed using a confocal microscope.

B. Results

B.1. Neurons in N. atomata express a neuron-specific tubulin that shows cross-reactivity towards the commercial antibody Tub Ab-4.

Initially, it had been published that acetylated- α -tubulin labelled neuroblasts specifically in embryos of rhabdocoels and polyclads (Younossi-Hartenstein *et al.*, 1999; Younossi-Hartenstein & Hartenstein, 2000). However, when this antibody was screened in adult tissues of the polyclad *N. atomata*, it was revealed that the antibody not only cross-reacts against nervous tissue, but also the ciliated cells of the ventral epidermis, and the cilia lining the gut lumen (**Fig. 23**). Upon initial observations, virtually all nervous tissue appears to label strongly against acetylated- α -tubulin (**Fig. 23a**). Cell bodies within the brain (**Fig. 23a**, solid arrow) are apparent, as are lateral nerve cords, the dorsal and ventral submuscular plexuses, dorsal-ventral commissural tracts, and secretory and

sensory neurons within the epidermis. However, sectioned material also reveals that the cilia lining the gut diverticula label against this antibody (**Fig. 23b**), and in gut cells, and individual cilia ranging between 10-20 μm in length and not the cell bodies show cross-reactivity (**Fig. 23c**). This is in contrast to the epidermal ciliated cells lining the ventral surface where both the cilia and the ciliated cells show cross-reactivity. Because the acetylated- α -tubulin antibody cross-reacted with various cellular phenotypes, it would not be suitable as a marker for neuronal phenotype, thus other commercial tubulin antibodies were tested to determine whether they would react specifically to neuronal tissues.

When compared to the staining observed using acetylated- α -tubulin antibodies, staining with Tub Ab-4 reveals that virtually the same neuronal elements label strongly, but not ciliated epidermal cells, nor the lining the gut lumen (**Fig. 24**). In a reconstructed 10 μm coronal section of a worm over 6 mm wide, nervous tissue and cilia clearly cross-react with the acetylated- α -tubulin antibody (**Fig. 24a**). However, in sections where Tub Ab-4 was screened, the same nervous tissue from the dorsal and ventral submuscular plexuses as well as the dorsal-ventral commissures label, but there is a distinct lack of cross-reactivity in the epidermis and the gut lumen (**Fig. 24b**). When this antibody was tested in neurons dissociated from the brain, cross-reactivity was clearly observed (**Fig. 25**). Thus, it was concluded that the Tub Ab-4 antibody would be useful as an indicator of neuronal phenotype in cultured cells.

Literature Cited

Buckingham, S.D., & Spencer, A.N. (2000). K⁺ currents in cultured neurones from a polyclad flatworm. *The Journal of Experimental Biology*, 203:3189-3198

Schurmann, W., & Peter, R. (2001). Planarian cell culture: A comparative review of methods and an improved protocol for primary cultures of neoblasts. *Belgian Journal of Zoology*, 131(Supplement 1):123-130

Schurmann, W., Betz, S., & Peter, R. (1998). Separation and subtyping of planarian neoblasts by density-gradient centrifugation and staining. *Hydrobiologia*, 383:117-124

Wong, R.G., Hadley, R.D., Kater, S.B., & Hauser, G.C. (1981). Neurite outgrowth in molluscan organ and cell cultures: the role of conditioning factors. *The Journal of Neuroscience*, 1:1008-1021

Wong, R.G., Barker, D.L., Kater, S.B., & Bodnar, D.A. (1984). Nerve growth-promoting factor produced in culture media conditioned by specific CNS tissues of the snail *Helisoma*. *Brain Research*, 292:81-91

Younossi-Hartenstein, A., Ehlers, U., & Hartenstein, V. (1999). Embryonic development of the nervous system of the rhabdocoel flatworm *Mesostoma lingua* (Abildgaard, 1789). *The Journal of Comparative Neurology*, 416:461-474

Younossi-Hartenstein, A., & Hartenstein, V. (2000). The embryonic development of the polyclad flatworm *Imogine mcgrathi*. *Development Genes and Evolution*, 210:383-398

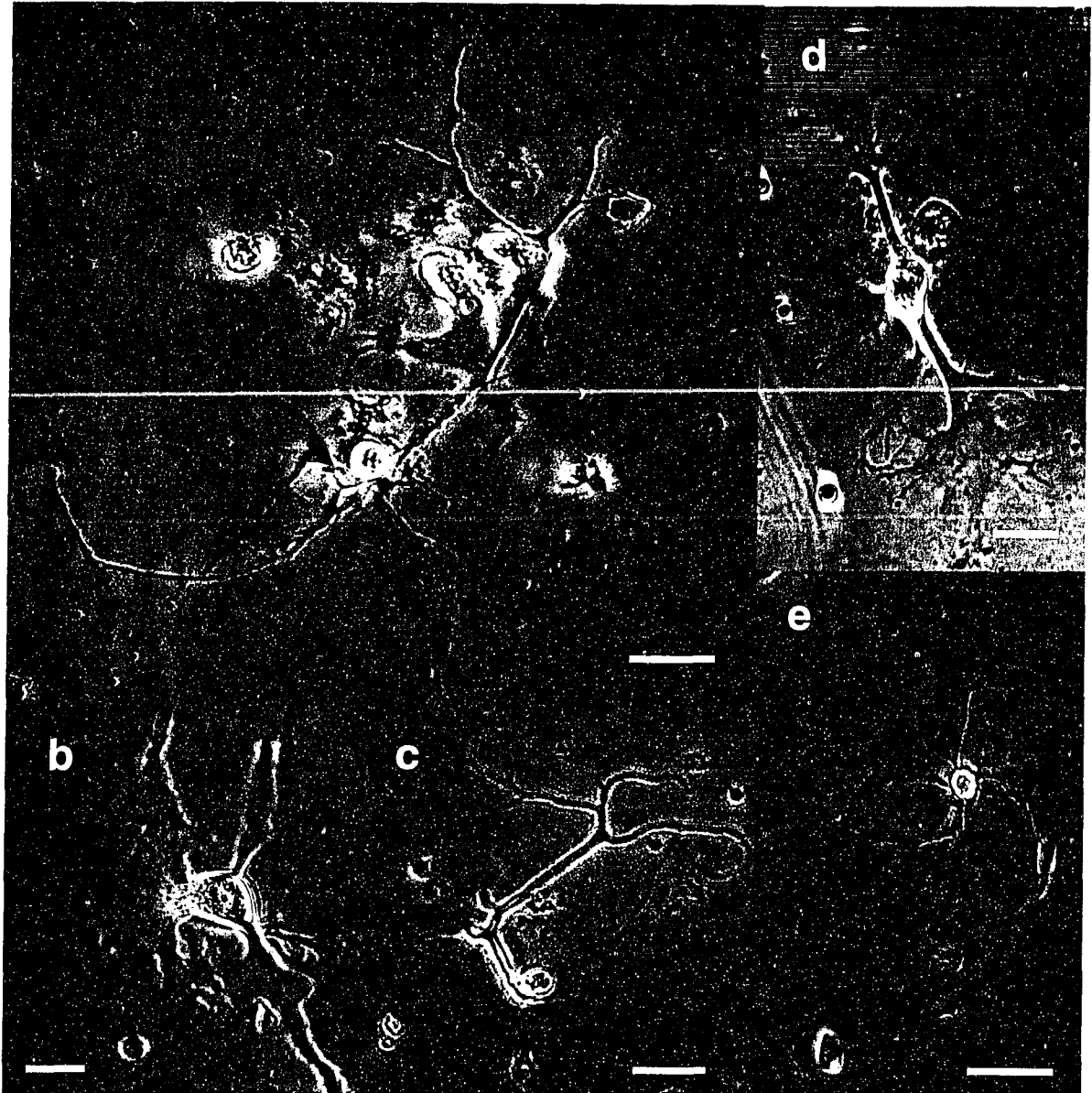


Figure A.1. Cultured brain neurons from *Notoplana atomata* develop growth cones within 3 h of plating and begin extending neurites soon after. (a) After 7 days in culture, brain neurons acquire various morphologies including cells without neurites, cells with developing growth cones, mono- and multipolar and homo- or heteropolar neurites. Between 3 h and 7 days, the proportion of cells with developing growth cones (b), neurons developing short (= 1 soma diameter in length) and long (> 2 soma diameters in length), and the number of neurites extended were measured. Monopolar (c) neurons, bipolar (d), and multipolar neurons (e) were all present after 7 days in culture. Scale bars represents 50 μm .

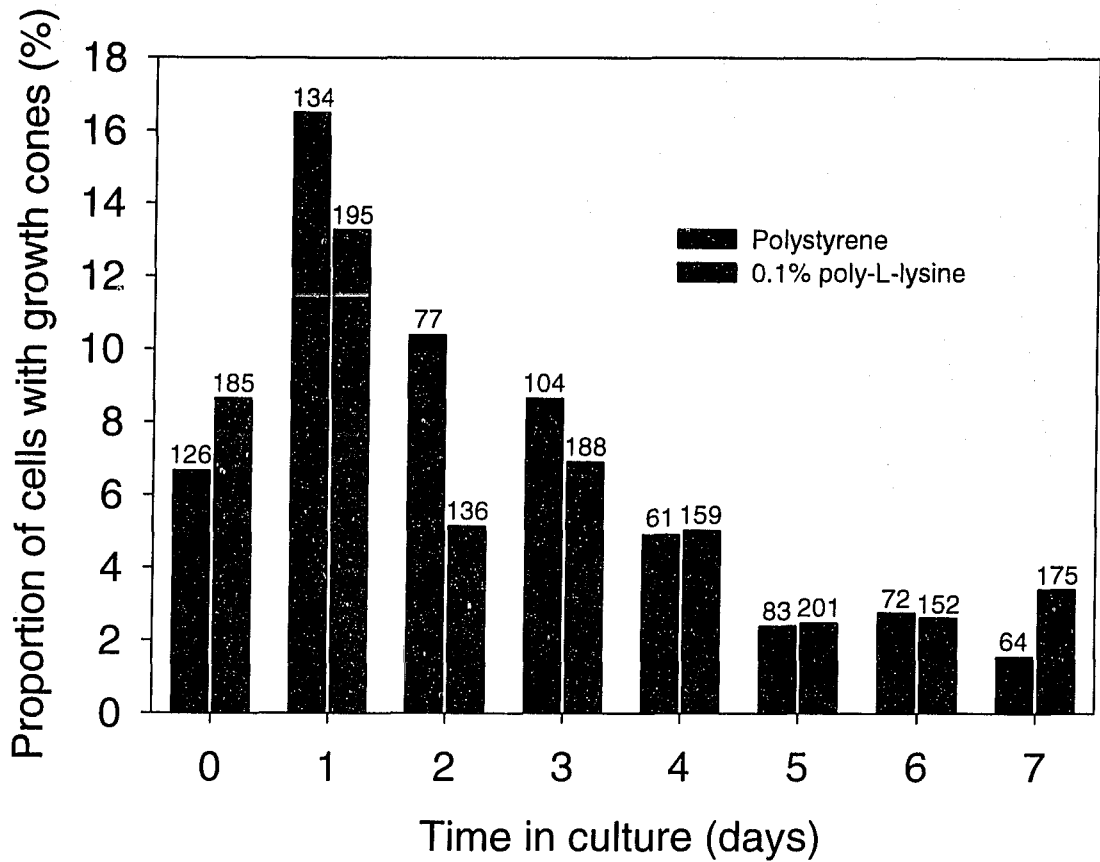


Figure A.2. Brain neurons from *N. atomata* developed growth cones during the first 24 h in culture in absence of exogenous biological factors. When plated on polystyrene culture dishes, or dishes coated with 0.1% poly-L-lysine, the proportion of cells extending growth cones increased and reached a maximum after 24 h in culture. After the first 24 h in culture, cells either lost or began retracting growth cones and only a small proportion (< 5%) of cells retained or developed new growth cones after 5 days in culture. There were no observable effects of plating neurons onto different substrates. Numbers above bars represent the sample size.

Figure A.3. The rate of neurite outgrowth is similar between brain neurons cultured on polystyrene dishes and cells grown on 0.1% poly-L-lysine. **(a)** The proportion of cells with neurites (equal to one soma diameter or longer in length) increased rapidly during the first two days when plated on either polystyrene or 0.1% poly-L-lysine. The number of cells with neurites continued to increase, but at a slower rate until 5 days in culture, after which there was no change in the proportion of cells with neurites. No differences were observed between cells plated on polystyrene and those plated on 0.1% poly-L-lysine. **(b)** The majority of cells eventually developed long neurites (equal to at least two soma diameters in length). Neurons developed long neurites rapidly during the first 48 h in culture, then at a slower rate, until reaching a plateau after 5 days in culture. Maintaining neurons in culture longer than 5 days had little or no effect on the proportion of cells extending long neurites. Substrate did not seem to influence the rate of neurite outgrowth in brain cells. Numbers above bars represent the sample size.

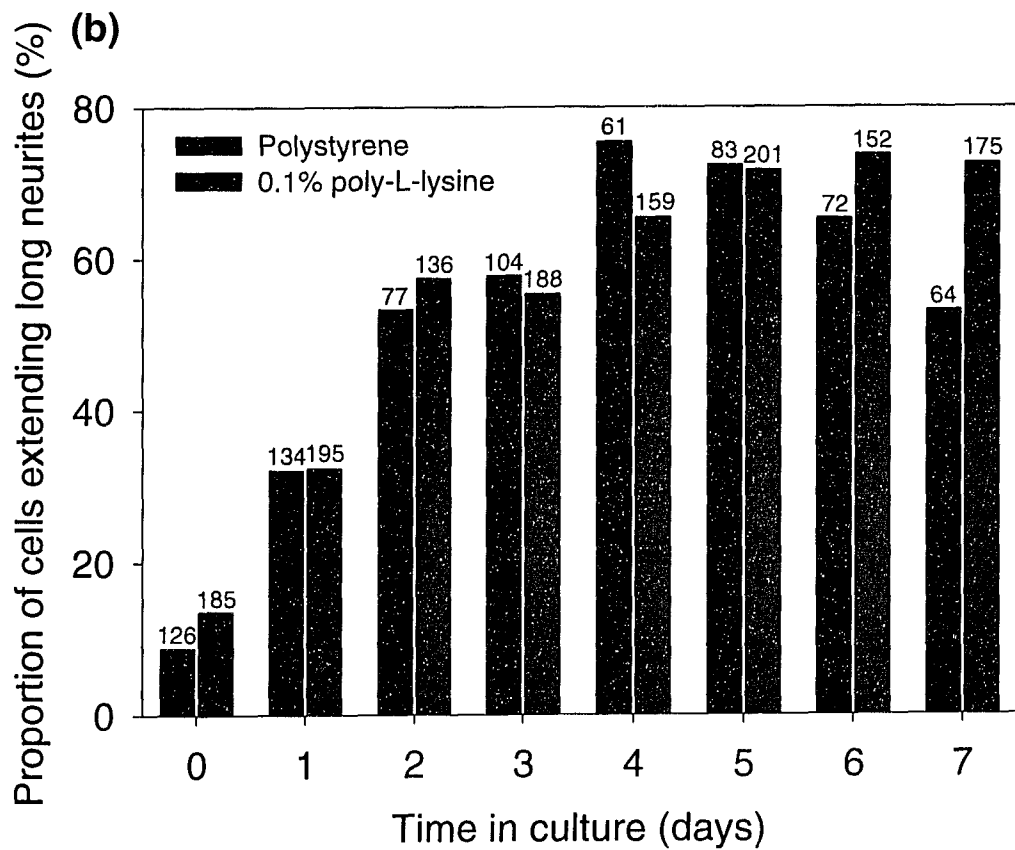
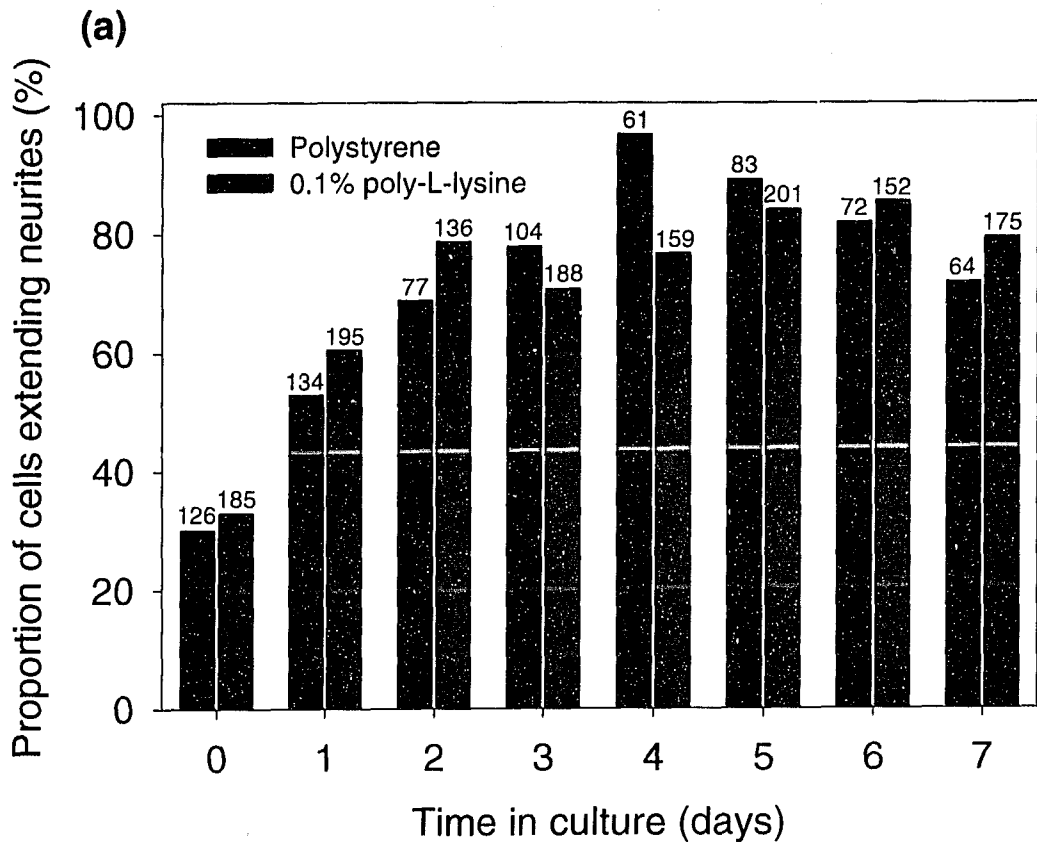
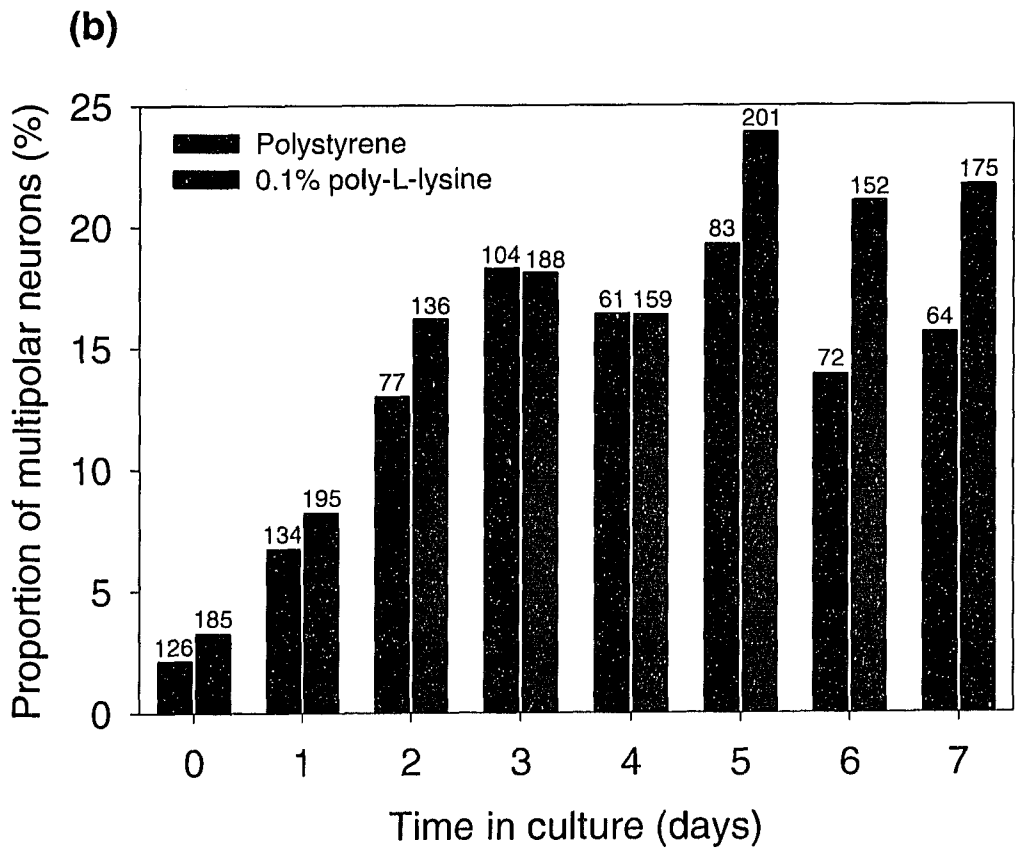
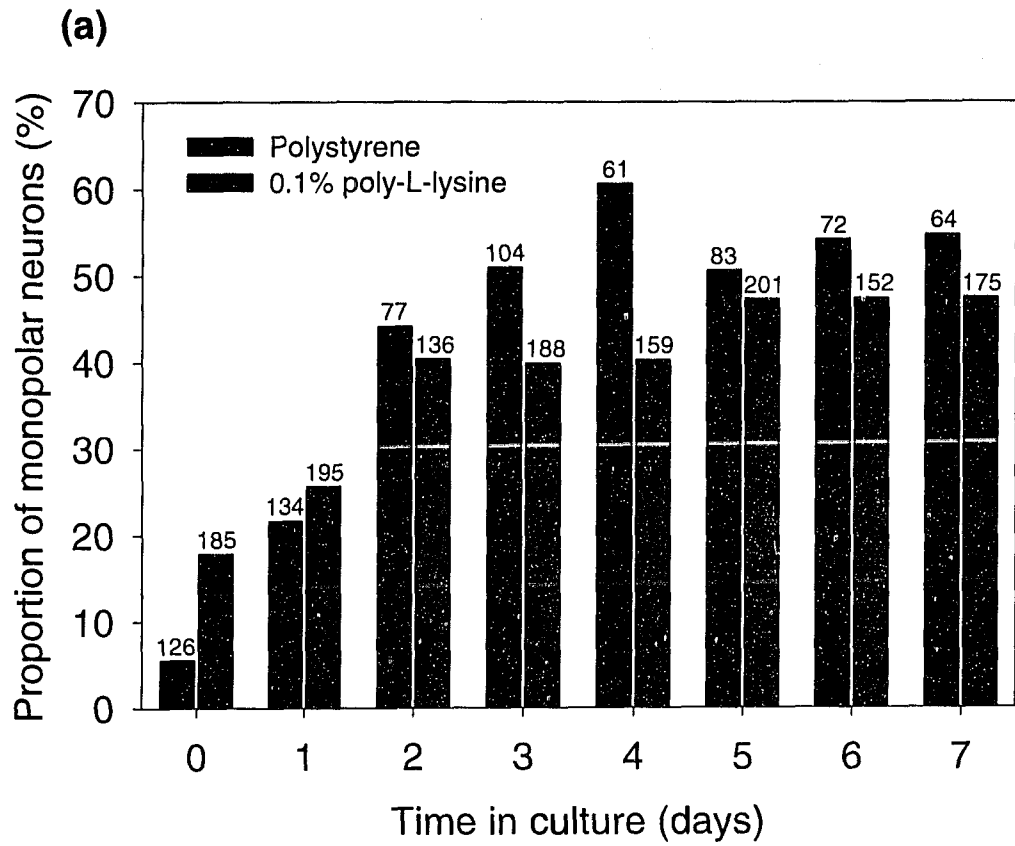


Figure A.4. The substrate on which brain neurons from *N. atomata* are culture upon has no effect on the number of neurites extended. **(a)** The number of monopolar neurons increased gradually and approximately doubled during the first 4 days in culture before reaching a plateau after 5 days. After 5 days in culture, nearly 50% of neurons had developed a monopolar morphology having extended only one neurite that was at least one soma diameter in length. There was no difference in the number of monopolar neurons when cells were plated on either untreated polystyrene or 0.1% poly-L-lysine. **(b)** The number of bi- and multipolar cells increased gradually for 3 days when brain neurons were plated on either untreated polystyrene or 0.1% poly-L-lysine. After 5 days in culture, the proportion of bi- or multipolar neurons reached a maximum. Nearly 20% of cultured cells developed bi- or multi-polar morphologies. The substrate had no effect on the number of multipolar neurons in culture. Numbers above bars represent the sample size.



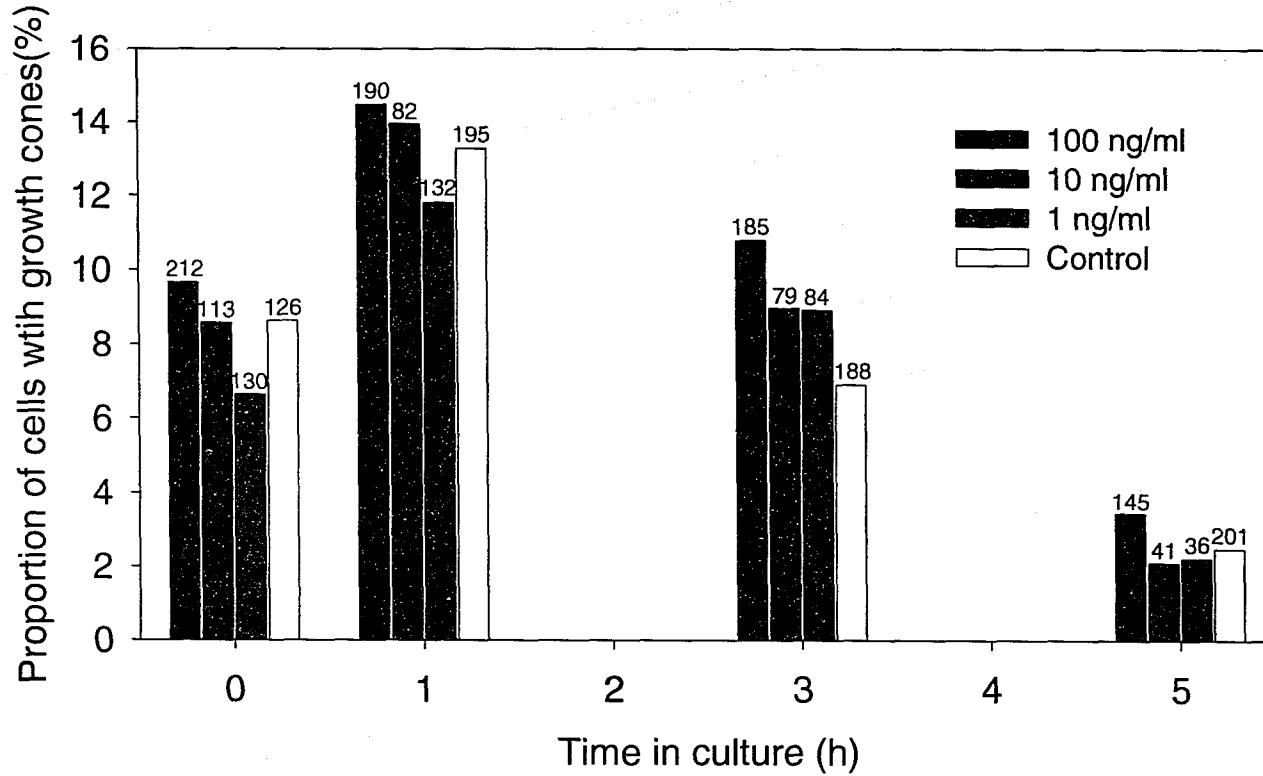


Figure A.5. Treatment of brain neurons from *N. atomata* with basic fibroblast growth factor increased the proportion of cells developing growth cones. Exogenously applied bFGF marginally increased the proportion of neurons developing growth cones in a dose-dependent manner. As in the control samples, cells treated with bFGF developed growth cones within the first 24 h in culture, which was followed by retraction and disappearance of distinct growth cones. Numbers represent the sample size.

Figure A.6. Basic fibroblast growth factor applied exogenously to brain neurons culture on 0.1% poly-L-lysine coated dishes had a slight inhibitory effect on neurite outgrowth. The presence of bFGF in the culture medium decreased the proportion of neurons developing short **(a)** or long **(b)** neurites in a dose-dependent manner. **(a)** The proportion of cells sprouting neurites increase gradually over 5 days, but treatment with high concentrations of bFGF (100 ng/ml) resulted in fewer cells sprouting neurites when compared to the control. **(b)** Treatment with bFGF also inhibited the extension of neurites and reduced the proportion of cells developing long neurites in a dose-dependent manner. Numbers above bars represent the sample size.

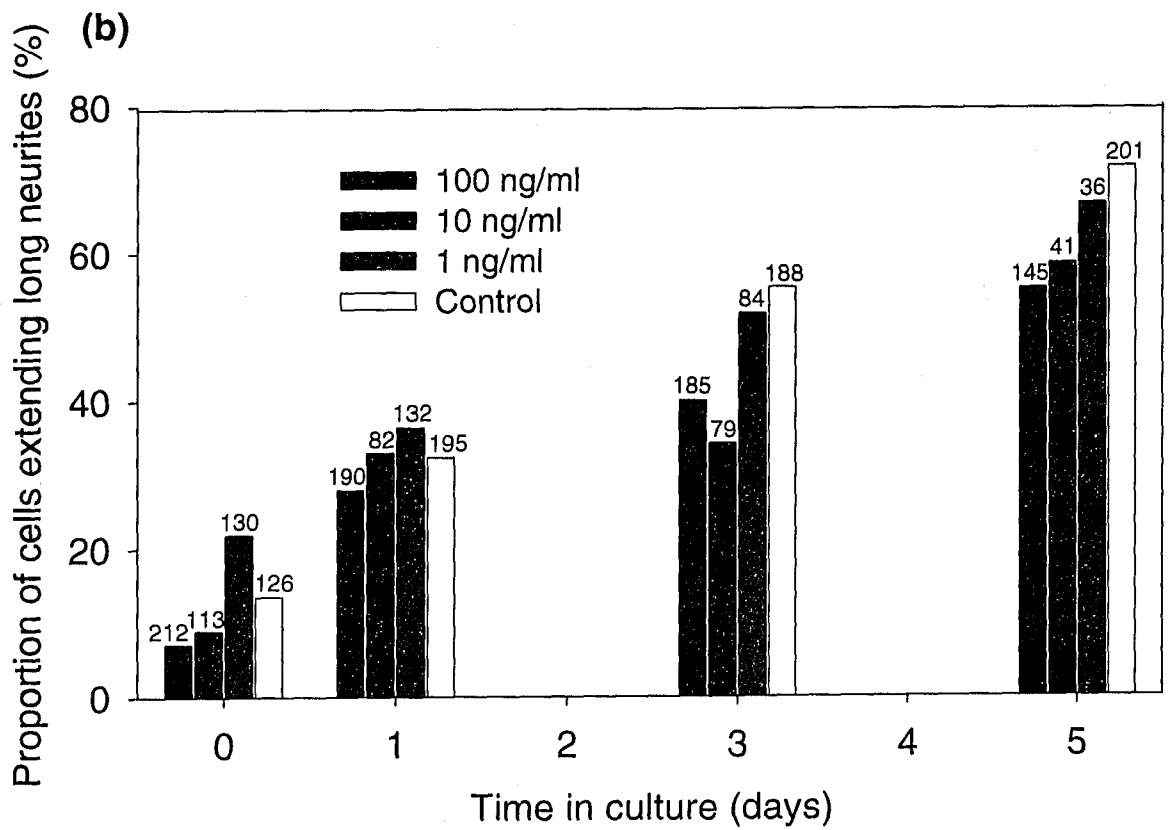
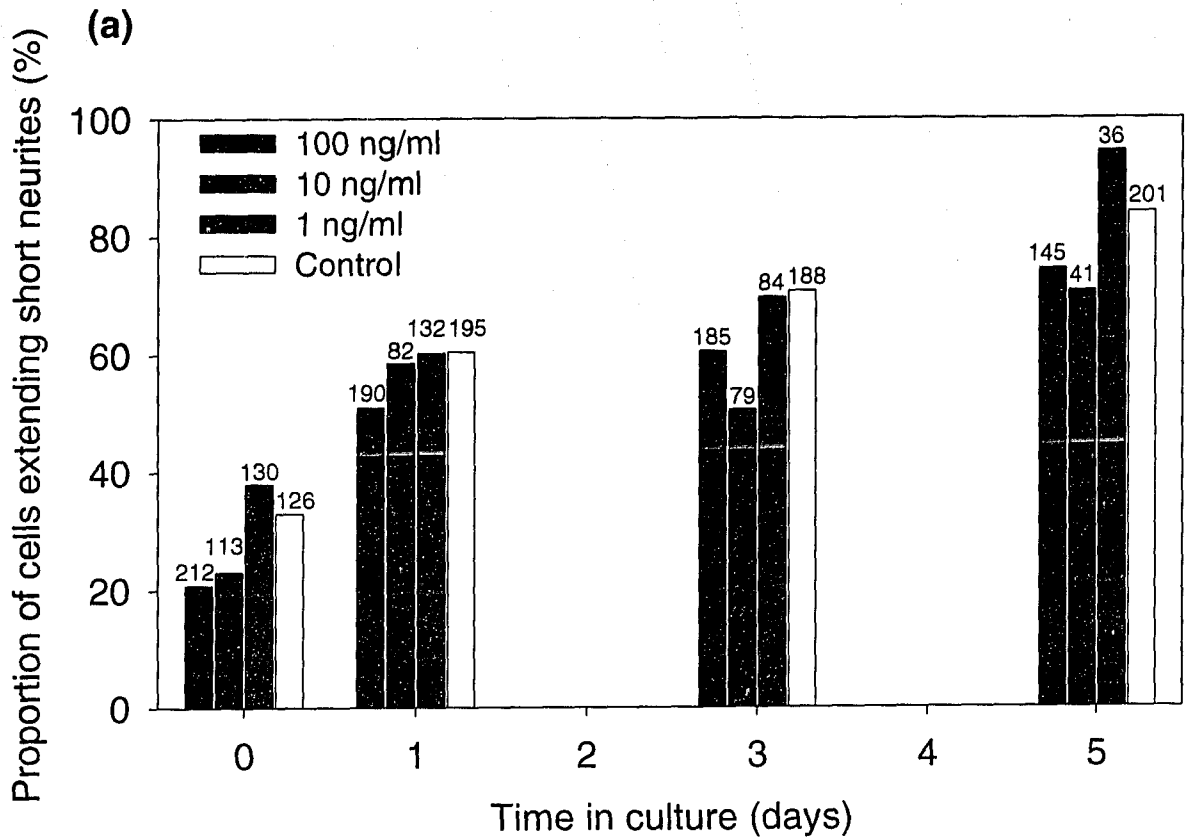
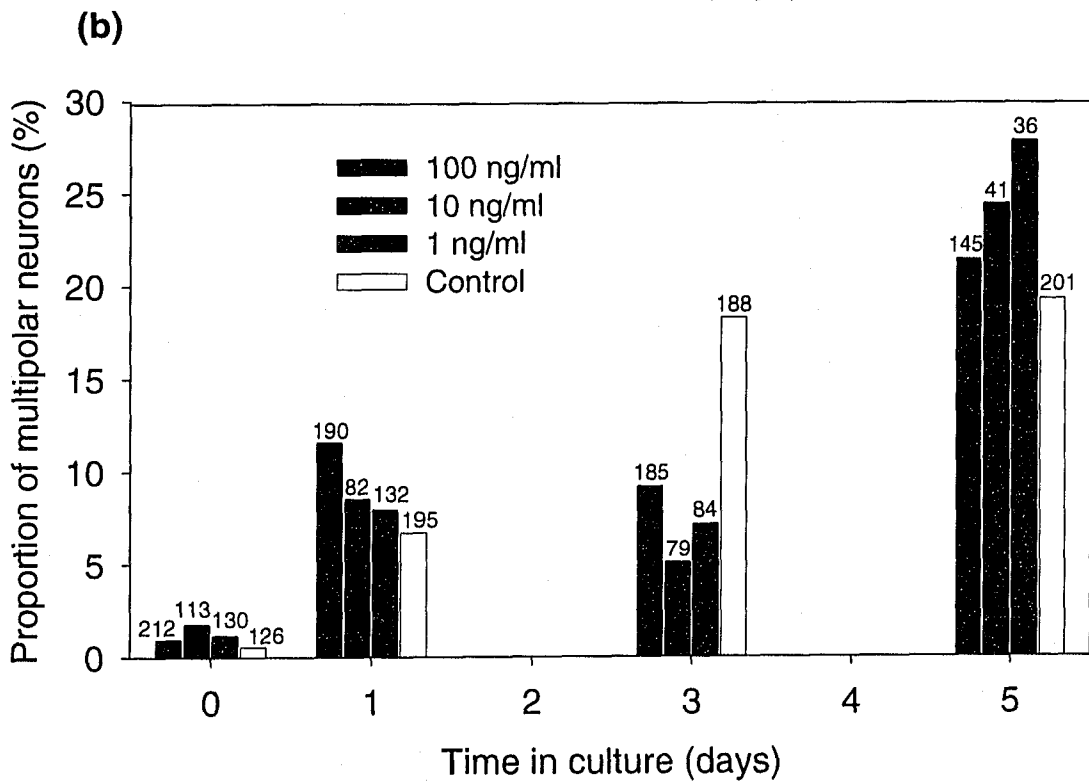
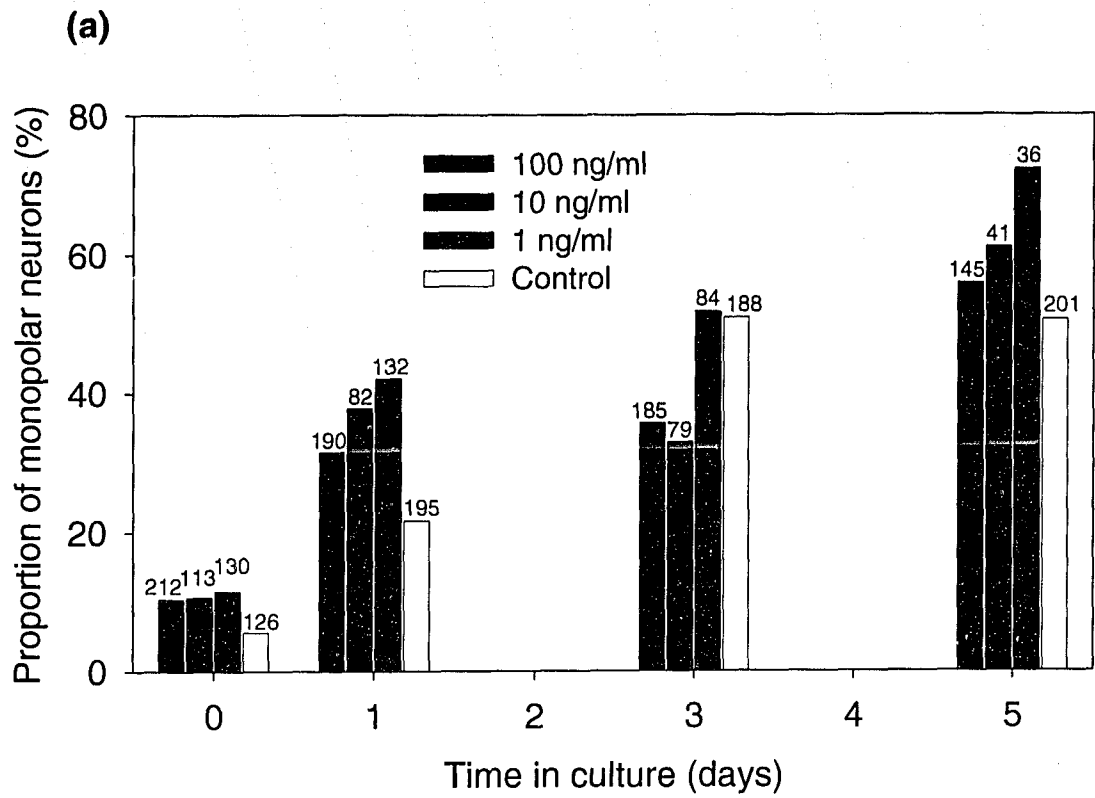


Figure A.7. Basic fibroblast growth factor applied exogenously to brain neurons cultured on 0.1% poly-L-lysine coated dishes had no effect the number of neurites extended. **(a)** The proportion of monopolar neurons increased gradually during the first 3 days in culture before reaching a plateau. After 72 h in culture, nearly 50% of neurons were monopolar having extended only one neurite that was at least one soma diameter in length. There was no observable dose-dependent response of neurons to bFGF. Treatment with bFGF did not induce more cells to develop a monopolar morphology. **(b)** The number of bi- and multipolar cells increased gradually for three days when brain neurons were plated on 0.1% poly-L-lysine, but this proportion was unaffected by bFGF. After 3 days in culture, the proportion of bi- or multipolar neurons reached a maximum. Nearly 20% of cultured cells developed bi- or multi-polar morphologies. Basic FGF applied exogenously had no effect on the number of multipolar neurons in culture. Numbers above bars represent the sample size.



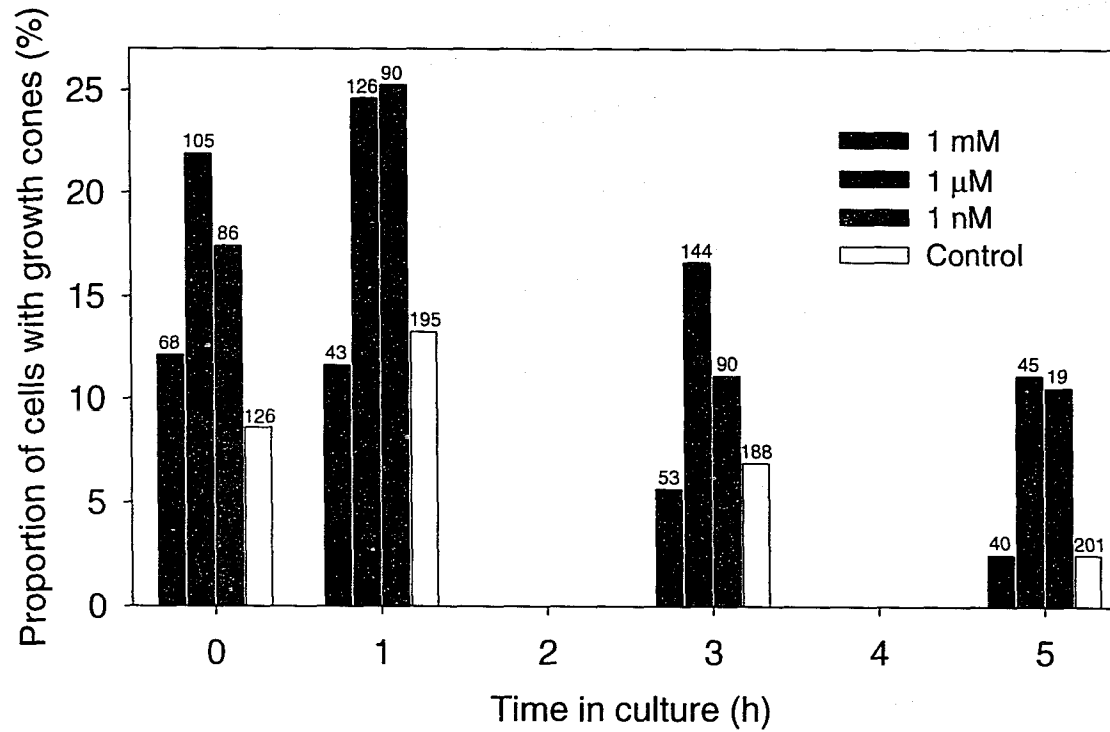


Figure A.8. Serotonin increases the proportion of cultured neurons extending growth cones. Neurons cultured in the presence of 5-HT developed growth cones sooner when compared to control samples. Within 30 min of plating with 5-HT added to the culture medium, the proportion of cells developing growth cones increased between 2 to 4 times compared to cells plated on 0.1% poly-L-lysine alone and bathed in control medium. Cells showed no response when exposed to the higher dose of 5-HT (1 mM). The proportion of cells with growth cones reached a maximum after 24 h, after which they were gradually retracted or lost. Numbers represent the sample size.

Figure A.9. Serotonin applied exogenously inhibited neurite outgrowth in brain neurons from *N. atomata*. **(a)** Both the rate and the maximum number of cells sprouting neurites (greater than one soma diameter in length) was smaller when brain neurons were cultured in the presence of 5-HT. Inhibition of neurite outgrowth was dose-dependent and more pronounced with higher doses of 5-HT. The rate of neurite outgrowth was inhibited by nearly 50% with as little as 1 nM 5-HT in the culture media. A small proportion of cells (~40%) appeared to be unaffected by exogenous 5-HT. **(b)** The proportion of neurons developing long neurites (greater than two soma diameters in length) was decreased when cells were cultured in the presence of 5-HT. The rate of neurite outgrowth was inhibited in a dose-dependent manner when 5-HT was applied. The proportion of cells extending long neurites increased rapidly during the first 72 h in culture, then reached a peak. There appeared to be a small proportion of neurons that were unaffected by 5-HT and produced long neurites after a few days in culture. Numbers above bars represent the sample size.

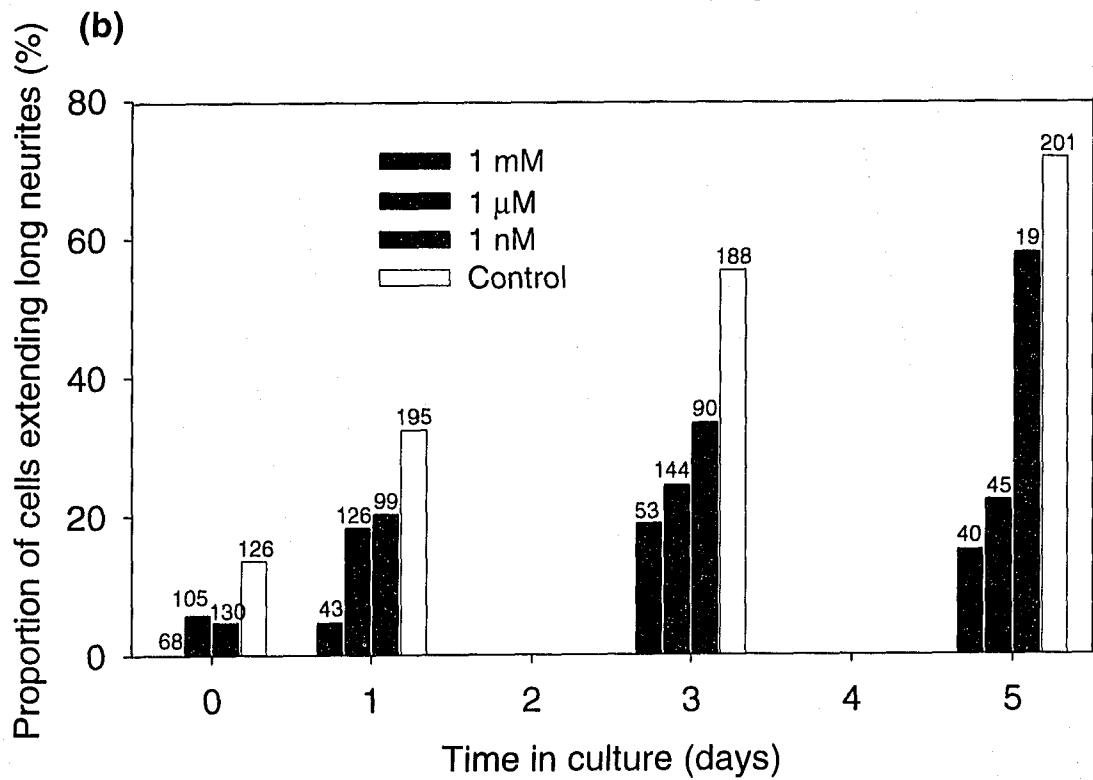
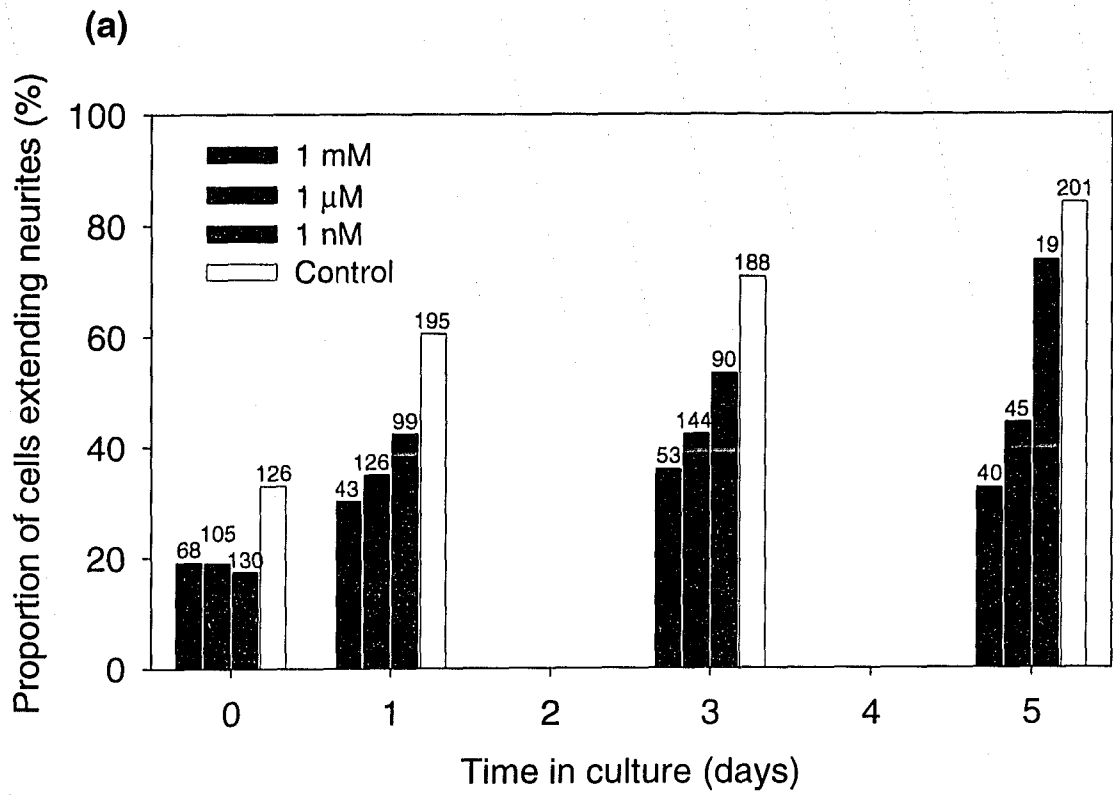
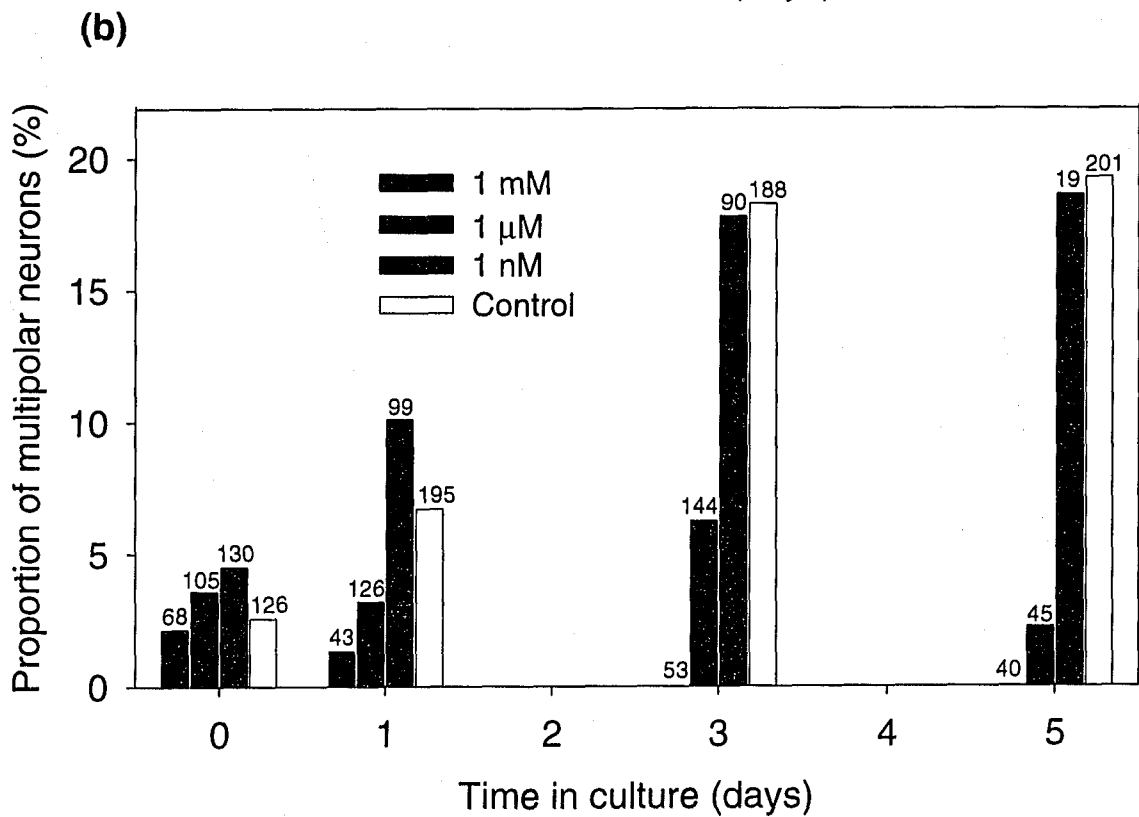
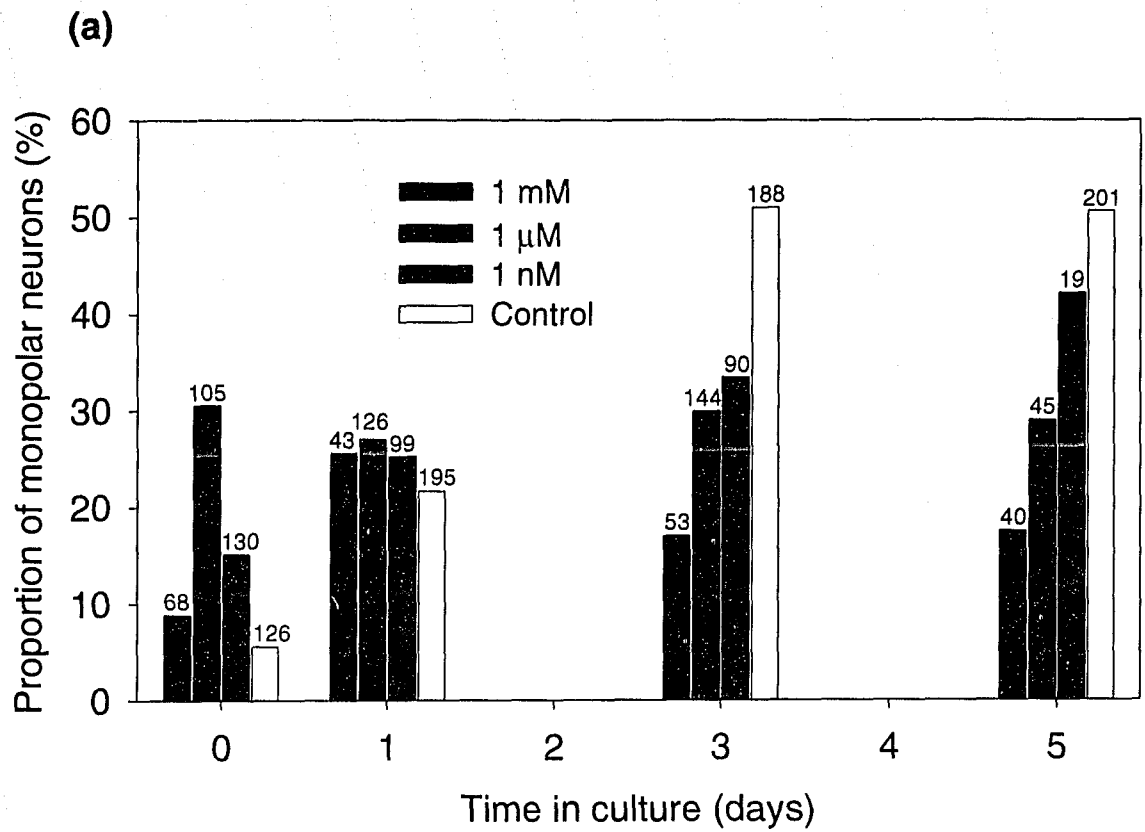


Figure A.10. Serotonin applied exogenously to brain neurons cultured on 0.1% poly-L-lysine coated dishes inhibited neurite extension. **(a)** Serotonin applied to the culture medium inhibited cells from developing a monopolar morphology when compared to cells cultured on 0.1% poly-L-lysine alone. Inhibition of neurite extension was dose-dependent and maximal at higher concentrations of 5-HT. There remained a small population of neurons (~20%) that were unaffected by 5-HT application and developed a monopolar morphology after a few days in culture. **(b)** The number of cells developing bi- or multi-polar morphologies was inhibited by application of 5-HT to the culture medium. This response was dose-dependent and largest at high concentrations of 5-HT. When 1 mM 5-HT was applied to the culture medium, there were no cells that developed either a bipolar or multipolar morphology. At reduced concentrations of 5-HT, a small population of cells appeared unaffected and developed bi- or multi-polar morphologies. Neither 1 μ M nor 1 nM reduced the number of multipolar neurons extending neurites compared with control cells plated on 0.1% poly-L-lysine and bathed in control medium. Numbers above bars represent the sample size.



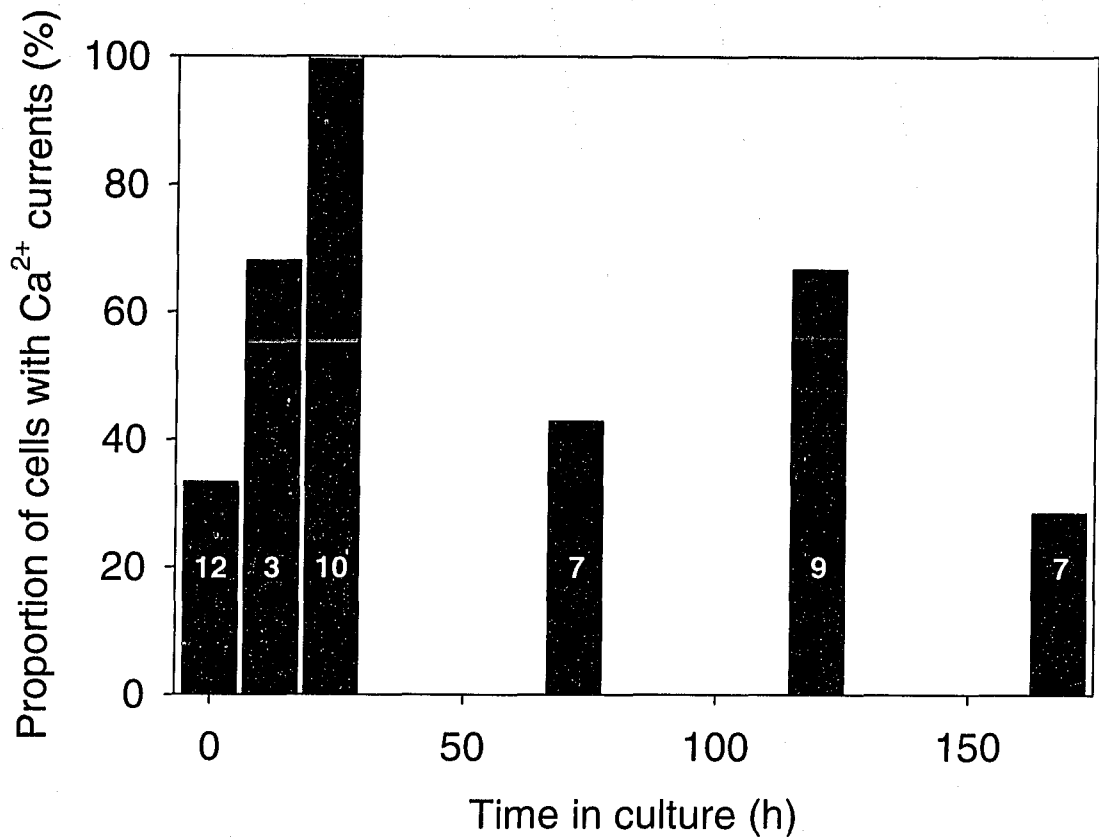


Figure A.11. Appearance of Vg-Ca²⁺ channels in cultured brain cells from *N. atomata*. Brain neurons expressed Vg-Ca²⁺ channels when cultured on 0.1% poly-L-lysine and bathed in control culture medium. Expression of Ca²⁺ channels increased gradually over the first day in culture and peaked at 24 h when 100% of cells (n= 10) examined possessed at least one type of Ca²⁺ current. The proportion of cells expressing a Vg-Ca²⁺ current decreased after 3 days in culture (42.9%, n = 7), and was further diminished after 7 days in culture (28.6%, n = 7). Bold numbers within bars represents the sample size.

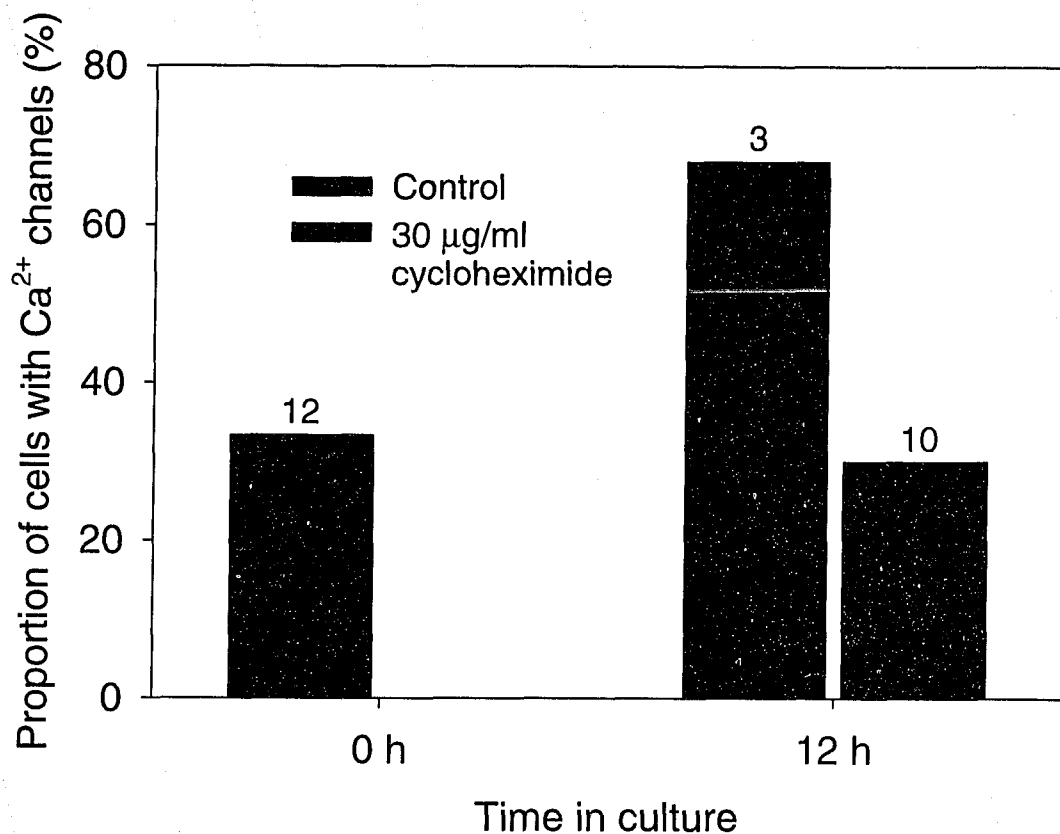


Figure A.12. Expression of Ca^{2+} currents in brain neurons during neurite outgrowth requires *de novo* protein expression. The increase in neurons expressing Ca^{2+} channels requires new protein synthesis. After 12 h in culture, the proportion of neurons expressing Ca^{2+} currents increases to 66.0% (n=3) from 33.0% (n=12) in cells immediately after plating. When the protein transcription inhibitor cycloheximide is applied to cultures for 12 h, no increase in the proportion of cells expressing Ca^{2+} channels is observed. The numbers above bars represent the sample size.

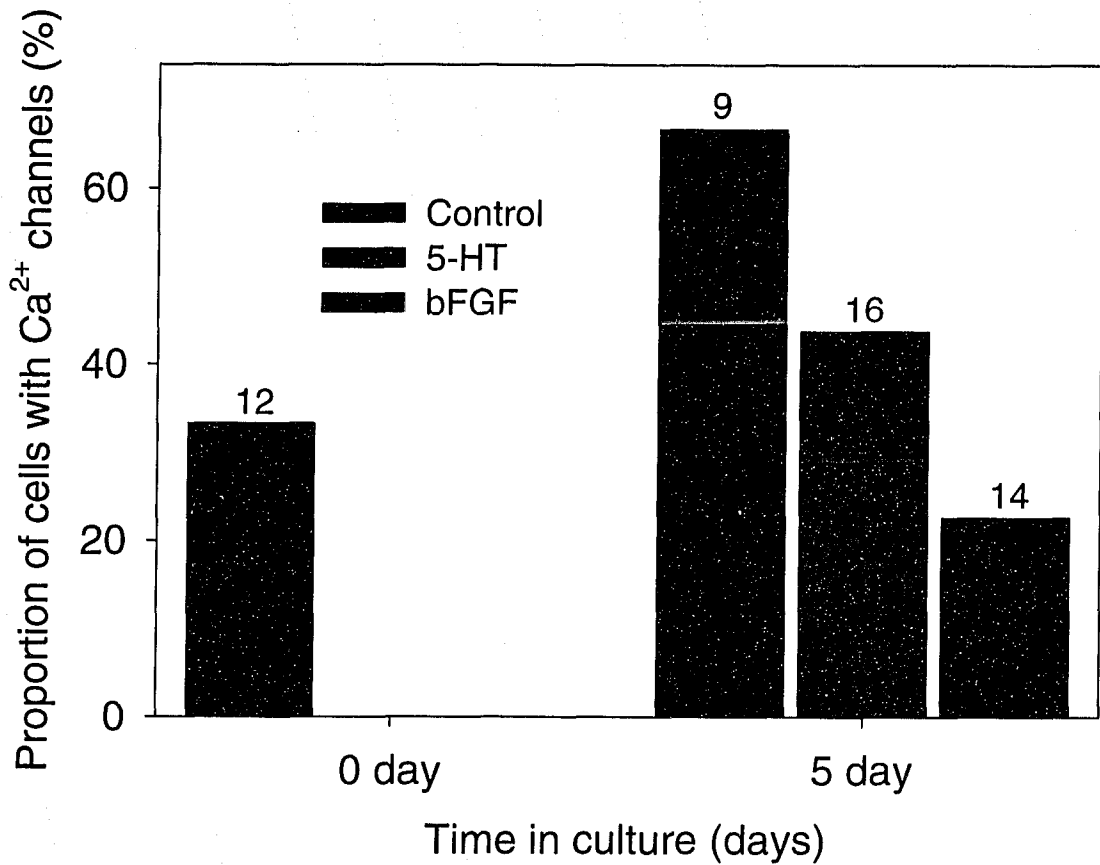


Figure A.13. Treatment with morphogens inhibits expression of Ca^{2+} currents in brain neurons cultured from *N. atomata*. After 5 days in culture, the proportion of control brain neurons cultured on 0.1% poly-L-lysine expressing at least one type of Ca^{2+} current doubled from 33.3% (n=12) to 66.7% (n=9). Treatment with both serotonin (Chi-square test, $p < 0.05$, $n = 25$) and bFGF (Chi-square test, $p < 0.05$, $n = 23$) significantly inhibited expression of Ca^{2+} currents after 5 days in culture. Application of 1 μM serotonin decreased the proportion of cells with Ca^{2+} currents to 43.8% (n=16), while application of 10 ng/ml of bFGF resulted in a decrease in the proportion of cells expressing a Ca^{2+} current to 21.4% (n=14).

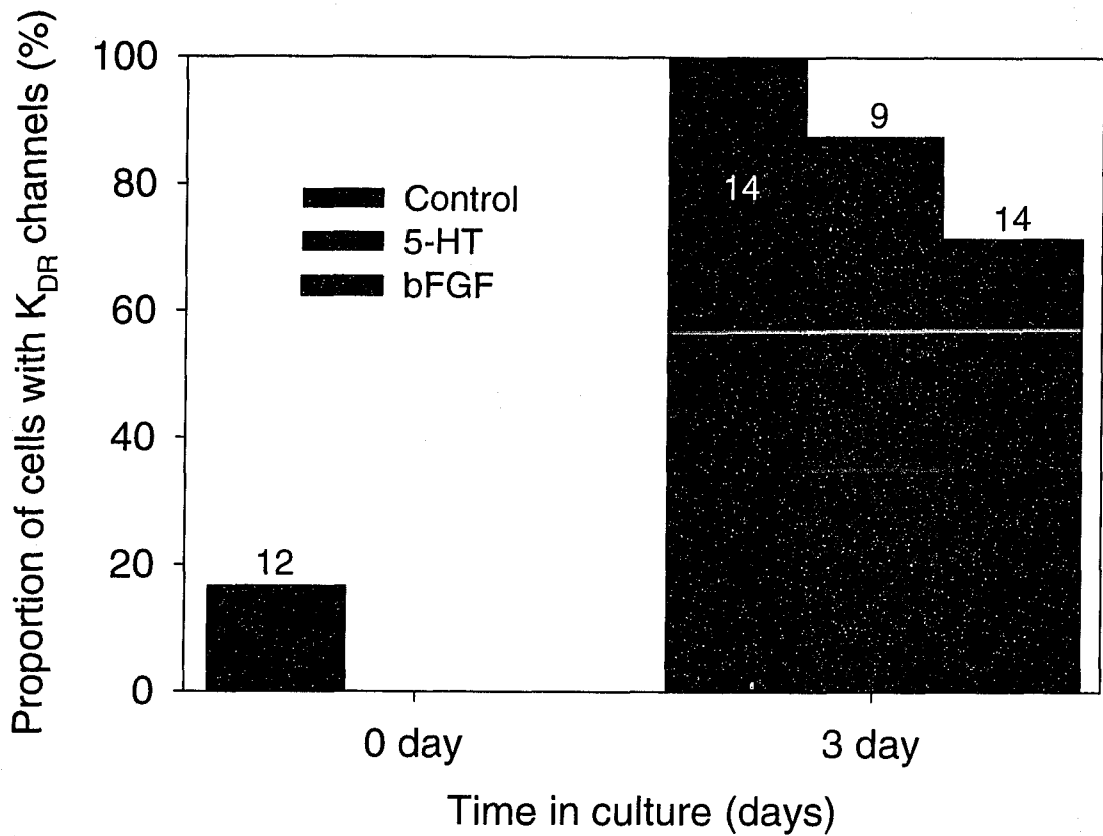


Figure A.14. Maintaining brain cells from *N. atomata* in culture resulted in an increase in the proportion of cells expressing a K_{DR} -like channel. When plated on control substrate (0.1% poly-L-lysine) alone, there was a significant increase in the proportion of neurons expressing a K_{DR} channel from 16.7% to 100% (Chi-Square test, $p < 0.05$, $n = 26$), after 3 days in culture. Treating brain neurons with $1 \mu\text{M}$ 5-HT or 10 ng/ml bFGF for 3 days had no effect on the proportion of cells expressing K_{DR} channels when compared to the control (Chi-Square test, $p > 0.05$, $n = 37$).

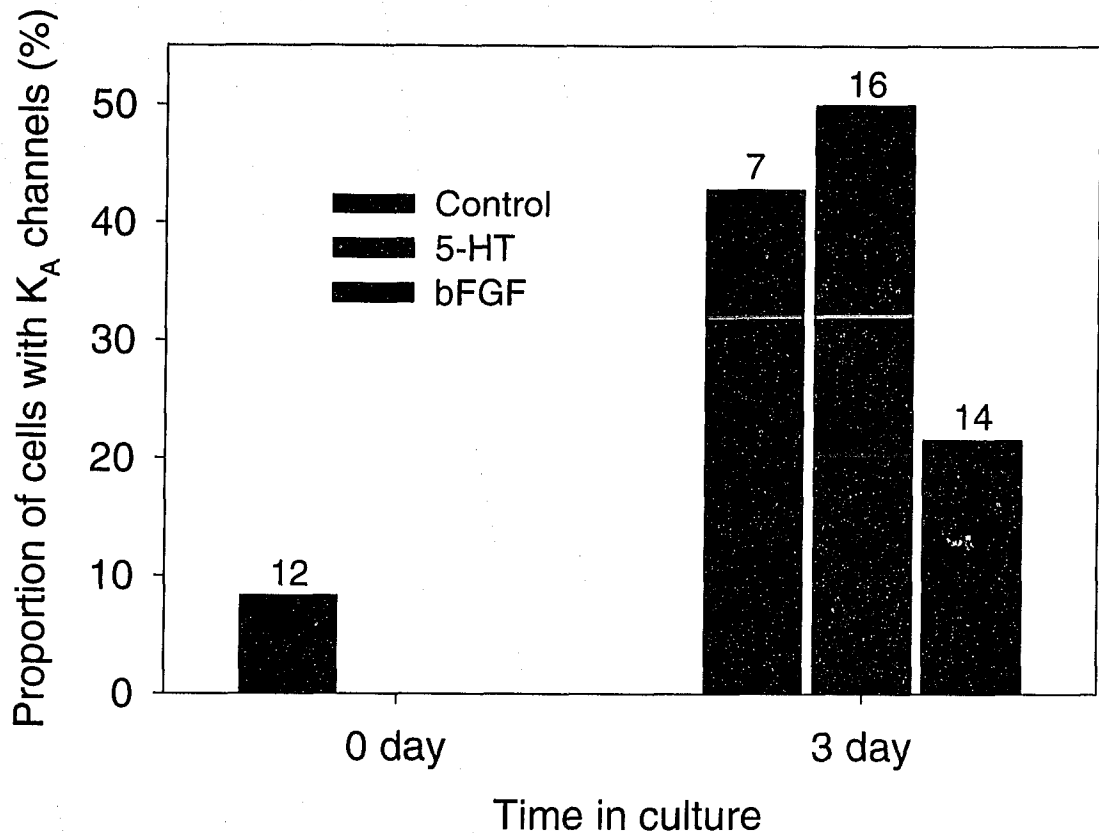


Figure A.15. The effect of diffusible factors on the proportion of cultured brain neurons expressing a K_A channel. The proportion of cells expressing a K_A current increased under control conditions from 8.3% (n=12) to 42.9% (n=7) after 3 days in culture. Treatment with 5-HT increased the proportion of cells with K_A currents to 50% but the difference was not significantly larger than the control (Chi-Square test, $p > 0.05$, n=23). Treatment with 10 ng/ml bFGF resulted in a significantly smaller proportion of cells expressing K_A channels than in the control after 3 days (Chi-Square test, $p > 0.05$, n=21). Numbers above the bars represent the sample size.

Figure A.16. V_g - Ca^{2+} currents recorded in brain cells from *N. atomata*. **(a)** A typical inward current recorded from a voltage-clamped brain neuron bathed in solutions designed to isolate for Ca^{2+} currents. At least two components were observed in some cells, that included both a sustained current and an inactivating current. Currents were evoked by stepping the holding potential from -70 mV in 10 mV increments between -90 mV and +70 mV for 150 ms. The scale bar is included in the inset. **(b)** The current-voltage relationship of Ca^{2+} currents show that channels activate at around -30 mV, peaked at +10 mV, and the mean reversal potential was 45.7 ± 3.2 mV ($n=17$). Data represent the mean from 17 cells.

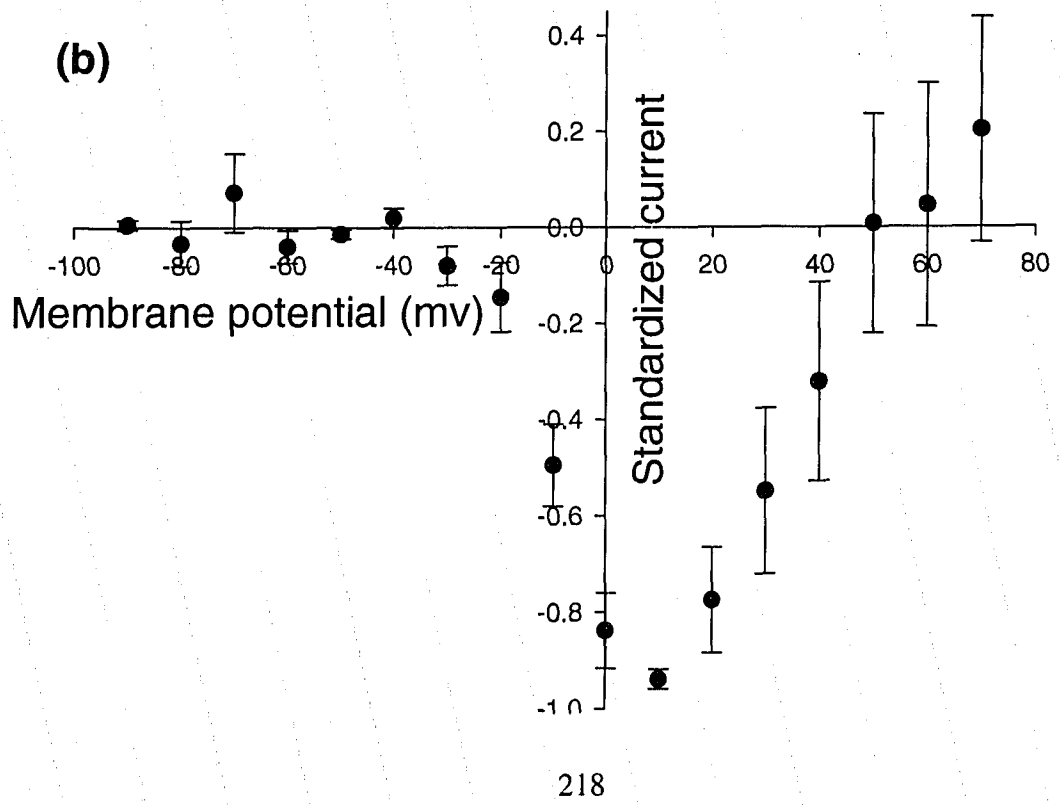
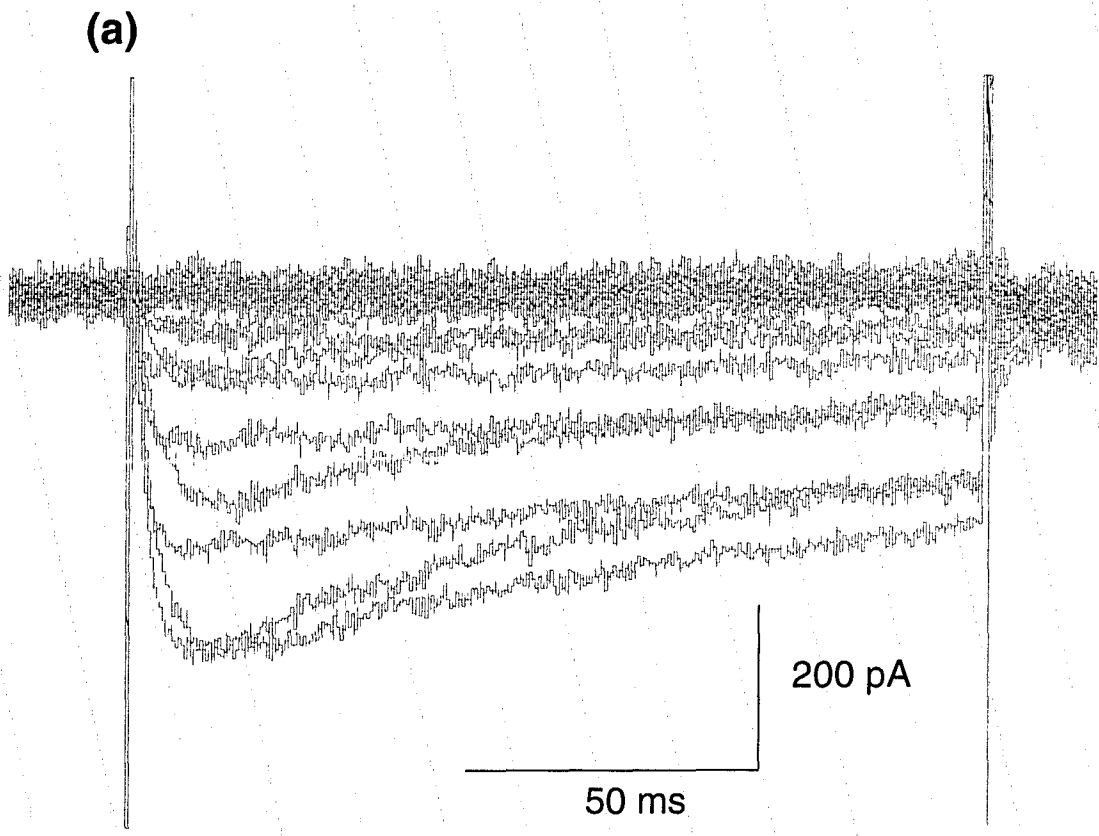
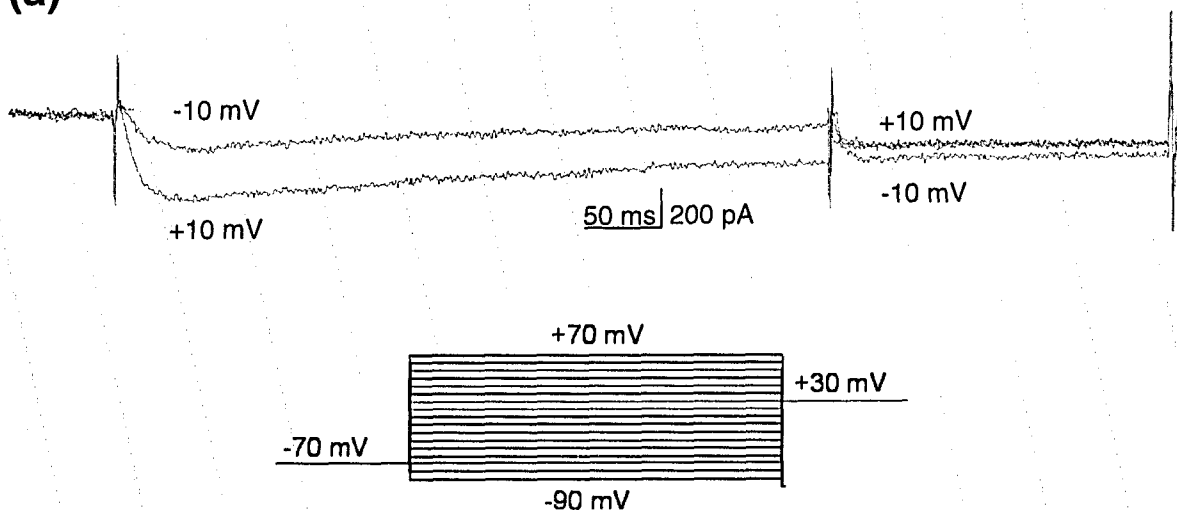
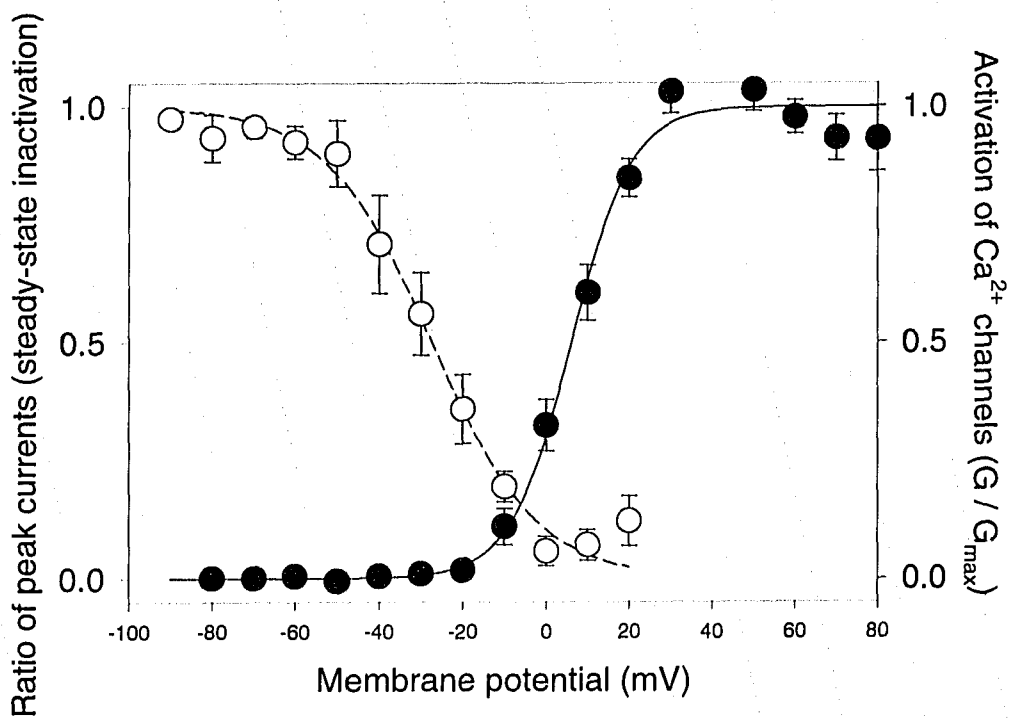


Figure A.17. Activation and steady-state inactivation properties of $V_g\text{-Ca}^{2+}$ channels recorded from brain neurons. (a) Two components could be separated from each other by using a simple depolarizing prepulse experiment to eliminate the inactivating component and isolate the non-inactivating component. Cells were held at -70 mV then stepped by 10 mV increments through a series of potentials between -90 mV and +70 mV for 450 ms. The prepulse was followed immediately by a 225 ms depolarizing test pulse to +10 mV. A depolarizing test pulse to +10 mV was sufficient to reduce the total current by more than 50%. (b) Activation properties were measured by stepping the holding potential 10 mV from -70 mV to a series of values between -90 mV and +70 mV, and the reversal potential was estimated from the I-V relationship. Currents were normalized to the maximal evoked current then plotted against the holding potential of the test pulse. Activation curves for individual cells were fitted to a multi-stage Boltzmann function to determine the voltage of half-activation and the slope factor. These values were used to generate a mean activation curve (solid curve). Ca^{2+} channels began to activate near -30 mV and were fully activated at +40 mV. The voltage of half-activation was 7.4 ± 1.1 mV ($n=10$) and the slope factor was 6.3 ± 1.2 ($n=10$). Steady state inactivation was obtained by determining the amplitude of the rapidly inactivating component by subtracting the transient component assuming that full inactivation had occurred during the prepulse. The data were normalized to the peak current and plotted against the potential of the prepulse. Channels began to inactivate between -60 mV and +10 mV. The voltage of half-inactivation was -26.6 ± 1.5 mV ($n=10$) and the slope factor was -12.0 ± 1.3 ($n=10$). The mean inactivation curve is shown by the dotted line.

(a)



(b)



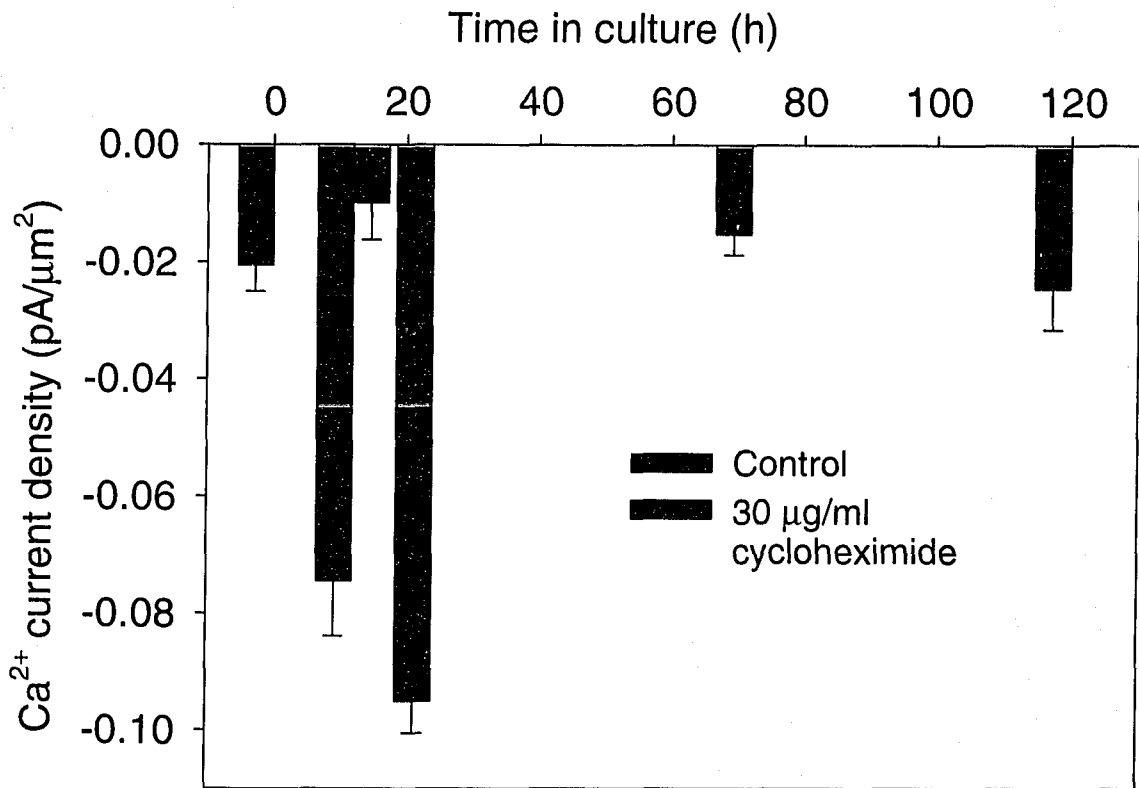
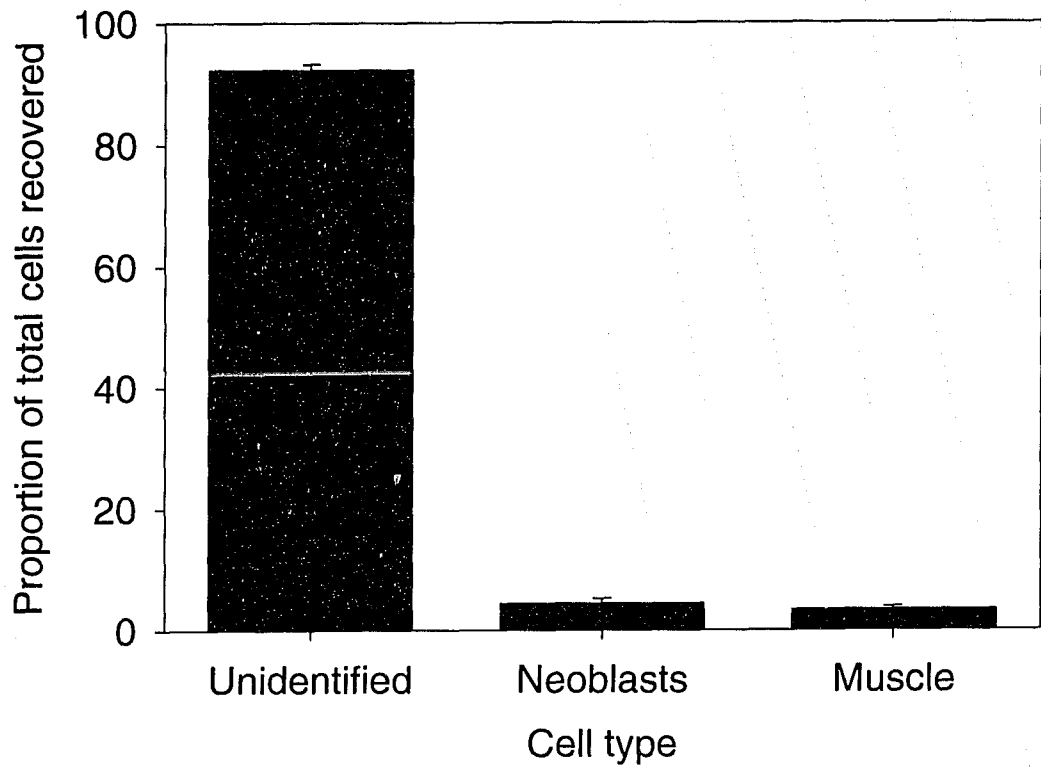


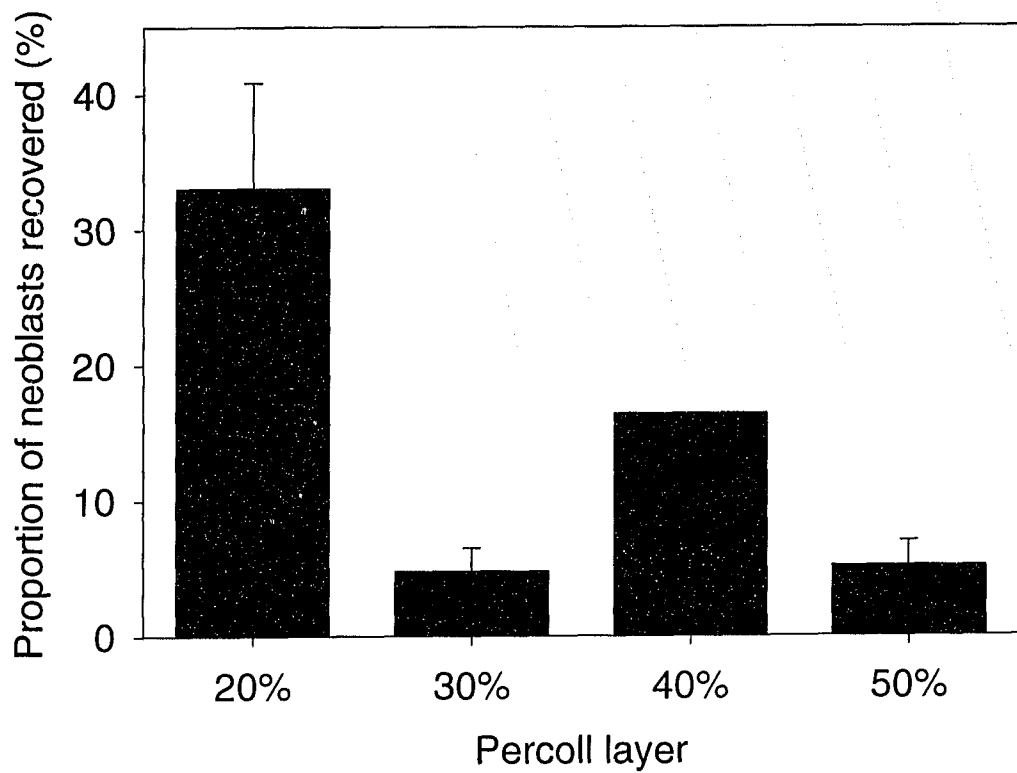
Figure A.18. Expression of Ca^{2+} channels increases during the first 24 h in cultured brain neurons. Ca^{2+} currents were evoked by depolarizing brain neurons voltage clamped in the whole-cell configuration in Ca^{2+} isolating medium. Cells were held at -70 mV then depolarized to $+10$ mV. Peak currents were standardized to cell size which was determined by the membrane capacitance (assuming a standard membrane capacitance of $1 \text{ pF}/\mu\text{m}^2$). Ca^{2+} currents were relatively small ($-0.021 \pm 0.004 \text{ pA}/\mu\text{m}^2$, $n=7$) in neurons immediately after plating but increased nearly five-fold to $-0.095 \pm 0.005 \text{ pA}/\mu\text{m}^2$ ($n=7$). The mean current density peaked at 24 h then declined back to initial levels after 3 days in culture. Treatment with $30 \text{ }\mu\text{g}/\text{ml}$ of the protein transcription inhibitor cycloheximide for 12 h prevented the increase in current density. This suggests that the increase in current density was caused by an increase in the number of Vg channels and not changes in single channel conductance. Data represent the mean \pm S.E.M. for 5 cells unless otherwise indicated.

Figure A.19. Isolation and purification of neoblasts from whole organism dissociations of *Notoplana atomata*. **(a)** Three to five worms were mechanically and enzymatically separated into single cell suspensions. Whole organism suspensions were plated and processed for histological identification of neoblasts and other cell types. Cell suspensions contained many cellular phenotypes, but neoblasts and muscle cells in particular were easily identifiable after staining with azure-A and eosin-B. Muscle cells were stained lightly pink and made up $3.3\pm 0.5\%$ ($n=10$) of the total cell fraction. Neoblast were identified as cells with high nucleus to cytoplasm ratios, that had a distinctly dark blue cytoplasmic staining. Neoblasts made up $4.4\pm 0.8\%$ ($n=10$) of the total cells recovered. **(b)** Whole organism suspensions were then process to separated and purify neoblasts by size and density using discontinuous Percoll gradients. The highest concentration of neoblasts was recovered from the boundary between 20% and 30% Percoll where $33.0\pm 7.8\%$ ($n=3$) of cells were identified as neoblasts. Neoblasts were also recovered from the boundaries of the 30%, 40% and 50% Percoll layers, but at smaller proportions. Neoblasts of different densities most likely represent different subtypes of neoblasts at various stages of cellular differentiation.

(a)



(b)



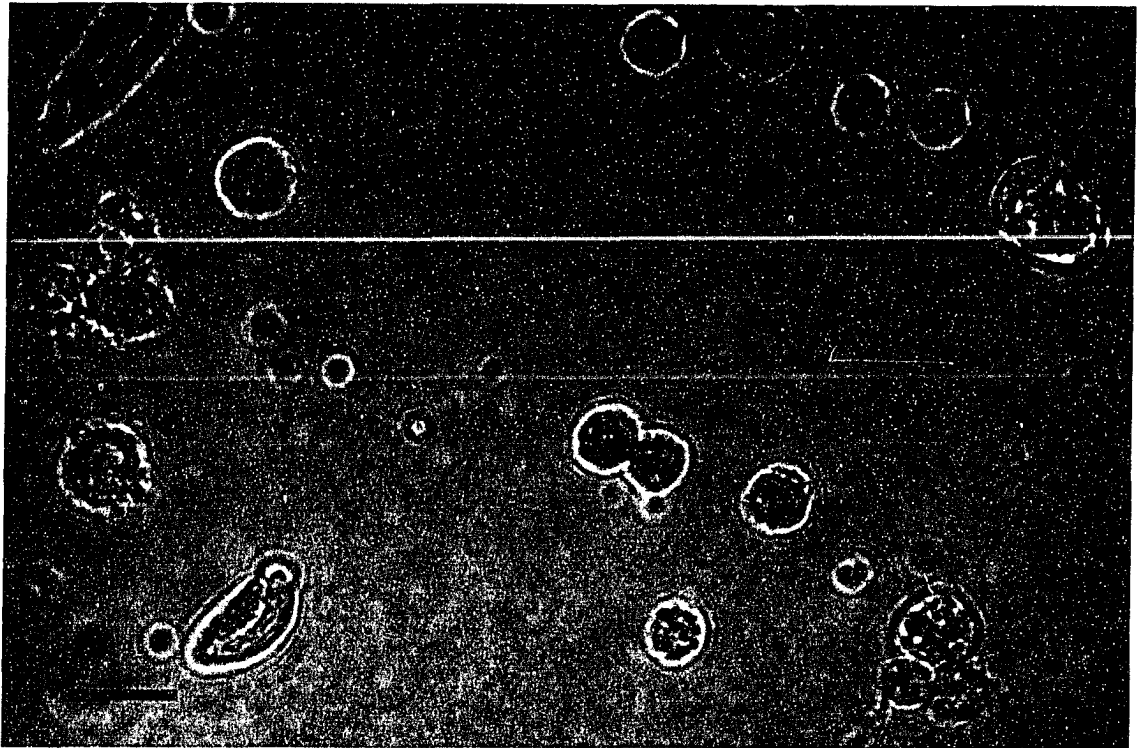
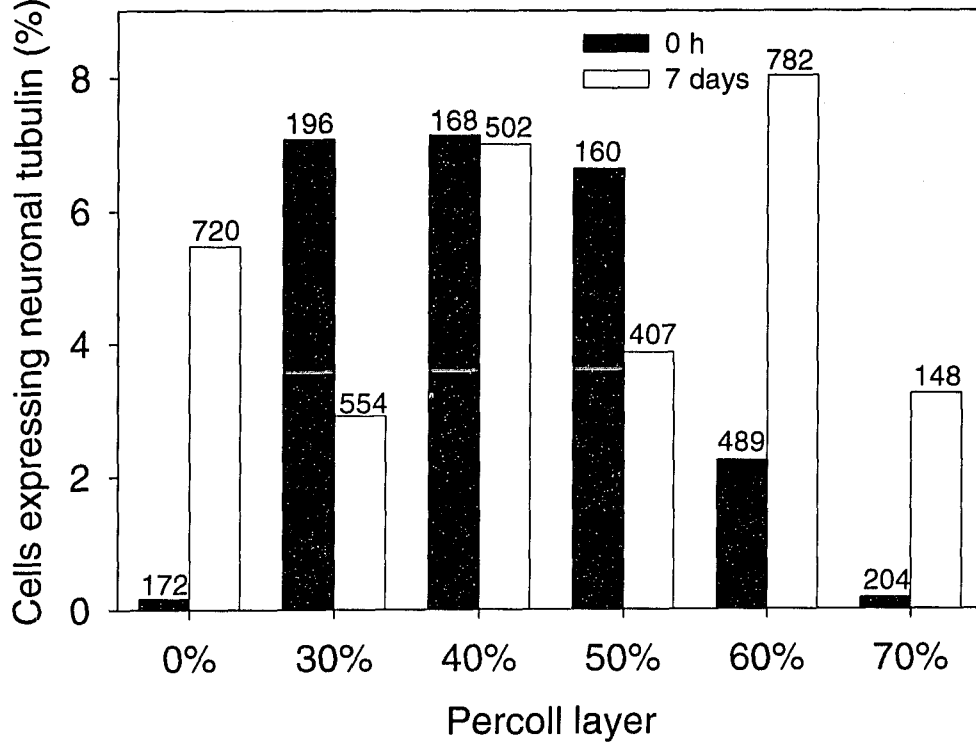


Figure 20. Neoblasts purified using Percoll gradients can be identified using histological stains. Cell suspensions isolated from the boundary between 20% and 30% Percoll were plated onto coated glass coverslips and processed for histological identification of neoblasts. This method was very specific for labeling neoblasts dark blue, and staining other cells light pink in colour. Contaminating cells found consistently included muscle cells and rhabdite-forming cells. Scale bar represents 10 μm .

Figure A.21. Effect of diffusible morphogens on the expression of a neuron-specific tubulin in neoblasts cultured for 7 days on 0.1% poly-L-lysine coated glass slides. **(a)** The proportion of tubulin expressing cells tended to increase after 7 days in culture compared to neoblast suspensions immediately after plating. Cells from the 30% and 50% Percoll layer were an exception where the proportion of cells expressing neuronal tubulin was smaller after 7 days than immediately after plating. The greatest change in the proportion of cells expressing neuronal tubulin occurred in cells from the 60% Percoll layer. **(b)** Treatment of cells isolated and purified in discontinuous Percoll gradients with bFGF and 5-HT for 7 days had little effect on the proportion of neurons in neoblast cultures. In general, bFGF tended to slightly increase the proportion of neurons in the cultures, with the exception of cells from the 40% Percoll layer when compared to the control. Serotonin had the opposite effect and tended to decrease the proportion of neurons in cultures following 7 day treatments. Numbers above bars represent the sample size.

(a)



(b)

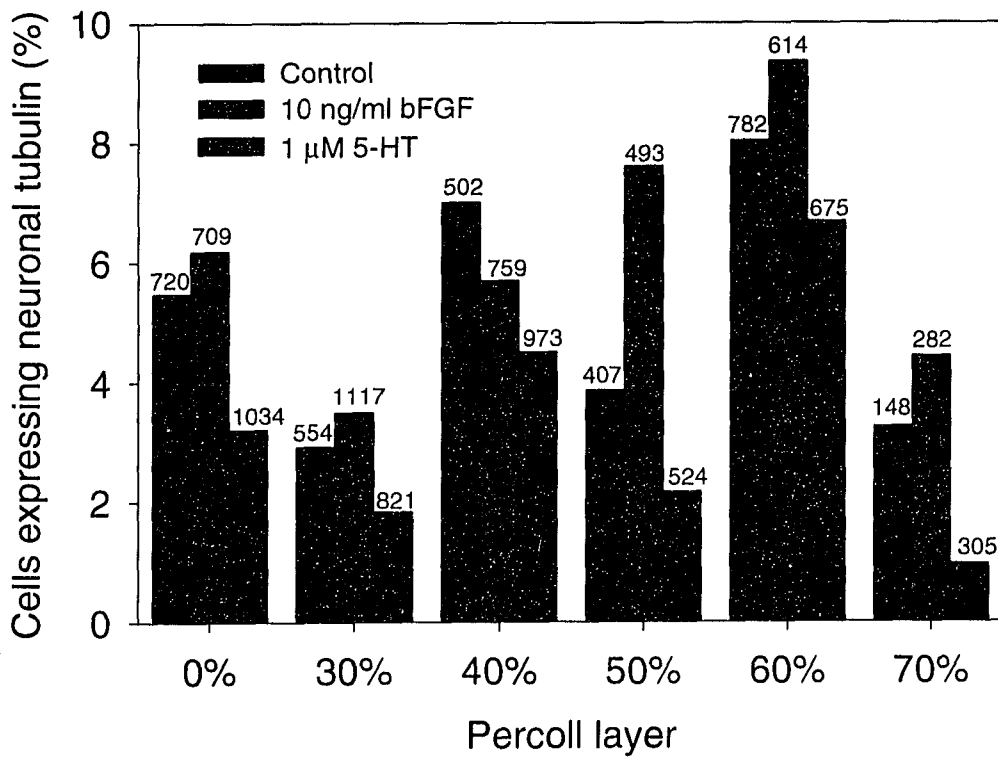
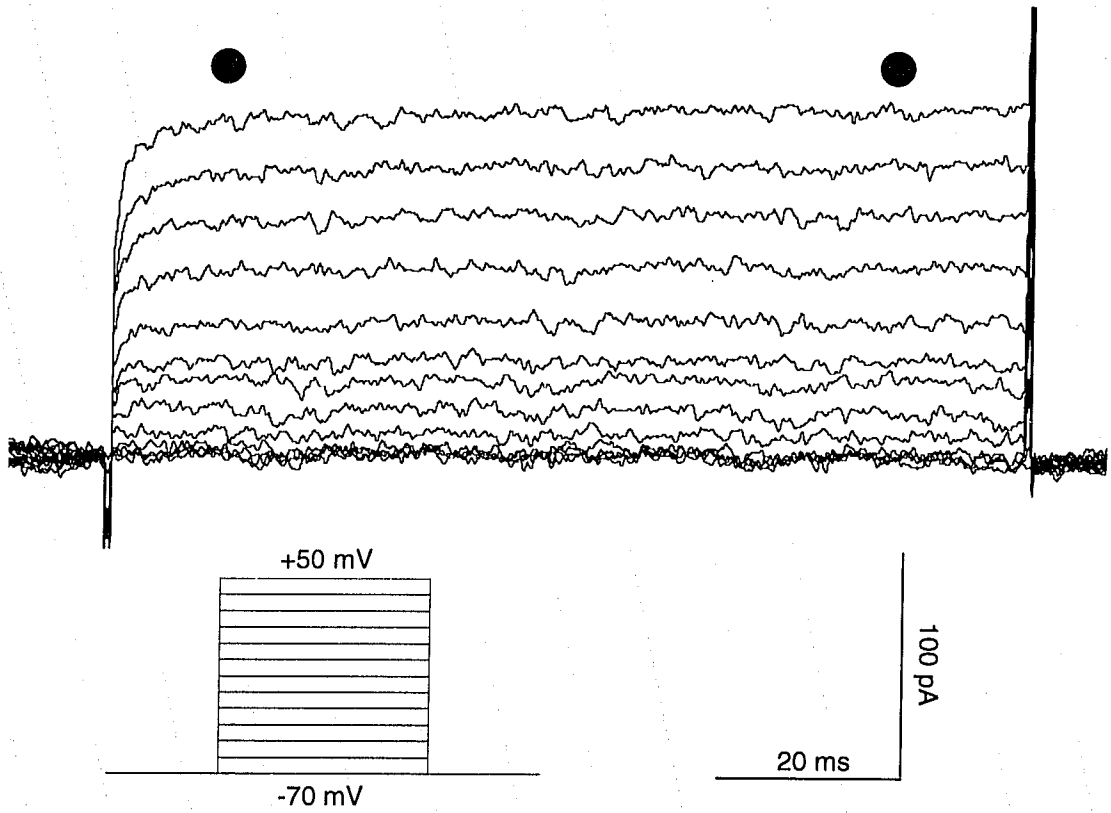
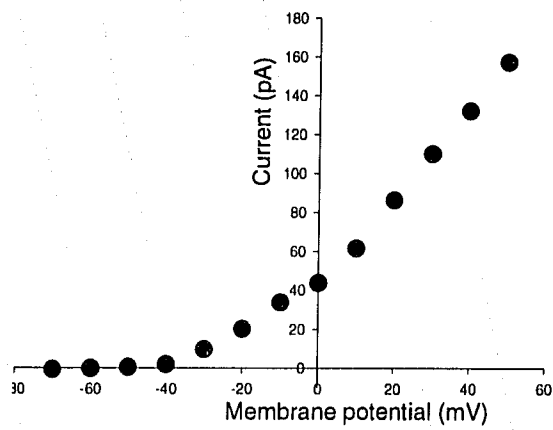


Figure A.22. V_g - K^+ currents recorded in undifferentiated neoblasts from *N. atomata*. (a) A typical outward current recorded from a voltage-clamped neoblast bathed artificial seawater. Outward currents were only observed in 30.0% (n=10) of neoblasts. Currents were evoked by stepping the holding potential from -70 mV in 10 mV increments between -70 mV and +50 mV for 100 ms. The scale bar and voltage waveform are included in the inset. (b) The current-voltage relationship of K^+ currents show that channels activate at around -30 mV and increases proportionally to the depolarizing test pulse. Mean peak current was taken between 10 ms and 90 ms into the test pulse (black dots above trace). (c) Steady-state activation properties of K^+ channels recorded from undifferentiated neoblasts. Activation curves from individual cells were fitted to a multi-stage Boltzmann function to determine the voltage of half-activation and the slope factor. These values were used to generate a mean activation curve (solid curve). K^+ channels activate at approximately -30 mV, and become fully activated at +30 mV. The voltage of half-activation was 16.2 ± 3.0 mV (n=3) and the slope factor was 15.7 ± 1.1 (n=3).

(a)



(b)



(c)

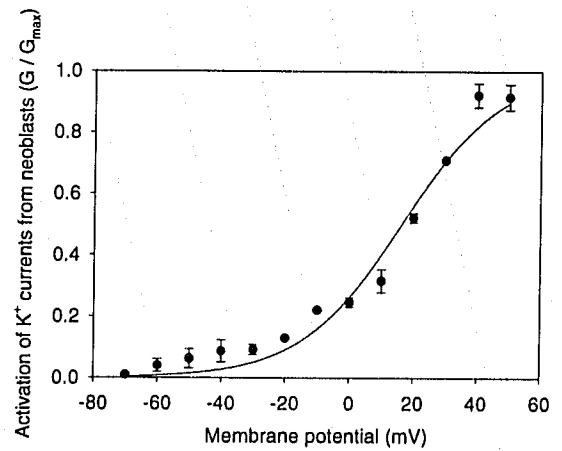


Figure A.23. Acetylated tubulin labels neurons, ciliated cells, and cilia non-discriminately in *Notoplana atomata*. **(a)** A coronal section reveals many elements that label strongly against an acetylated- α -tubulin antibody. Tubulin staining reveals the bilaterally symmetrical brain (solid arrow) and a pair of nerves exiting at the ventral side above a layer of muscle and the epidermis. The paired nerves can be followed laterally to the left and right margins of the animal (not shown). Cell bodies and axons of neurons from the dorsal submuscular nerve plexus are also visible below the dorsal layer of muscle and epidermis. Many tubulin positive cells are found inbetween epidermal cells, presumably secretory and sensory neurons. The tubulin antibody also labels the ciliated cells of the ventral epidermis, and the cilia of the gut diverticula (dashed arrow). **(b)** A magnified view of one of the chambers of the gut diverticula clearly shows that cilia label intensely against acetylated- α -tubulin. **(c)** Individual cilia are larger in the main gut chamber. It appears that only the cilia themselves and not the adjoining ciliated gut cells label against acetylated- α -tubulin.

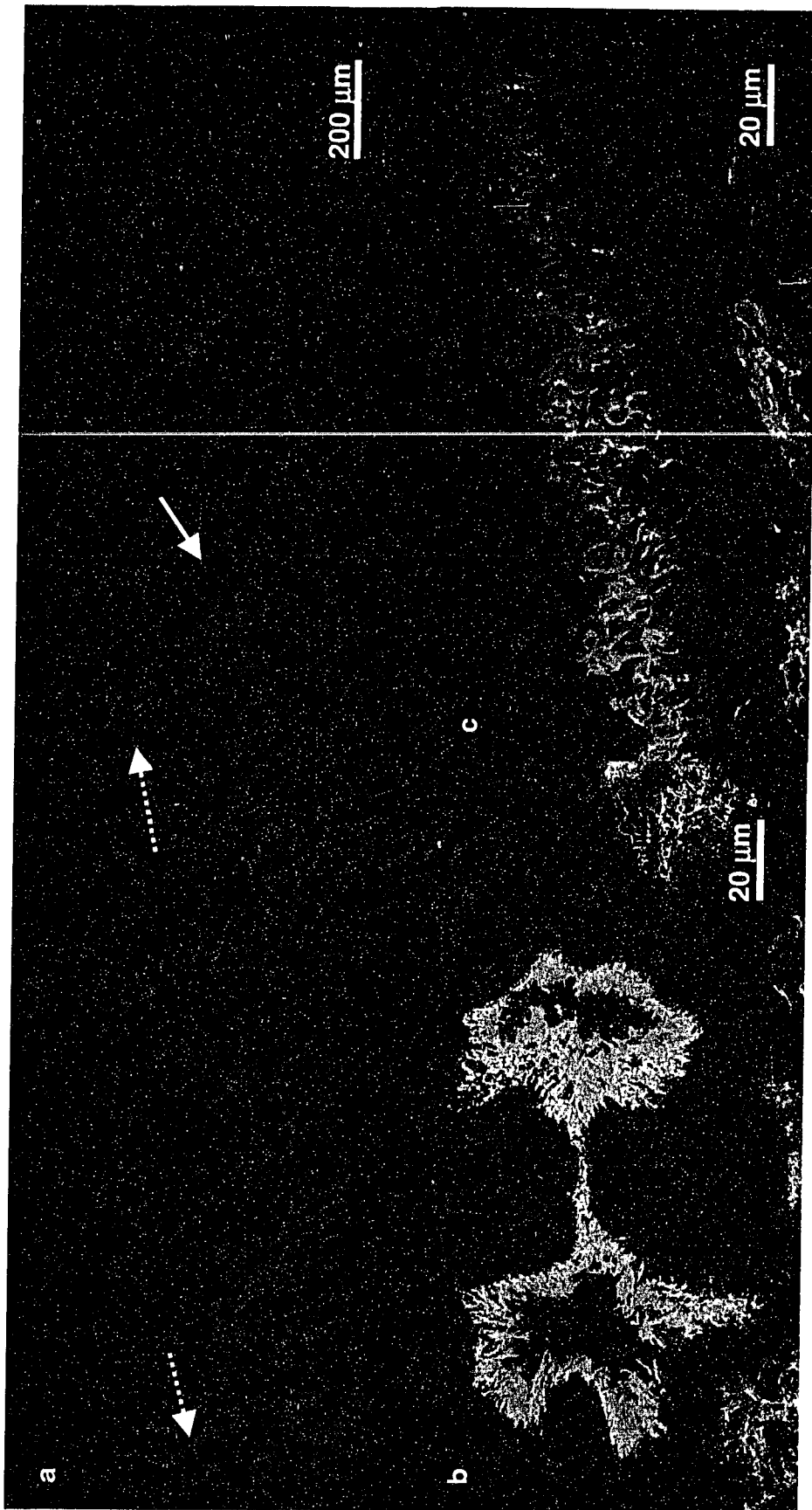
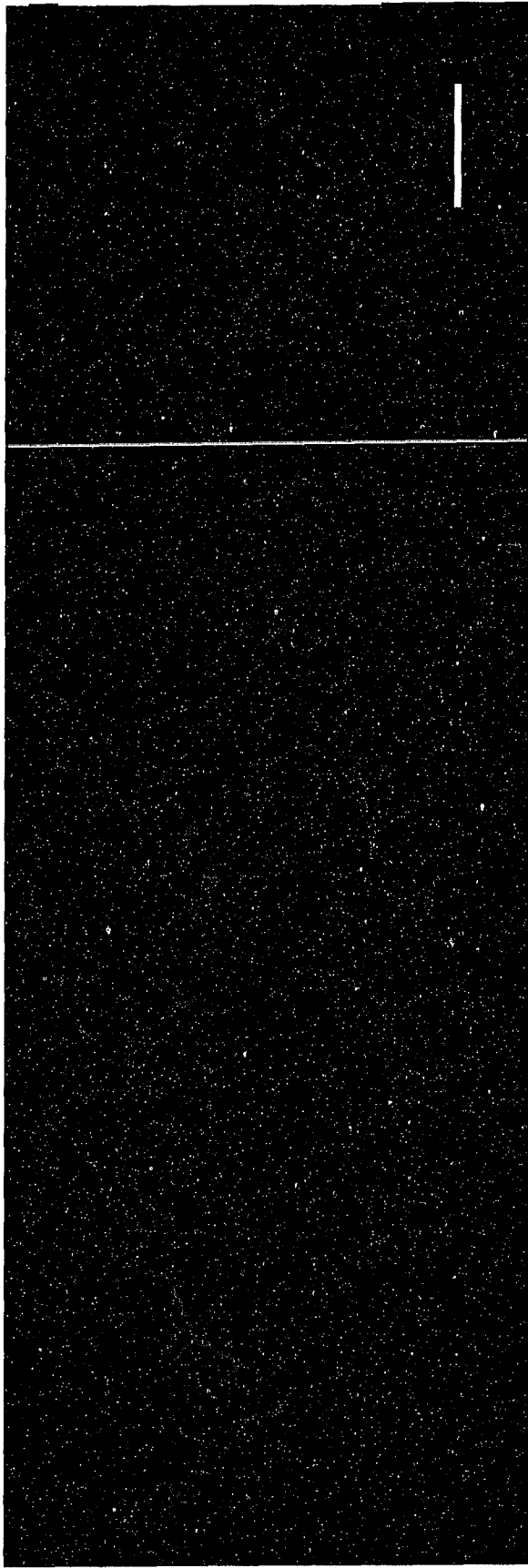


Figure A.24. Neurons from *Notoplana atomata* are labelled specifically by the Tub Ab-4 antibody. **(a)** A coronal section labelled against acetylated- α -tubulin reveals immunoreactivity from neurons, ciliated cells, and cilia. This suggests that acetylated- α -tubulin is not a suitable marker for neuronal differentiation since various cellular phenotypes are cross-reactive. **(b)** Neurons are labelled specifically against the Tub Ab-4 antibody. Note that in both the ventral and dorsal boundaries, no immunoreactivity is observed in ciliated cells or in cilia. Also, the cilia of the gut diverticula do not show immunoreactivity towards Tub Ab-4. Taken together, these results show that Tub Ab-4 relatively neuron-specific and a better marker for neuronal phenotype.

(a)



(b)



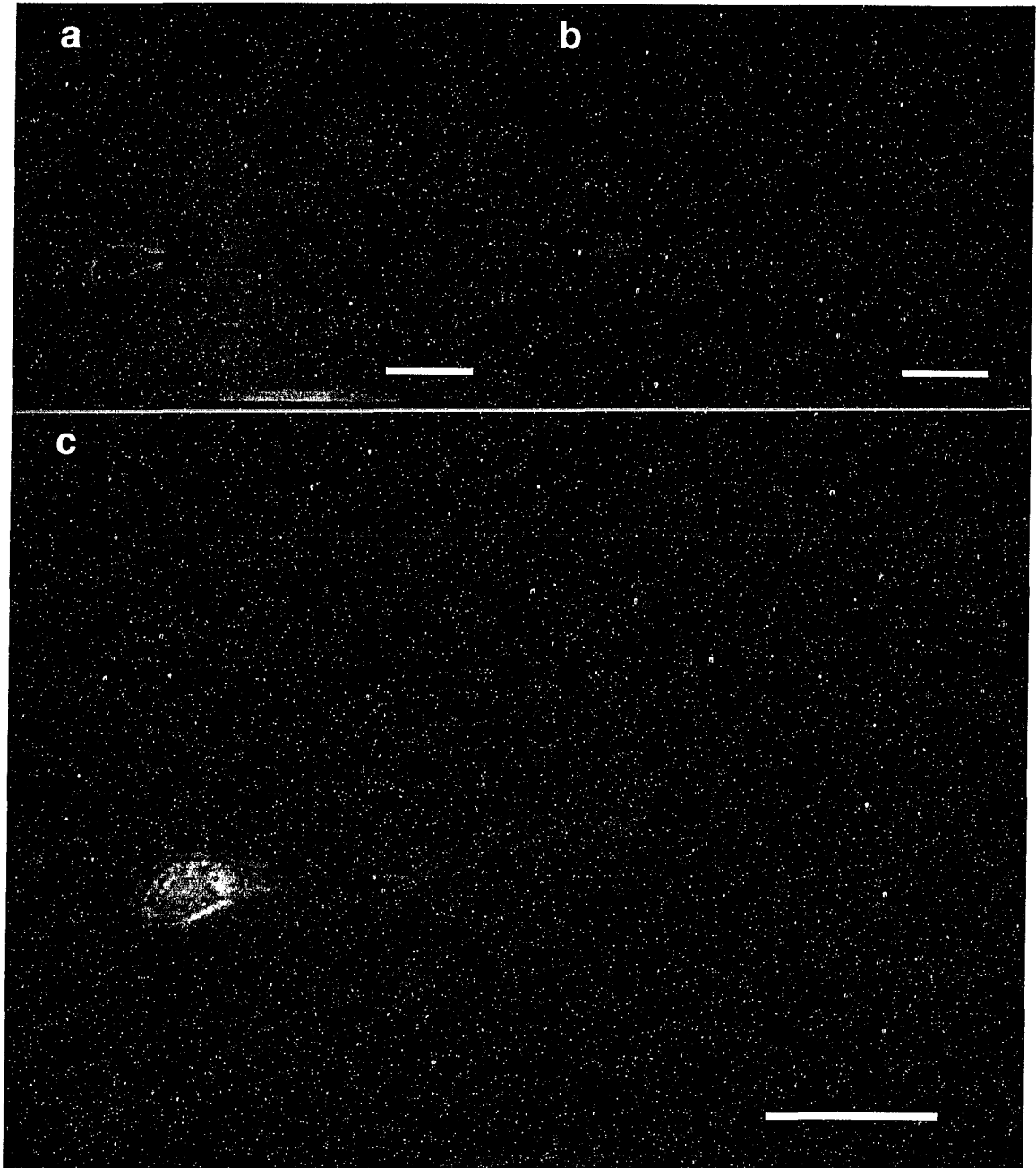


Figure A.25. Cultured brain neurons can be identified in culture by immunoreactivity towards the Tub Ab-4 antibody. (a) A bipolar brain neuron with prominent secondary neurites and growth cones imaged with bright field microscopy. (b) Brain neurons label specifically against a neuron-specific tubulin antibody. (c) Tubulin is present in all regions of the neurons including the soma, primary and secondary neurites, as well as in the growth cones. Scale bars represent 50 μm .